Development of a Chemoproteomic Approach to Study Kinase-Substrate Interactions and the Discovery of CDK4 as a 4E-BP1 Kinase

By

Dylan Charles Mitchell

A dissertation submitted in partial fulfillment
of the requirements for the degree of
Doctor of Philosophy
(Chemical Biology)
in the University of Michigan
2019

Doctoral Committee:

      Assistant Professor Amanda L. Garner, Chair
      Assistant Professor Brent R. Martin
      Professor Alexey Nesvizhskii
      Assistant Professor Matthew B. Soellner

Dylan C. Mitchell

dylancm@umich.edu

ORCID iD: 0000-0002-1676-8757

DEDICATION

I dedicate this to my wife, Lindsay, who is my best friend and biggest supporter.

Acknowledgements

I would first like to thank my committee members for all of the guidance over the past four years. To my advisor Dr. Amanda Garner, thank you for putting your trust in me from day one, and allowing me to follow my interests while pursuing areas of science in which neither of us were an expert. Your hands-off approach, which took a lot of faith that I would find the right path, was instrumental in allowing me to become an independent scientist and I will be forever grateful. To Dr. Brent Martin, Dr. Alexey Nesvizhskii, and Dr. Matt Soellner: thank you for providing me with helpful suggestions on how to solve the questions for which I was seeking answers, and for aiding in my quest to become a successful chemical biologist.

I also thank each of my friends in the Garner lab, who created a great environment in which to do science. Dr. Dan Lorenz, while your stubbornness in refusing to believe any of my data often made me incredibly frustrated, it stimulated so many conversations that helped me see an important outside perspective on my work. Discussing our work together truly made me a better scientist. Arya Menon, thank you for being a great partner with whom to study 4E-BP1 biology; I am grateful that you never got too mad at me for requesting hundreds of Western blots. Emily Sherman, having you in lab to discuss everything from science to being a meathead made working long hours substantially better. To Jorge Sandoval, you have been a great friend both in and out of the lab. I already miss sharing an office with you; I always enjoyed trading stories and talking about food. To Dr. Tanpreet Kaur thank you for the countless, long-winded conversations, and for keeping me abreast of all that was happening in the lab.

Dr. Ken Takeuchi, thank you for providing instrumental early stage guidance for me as I attempted to learn cancer biology. You were an unofficial mentor and great friend during a time that I found myself in over my head. The general knowledge and expertise you shared with me were essential to my success, and have been passed on to others that I have helped train.

iii

I also thank my family for their continual support. My parents, who were great role models for me throughout my life, taught me the value of hard work and perseverance. You truly put me in the best possible position for me to be successful in my career and in life. To my brother Scott, our weekly conversations were so important to me and kept me from losing perspective after long hours in the lab. To my sister Kelly, thank you for constantly for barraging me with pictures of my niece and nephews; you made me feel like I was still a small part of their lives even from the other side of the country.

Finally, I thank the most important person of all, Lindsay. This would not have happened if not for all of your tireless work behind the scenes. You moved with me across the country to the frozen tundra of Michigan, and did it with excitement even though you were more nervous than I was. You put up with my long hours, and my "I'll be home in 30 minutes" texts, that we both knew meant at least 2 hours. You made sure I always had food during the day and that I came home to a hot meal (or warm, depending on how late I was) at night. You listened to me when I was continually frustrated, with science or otherwise, and always kept me level-headed. I wish I could give you half of my Ph.D., because you deserve at least that for how instrumental you were in me getting to this point. Thank you for being such a great wife and an even better friend.

TABLE OF CONTENTS

LIST OF FIGURES

LIST OF TABLES

LIST OF APPENDICES

LIST OF ACRONYMS AND ABBREVIATIONS

4E-BP1..Eukaryotic initiation factor 4E Binding Protein 1
eIF4E.. Eukaryotic initiation factor 4E
eIF4G .... Eukaryotic initation factor 4G
CDK4.. Cyclin Dependent Kinase 4
CDK6.. Cyclin Dependent Kinase 6
CDT.. Cap Dependent Translation
VEGF ....Vascular Endothelial Growth Factor
mTORC1/2.. mechanistic Target of Rapamycin Complexes 1/2
ATP ....Adenosine Triphosphate
PhAXA ....Phosphosite Accurate Crosslinking Assay
LC-MS..Liquid Chromatography Mass Spectrometry
PPI ....Protein-Protein Interaction
GOI.. Gene of interest
JNK1/2 ....c-Jun N-terminal Kinase 1 and 2
MAPK8/9.. Mitogen Activated Protein Kinase 8 and 9
ERK2.. Extracellular Regulated Kinase 2
MEK1/2 ....MAPK/ERK Kinase 1 and 2
PhAXA ....Phosphosite Accurate Crosslinking Assay
PhAXA-MS......Phosphosite Accurate Crosslinking Assay coupled to Mass Spectrometry
RB1 ....Retinoblastoma-associated protein
KO .... Knockout
PPI ....Protein-Protein Interactions
AP-MS...Affinity Purification Coupled to Mass Spectrometry
PTM.. Post-Translational Modification
as-Kinase ....Analog-sensitive kinase
B5A .... Biotinoyl-5'-adenylate
PKA..Protein Kinase A
PSM .... Peptide Spectrum Match

ABSTRACT

An instrumental aspect of cancer progression is the acquired deregulation of the cellular processes that regulate growth and proliferation. Most of these processes are, at some level, controlled by a kinase-catalyzed change in the phosphorylation status of key signaling intermediates. Given the role of kinases in regulating every key cellular process, kinase inhibitors have emerged as an important class of anticancer therapeutics. However, as our knowledge of the phosphoproteome grows, our understanding of the identified phosphorylation sites remains limited. However, the ability to fully deconvolute kinase signaling networks is hampered by the transient nature of kinase-substrate interactions, a property that renders traditional methods of identifying novel protein-protein interactions ineffectual. Thus, new tools are needed with which to identify kinases that act on phosphorylation sites known to contribute to the pathophysiology of cancer.

Cap-dependent translation (CDT) is a critical cellular process that enables the expression of mRNA transcripts encoding for growth and survival proteins, many of which contribute to malignancy. Consequently, regulation of CDT is typically maintained at different levels by numerous signaling cascades. However, these pathways ultimately converge to alter the phosphorylation status of the translational suppressor eukaryotic initiation factor 4E binding protein (4E-BP1). 4E-BP1 serves as a gate-keeper of CDT by competing with translation initiation factors for binding to the m^7G-cap-binding protein eIF4E. In cancers, oncogenic signaling results in hyperphosphorylation of 4E-BP1, eliminating the negative repression on eIF4E, leading to constitutive CDT. This has provided rationale for the development of mechanistic Target Of Rapamycin (mTOR) inhibitors as cancer therapeutics, as mTOR complex 1 (mTORC1) is thought to be responsible for the ultimate regulation of 4E-BP1 phosphorylation. However, resistance to allosteric and active site mTOR inhibitors is a hallmark of many cancers, which has decreased the clinical efficacy of mTOR-targeted therapeutics. Moreover, 4E-BP1 contains several uncharacterized phosphorylation sites, the function and regulation of which are unknown. These findings have resulted in speculation about the possibility of

uncharacterized 4E-BP1 kinases that promote 4E-BP1 hyperphosphorylation, CDT, and tumorigenesis.

To facilitate the identification of kinases capable of acting on phosphorylation sites of interest, a kinase crosslinking assay (termed PhAXA) was developed. When coupled to LC-MS/MS analysis, PhAXA yields high confidence kinase-substrate interactions with phosphosite specificity. Proof-of-concept studies demonstrated the broad applicability of this approach by validating known relationships for three distinct kinase-substrate pairs. This chemoproteomic pipeline was then used to uncover the role of CDK4 in regulating 4E-BP1 phosphorylation. Dissection of this relationship revealed that CDK4 activity maintains CDT under conditions of mTORC1 inhibition in CDK4/6 inhibitor-sensitive cell lines. Moreover, Ser101, an orphan, understudied 4E-BP1 phosphorylation site, was identified and validated as a CDK4 substrate. Evaluation of this event provided a mechanism by which inhibition of CDK4 regulates translation of the oncoprotein c-Myc, which drives a host of known cancers. The discovery of this signaling axis has uncovered a novel function of clinically approved CDK4/6 inhibitors, and sheds light on the mechanism by which these drugs synergize with mTORC1-targeted therapies. The successful implementation of this approach to uncover new biology should result in wide-spread adaptation of the PhAXA platform for elucidating novel drug targets for the treatment of cancers and other kinase-driven diseases.

Chapter 1

Kinases and Activity Based Probes

1.1 Abstract

Kinase-catalyzed addition of a phosphate to a substrate serine, threonine or tyrosine is the most ubiquitous post-translational modification in eukaryotes, serving as a robust mechanism for intracellular information transfer. Aberrant kinase signaling contributes to the pathophysiology of many diseases such as cancer, lung fibrosis and rheumatoid disorders.[1-3] However, despite the important role protein phosphorylation plays in mediating important cellular processes, most of identified phosphorylation sites remain uncharacterized. Elucidation of the kinases responsible for mediating the modification of clinically relevant phosphorylation sites would lead to new targets for modulation with therapeutics.

Because of the transient nature of kinase-substrate interactions, traditional affinity purification followed by mass spectrometry approaches for mapping protein-protein interactions have been ineffective for solving this problem.[4,5] Thus, tools such as yeast-two hybrid assays, promiscuous crosslinkers, and proximity labeling techniques have been implemented to directly identify novel substrates for a kinase-of-interest; however, these methods provide little information about phospho-site specificity.[6-12] Identifying kinases capable of phosphorylating a specific residue has proven difficult; very few methods are available to answer this question and each has considerable limitations.[13] Given the limitations of currently available technology, new tools are needed to assign kinases to site-specific phosphorylation sites, allowing for a better understanding of the interplay between signaling networks and the identification of therapeutically relevant protein targets.

1.2 Signal Transduction, Kinases and the Phosphoproteome

Cells are capable of responding to a diverse set of environmental stimuli, including nutrient availability, stress and a variety of small molecule effectors, using many different methods of signal transduction. These extracellular stimuli are recognized by intra- or extra-cellular receptors, which activate or inactivate signaling cascades required to elicit the appropriate cellular response. Following activation of a surface receptor, the signal is transduced through an ordered list of intermediary proteins until an end result, such as increased/decreased translation or transcription, is achieved. These intermediary proteins propagate and amplify the appropriate signal upon modulation of their activity by post-translational modifications (PTMs). PTMs that modify protein activity include phosphorylation, glycosylation, hydroxylation, acetylation, lipidation and ubiquitylation[14] (Table 1.1). Accounting for these modifications yields an estimated 1,000,000 distinct proteins in the human proteome,[15] each of which may perform a diverse array of functions.

Modification Type	Amino Acid	Enzyme Class	Review
Phosphorylation	Ser/Thr/Tyr	Kinase	16
Glycosylation	Asn/Ser/Thr	Glycosidase & Glycosyltransferase	17
Acetylation	Lys/Nterm*	Acetyltransferase	18
Amidation	Cterm**		19
Hydroxylation	Pro/Asn	Hydroxylase	20
Methylation	Lys/Arg	Methyltransferase	21
Lipidation	Cys/N-Gly***	Various****	22

Table 1.1 | Common Post-Translational Modifications. A table listing the seven most common[14] PTMs in eukaryotes. *Nterm = N-terminus of protein. **Cterm = Carboxy-terminus of protein. *** N-Gly = N-terminal glycine (after cleavage of initiator methionine. ****Lipidation in this case groups palmitoylation, farnesylation, geranylgeranylation, myristoylation, and acylation. Therefore, many enzymes are responsible for these PTMs.

Phosphorylation is the kinase-catalyzed transfer of a phosphate from ATP to a substrate Serine, Threonine or Tyrosine, and constitutes the most ubiquitous method of intracellular signal transduction, with one-third of the human proteome containing at least one phosphorylation site. Recent estimates of the human proteome suggest that there

are ~20,000 protein-coding genes,[23,24] the protein products of which contain at least 146,306 identified phosphorylation sites.[25-27] When accounting for *in silico* predictions, the human phosphoproteome is expanded to over 500,000 phosphorylation sites, each of which is mediated by one of the 518 human kinases.[27,28] However, only ~7,000 of these sites have been assessed experimentally,[25] leaving a large gap in our knowledge of kinase signaling networks. (Figure 1.1)

Predicted (~500,000)

Identified (~140,000)

Annotated (~7,200)
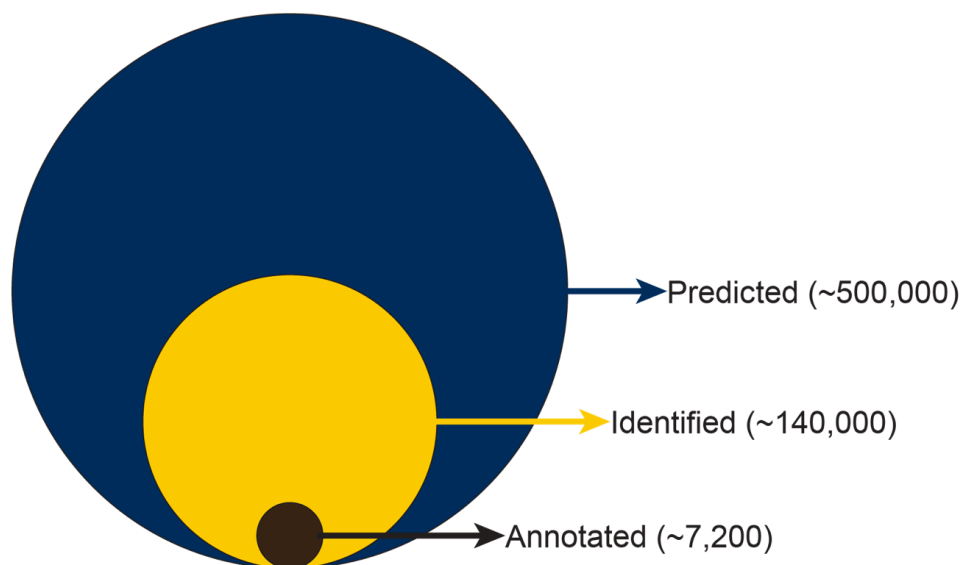
Figure 1.1 | Annotation of the Human Phosphoproteome

      The explosion in our knowledge of the phosphoproteome can be directly linked to advances in mass-spectrometry based phosphoproteomics. (Figure 1.2) While these experiments are capable of identifying tens of thousands of phosphorylation sites in a single run, they provide very little information about function and no value as far as kinase assignment. This in-depth examination of the human phosphoproteome has far outpaced the ability to annotate the kinases that mediate these PTMs, limiting the utility of this influx of data.[29] However, the field of phosphoproteomics is uniquely positioned for identifying phosphorylation-site-biomarkers that correlate with phenotypes such as drug resistance[30] or an increased propensity for metastasis.[31] This in-depth analysis of the phosphoproteome can aid in understanding viable combination treatments for cancer therapy,[32] though only if the identified phospho-biomarkers can be confidently assigned to a known kinase. Because phosphorylation can elicit dramatic effects on a substrate,

and many substrates affect numerous cellular processes that are implicated in disease, understanding the kinases that regulate each site individually is critically important in piecing together signaling networks.
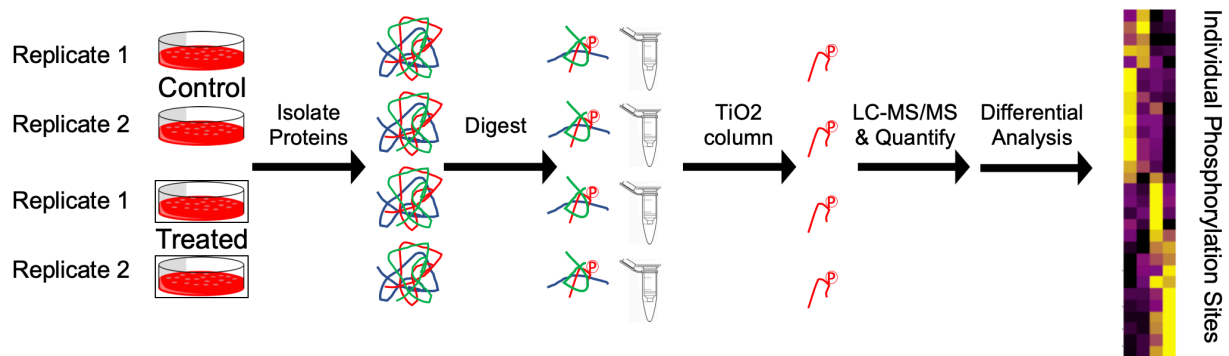
Figure 1.2 | Phosphoproteomics Workflow. A typical phosphoproteomics workflow is shown. Proteins from different types samples (cells, tissue, etc) are collected, then digested into peptides using a protease such as trypsin. Those peptides harboring a phosphate group are isolated by affinity purification (often titanium dioxide colums) and analysed by LC-MS/MS. After assignment of MS^2 spectra, phosphopeptides are quantified and differentially regulated sites are identified.[33]

1.3 Kinases and Kinase Inhibitors in the Treatment of Cancer

Kinases regulate every process in cell biology, from growth and proliferation to apoptosis and metabolism. As such, numerous kinases have been implicated in facilitating uncontrolled proliferation in diseases such as cancer and pulmonary fibrosis.[2,3,34] Indeed, a systematic evaluation of cancer-associated genetic mutations identified kinases as the most over-represented family in the dataset.[35] Similar observations have been made upon consideration of gene overexpression and amplification.[36] These findings, along with the unprecedented success of Imatinib, the second FDA approved, small-molecule kinase inhibitor,[37] led to a burgeoning field of kinase-targeted therapeutics for treating cancers.[34] Since Imatinib first gained FDA approval in 2001,[38] 46 small-molecule kinase inhibitors have been approved for use in oncology, 36 of which have been approved over the last 8 years (2011-2018). (Figure 1.3) This number does not include monoclonal antibody inhibitors such as Cetuximab and Trastuzumab, which target EGFR and ERBB2 respectively.[39]

Total Number of FDA Approved Kinase Inhibitors
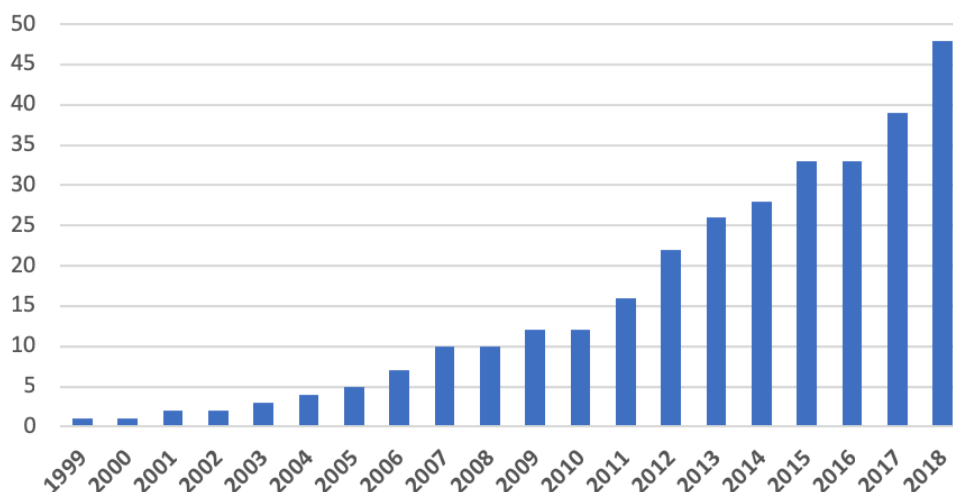
Figure 1.3 | FDA-Approved Small-Molecule Kinase Inhibitors Over the Years. Sirolimus, the first FDA-approved kinase inhibitor, gained approval in 1999 as an immunosuppressant for preventing organ rejection following kidney transplant. Aside from Sirolimus, Baricitinib[40] (rheumatoid arthritis), Netarsudil[41] (glaucoma), Fostamatinib[42] (thrombocytopenia), Nintedanib[43] (pulmonary fibrosis) and Tofacitinib[44] (rheumatoid arthritis) are the only FDA-approved kinase inhibitors used for a non-cancer indication.

While these inhibitors have realized success in clinical oncology, the overall impact of small molecule kinase inhibitors is in question, in part due to emerging resistance.[45,46] Applying selective pressure to cells in the form of chronic kinase inhibition induces resistance in the form of acquired gatekeeper mutations,[47] or via hyperactivation of compensatory pathways.[45] Strategies to overcome the former include development of type III, allosteric kinase inhibitors such as the MEK1/2 inhibitor Trametinib,[48,49] or by pursuing molecules that are not reliant upon the gatekeeper residue.[50] Identifying pathways that circumvent targeted kinase inhibitors is a question of uncovering and dissecting novel signaling paradigms, which requires a diverse array of biological and chemical tools. However, by achieving a better understanding of fundamental cancer biology in the context of kinase inhibitor resistance, new combination therapies can be pursued that lead to a more robust clinical outcome.[51]

1.4   Current Methods for Uncovering Protein-Protein Interactions

Protein-protein interactions (PPIs) mediate the vast majority of biological processes including many that are involved in initiating and/or maintaining malignancy.[52]

As such, many techniques have been developed by which to elucidate binding partners for a protein of interest. One of the most well-established methods used to accomplish this is affinity purification coupled to mass spectrometry (AP-MS) (Figure 1.4). AP-MS experiments typically utilize an antibody raised against an epitope fused to the bait protein of interest, and cells expressing this fusion protein are lysed and passed over antibody-conjugated resin. The bait protein is retained on the resin along with binding partners and non-specific interactors, while non-interacting partners are washed away. These proteins are then analyzed by LC-MS/MS to come up with a candidate list of bait-interacting protein partners. This technique has been successfully used to uncover a tremendous amount of biologically relevant PPIs, though identifying kinases that act on a substrate of interest using an AP-MS approach is difficult given the transient nature of kinase-substrate interactions. Indeed, one published analysis of ERK2 kinases using AP-MS failed to identify MAPK/ERK Kinase 1 or 2 (MEK1/2), the kinase known to phosphorylate ERK2.[53] Moreover, any kinase-substrate identification uncovered using affinity purification methods would provide no information regarding phosphorylation site specificity. As a result of this limitations, basic AP-MS techniques such as IP-MS (Figure 1.4) have largely failed to aid in the deconvolution of kinase mediated signaling events.
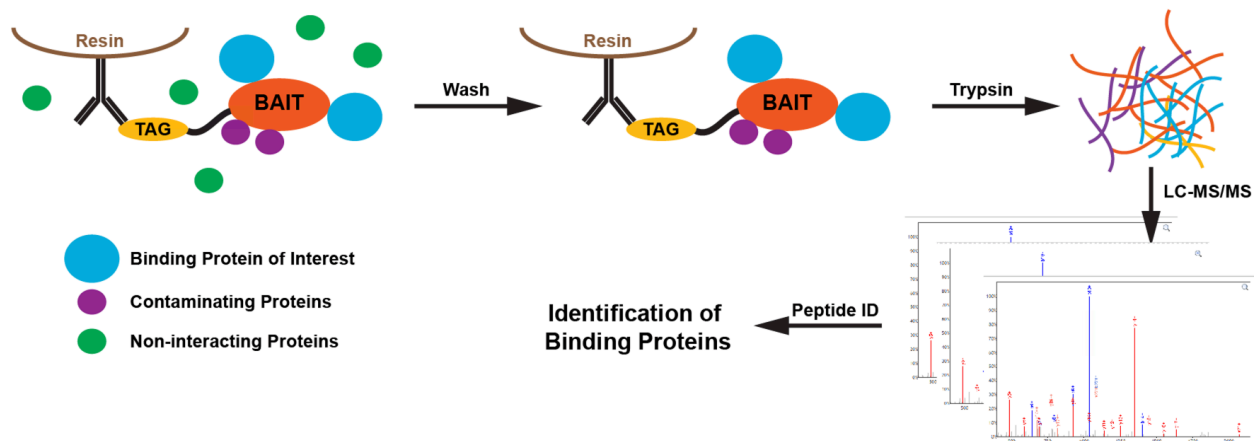
Figure 1.4 | Affinity Purification and Mass Spectrometry. A scheme for Immunoprecipitation coupled to Mass Spectrometry (IP-MS) is shown. Resin conjugated with antibodies specific for an affinity tag is used to isolate proteins bound to a bait protein of interest while non-interacting proteins are removed by washing. These proteins are digested into peptides using a protease (typically trypsin), separated by liquid chromatography (LC) and analyzed by tandem mass spectrometry (MS/MS). These MS^2 spectra are matched to known peptide sequences using database searching tools, which results in protein identification.

However, given the importance of phosphorylation in many diseases, and the emergence of clinically successful kinase inhibitors, significant effort has been put into illuminating these signaling events via the development of novel methodologies. Proximity labeling (PL) has gained significant traction in recent years, with the advent of BioID and BioID2.[11,54-57] (Figure 1.5A) These methods rely on the generation of a fusion protein between an promiscuous biotin ligase enzyme that generates biotinoyl-5'-Adenylate (B5A). (Figure 1.5B) This highly amine-reactive B5A diffuses away from the bait-ligase fusion protein, labeling surface-exposed lysines on proximal proteins with a biotin moiety. The biotinylated proteins are then isolated using streptavidin-conjugated affinity resin, and subsequently identified by LC-MS/MS. The proteins identified by this method should be largely comprised of proteins that interact with the bait, though proximal, non-interacting proteins are also isolated.

The two biggest benefits of this technology are 1) The ability to probe for interactions within live cells without disrupting the cellular organization, which is a requirement of AP-MS assays 2) The ability to capture transient interactions such as those between a kinase and a substrate. However, the drawbacks of PL methods include 1) Slow labeling rates with BioID (on the order of 18 hours), which limits the ability of this method to study discreet cellular signaling events. However, newer PL enzymes like Apex,[58,59] which generates a biotinyl radical instead of B5A, and TurboID[60] have been developed to work around this issue. 2) Isolation of thousands of proteins necessitates up-front fractionation of samples before LC-MS/MS analysis, which increases instrument time. 3) The need to engineer cell lines that stably express the required fusion protein increases the time required to set up this assay. 4) The size of the fusion protein, between 30-45 kDa, may influence (positively or negatively) the PPIs engaged in by the bait protein. 5) No information regarding phosphorylation site specificity is garnered by these techniques. Despite these limitations, PL assays have successfully uncovered a handful of new kinase-substrate interactions.[11,61]
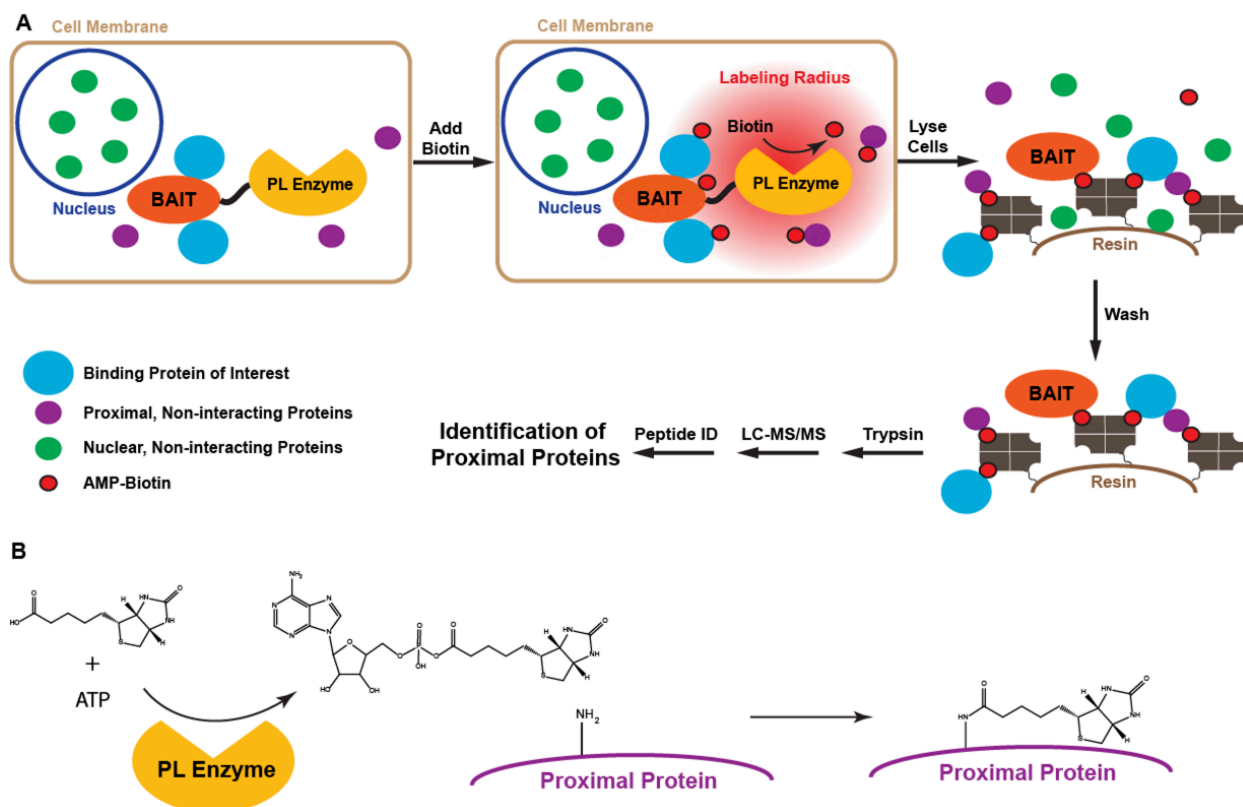
Figure 1.5 | Proximity Labeling Techniques Using Promiscuous Biotin Ligases. A) Cells expressing a bait-proximity labeling (PL) enzyme, or a no bait control, are treated with excess biotin to induce generation of biotinoyl-5'-Adenylate (B5A). Diffusion of B5A results in labeling of lysine residues on proximal proteins, allowing for purification using streptavidin resin. Bound proteins are then identified by LC-MS/MS based proteomics.

1.5 Chemical Probes for Kinase Discovery

AP-MS and PL approaches are useful for discovering new biology through uncovering novel PPIs. However, as each of these methods has significant drawbacks in the realm of uncovering novel kinase-substrate interactions, new technologies are required to fill this unmet need.[62] One unique approach to mapping kinase signaling networks utilizes a bump-in-hole strategy, whereby a kinase of interest is modified to accommodate a modified ATP substrate, commonly N6-(benzyl)ATP-γ-S, which is a poor substrate for endogenous kinases.[63] (Table 1.2A) In this approach, the N6-(benzyl)ATP-γ-S probe is added to cell lysate along with recombinant analog-sensitive kinase (as-kinase), which facilitates transfer of a thiophosphate group to all direct substrates. These thiophosphorylated peptides are then isolated using iodoacetamide conjugated resin,[64] or p-nitrobenzyl mesylate (PNBM) along with antibodies specific for the alkylated phosphorothioate epitope.[65,66] Mass-spec based proteomics is then used to identify the

8

direct as-kinase substrate peptides. This is an attractive approach to large-scale deconvolution of the phosphoproteome, as most kinases have bulky gatekeeper residues that, upon mutation to an amino acid with a smaller side-chain, can utilize one of several N6 modified ATP substrates.[67] While these probes have been used to uncover novel kinase-substrate interactions,[7,64] they are not useful when the goal is uncovering a kinase that phosphorylates a particular site of interest.
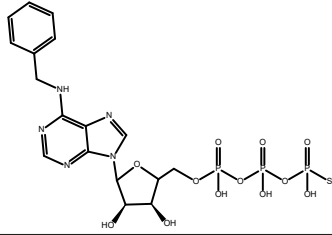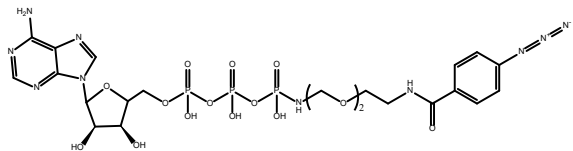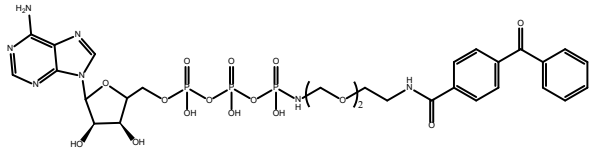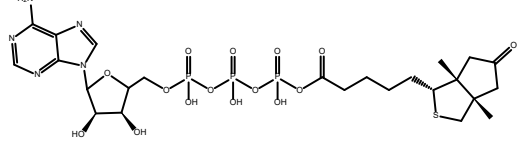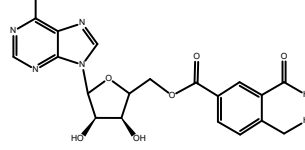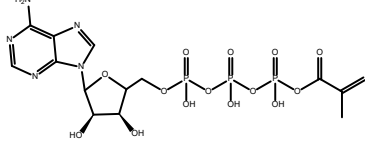
Probe Structure	Phosphosite Specific?	Bait Specific?	Refs
A	Yes. For kinase of interest	No	63-66
B	Maybe	Yes	68-71
C	Maybe	Yes	68-71
D	No	No	75-78
E	Yes	Yes	80
F	Yes	Yes	81

Table 1.2 | Chemical Probes for Unraveling the Phosphoproteome.

ATP-based photocrosslinkers have also explored for the purpose of interrogating the kinase-substrate interactome.[68-71] (Table 1.2B and 1.2C) These photocrosslinking probes rely on kinase catalyzed transfer of the gamma-phosphate, along with the PEG-linked photoreactive benzophenone or aryl azide, to the substrate. The kinase is then trapped on the "phosphorylated" bait by UV induced crosslinking, and the complex is isolated by affinity purification and proteins are identified by MS/MS. Initial experiments utilizing these probes provided proof-of-concept using recombinant protein kinase A (PKA) and a seven amino acid, biotinylated peptide pseudosubstrate.[68] However, a negative control peptide lacking the substreate serine residue still exhibited 50% labeling relative to the true substrate peptide. This finding calls into question the specificity of this approach, and the ability of the assay to find phosphosite specific kinases. When this assay (termed K-CLASP) was applied to cell lysate, PKA was positively identified by MS/MS.[68] However, no new biology was uncovered in this analysis, as the only other kinases enriched over the negative control samples were not relavent to the peptide substrate. A similar approach was then used to identify novel kinases using full-length p53 as a bait substrate.[69] As this method (termed K-CLIP) uses the full length substrate instead of a consensus substrate motif, it likely cannot identify kinases with phosphorylation site specificity. K-CLIP analysis of p53 kinases resulted in positive identification of a new p53 kinase, MRCKβ, though with very low abundance (1-3 PSMs) even in samples treated with 10 mM ATP-based photocrosslinker probe. However, this interaction was validated *in vitro* and in cells, though the exact site at which MRCKβ phosphorylates p53 was not identified.

K-CLIP is the first published method by which an ATP-based chemical probe has uncovered a novel kinase-substrate interaction. However, there are severe limitations to these aryl-azide (Table 1.2B) and benzophenone (Table 1.2C) photocrosslinker probes, including: 1) Many kinases cannot accommodate a bulky substitution on the gamma-phosphate of ATP.[72] Differential activity or ability of a kinase to utilize gamma phosphate functionalized ATP probes creates a biased survey of kinases capable of phosphorylating the bait. 2) Poor labeling efficiency of arylazides and benzophenones.[73] Increased labeling efficiency is only achieved under conditions that also cause protein damage. 3) The propensity of these groups to promote nonspecific crosslinking, typically to highly

abundant proteins instead of low abundance kinases. 4) Many proteins exhibit high affinity for these molecules even without UV activation, which can mask the reactive group for proteins of interest and increase nonspecific pulldown.[74] 5) The kinase-catalyzed photocrosslinker labeling is not bait specific, and the phospho-crosslinker can diffuse away from the kinase of interest before applying UV light. It is therefore possible that identified kinases are not acting on the bait substrate of interest. However, one benefit of this method is the possibility of performing the reverse experiment, where a kinase of interest is isolated along with potential substrates. Though this has not yet been done, this flexibility is attractive for achieving better annotation of the phosphoproteome.

To enable the unbiased quantification of kinases across several conditions, promiscuous ATP-based biotinylation probe was developed.[75-78] (Table 1.2D) This acyl-phosphate containing probes rely on a conserved lysine residue present in the active site of 98% of eukaryotic kinases, that normally coordinates the negative charge on the γ-phosphate of ATP.[79] Upon docking within the active site of a kinase, the carbonyl on the Biotinoyl-ATP probe is positioned near this conserved lysine. The amine of the lysine side chain attacks the carbonyl from the ATP analog, forming an amide linked biotin and releaseing free ATP. The biotinylated kinases are then purified using streptavidin resin and identified by MS/MS. This probe, which can engage and facilitate the purification of approximately 240 kinases,[75] has been commercialized by ActivX Biosciences for studying kinase inhibitor selectivity as part of the KiNativ platform.

These studies utilizing acyl-phosphate ATP probes opened up the possibility of leveraging similar techniques to uncover novel kinase-substrate interactions. The first approach that took advantage of this reactivity required a two-step mechanism between the conserved lysine, a cysteine residue on the bait peptide in place of the phosphorylated Ser/Thr/Tyr, and a dialdehyde group present on the probe.[80] (Table 1.2E) Proof-of-concept studies with this system left much to be desired, as the labeling was proven to be very inefficient.[81] However, a second generation of this crosslinker demonstrated much more favorable characteristics, and will be discussed further in Chapter 3.[81] (Table 1.2F) Though these methods proved valueable conceptually, each method utilized a peptide pseudosubstrate for *in vitro* characterization, thus limiting the biological relevance of the

approach. Likely as a result of this, neither probe successfully uncovered novel biology, though they set the groundwork for successful experiments to be discussed in Chapter 3.

1.6 Conclusions

The human proteome is highly dynamic, with ~20,000 protein coding genes giving rise to over 1,000,000 distict proteins after accounting for alternate splicing and post translational modifications (PTMs). Phosphorylation is one of the most relevant PTMs in the context of cancer, highlighted by the clinical success of many kinase inhibitors. However, as mass spectrometry technologies improve the ability of scientists to identify clinically relevant phosphorylation sites, new tools are required to provide actionable information for subsequent development and clinical implementation of kinase inhibitors. The standard toolkit for elucidating protein-protein interactions has proven incapable of rising to this challenge, and lead to the development of kinase-directed chemoproteomic probes. Previous attempts at designing activity-based, phosphosite-specific probes for kinase identification have used two approaches: (1) Assays that utilize peptide substrates that poorly recapitulate the activity of the bait protein[62,80,81] (2) Photoaffinity probes, which are inherently promiscuous and favor the identification of high abundance proteins, preventing the identification of low-abundance kinases.[68,71] These techniques have largely been unable to live up to their billing; however, each method has proven valuable in the context of establishing proof-of-concept for ways by which to more effectively uncover kinase-substrate interactions.

1.7 References

1   Gross, S., Rahal, R., Stransky, N., Lengauer, C. & Hoeflich, K. P. Targeting cancer with kinase inhibitors. *The Journal of clinical investigation* **125**, 1780-1789, doi:10.1172/JCI76094 (2015).

2   Walker, N. M., Mazzoni, S. M., Vittal, R., Fingar, D. C. & Lama, V. N. c-Jun N-terminal kinase (JNK)-mediated induction of mSin1 expression and mTORC2 activation in mesenchymal cells during fibrosis. *The Journal of biological chemistry* **293**, 17229-17239, doi:10.1074/jbc.RA118.003926 (2018).

3   Garneau-Tsodikova, S. & Thannickal, V. J. Protein kinase inhibitors in the treatment of pulmonary fibrosis. *Curr Med Chem* **15**, 2632-2640 (2008).

4   Jorgensen, C. & Linding, R. Directional and quantitative phosphorylation networks. *Brief Funct Genomic Proteomic* **7**, 17-26, doi:10.1093/bfgp/eln001 (2008).

5   Tan, C. S. H. & Linding, R. Experimental and computational tools useful for (re)construction of dynamic kinase-substrate networks. *Proteomics* **9**, 5233-5242, doi:10.1002/pmic.200900266 (2009).

6   Guo, X. *et al.* Site-specific proteasome phosphorylation controls cell proliferation and tumorigenesis. *Nat Cell Biol*, doi:10.1038/ncb3289 (2015).

7   Eblen, S. T. *et al.* Identification of novel ERK2 substrates through use of an engineered kinase and ATP analogs. *The Journal of biological chemistry* **278**, 14926-14935, doi:10.1074/jbc.M300485200 (2003).

8   Garber, K. C. & Carlson, E. E. Thiol-ene enabled detection of thiophosphorylated kinase substrates. *ACS chemical biology* **8**, 1671-1676, doi:10.1021/cb400184v (2013).

9   Hodgson, D. R. & Schroder, M. Chemical approaches towards unravelling kinase-mediated signalling pathways. *Chemical Society reviews* **40**, 1211-1223, doi:10.1039/c0cs00020e (2011).

10   Suwal, S. & Pflum, M. K. Phosphorylation-dependent kinase-substrate cross-linking. *Angewandte Chemie* **49**, 1627-1630, doi:10.1002/anie.200905244 (2010).

11   Couzens, A. L. *et al.* Protein interaction network of the mammalian Hippo pathway reveals mechanisms of kinase-phosphatase interactions. *Science signaling* **6**, rs15, doi:10.1126/scisignal.2004712 (2013).

12   Yuryev, A. & Wennogle, L. P. Novel Raf kinase protein-protein interactions found by an exhaustive yeast two-hybrid analysis. *Genomics* **81**, 112-125, doi:10.1016/S0888-7543(02)00008-3 (2003).

13   Chuh, K. N., Batt, A. R. & Pratt, M. R. Chemical methods for encoding and decoding of posttranslational modifications. *Cell Chem. Biol.* **23**, 86-107 (2016).

14   Khoury, G. A., Baliban, R. C. & Floudas, C. A. Proteome-wide post-translational modification statistics: frequency analysis and curation of the swiss-prot database. *Sci Rep* **1**, doi:10.1038/srep00090 (2011).

15   Jensen, O. N. Modification-specific proteomics: characterization of post-translational modifications by mass spectrometry. *Curr Opin Chem Biol* **8**, 33-41, doi:10.1016/j.cbpa.2003.12.009 (2004).

16   Ardito, F., Giuliani, M., Perrone, D., Troiano, G. & Lo Muzio, L. The crucial role of protein phosphorylation in cell signaling and its use as targeted therapy. *Int J Mol Med* **40**, 271-280, doi:10.3892/ijmm.2017.3036 (2017).

17   Ohtsubo, K. & Marth, J. D. Glycosylation in cellular mechanisms of health and disease. *Cell* **126**, 855-867, doi:10.1016/j.cell.2006.08.019 (2006).

18   Drazic, A., Myklebust, L. M., Ree, R. & Arnesen, T. The world of protein acetylation. *Biochim Biophys Acta* **1864**, 1372-1401, doi:10.1016/j.bbapap.2016.06.007 (2016).

19   Bradbury, A. F. & Smyth, D. G. Peptide amidation. *Trends in biochemical sciences* **16**, 112-115 (1991).

20   Zurlo, G., Guo, J. P., Takada, M., Wei, W. Y. & Zhang, Q. New Insights into Protein Hydroxylation and Its Important Role in Human Diseases. *Bba-Rev Cancer* **1866**, 208-220, doi:10.1016/j.bbcan.2016.09.004 (2016).

21   Murn, J. & Shi, Y. The winding path of protein methylation research: milestones and new frontiers. *Nat Rev Mol Cell Biol* **18**, 517-527, doi:10.1038/nrm.2017.35 (2017).

22   Nadolski, M. J. & Linder, M. E. Protein lipidation. *FEBS J* **274**, 5202-5210, doi:10.1111/j.1742-4658.2007.06056.x (2007).

23   Nesvizhskii, A. I. Proteogenomics: concepts, applications and computational strategies. *Nature methods* **11**, 1114-1125, doi:10.1038/nmeth.3144 (2014).

24   Omenn, G. S. *et al.* Metrics for the Human Proteome Project 2016: Progress on Identifying and Characterizing the Human Proteome, Including Post-Translational Modifications. *J Proteome Res* **15**, 3951-3960, doi:10.1021/acs.jproteome.6b00511 (2016).

25   Hornbeck, P. V. *et al.* PhosphoSitePlus, 2014: mutations, PTMs and recalibrations. *Nucleic acids research* **43**, D512-520, doi:10.1093/nar/gku1267 (2015).

26   Trost, B., Kusalik, A. & Napper, S. Computational Analysis of the Predicted Evolutionary Conservation of Human Phosphorylation Sites. *PloS one* **11**, doi:ARTN e0152809 10.1371/journal.pone.0152809 (2016).

27   Lemeer, S. & Heck, A. J. The phosphoproteomics data explosion. *Curr Opin Chem Biol* **13**, 414-420, doi:10.1016/j.cbpa.2009.06.022 (2009).

28   Manning, G., Whyte, D. B., Martinez, R., Hunter, T. & Sudarsanam, S. The protein kinase complement of the human genome. *Science* **298**, 1912-+, doi:DOI 10.1126/science.1075762 (2002).

29   Liu, Y. C. & Tozeren, A. Modular composition predicts kinase/substrate interactions. *Bmc Bioinformatics* **11**, doi:Artn 349 10.1186/1471-2105-11-349 (2010).

30   Hsu, P. P. *et al.* The mTOR-regulated phosphoproteome reveals a mechanism of mTORC1-mediated inhibition of growth factor signaling. *Science* **332**, 1317-1322, doi:10.1126/science.1199498 (2011).

31   Schunter, A. J., Yue, X. & Hummon, A. B. Phosphoproteomics of colon cancer metastasis: comparative mass spectrometric analysis of the isogenic primary and metastatic cell lines SW480 and SW620. *Analytical and bioanalytical chemistry* **409**, 1749-1763, doi:10.1007/s00216-016-0125-5 (2017).

32   Wei, W. *et al.* Single-Cell Phosphoproteomics Resolves Adaptive Signaling Dynamics and Informs Targeted Combination Therapy in Glioblastoma. *Cancer Cell* **29**, 563-573, doi:10.1016/j.ccell.2016.03.012 (2016).

33   Kauko, O. *et al.* Label-free quantitative phosphoproteomics with novel pairwise abundance normalization reveals synergistic RAS and CIP2A signaling. *Sci Rep* **5**, 13099, doi:10.1038/srep13099 (2015).

34   Bhullar, K. S. *et al.* Kinase-targeted cancer therapies: progress, challenges and future directions. *Mol Cancer* **17**, 48, doi:10.1186/s12943-018-0804-2 (2018).

35   Futreal, P. A. *et al.* A census of human cancer genes. *Nature reviews. Cancer* **4**, 177-183, doi:10.1038/nrc1299 (2004).

36   Santarius, T., Shipley, J., Brewer, D., Stratton, M. R. & Cooper, C. S. A census of amplified and overexpressed human cancer genes. *Nature reviews. Cancer* **10**, 59-64, doi:10.1038/nrc2771 (2010).

37   Druker, B. J. *et al.* Effects of a selective inhibitor of the Abl tyrosine kinase on the growth of Bcr-Abl positive cells. *Nat Med* **2**, 561-566 (1996).

38   Moen, M. D., McKeage, K., Plosker, G. L. & Siddiqui, M. A. A. Imatinib - A review of its use in chronic myeloid leukaemia. *Drugs* **67**, 299-320, doi:Doi 10.2165/00003495-200767020-00010 (2007).

39   Gharwan, H. & Groninger, H. Kinase inhibitors and monoclonal antibodies in oncology: clinical implications. *Nat Rev Clin Oncol* **13**, 209-227, doi:10.1038/nrclinonc.2015.213 (2016).

40   Genovese, M. C. *et al.* Baricitinib in Patients with Refractory Rheumatoid Arthritis. *N Engl J Med* **374**, 1243-1252, doi:10.1056/NEJMoa1507247 (2016).

41   Kopczynski, C. C. & Heah, T. Netarsudil ophthalmic solution 0.02% for the treatment of patients with open-angle glaucoma or ocular hypertension. *Drugs Today (Barc)* **54**, 467-478, doi:10.1358/dot.2018.54.8.2849627 (2018).

42   Bussel, J. *et al.* Fostamatinib for the treatment of adult persistent and chronic immune thrombocytopenia: Results of two phase 3, randomized, placebo-controlled trials. *Am J Hematol* **93**, 921-930, doi:10.1002/ajh.25125 (2018).

43   Fala, L. Ofev (Nintedanib): First Tyrosine Kinase Inhibitor Approved for the Treatment of Patients with Idiopathic Pulmonary Fibrosis. *Am Health Drug Benefits* **8**, 101-104 (2015).

44   Bergrath, E. *et al.* Tofacitinib versus Biologic Treatments in Moderate-to-Severe Rheumatoid Arthritis Patients Who Have Had an Inadequate Response to Nonbiologic DMARDs: Systematic Literature Review and Network Meta-Analysis. *Int J Rheumatol* **2017**, 8417249, doi:10.1155/2017/8417249 (2017).

45   Barouch-Bentov, R. & Sauer, K. Mechanisms of drug resistance in kinases. *Expert Opin Investig Drugs* **20**, 153-208, doi:10.1517/13543784.2011.546344 (2011).

46   Ferrarelli, L. K. Tackling kinase inhibitor resistance. *Science signaling* **9**, ec97 (2016).

47   Wilson, T. R. *et al.* Widespread potential for growth-factor-driven resistance to anticancer kinase inhibitors. *Nature* **487**, 505-509, doi:10.1038/nature11249 (2012).

48   Yamaguchi, T., Kakefuda, R., Tajima, N., Sowa, Y. & Sakai, T. Antitumor activities of JTP-74057 (GSK1120212), a novel MEK1/2 inhibitor, on colorectal cancer cell lines in vitro and in vivo. *Int J Oncol* **39**, 23-31, doi:10.3892/ijo.2011.1015 (2011).

49   Hatzivassiliou, G. *et al.* Mechanism of MEK inhibition determines efficacy in mutant KRAS- versus BRAF-driven cancers. *Nature* **501**, 232-236, doi:10.1038/nature12441 (2013).

50   Weisberg, E. *et al.* Characterization of AMN107, a selective inhibitor of native and mutant Bcr-Abl. *Cancer Cell* **7**, 129-141, doi:10.1016/j.ccr.2005.01.007 (2005).

51   Ma, X. D., Lv, X. Q. & Zhang, J. K. Exploiting polypharmacology for improving therapeutic outcome of kinase inhibitors (KIs): An update of recent medicinal chemistry efforts. *Eur J Med Chem* **143**, 449-463, doi:10.1016/j.ejmech.2017.11.049 (2018).

52   Li, Z. *et al.* The OncoPPi network of cancer-focused protein-protein interactions to inform biological insights and therapeutic strategies. *Nat Commun* **8**, 14356, doi:10.1038/ncomms14356 (2017).

53   Varjosalo, M. *et al.* The Protein Interaction Landscape of the Human CMGC Kinase Group. *Cell Reports* **3**, 1306-1320, doi:http://dx.doi.org/10.1016/j.celrep.2013.03.027 (2013).

54   Roux, K. J., Kim, D. I., Raida, M. & Burke, B. A promiscuous biotin ligase fusion protein identifies proximal and interacting proteins in mammalian cells. *J Cell Biol* **196**, 801-810, doi:10.1083/jcb.201112098 (2012).

55   Dingar, D. *et al.* BioID identifies novel c-MYC interacting partners in cultured cells and xenograft tumors. *J Proteomics* **118**, 95-111, doi:10.1016/j.jprot.2014.09.029 (2015).

56   Chen, A. L. *et al.* Novel components of the Toxoplasma inner membrane complex revealed by BioID. *MBio* **6**, e02357-02314, doi:10.1128/mBio.02357-14 (2015).

57   Kim, D. I. *et al.* Probing nuclear pore complex architecture with proximity-dependent biotinylation. *Proceedings of the National Academy of Sciences of the United States of America* **111**, E2453-2461, doi:10.1073/pnas.1406459111 (2014).

58   Mick, D. U. *et al.* Proteomics of Primary Cilia by Proximity Labeling. *Dev Cell* **35**, 497-512, doi:10.1016/j.devcel.2015.10.015 (2015).

59   Rhee, H. W. *et al.* Proteomic mapping of mitochondria in living cells via spatially restricted enzymatic tagging. *Science* **339**, 1328-1331, doi:10.1126/science.1230593 (2013).

60   Branon, T. C. *et al.* Efficient proximity labeling in living cells and organisms with TurboID. *Nature biotechnology* **36**, 880-887, doi:10.1038/nbt.4201 (2018).

61   Steed, E. *et al.* MarvelD3 couples tight junctions to the MEKK1-JNK pathway to regulate cell behavior and survival. *J Cell Biol* **204**, 821-838, doi:10.1083/jcb.201304115 (2014).

62   Statsuk, A. V. & Shokat, K. M. Covalent cross-linking of kinases with their corresponding peptide substrates. *Methods in molecular biology* **795**, 179-190, doi:10.1007/978-1-61779-337-0_12 (2012).

63   Lopez, M. S., Kliegman, J. I. & Shokat, K. M. The logic and design of analog-sensitive kinases and their small molecule inhibitors. *Methods Enzymol* **548**, 189-213, doi:10.1016/B978-0-12-397918-6.00008-2 (2014).

64   Blethrow, J. D., Glavy, J. S., Morgan, D. O. & Shokat, K. M. Covalent capture of kinase-specific phosphopeptides reveals Cdk1-cyclin B substrates. *Proceedings of the National Academy of Sciences of the United States of America* **105**, 1442-1447, doi:10.1073/pnas.0708966105 (2008).

65   Allen, J. J., Lazerwith, S. E. & Shokat, K. M. Bio-orthogonal affinity purification of direct kinase substrates. *Journal of the American Chemical Society* **127**, 5288-5289, doi:10.1021/ja050727t (2005).

66   Allen, J. J. *et al.* A semisynthetic epitope for kinase substrates. *Nature methods* **4**, 511-516, doi:10.1038/nmeth1048 (2007).

67   Bishop, A. C. *et al.* A chemical switch for inhibitor-sensitive alleles of any protein kinase. *Nature* **407**, 395-401, doi:Doi 10.1038/35030148 (2000).

68   Dedigama-Arachchige, P. M. & Pflum, M. K. K-CLASP: A Tool to Identify Phosphosite Specific Kinases and Interacting Proteins. *ACS chemical biology* **11**, 3251-3255, doi:10.1021/acschembio.6b00289 (2016).

69   Garre, S., Gamage, A. K., Faner, T. R., Dedigama-Arachchige, P. & Pflum, M. K. H. Identification of Kinases and Interactors of p53 Using Kinase-Catalyzed Cross-Linking and Immunoprecipitation. *Journal of the American Chemical Society* **140**, 16299-16310, doi:10.1021/jacs.8b10160 (2018).

70   Garre, S., Senevirathne, C. & Pflum, M. K. A comparative study of ATP analogs for phosphorylation-dependent kinase-substrate crosslinking. *Bioorg Med Chem* **22**, 1620-1625, doi:10.1016/j.bmc.2014.01.034 (2014).

71   Parang, K., Kohn, J. A., Saldanha, S. A. & Cole, P. A. Development of photo-crosslinking reagents for protein kinase-substrate interactions. *FEBS Lett* **520**, 156-160 (2002).

72   Suwal, S., Senevirathne, C., Garre, S. & Pflum, M. K. Structural analysis of ATP analogues compatible with kinase-catalyzed labeling. *Bioconjug Chem* **23**, 2386-2391, doi:10.1021/bc300404s (2012).

73   Kotzybahibert, F., Kapfer, I. & Goeldner, M. Recent Trends in Photoaffinity-Labeling. *Angewandte Chemie-International Edition* **34**, 1296-1312, doi:DOI 10.1002/anie.199512961 (1995).

74   Park, J., Koh, M., Koo, J. Y., Lee, S. & Park, S. B. Investigation of Specific Binding Proteins to Photoaffinity Linkers for Efficient Deconvolution of Target Protein. *ACS chemical biology* **11**, 44-52, doi:10.1021/acschembio.5b00671 (2016).

75   Patricelli, M. P. *et al.* Functional interrogation of the kinome using nucleotide acyl phosphates. *Biochemistry* **46**, 350-358, doi:DOI 10.1021/bi062142x (2007).

76   Villamor, J. G. *et al.* Profiling Protein Kinases and Other ATP Binding Proteins in Arabidopsis Using Acyl-ATP Probes. *Molecular & Cellular Proteomics* **12**, 2481-2496, doi:10.1074/mcp.M112.026278 (2013).

77   Rosenblum, J. S., Nomanbhoy, T. K. & Kozarich, J. W. Functional interrogation of kinases and other nucleotide-binding proteins. *FEBS Lett* **587**, 1870-1877, doi:10.1016/j.febslet.2013.05.008 (2013).

78   Zhao, Q. *et al.* Broad-Spectrum Kinase Profiling in Live Cells with Lysine-Targeted Sulfonyl Fluoride Probes. *Journal of the American Chemical Society* **139**, 680-685, doi:10.1021/jacs.6b08536 (2017).

79   Hanks, S. K. & Hunter, T. Protein kinases 6. The eukaryotic protein kinase superfamily: kinase (catalytic) domain structure and classification. *The FASEB Journal* **9**, 576-596 (1995).

80   Maly, D. J., Allen, J. A. & Shokat, K. M. A mechanism-based cross-linker for the identification of kinase-substrate pairs. *Journal of the American Chemical Society* **126**, 9160-9161, doi:10.1021/ja048659i (2004).

81   Riel-Mehan, M. M. & Shokat, K. M. A crosslinker based on a tethered electrophile for mapping kinase-substrate networks. *Chemistry & biology* **21**, 585-590, doi:10.1016/j.chembiol.2014.02.022 (2014).

Chapter 2

4E-BP1 Biology: An Overview

2.1 Abstract

Cap-dependent translation (CDT) is a critical cellular process that enables the expression of mRNA transcripts encoding for growth and survival proteins. Consequently, under normal growth conditions, CDT is under tight regulation, primarily through alteration of the phosphorylation status of the eukaryotic initiation factor 4E binding protein (4E-BP1). 4E-BP1 serves as a gate-keeper of CDT by competing with translation initiation factors for binding to the m^7G-cap-binding protein eIF4E. Under mitogenic stimulation and high nutrient availability, 4E-BP1 becomes hyperphosphorylated, dissociates from eIF4E, and translation is initiated. In many cancers, this process becomes dysregulated conferring constitutive CDT, and thus, cell proliferation, due to increased phosphorylation of 4E-BP1. This has provided rationale for the development of mechanistic Target Of Rapamycin (mTOR) inhibitors as cancer therapeutics since mTOR complex 1 (mTORC1) is responsible for phosphorylation of four of the seven *bona fide* phosphorylation sites on 4E-BP1. Yet, there is speculation about the exclusivity of these sites due to reports of 4E-BP1 hyperphosphorylation in cells treated with allosteric and active site mTOR inhibitors. Additionally, at least three other residues are also phosphorylated *in vivo* although there is no consensus as to which kinases are responsible for these post-translational modifications. Identification of these kinases will uncover new targets for therapeutic intervention in patients with hyperphosphorylated 4E-BP1 and be invaluable in further elucidating the signaling intermediates involved in regulating CDT in cancer.

2.2 Cap-Dependent Translation and 4E-BP1

Synthesis of new proteins in eukaryotes is a highly regulated, key step in gene expression, necessary for both cellular maintenance and proliferation. Eukaryotic protein translation can be divided into two distinct processes: 1) Cap-Dependent Translation (CDT) (Figure 2.1) and 2) Cap-Independent Translation. CDT refers to eIF4E-driven translation of mRNA transcripts via assembly of initiation factors around the 7-methylguanosine (m^7G) cap at the 5' end of the transcript. Transcripts translated strictly via CDT are those encoding proteins important for growth, proliferation and survival, such as the cyclins, VEGF, c-myc, and HIF-1α among other proteins implicated in oncogenesis.[1-5] (Table 2.1) Conversely, cap-independent translation is largely responsible for translating housekeeping genes via an internal ribosomal entry site (IRES) mediated initiation mechanism.[6]

Transcript	Protein Function
Cyclin D1/2/3	Cell cycle progression (G1$\rightarrow$S)[7]
c-Myc	Proliferation, Promotes Malignant Transformation[8]
Ornithine Decarboxylase	Synthesis of Polyamines[9]
VEGF	Promotes Angiogenesis[10]
Bcl-2	Inhibits Apoptosis[11]
FGF-2	Proliferation and Angiogenesis[12]
Pim-1	Proliferation, Stabilization of MYC[13]

Table 2.1 | mRNA Transcripts Regulated by Cap-Dependent Translation

CDT is an anabolic cellular process that is divided into four distinct steps: initiation, elongation, termination and recycling, with initiation acting as the rate limiting step.[14,15] As protein translation is the most energy-expensive cellular process,[14-16] it is highly regulated at several levels by many different signaling pathways following activation by extracellular signals such as high nutrient availability and mitogens. These stimuli activate the PI3K/AKT/MAPK signaling cascades, which converge on mTOR, (Figure 2.1) a highly-conserved protein kinase present in two functionally distinct complexes, mTOR complex 1 (mTORC1) and 2 (mTORC2).[17] mTORC1, a master regulator of cellular anabolism, is essential for integrating input from several discrete pathways to promote a wide range of processes, from protein synthesis and autophagy, to mitochondrial biogenesis and lipid metabolism.[18-20] mTORC1 positively regulates protein translation via phosphorylation of two main substrates: the ribosomal protein kinase p70S6K, which is activated by

phosphorylation, and the translational gatekeeper protein 4E-BP1, which becomes inactivated by phosphorylation.[21-24] (Figure 2.1)

Hyperphosphorylated 4E-BP1 has a weakened affinity for eIF4E, the 7-methylguanosine (m^7G) cap binding protein, allowing it to be outcompeted by the scaffolding protein eIF4G for a common binding site on eIF4E.[25-32] Upon eIF4G binding, assembly of the eIF4F translation initiation complex is promoted, thus stimulating initiation of CDT.[33-37] Therefore, this interplay between eIF4E and its binding partners 4E-BP1 and eIF4G is the key event in the regulation of CDT, one that has been the subject of many drug discovery efforts.
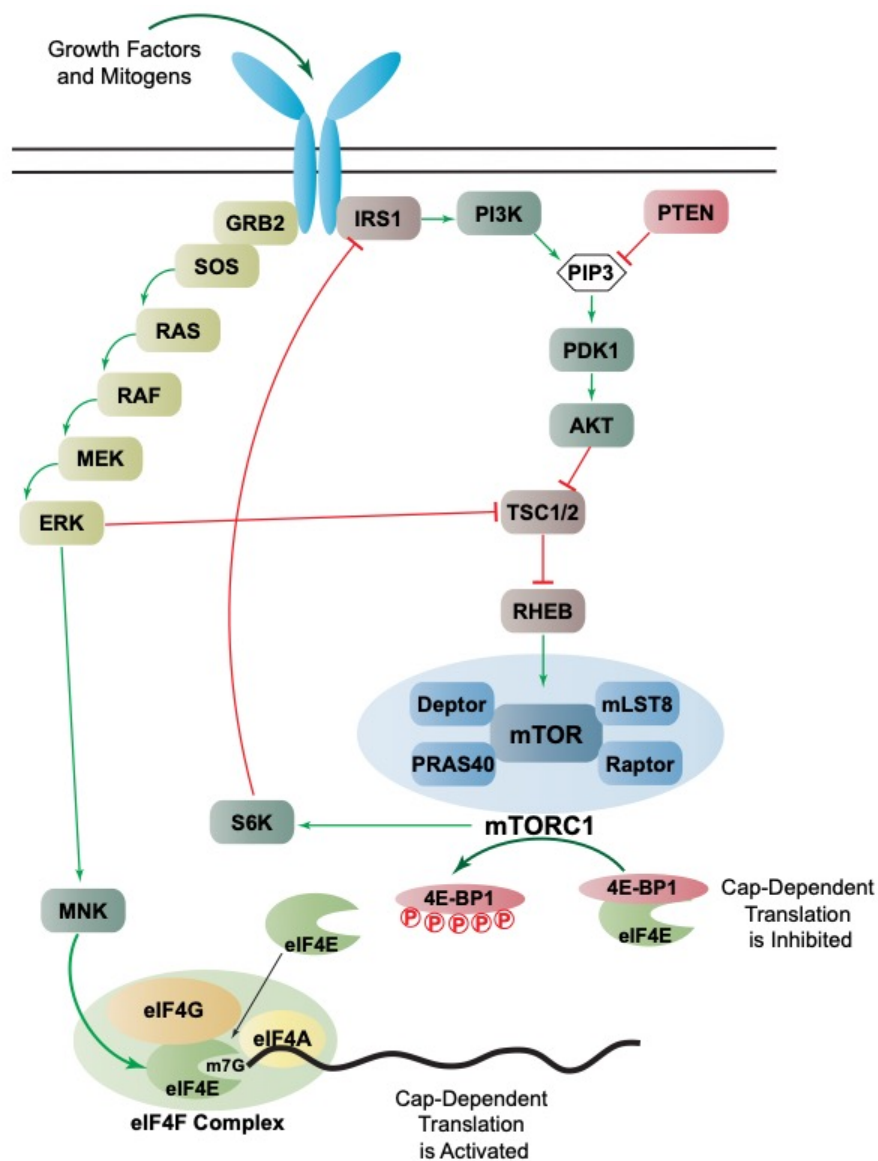
Figure 2.1 | Pathways Leading to mTORC1 and CDT

2.3 CDT and 4E-BP1 Phosphorylation in Cancer

mTOR hyperactivation has been identified in most human tumors (>70% of patients),[38,39] resulting in uncontrolled cell growth and proliferation. As mTOR promotes CDT, and this process facilitates the expression of proteins implicated in oncogenesis, the potential ramifications of dysregulated CDT in cancer are clear.[22] It is therefore unsurprising that many cancers also show hallmarks of deregulated CDT.[34,40] Through in-depth analysis of mTOR-driven cancer dependencies, CDT (via 4E-BP1 hyperphosphorylation) has emerged as a principle mechanism by which oncogenic mTORC1 signaling promotes malignant transformation.[5,41-44] As such, phosphorylated 4E-BP1 has been implicated as a biomarker for interpreting the severity and aggressiveness of colorectal, prostate, gastric, ovarian, breast, lung, and pancreatic cancers. Relatedly, analysis of patient samples has uncovered a positive correlation between hyperphosphorylated 4E-BP1 and poor prognosis.[45-54] In the laboratory, ectopic delivery of hypophosphorylated 4E-BP1 has been shown to reduce *in vivo* tumor progression,[55] and non-phosphorylatable 4E-BP1 mutants inhibit cell migration and colony formation in cancer cell lines.[56,57] Thus, these studies point to the hyperphosphorylation of 4E-BP1 as a key event in cancer progression, and emphasize the importance of fully deconvoluting the mechanisms of 4E-BP1 inactivation in cancer.[58]

2.4 Current Efforts for Targeting Cap-Dependent Translation

Given the role that aberrant CDT plays in many cancers, and the identification of this process as a "druggable addiction",[5,59] significant effort has been put forth to develop mTORC1 inhibitors as therapeutics. First generation mTORC1 inhibitors were derivatives of rapamycin, the rapalogs (everolimus and temsirolimus), (Figure 2.2) that inhibit mTORC1 activity by dissociating mTOR from Raptor, preventing the recruitment of substrates to mTOR. Currently, two rapalogs are approved for the treatment of cancer; however, these drugs are only modestly effective for treating most malignancies outside of renal cell carcinoma.[60-63] Many explanations for the limited efficacy of these drugs have been postulated, including rapalog-induced AKT activation and increased MAPK signaling due to the release of S6K1-mediated negative feedback signaling (Figure 2.1).[38,64-79] Of particular significance, nearly all reports of rapalog resistance refer to the

inability of these drugs to prevent the phosphorylation of 4E-BP1, although inhibition of S6K1 phosphorylation is maintained.[80-82]
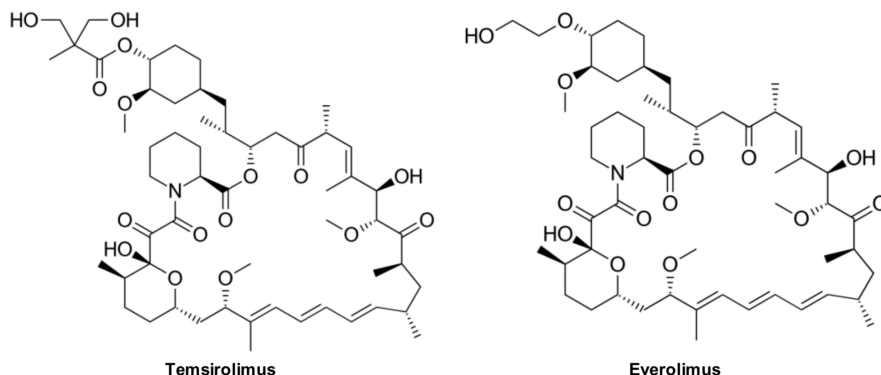
Figure 2.2 | Clinically Approved Allosteric mTORC1 Inhibitors

These observed mechanisms of resistance have fueled the development of ATP-competitive mTOR inhibitors (mTORKis) (Figure 2.3) capable of inhibiting both mTOR complexes, thereby completely inhibiting 4E-BP1 phosphorylation, and abrogating the negative feedback loops that drive AKT activation downstream of mTORC2.[65] While this is generally the case, a high incidence of resistance to these new mTOR inhibitors is still observed.[81,83] The mechanisms driving this phenotype include incomplete inhibition of 4E-BP1,[81,84] and the mTORKi induced reduction of 4E-BP1 levels in a Snail-dependent downregulation of 4E-BP1 transcription.[85] Despite these observed patterns of resistance, mTORKis have achieved great success in preclinical models, as well as some clinical efficacy, for treating certain malignancies, including NSCLC, hepatocellular carcinoma and ER+ breast cancers.[86-90] However, an in-depth analysis of the factors leading to this efficacy over other cancers has not been performed. Because of this lack of information, as well as the broad toxicity profiles observed,[91,92] most clinical trials using mTORKis have failed to achieve desired endpoints.[93,94]

AZD2014/Vistusertib   CC-223   MLN-128/Sapanisertib
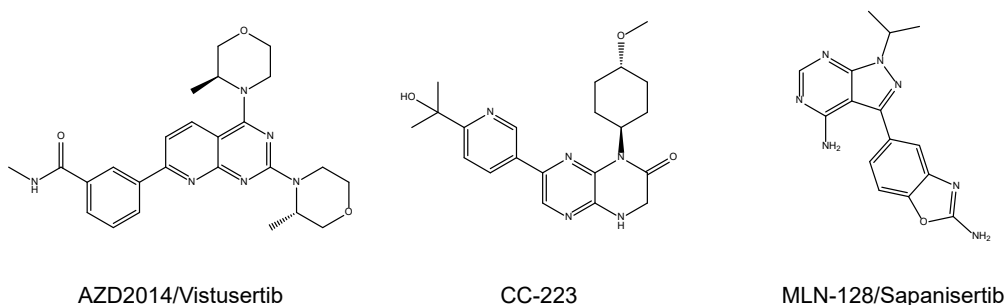
Figure 2.3 | Select mTORKis Used in Clinical Trials

Interestingly, mTOR inhibitor resistance is particularly evident in patients and cell lines with activating mutations of the GTPase KRAS.[64,81,95-97] Indeed, several studies have identified 4E-BP1 inactivation as a key step in initiating and maintaining a metastatic phenotype in KRAS mutant cancers, due to an altered translational program that promotes epithelial-to-mesenchymal transition.[57,98,99] RAS and PI3K pathways cooperate to promote eIF4E-driven CDT in situations with intact mTORC1 signaling, as well as in situations where mTORC1 activity has been compromised by allosteric inhibitors. This signaling dynamic has provided rationale for the use dual PI3K-mTOR inhibitors (Figure 2.4) as a therapeutic strategy in cancer.[100-102] These agents have shown great potential in cell lines and other preclinical models due to their ability to inhibit mTORC1/2 signaling, reduce AKT/MAPK activity, and induce apoptosis.[100,103,104] These inhibitors have a similar story to mTORKis; strong activity in preclinical models followed by limited clinical efficacy.[100] A phase I study comparing two such inhibitors, Gedatolisib and PF-04691502, demonstrated only a 5% response rate in advanced cancers.[105] However, due to poor tolerability, the desired maximal dose was not achieved. This limitation highlights the difficulties with targeting two critical signaling nodes, as the propensity for inducing significant toxicities dramatically increases with this class of inhibtors.[106,107]

NVP-BEZ235/Dactolisib   GDC0980   PF-05212384/Gedatolisb
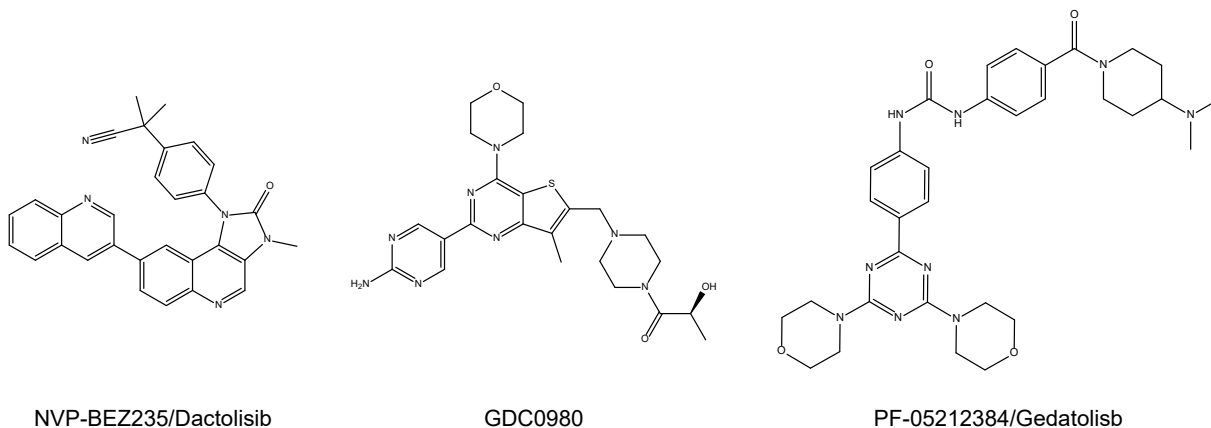
Figure 2.4 | Select Dual mTOR-PI3K Inhibitors Used in Clinical Trials

Another therapeutic strategy for inhibiting CDT has come in the form of directly modulating the eIF4E-4E-BP1 and eIF4E-eIF4G protein-protein interactions.[108] (Figure 2.5) 4EGI-1, which was identified by a fluorescence-polarization-based high-throughput screening assay,[109] showed antiproliferative activity in a range of cancer cell lines. This

compound disrupts CDT by allegedly stabilizing the interaction between eIF4E-4E-BP1, while inhibiting the eIF4E-eIF4G interaction, thus preventing eIF4F complex assembly.[110] However, with a reported K_D of 25μM,[109] this molecule is only useful as a tool compound for *in vitro* assays. 4E1RCat and 4E2RCat, two other small molecule inhibitors of eIF4E, were identified by another highthroughput screening campaign using a TR-FRET platform.[108,111] 4E1RCat showed *in vivo* activity against a Eμ-Myc model of lymphoma, while 4E2RCat effectively inhibited coronavirus replication in cells, albeit at concentrations in excess of 50μM. Other groups have also successfully to modulated CDT using peptide mimetics of 4E-BP1 and eIF4G.[112-115] While these peptides can effectively inhibit CDT in cell lines, the viability of this approach as a therapeutic is in question due to their poor drug-like properties of most peptides.[116] While it is understood that all of these eIF4E-inhibiting molecules are best utilized as tool compounds, their success both *in vitro* and in cells provides evidence that it might be possible to inhibit eIF4E activity without directly modulating 4E-BP1 phosphorylation. However, until these molecules improve in selectivity, specificity and cell penetrability, this approach will not be a viable means by which to target CDT in a clinical setting.

4EGI-1   **4E1RCat**   **4E2RCat**
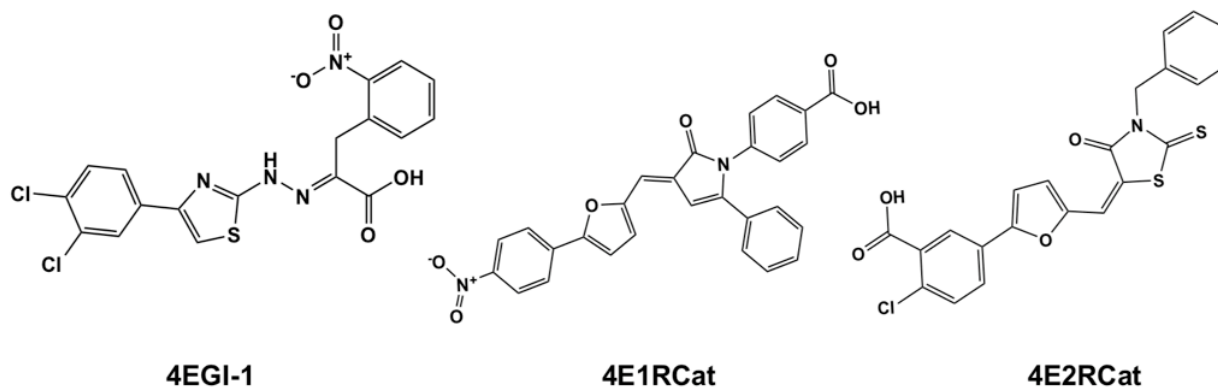
Figure 2.5 | Small Molecule Inhibitors of eIF4E

2.5 Intricacies of 4E-BP1 Phosphorylation

4E-BP1 is phosphorylated in a hierarchical fashion, with phosphorylation of Thr37/46 "priming" the subsequent phosphorylation of Ser65 and Thr70.[117-119] Therefore, it is often difficult to assess the impact of each phosphorylation site individually. It is clear that 4E-BP1 inactivation is mediated by hyperphosphorylation at these four canonical

mTORC1-dependent sites, each of which immediately flanks the eIF4E binding region of the protein; though Ser65 and T70 are thought to make the largest contributions towards weakening the affinity between the two proteins.[118-123] (Figure 2.6) However, up to 21 phosphorylation sites have been identified by phosphoproteomic methods, many of which have been confirmed through experiments described in Chapter 3 and 4.[124] Though each of these sites have been identified with high confidence, very few have been validated mechanistically or experimentally, leaving potentially interesting mechanisms of CDT regulation undiscovered.
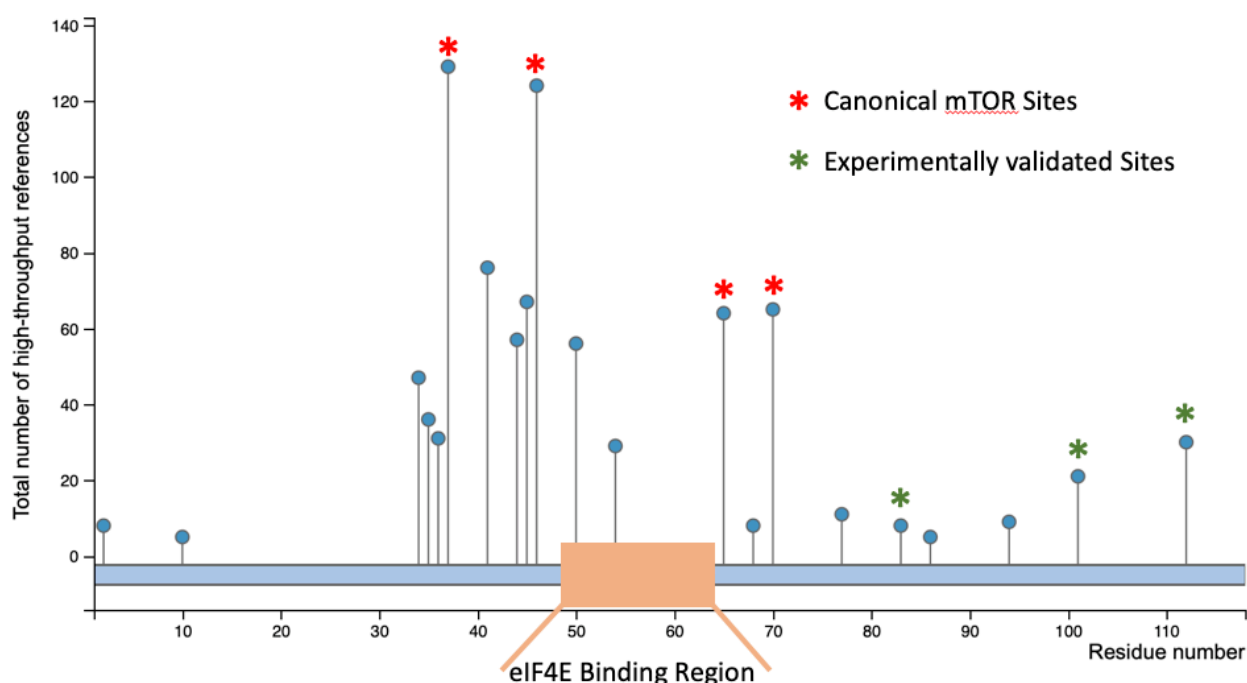
Figure 2.6 | 4E-BP1 Phosphorylation Sites Identified by Phosphoproteomics. All high-throughput phosphorylation sites identified in at least 5 experiments. The base of this figure was generated using phosphosite.org.[124]

2.6 mTOR-Independent Phosphorylation of 4E-BP1

Inhibition of mTORC1 activity with allosteric rapalog inhibitors reactivates 4E-BP1 via inducing hypophosphorylation. However, in cell lines and *in vivo* models, this phenotype is transient; within a few hours 4E-BP1 phosphorylation is restored, while S6K phosphorylation is fully abrogated throughout the duration of the treatment.[125] The mechanism of phosphorylation for proteins is similar, with each substrate competing for binding to the mTORC1 subunit Raptor, which facilitates recruitment of substrates to

mTOR kinase.[126-128] Therefore, the differential phosphorylation pattern between two of the best-validated mTORC1 substrates has led to speculation about the presence of additional kinases filling in for mTOR under conditions of mTORC1 inhibition.[96,129] The poor clinical efficacy of second-generation mTORKis has also increased support for this hypothesis.[96]

Indeed, many kinases have been reported to phosphorylate 4E-BP1 *in vitro* and in cells including: ATM,[130] casein kinase,[131] ERK2,[132] CDK1,[133,134] GSK3β,[135] p38 MAPK,[136] PIM2[137] and PLK1.[138] Though each of these have been reported, most have not been sufficiently validated outside of an *in vitro* kinase assay setting. As all four of the canonical phosphorylation sites are directly adjacent to the eIF4E binding site,[139] 4E-BP1 phosphorylation is only relevant in the context of eIF4E binding; any kinase recognition motif surrounding these sites is blocked by eIF4E.[140,141] In previous reports, many kinases exhibiting activity towards 4E-BP1 *in vitro* were not examined following pre-incubation with eIF4E.[135,136] Several that have been tested lost activity towards 4E-BP1 as a substrate,[142] shedding light on the importance of probing for kinase-substrate interactions *in situ*. However, the CDK1-4E-BP1 interaction was thoroughly validated across many cell types.[133,134] Yet CDK1 is only capable of phosphorylating 4E-BP1 during the early stages of mitosis, a stage of the cell cycle which has long been known to exhibit mTOR-independent phosphorylation of 4E-BP1.

The identification of these kinases has, in some cases, contributed to our knowledge and understanding of mTORC1-independent regulation of 4E-BP1 phosphorylation. However, these relationships have not been established *in vivo*, and have not uncovered novel treatments for treating patients with cancer that is refractory to mTORC1 allosteric inhibitors. By elucidating definitive compensatory kinases capable of regulating CDT in the absence of mTORC1 signaling, combination therapies can be developed for creating a larger clinical impact.

2.7 Conclusions

mTOR is one of the best-known oncoproteins in human cancer. Hyperactivation of this pathway induces controlled proliferation partly through increasing cap-dependent protein synthesis and lipid metabolism, while decreasing autophagy and apoptosis.

mTOR has long been considered a viable drug target for many diseases, however current therapies have fallen short of expectations due to poor tolerability, as well as drug resistance as a result of mTORC1 independent phosphorylation of 4E-BP1. Positive identification of a kinase that phosphorylates 4E-BP1 under conditions of mTORC1 inhibition would be instrumental in understanding the observed resistance to each category of mTOR inhibitors, and would drive the design of rational combination therapies in cancer and fibrotic diseases.

2.8 References

1   Willis, A. E. Translational control of growth factor and proto-oncogene expression. *Int. J. Biochem. Cell. Biol.* **31**, 73-86 (1999).

2   Mamane, Y. *et al.* eIF4E-from translation to transformation. *Oncogene* **23**, 3172-3179 (2004).

3   Hsieh, A. C. & Ruggero, D. Targeting eukaryotic translation initiation factor 4E (eIF4E) in cancer. *Clin. Cancer Res.* **16**, 4914-4920 (2010).

4   Pelletier, J., Graff, J., Ruggero, D. & Sonenberg, N. Targeting the eIF4F translation initiation complex: a critical nexus for cancer development. *Cancer Res.* **75**, 250-263 (2015).

5   Hsieh, A. C. *et al.* Genetic dissection of the oncogenic mTOR pathway reveals druggable addiction to translational control via 4EBP-eIF4E. *Cancer Cell* **17**, 249-261, doi:10.1016/j.ccr.2010.01.021 (2010).

6   Komar, A. A. & Hatzoglou, M. Internal ribosome entry sites in cellular mRNAs: mystery of their existence. *The Journal of biological chemistry* **280**, 23425-23428, doi:10.1074/jbc.R400041200 (2005).

7   Rosenwald, I. B., Lazaris-Karatzas, A., Sonenberg, N. & Schmidt, E. V. Elevated levels of cyclin D1 protein in response to increased expression of eukaryotic initiation factor 4E. *Molecular and cellular biology* **13**, 7358-7363 (1993).

8   Lin, C. J., Cencic, R., Mills, J. R., Robert, F. & Pelletier, J. c-Myc and eIF4F are components of a feedforward loop that links transcription and translation. *Cancer research* **68**, 5326-5334, doi:10.1158/0008-5472.Can-07-5876 (2008).

9   Manzella, J. M., Rychlik, W., Rhoads, R. E., Hershey, J. W. B. & Blackshear, P. J. Insulin Induction of Ornithine Decarboxylase - Importance of Messenger-Rna Secondary Structure and Phosphorylation of Eukaryotic Initiation Factor-Eif-4b and Factor-Eif-4e. *Journal of Biological Chemistry* **266**, 2383-2389 (1991).

10   Kevil, C. G. *et al.* Translational regulation of vascular permeability factor by eukaryotic initiation factor 4E: implications for tumor angiogenesis. *Int J Cancer* **65**, 785-790, doi:10.1002/(SICI)1097-0215(19960315)65:6<785::AID-IJC14>3.0.CO;2-3 (1996).

11   Clemens, M. J. Translational regulation in cell stress and apoptosis. Roles of the eIF4E binding proteins. *J Cell Mol Med* **5**, 221-239, doi:DOI 10.1111/j.1582-4934.2001.tb00157.x (2001).

12   Kevil, C., Carter, P., Hu, B. & DeBenedetti, A. Translational enhancement of FGF-2 by eIF-4 factors, and alternate utilization of CUG and AUG codons for translation initiation. *Oncogene* **11**, 2339-2348 (1995).

13   De Benedetti, A. & Harris, A. L. eIF4E expression in tumors: its possible role in progression of malignancies. *Int J Biochem Cell Biol* **31**, 59-72 (1999).

14   Roux, P. P. & Topisirovic, I. Regulation of mRNA translation by signaling pathways. *Cold Spring Harb Perspect Biol* **4**, doi:10.1101/cshperspect.a012252 (2012).

15   Roux, P. P. & Topisirovic, I. Signaling Pathways Involved in the Regulation of mRNA Translation. *Molecular and cellular biology* **38**, doi:10.1128/MCB.00070-18 (2018).

16   Buttgereit, F. & Brand, M. D. A hierarchy of ATP-consuming processes in mammalian cells. *The Biochemical journal* **312 (Pt 1)**, 163-167 (1995).

17   Saxton, R. A. & Sabatini, D. M. mTOR signaling in growth, metabolism, and disease. *Cell* **168**, 960-976 (2017).

18   Saxton, R. A. & Sabatini, D. M. mTOR Signaling in Growth, Metabolism, and Disease. *Cell* **168**, 960-976 (2017).

19   Dennis, P. B. *et al.* Mammalian TOR: A homeostatic ATP sensor. *Science* **294**, 1102-1105, doi:DOI 10.1126/science.1063518 (2001).

20   Rohde, J., Heitman, J. & Cardenas, M. E. The TOR kinases link nutrient sensing to cell growth. *The Journal of biological chemistry* **276**, 9583-9586, doi:10.1074/jbc.R000034200 (2001).

21   Holz, M. K., Ballif, B. A., Gygi, S. P. & Blenis, J. mTOR and S6K1 mediate assembly of the translation preinitiation complex through dynamic protein interchange and ordered phosphorylation events. *Cell* **123**, 569-580, doi:10.1016/j.cell.2005.10.024 (2005).

22   Mamane, Y., Petroulakis, E., LeBacquer, O. & Sonenberg, N. mTOR, translation initiation and cancer. *Oncogene* **25**, 6416-6422, doi:10.1038/sj.onc.1209888 (2006).

23   Guertin, D. A. & Sabatini, D. M. Defining the Role of mTOR in Cancer. *Cancer Cell* **12**, 9-22, doi:http://dx.doi.org/10.1016/j.ccr.2007.05.008 (2007).

24   Laplante, M. & Sabatini, D. M. mTOR signaling in growth control and disease. *Cell* **149**, 274-293, doi:10.1016/j.cell.2012.03.017 (2012).

25   Richter, J. D. & Sonenberg. Regulation of cap-dependent translation by eIF4E inhibitory proteins. *Nature* (2005).

26   Pause, A. *et al.* Insulin-dependent stimulation of protein synthesis by phosphorylation of a regulator of 5'-cap function. *Nature* **371**, 762-767 (1994).

27   Lin, T.-A. *et al.* PHAS-I as a link between mitogen-activated protein kinase and translation initiation. *Science* **266**, 653-656 (1994).

28   Haghighat, A., Mader, S., Pause, A. & Sonenberg, N. Repression of cap-dependent translation by 4E-binding protein 1: competition with p220 for binding to eukaryotic initiation factor-4E. *EMBO J.* **14**, 5701-5709 (1995).

29   Mader, S., Lee, H., Pause, A. & Sonenberg, N. The translation initiation factor eIF-4E binds to a common motif shared by the translation factor eIF-4 gamma and the translational repressors 4E-binding proteins. *Mol. Cell. Biol.* **15**, 4990-4997 (1995).

30   Marcotrigiano, J., Gingras, A. C., Sonenberg, N. & Burley, S. K. Cap-dependent translation initiation in eukaryotes is regulated by a molecular mimic of eIF4G. *Mol. Cell* **3**, 707-716 (1999).

31   Ptushkina, M., von der Haar, T., Karim, M. M., Hughes, J. M. X. & McCarthy, J. E. G. Repressor binding to a dorsal regulatory site traps human eIF4E in a high cap-affinity state. *EMBO J.* **18**, 4068-4075 (1999).

32   Richter, J. D. & Sonenberg, N. Regulation of cap-dependent translation by eIF4E inhibitory proteins. *Nature* **433**, 477-480 (2005).

33   Yanagiya, A. *et al.* Translational homeostasis via the mRNA cap-binding protein, eIF4E. *Molecular cell* **46**, 847-858, doi:10.1016/j.molcel.2012.04.004 (2012).

34   Bhat, M. *et al.* Targeting the translation machinery in cancer. *Nat Rev Drug Discov* **14**, 261-278, doi:10.1038/nrd4505 (2015).

35   Pain, V. M. Initiation of protein synthesis in eukaryotic cells. (1996).

36   Modrak-Wojcik, A. *et al.* Eukaryotic translation initiation is controlled by cooperativity effects within ternary complexes of 4E-BP1, eIF4E, and the mRNA 5' cap. *FEBS Lett* **587**, 3928-3934, doi:10.1016/j.febslet.2013.10.043 (2013).

37   Boussemart, L. *et al.* eIF4F is a nexus of resistance to anti-BRAF and anti-MEK cancer therapies. *Nature* **513**, 105-109, doi:10.1038/nature13572 (2014).

38   Zoncu, R., Efeyan, A. & Sabatini, D. M. mTOR: from growth signal integration to cancer, diabetes and aging. *Nat. Rev. Mol. Cell Biol.* **12**, 21-35 (2011).

39   Menon, S. & Manning, B. D. Common corruption of the mTOR signaling network in human tumors. *Oncogene* **27**, S43-S51 (2008).

40   Pelletier, J., Graff, J., Ruggero, D. & Sonenberg, N. Targeting the eIF4F translation initiation complex: a critical nexus for cancer development. *Cancer research* **75**, 250-263, doi:10.1158/0008-5472.CAN-14-2789 (2015).

41   Signer, R. A., Magee, J. A., Salic, A. & Morrison, S. J. Haematopoietic stem cells require a highly regulated protein synthesis rate. *Nature* **509**, 49-54, doi:10.1038/nature13035 (2014).

42   Thoreen, C. C. *et al.* A unifying model for mTORC1-mediated regulation of mRNA translation. *Nature* **485**, 109-113 (2012).

43   Silvera, D., Formenti, S. C. & Schneider, R. J. Translational control in cancer. *Nat. Rev. Cancer* **10**, 254-266 (2010).

44   Blagden, S. P. & Willis, A. E. The biological and therapeutic relevance of mRNA translation in cancer. *Nat. Rev. Clin. Oncol.* **8**, 280-291 (2011).

45   Seki, N. *et al.* Prognostic significance of expression of eukaryotic initiation factor 4E and 4E binding protein 1 in patients with pathological stage I invasive lung adenocarcinoma. *Lung Cancer* **70**, 329-334, doi:10.1016/j.lungcan.2010.03.006 (2010).

46   Roh, M. S. *et al.* Phosphorylated 4E-binding protein 1 expression is associated with poor prognosis in small-cell lung cancer. *Virchows Arch*, doi:10.1007/s00428-015-1860-2 (2015).

47   Castellvi, J. *et al.* Phosphorylated 4E binding protein 1: A hallmark of cell signaling that correlates with survival in ovarian cancer. *Cancer* **107**, 1801-1811, doi:10.1002/cncr.22195 (2006).

48   Martineau, Y. *et al.* Pancreatic tumours escape from translational control through 4E-BP1 loss. *Oncogene* **33**, 1367-1374, doi:10.1038/onc.2013.100 (2014).

49   Salehi, Z. & Mashayekhi, F. Expression of the eukaryotic translation initiation factor 4E (eIF4E) and 4E-BP1 in esophageal cancer. *Clin Biochem* **39**, 404-409, doi:10.1016/j.clinbiochem.2005.11.007 (2006).

50   Coleman, L. J. *et al.* Combined analysis of eIF4E and 4E-binding protein expression predicts breast cancer survival and estimates eIF4E activity. *Br J Cancer* **100**, 1393-1399, doi:10.1038/sj.bjc.6605044 (2009).

51   Zhou, X. *et al.* Activation of the Akt/mammalian target of rapamycin/4E-BP1 pathway by ErbB2 overexpression predicts tumor progression in breast cancers. *Clinical cancer research : an official journal of the American Association for Cancer Research* **10**, 6779-6788, doi:10.1158/1078-0432.CCR-04-0112 (2004).

52   Armengol, G. *et al.* 4E-binding protein 1: a key molecular "funnel factor" in human cancer with clinical implications. *Cancer research* **67**, 7551-7555, doi:10.1158/0008-5472.CAN-07-0881 (2007).

53   Rojo, F. *et al.* 4E-binding protein 1, a cell signaling hallmark in breast cancer that correlates with pathologic grade and prognosis. *Clinical cancer research : an official journal of the American Association for Cancer Research* **13**, 81-89, doi:10.1158/1078-0432.CCR-06-1560 (2007).

54   Martin, M. E. *et al.* 4E binding protein 1 expression is inversely correlated to the progression of gastrointestinal cancers. *Int J Biochem Cell B* **32**, 633-642, doi:Doi 10.1016/S1357-2725(00)00007-8 (2000).

55   Chang, S. H. *et al.* Aerosol delivery of eukaryotic translation initiation factor 4E-binding protein 1 effectively suppresses lung tumorigenesis in K-rasLA1 mice. *Cancer gene therapy* **20**, 331-335, doi:10.1038/cgt.2013.24 (2013).

56   Avdulov, S. *et al.* Activation of translation complex eIF4F is essential for the genesis and maintenance of the malignant phenotype in human mammary epithelial cells. *Cancer Cell* **5**, 553-563, doi:10.1016/j.ccr.2004.05.024 (2004).

57   Ye, Q., Cai, W., Zheng, Y., Evers, B. M. & She, Q. B. ERK and AKT signaling cooperate to translationally regulate survivin expression for metastatic progression of colorectal cancer. *Oncogene* **33**, 1828-1839, doi:10.1038/onc.2013.122 (2014).

58   Martineau, Y., Azar, R., Bousquet, C. & Pyronnet, S. Anti-oncogenic potential of the eIF4E-binding proteins. *Oncogene* **32**, 671-677, doi:10.1038/onc.2012.116 (2013).

59   Schwarzer, A. *et al.* Hyperactivation of mTORC1 and mTORC2 by multiple oncogenic events causes addiction to eIF4E-dependent mRNA translation in T-cell leukemia. *Oncogene* **34**, 3593-3604, doi:10.1038/onc.2014.290 (2015).

60   Hudes, G. *et al.* Temsirolimus, interferon alfa, or both for advanced renal-cell carcinoma. *New Engl J Med* **356**, 2271-2281, doi:DOI 10.1056/NEJMoa066838 (2007).

61   Motzer, R. J. *et al.* Efficacy of everolimus in advanced renal cell carcinoma: a double-blind, randomised, placebo-controlled phase III trial. *Lancet* **372**, 449-456, doi:10.1016/S0140-6736(08)61039-9 (2008).

62   Zibelman, M. *et al.* Phase I study of the mTOR inhibitor ridaforolimus and the HDAC inhibitor vorinostat in advanced renal cell carcinoma and other solid tumors. *Invest New Drugs*, doi:10.1007/s10637-015-0261-3 (2015).

63   Tamburini, J. *et al.* Protein synthesis is resistant to rapamycin and constitutes a promising therapeutic target in acute myeloid leukemia. *Blood* **114**, 1618-1627, doi:10.1182/blood-2008-10-184515 (2009).

64   Carew, J. S., Kelly, K. R. & Nawrocki, S. T. Mechanisms of mTOR inhibitor resistance in cancer therapy. *Target Oncol* **6**, 17-27, doi:10.1007/s11523-011-0167-8 (2011).

65   Feldman, M. E. *et al.* Active-site inhibitors of mTOR target rapamycin-resistant outputs of mTORC1 and mTORC2. *PLoS Biol* **7**, e38, doi:10.1371/journal.pbio.1000038 (2009).

66   Hosoi, H. *et al.* Rapamycin causes poorly reversible inhibition of mTOR and induces p53-independent apoptosis in human rhabdomyosarcoma cells. *Cancer research* **59**, 886-894 (1999).

67   Kang, S. A. *et al.* mTORC1 phosphorylation sites encode their sensitivity to starvation and rapamycin. *Science* **341**, 1236566, doi:10.1126/science.1236566 (2013).

68   Thoreen, C. C. *et al.* An ATP-competitive mammalian target of rapamycin inhibitor reveals rapamycin-resistant functions of mTORC1. *The Journal of biological chemistry* **284**, 8023-8032, doi:10.1074/jbc.M900301200 (2009).

69   Shi, Y., Yan, H., Frost, P., Gera, J. & Lichtenstein, A. Mammalian target of rapamycin inhibitors activate the AKT kinase in multiple myeloma cells by up-regulating the insulin-like growth factor receptor/insulin receptor substrate-1/phosphatidylinositol 3-kinase cascade. *Mol Cancer Ther* **4**, 1533-1540, doi:10.1158/1535-7163.MCT-05-0068 (2005).

70   Tamburini, J. *et al.* Mammalian target of rapamycin (mTOR) inhibition activates phosphatidylinositol 3-kinase/Akt by up-regulating insulin-like growth factor-1 receptor

signaling in acute myeloid leukemia: rationale for therapeutic inhibition of both pathways. *Blood* **111**, 379-382, doi:10.1182/blood-2007-03-080796 (2008).

71   Carriere, A. *et al.* ERK1/2 phosphorylate Raptor to promote Ras-dependent activation of mTOR complex 1 (mTORC1). *The Journal of biological chemistry* **286**, 567-577, doi:10.1074/jbc.M110.159046 (2011).

72   Roux, P. P. *et al.* RAS/ERK signaling promotes site-specific ribosomal protein S6 phosphorylation via RSK and stimulates cap-dependent translation. *The Journal of biological chemistry* **282**, 14056-14064, doi:10.1074/jbc.M700906200 (2007).

73   Wander, S. A., Hennessy, B. T. & Slingerland, J. M. Next-generation mTOR inhibitors in clinical oncology: how pathway complexity informs therapeutic strategy. *J. Clin. Invest.* **121**, 1231-1241 (2011).

74   Guertin, D. A. & Sabatini, D. M. The pharmacology of mTOR inhibition. *Sci. Signal.* **2**, pe24 (2009).

75   Li, J., Kim, S. G. & Blenis, J. Rapamycin: one drug, many effects. *Cell Metab.* **19**, 373-379 (2014).

76   Sun, S.-Y. *et al.* Activation of Akt and eIF4E survival pathways by rapamycin-mediated mammalian target of rapamycin inhibition. *Cancer Res.* **65**, 7052-7058 (2005).

77   O'Reilly, K. E. *et al.* mTOR inhibition induces upstream receptor tyrosine kinase signaling and activates Akt. *Cancer Res.* **66**, 1500-1508 (2006).

78   Carracedo, A. *et al.* Inhibition of mTORC1 leads to MAPK pathway activation through a PI3K-dependent feedback loop in human cancer. *J. Clin. Invest.* **118**, 3065-2074 (2008).

79   She, Q.-B. *et al.* 4E-BP1 is a key effector of the oncogenic activation of the AKT and ERK signaling pathways that integrates their function in tumors. *Cancer Cell* **18**, 39-51 (2010).

80   Choo, A. Y., Yoon, S. O., Kim, S. G., Roux, P. P. & Blenis, J. Rapamycin differentially inhibits S6Ks and 4E-BP1 to mediate cell-type-specific repression of mRNA translation. *Proceedings of the National Academy of Sciences of the United States of America* **105**, 17414-17419, doi:10.1073/pnas.0809136105 (2008).

81   Ducker, G. S. *et al.* Incomplete inhibition of phosphorylation of 4E-BP1 as a mechanism of primary resistance to ATP-competitive mTOR inhibitors. *Oncogene* **33**, 1590-1600, doi:10.1038/onc.2013.92 (2014).

82   Choo, A. Y. & Blenis, J. Not all substrates are treated equally: Implications for mTOR, rapamycin-resistance, and cancer therapy. *Cell Cycle* **8**, 567-572, doi:10.4161/cc.8.4.7659 (2009).

83   Alain, T. *et al.* eIF4E/4E-BP ratio predicts the efficacy of mTOR targeted therapies. *Cancer research* **72**, 6468-6476, doi:10.1158/0008-5472.CAN-12-2395 (2012).

84   Wei, W. *et al.* Single-Cell Phosphoproteomics Resolves Adaptive Signaling Dynamics and Informs Targeted Combination Therapy in Glioblastoma. *Cancer Cell* **29**, 563-573, doi:10.1016/j.ccell.2016.03.012 (2016).

85   Wang, J. *et al.* Snail determines the therapeutic response to mTOR kinase inhibitors by transcriptional repression of 4E-BP1. *Nat Commun* **8**, 2207, doi:10.1038/s41467-017-02243-3 (2017).

86   Banerji, U. *et al.* First-in-human phase I trial of the dual mTORC1 and mTORC2 inhibitor AZD2014 in solid tumors. *J Clin Oncol* **30** (2012).

87   Guichard, S. M. *et al.* AZD2014, an Inhibitor of mTORC1 and mTORC2, Is Highly Effective in ER+ Breast Cancer When Administered Using Intermittent or Continuous Schedules. *Molecular Cancer Therapeutics* **14**, 2508-2518, doi:10.1158/1535-7163.Mct-15-0365 (2015).

88   Shih, K. C. *et al.* Phase I trial of an oral TORC1/TORC2 inhibitor (CC-223) in advanced solid and hematologic cancers. *J Clin Oncol* **30** (2012).

89   Varga, A. *et al.* Phase I expansion trial of an oral TORC1/TORC2 inhibitor (CC-223) in advanced solid tumors. *J Clin Oncol* **31** (2013).

90   Venkatesha, V. A. *et al.* P7170, a novel inhibitor of mTORC1/mTORC2 and Activin receptor-like Kinase 1 (ALK1) inhibits the growth of non small cell lung cancer. *Mol Cancer* **13**, 259, doi:10.1186/1476-4598-13-259 (2014).

91   Kaplan, B., Qazi, Y. & Wellen, J. R. Strategies for the management of adverse events associated with mTOR inhibitors. *Transplant Rev (Orlando)* **28**, 126-133, doi:10.1016/j.trre.2014.03.002 (2014).

92   Pallet, N. & Legendre, C. Adverse events associated with mTOR inhibitors. *Expert Opin Drug Saf* **12**, 177-186, doi:10.1517/14740338.2013.752814 (2013).

93   Graham, L. *et al.* A phase II study of the dual mTOR inhibitor MLN0128 in patients with metastatic castration resistant prostate cancer. *Invest New Drugs* **36**, 458-467, doi:10.1007/s10637-018-0578-9 (2018).

94   Xie, J., Wang, X. & Proud, C. G. mTOR inhibitors in cancer therapy. *F1000Res* **5**, doi:10.12688/f1000research.9207.1 (2016).

95   Nawroth, R. *et al.* S6K1 and 4E-BP1 are independent regulated and control cellular growth in bladder cancer. *PloS one* **6**, e27509, doi:10.1371/journal.pone.0027509 (2011).

96   Zhang, Y. & Zheng, X. F. mTOR-independent 4E-BP1 phosphorylation is associated with cancer resistance to mTOR kinase inhibitors. *Cell Cycle* **11**, 594-603, doi:10.4161/cc.11.3.19096 (2012).

97   Di Nicolantonio, F. *et al.* Deregulation of the PI3K and KRAS signaling pathways in human cancer cells determines their response to everolimus. *Journal of Clinical Investigation* **120**, 2858-2866, doi:10.1172/Jci37539 (2010).

98   Wang, J., Ye, Q. & She, Q.-B. New insights into 4E-BP1-regulated translation in cancer progression and metastasis. *Cancer cell & microenvironment* **1**, e331, doi:10.14800/ccm.331 (2014).

99   Cai, W., Ye, Q. & She, Q. B. Loss of 4E-BP1 function induces EMT and promotes cancer cell migration and invasion via cap-dependent translational activation of snail. *Oncotarget* **5**, 6015-6027, doi:10.18632/oncotarget.2109 (2014).

100   Dienstmann, R., Rodon, J., Serra, V. & Tabernero, J. Picking the point of inhibition: a comparative review of PI3K/AKT/mTOR pathway inhibitors. *Mol Cancer Ther* **13**, 1021-1031, doi:10.1158/1535-7163.MCT-13-0639 (2014).

101   Dogan Turacli, I., Ozkan, A. C. & Ekmekci, A. The comparison between dual inhibition of mTOR with MAPK and PI3K signaling pathways in KRAS mutant NSCLC cell lines. *Tumour Biol*, doi:10.1007/s13277-015-3671-0 (2015).

102   Gravina, G. L. *et al.* Dual PI3K/mTOR inhibitor, XL765 (SAR245409), shows superior effects to sole PI3K [XL147 (SAR245408)] or mTOR [rapamycin] inhibition in prostate cancer cell models. *Tumour Biol*, doi:10.1007/s13277-015-3725-3 (2015).

103   Serra, V. *et al.* NVP-BEZ235, a dual PI3K/mTOR inhibitor, prevents PI3K signaling and inhibits the growth of cancer cells with activating PI3K mutations. *Cancer research* **68**, 8022-8030, doi:10.1158/0008-5472.CAN-08-1385 (2008).

104   Wallin, J. J. *et al.* GDC-0980 Is a Novel Class I PI3K/mTOR Kinase Inhibitor with Robust Activity in Cancer Models Driven by the PI3K Pathway. *Molecular Cancer Therapeutics* **10**, 2426-2436, doi:10.1158/1535-7163.Mct-11-0446 (2011).

105   Wainberg, Z. A. *et al.* A Multi-Arm Phase I Study of the PI3K/mTOR Inhibitors PF-04691502 and Gedatolisib (PF-05212384) plus Irinotecan or the MEK Inhibitor PD-0325901 in Advanced Cancer. *Target Oncol* **12**, 775-785, doi:10.1007/s11523-017-0530-5 (2017).

106   Chia, S. *et al.* Novel agents and associated toxicities of inhibitors of the pi3k/Akt/mtor pathway for the treatment of breast cancer. *Curr Oncol* **22**, 33-48, doi:10.3747/co.22.2393 (2015).

107   Zhou, Y. *et al.* Developing a novel dual PI3K-mTOR inhibitor from the prodrug of a metabolite. *Onco Targets Ther* **10**, 5077-5087, doi:10.2147/OTT.S142492 (2017).

108   Cencic, R. *et al.* Reversing chemoresistance by small molecule inhibition of the translation initiation complex eIF4F. *Proceedings of the National Academy of Sciences of the United States of America* **108**, 1046-1051, doi:10.1073/pnas.1011477108 (2011).

109   Moerke, N. J. *et al.* Small-molecule inhibition of the interaction between the translation initiation factors eIF4E and eIF4G. *Cell* **128**, 257-267, doi:10.1016/j.cell.2006.11.046 (2007).

110   Sekiyama, N. *et al.* Molecular mechanism of the dual activity of 4EGI-1: Dissociating eIF4G from eIF4E but stabilizing the binding of unphosphorylated 4E-BP1. *Proceedings of the National Academy of Sciences of the United States of America* **112**, E4036-E4045, doi:10.1073/pnas.1512118112 (2015).

111   Cencic, R. *et al.* Blocking eIF4E-eIF4G Interaction as a Strategy To Impair Coronavirus Replication. *Journal of Virology* **85**, 6381-6389, doi:10.1128/Jvi.00078-11 (2011).

112   Herbert, T. P., Fahraeus, R., Prescott, A., Lane, D. P. & Proud, C. G. Rapid induction of apoptosis mediated by peptides that bind initiation factor eIF4E. *Current Biology* **10**, 793-796, doi:Doi 10.1016/S0960-9822(00)00567-4 (2000).

113   Ko, S. Y., Guo, H. F., Barengo, N. & Naora, H. Inhibition of Ovarian Cancer Growth by a Tumor-Targeting Peptide That Binds Eukaryotic Translation Initiation Factor 4E. *Clinical Cancer Research* **15**, 4336-4347, doi:10.1158/1078-0432.Ccr-08-2924 (2009).

114   Masse, M. *et al.* An eIF4E-interacting peptide induces cell death in cancer cell lines. *Cell Death & Disease* **5**, doi:10.1038/cddis.2014.457 (2014).

115   Zhou, W. Z. *et al.* Improved eIF4E Binding Peptides by Phage Display Guided Design: Plasticity of Interacting Surfaces Yield Collective Effects. *PloS one* **7**, doi:10.1371/journal.pone.0047235 (2012).

116   Fosgerau, K. & Hoffmann, T. Peptide therapeutics: current status and future directions. *Drug Discov Today* **20**, 122-128, doi:10.1016/j.drudis.2014.10.003 (2015).

117   Heesom, K. J. & Denton, R. M. Dissociation of the eukaryotic initiation factor-4E/4E-BP1 complex involves phosphorylation of 4E-BP1 by an mTOR-associated kinase. *FEBS Lett* **457**, 489-493 (1999).

118   Gingras, A.-C. *et al.* Hierarchical phosphorylation of the translation inhibitor 4E-BP1. *Genes & development* **15**, 2852-2864, doi:10.1101/gad.912401 (2001).

119   Gingras, A.-C. *et al.* Regulation of 4E-BP1 phosphorylation: a novel two-step mechanism. *Genes & development* **13**, 1422-1437 (1999).

120   Burnett, P. E., Barrow, R. K., Cohen, N. A., Solomon, H. S. & Sabatini, D. M. RAFT1 Phosphorylation of the Translational Regulators p70 S6 Kinase and 4E-BP1. *Proceedings of the National Academy of Sciences of the United States of America* **95**, 1432-1437, doi:10.2307/44300 (1998).

121   Haystead, T. A. J. Identification of Phosphorylation Sites in the Translational Regulator, PHAS-I, That Are Controlled by Insulin and Rapamycin in Rat Adipocytes. *Journal of Biological Chemistry* **272**, 10240-10247, doi:10.1074/jbc.272.15.10240 (1997).

122   Lawrence, J. C. PHAS/4E-BPs as reguators of mRNA translation and cell proliferation. *Trends in biochemical sciences* **22**, 345-349, doi:doi:10.1016/S0968-0004(97)01101-8 (1997).

123   Lawrence, J. C., Fadden, P., Haystead, T. A. J. & Lin, T. A. PHAS proteins as mediators of the actions of insulin, growth factors and cAMP on protein synthesis and cell proliferation. *Adv Enzyme Regul* **37**, 239-267, doi:Doi 10.1016/S0065-2571(96)00016-7 (1997).

124   Hornbeck, P. V. *et al.* PhosphoSitePlus, 2014: mutations, PTMs and recalibrations. *Nucleic acids research* **43**, D512-520, doi:10.1093/nar/gku1267 (2015).

125   Magnuson, B., Ekim, B. & Fingar, D. C. Regulation and function of ribosomal protein S6 kinase (S6K) within mTOR signalling networks. *The Biochemical journal* **441**, 1-21, doi:10.1042/BJ20110892 (2012).

126   Nojima, H. *et al.* The mammalian target of rapamycin (mTOR) partner, raptor, binds the mTOR substrates p70 S6 kinase and 4E-BP1 through their TOR signaling (TOS) motif. *The Journal of biological chemistry* **278**, 15461-15464, doi:10.1074/jbc.C200665200 (2003).

127   Schalm, S. S., Fingar, D. C., Sabatini, D. M. & Blenis, J. TOS Motif-Mediated Raptor Binding Regulates 4E-BP1 Multisite Phosphorylation and Function. *Current Biology* **13**, 797-806, doi:10.1016/s0960-9822(03)00329-4 (2003).

128   Beugnet, A., Wang, X. & Proud, C. G. Target of rapamycin (TOR)-signaling and RAIP motifs play distinct roles in the mammalian TOR-dependent phosphorylation of initiation factor 4E-binding protein 1. *The Journal of biological chemistry* **278**, 40717-40722, doi:10.1074/jbc.M308573200 (2003).

129   Batool, A., Aashaq, S. & Andrabi, K. I. Reappraisal to the study of 4E-BP1 as an mTOR substrate - A normative critique. *Eur J Cell Biol* **96**, 325-336, doi:10.1016/j.ejcb.2017.03.013 (2017).

130   Yang, D. Q. & Kastan, M. B. Participation of ATM in insulin signalling through phosphorylation of eIf-4E-binding protein 1. *Nat Cell Biol* **2**, 893-898 (2000).

131   Shin, S., Wolgamott, L., Roux, P. P. & Yoon, S. O. Casein kinase 1epsilon promotes cell proliferation by regulating mRNA translation. *Cancer research* **74**, 201-211, doi:10.1158/0008-5472.CAN-13-1175 (2014).

132   Herbert, T. P., Tee, A. R. & Proud, C. G. The extracellular signal-regulated kinase pathway regulates the phosphorylation of 4E-BP1 at multiple sites. *The Journal of biological chemistry* **277**, 11591-11596, doi:10.1074/jbc.M110367200 (2002).

133   Shuda, M. *et al.* CDK1 substitutes for mTOR kinase to activate mitotic cap-dependent protein translation. *Proceedings of the National Academy of Sciences of the United States of America* **112**, 5875-5882, doi:10.1073/pnas.1505787112 (2015).

134   Velasquez, C. *et al.* Mitotic protein kinase CDK1 phosphorylation of mRNA translation regulator 4E-BP1 Ser83 may contribute to cell transformation. *Proceedings of the National Academy of Sciences of the United States of America* **113**, 8466-8471, doi:10.1073/pnas.1607768113 (2016).

135   Shin, S. *et al.* Glycogen synthase kinase-3beta positively regulates protein synthesis and cell proliferation through the regulation of translation initiation factor 4E-binding protein 1. *Oncogene* **33**, 1690-1699, doi:10.1038/onc.2013.113 (2014).

136   Liu, G. M., Zhang, Y. G., Bode, A. M., Ma, W. Y. & Dong, Z. G. Phosphorylation of 4E-BP1 is mediated by the p38/MSK1 pathway in response to UVB irradiation. *Journal of Biological Chemistry* **277**, 8810-8816, doi:10.1074/jbc.M110477200 (2002).

137   Fox, C. J. *et al.* The serine/threonine kinase Pim-2 is a transcriptionally regulated apoptotic inhibitor. *Genes & development* **17**, 1841-1854, doi:10.1101/gad.1105003 (2003).

138   Shang, Z. F. *et al.* 4E-BP1 participates in maintaining spindle integrity and genomic stability via interacting with PLK1. *Cell Cycle* **11**, 3463-3471, doi:10.4161/cc.21770 (2012).

139   Tait, S. *et al.* Local control of a disorder-order transition in 4E-BP1 underpins regulation of translation via eIF4E. *Proceedings of the National Academy of Sciences of the United States of America* **107**, 17627-17632, doi:10.1073/pnas.1008242107 (2010).

140   Peter, D. *et al.* Molecular architecture of 4E-BP translational inhibitors bound to eIF4E. *Molecular cell* **57**, 1074-1087, doi:10.1016/j.molcel.2015.01.017 (2015).

141   Gruner, S. *et al.* The Structures of eIF4E-eIF4G Complexes Reveal an Extended Interface to Regulate Translation Initiation. *Molecular cell* **64**, 467-479, doi:10.1016/j.molcel.2016.09.020 (2016).

142   Gingras, A. C. *et al.* Regulation of 4E-BP1 phosphorylation: a novel two-step mechanism. *Genes & development* **13**, 1422-1437, doi:DOI 10.1101/gad.13.11.1422 (1999).

Chapter 3

Development of a Phosphosite Accurate Crosslinking Assay

3.1   Abstract

Given the importance of kinase-catalyzed phosphorylation (discussed in Chaper 2), and the dearth of available tools with which to reliably identify phosphorylation site specific kinases (discussed in Chapter 1), a new assay for allowing an unbiased query of the kinome was sorely needed. To address this need, a kinase crosslinking assay (PhAXA) was developed that, when coupled to LC-MS/MS analysis, provides a list of possible kinases for a phosphorylation site of interest. This chapter discusses the concept behind PhAXA, and the three kinase-substrate systems used as proof-of-concept for this activity-based, chemoproteomic pipeline.

3.2   A Phosphosite Accurate Crosslinking Assay (PhAXA)

To improve upon a previous method of implementing biotinylated peptide pseudosubstrates for phosphosite specific kinase identification, a new assay was developed: the Phosphosite Accurate Crosslinking Assay, or PhAXA. (Figure 3.1) PhAXA was inspired by a previously reported[1] ATP crosslinker probe in which the γ-phosphate of ATP has been modified with a methacrylate moiety (Figure 3.1), allowing for the selective conversion of highly conserved active site lysines to an acrylamide. The position of this electrophilic handle within the active site of a kinase allows for a crosslinking reaction to occur via Michael addition with a cysteine thiol, which has been inserted in place of the serine, threonine, or tyrosine of a substrate protein of interest. The result is a hydrolytically stable bond formed between the acrylamide-kinase and cysteine mutant probe, allowing

this complex to be isolated by immunoprecipitation using anti-FLAG affinity resin and the kinase(s) identified via mass spectrometry (MS)-based proteomics.
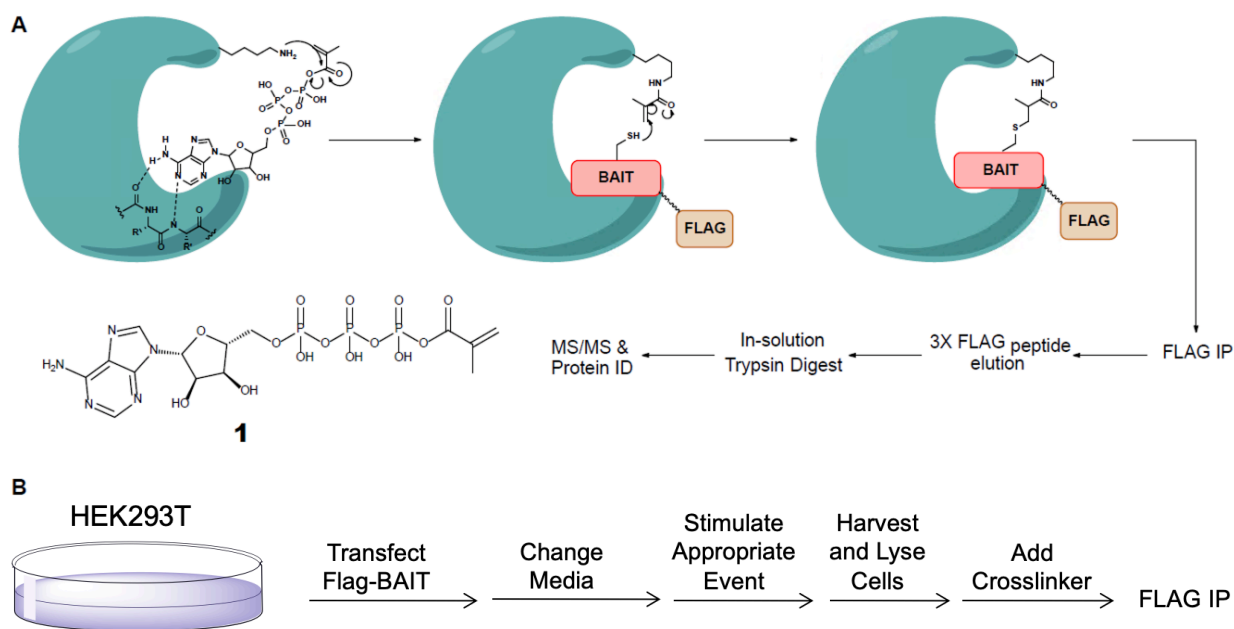
Figure 3.1 | Workflow for identifying site-specific kinase-substrate interactions. **A)** PhAXA schematic and structure of ATP crosslinker probe 1. **B)** Generic workflow for the cell-based aspect of PhAXA.

The benefits of PhAXA are two-fold: (1) Kinases have been shown to achieve substrate specificity through complex docking interactions.[2,3] As such, these interactions are impossible to achieve by using a peptide or partial substrate as bait for activity-based pulldown. In this method, the full-length protein is used, and thus, more biologically relevant. (2) By transiently expressing the substrate protein, as opposed to adding exogenous protein or peptide, the bait is present *in situ* and can engage in all physiologically relevant interactions prior to cell lysis, aiding in specificity. Moreover, 98% of all human protein kinases utilize an active site lysine to coordinate the negative charge of the gamma-phosphate on ATP.[4] Because of this highly conserved residue, and the fact that all kinases utilize ATP as a phosphate donor, the ATP-methacrylate crosslinker is likely capable of converting the vast majority of the human kinome into a suitable electrophile for a Michael addition with a cysteine thiol. Therefore, this approach is likely amenable to the majority of kinase-substrate interactions, which is essential to achieve an unbiased scan of the kinome.

3.3 Assay Validation using c-Jun – MAPK8/9

Development of a phosphosite specific crosslinking assay required a model system for which the kinase, and the exact phosphorylation site, is known with absolute certainty. For initial proof-of-concept studies, the Jnk1/2-c-Jun kinase-substrate interaction was used, as phosphorylation-mediated activation of c-Jun has been of significant interest since the discovery of *JUN* as an oncogene in the 1980's.[5,6] c-Jun is a member of the AP-1 transcription factor complex, which is present as both homodimers and heterodimers comprised of Fos (c-Fos, FosB, Fra1, and Fra2), Jun (c-Jun, JunB, and JunD), Jun dimerization partners (JDP1 and JDP2), and the activating transcription factors (B-ATF, ATF2 and ATF3).[6,7] Each homo- and heterodimer activates transcription of a different subset of genes, though c-Jun can independently drive cell proliferation via downregulation of p53, p21 and p16, while upregulating Cyclin D1 and FasL.[8] These findings implicated c-Jun in oncogenesis,[9-12] and resulted in extensive investigation of the mechanism by which c-Jun is activated. Mechanistic evaluation of the cellular UV response found that the c-Jun N-terminal Kinases 1 and 2 (JNK1/2), also known as mitogen activated kinases 8 and 9 (MAPK8/9), phosphorylate the c-Jun transactivation domain at Ser63 and Ser73.[13-16] This led to several drug discovery efforts for developing JNK inhibitors,[17-22] the results of which further validated the JNK-c-Jun interaction.

JNK1/2-mediated c-Jun phosphorylation is induced by stress, UV light, loss of contact inhibition, and reactive oxygen species.[13,15,23,24] In an *in vitro* setting, this is commonly induced via ionizing radiation,[24] or by treatment with the protein synthesis inhibitor[25] anisomycin.[16] Due to ease of use, pharmacological induction of c-jun phosphorylation was preferable to using UV radiation, so anisomycin was used to stimulate JNK activity. JNK activation was verified by treating 293Ts with increasing doses of anisomycin for different times, leading to increased phosphorylation of both endogenous and transfected FLAG-c-Jun at each concentration and time that was examined. (Figure 3.2A) c-Jun is a transcription factor, which translocates to the nucleus upon activation. As kinases are known to exhibit differential activity *in vitro* in response to detergents, it was important to determine whether both Jnk1/2 and c-Jun could still be isolated with a mild, detergent-free kinase-assay buffer.[26,27] Therefore, 293T cells were

stimulated with anisomycin and lysed with SDS-containing buffer (for whole-cell extract), or with buffer lacking detergent (cytoplasmic proteins only). (Figure 3.2B) Jnk was found in equal amounts in both cytoplasmic and whole cell fractions, while active, phosphorylated c-Jun was less abundant in the cytoplasmic fraction. However, there was still a relatively high proportion of c-Jun in lysate isolated from high density cells without using detergent. (Figure 3.2B) These initial optimization experiments provide the cellular conditions under which to observe the interaction of c-Jun and Jnk1/2 using PhAXA.
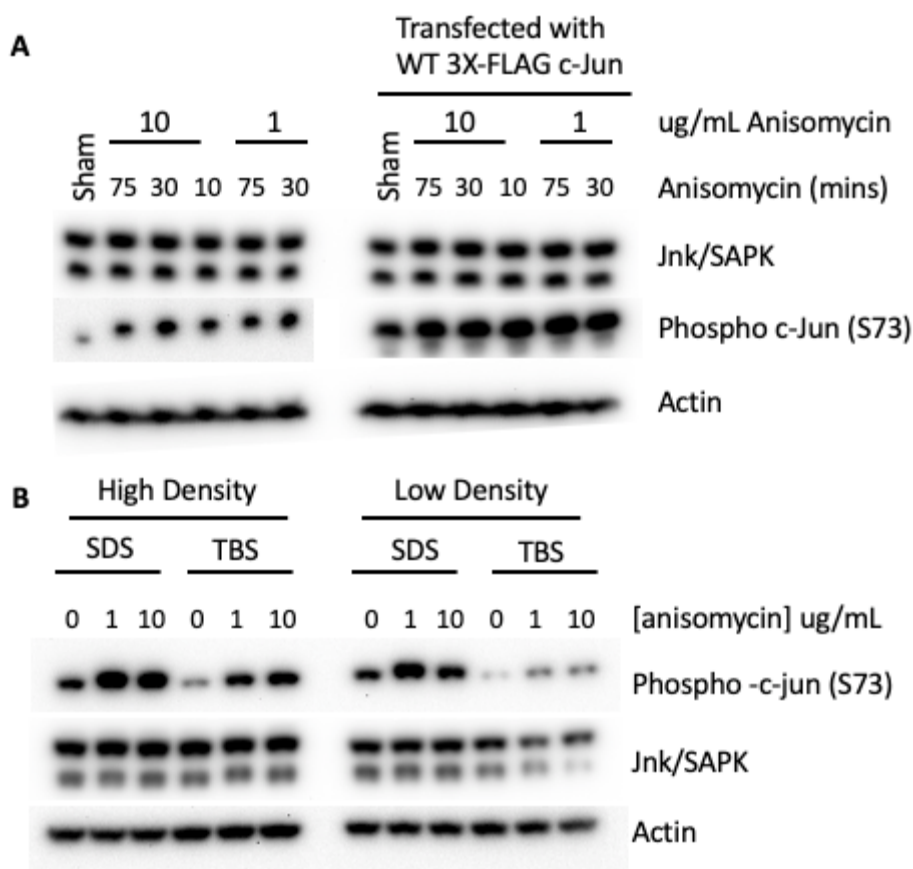
Figure 3.2 | Evaluating the the Activation of c-Jun Using Anisomycin. A) Western Blot of 293T cells left untransfected or transfected with wild-type 3x-FLAG c-Jun after treatment with different concentrations and durations of anisomycin. Western Blot of 293T cells at high or low density treated with different concentrations of anisomycin. Cells were harvested in Tris-buffered saline (TBS) +/- 0.1% sodium dodecyl sulfate.

Finally, PhAXA was attempted using wild-type (WT) c-Jun as a bait protein. Unfortunately, Jnk was highly enriched from lysate expressing wild-type Flag-c-Jun protein when treated with crosslinker, with the observed mass shift indicating successful crosslinking between the kinase and substrate. (Figure 3.3A) However, no crosslinking

was observed without the addition of crosslinker, suggesting background labeling occurred through an endogenous cysteine. (Figure 3.3A) It was reasoned that pulldown with the WT probe was likely due to labeling at Cys99, which is located near three other JNK phosphorylation sites, Thr91, Thr93, and Thr95.[28,29] This was confirmed by performing PhAXA using Flag-c-Jun (C99A) as bait, as very little crosslinking was observed upon removal of the endogenous cysteine. (Figure 3.3A) Robust pulldown was achieved with the C99A/S63C and C99A/S73A mutant probes relative to the C99A control. (Figure 3.3B) Jnk was also enriched over background with the cysteine mutant probes corresponding to the other Jnk substrate residues (C99A/T91A, C99A/T93C, and C99A/T95C), however the pulldown efficiency was lower. (Figure 3.3B)

Kinase-substrate crosslinking was determined to be dependent on the catalytic lysine via utilizing an active site kinase inhibitor. Pre-treatment of lysate with the ATP competitive inhibitor SP600125[19-21] prevented the pulldown of Jnk by Flag-c-Jun (S63C) probes from lysate treated with crosslinker, indicating that crosslinking occurs between the kinase active site and the incorporated cysteine. (Figure 3.3C,D**)** Moreover, enrichment of the Jnk was only abrogated at concentrations exceeding 40nM, the reported IC_{50} for this inhibitor.[21] This experiment provides evidence that the level of enrichment from cell lysate is representative of the activity of that kinase towards the cysteine mutant substrate, a necessary quality for activity based probes.
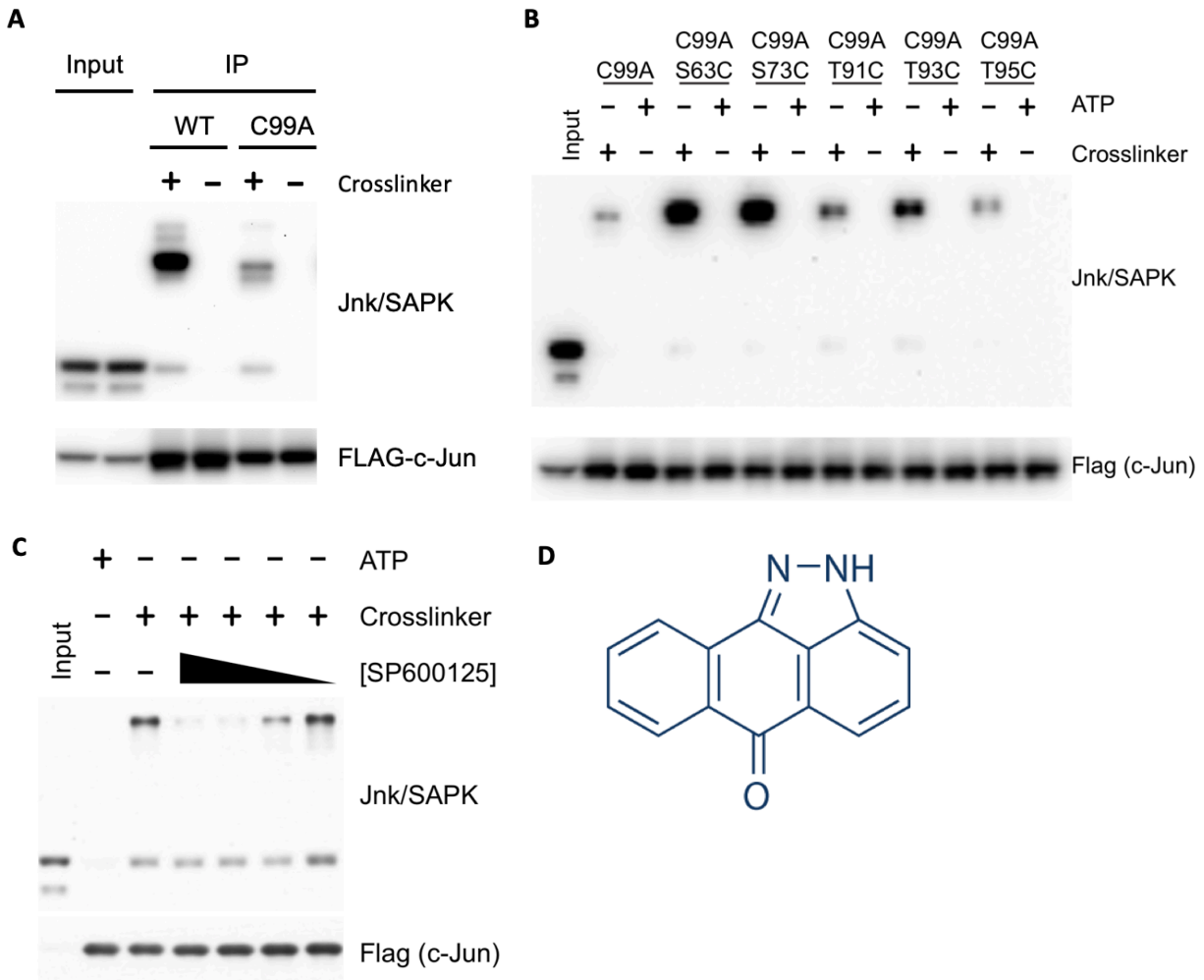
Figure 3.3 | Optimizing PhAXA Pulldown With c-Jun-Jnk1/2. A) Western blot comparing PhAXA pulldown efficiency between 3xFlag-c-Jun (WT) and (C99A) baits. **B)** 3xFlag-c-Jun phosphosite to cysteine mutant bait proteins selectively pull down Jnk when treated with crosslinker. **C)** SP600125 inhibition of Jnk pulldown from 5 μM − 10 nM **D)** Structure of the active-site Jnk inhibitor SP600125.

To demonstrate that PHAT-ELKCA can be used for kinase identification by mass-spectrometry (PhAXA-MS), and to profile selectivity of this method, the FLAG-c-Jun (C99A/S63C) and (C99A) probes were used to pulldown associated kinases from HEK293T lysate followed by LC-MS/MS analysis. Significant enrichment of high-scoring Jnk1/2 peptides from the sample prepared from C99A/S63C expressing cell lysate treated with the crosslinker 1, while very few Jnk1/2 peptides were identified in the ATP only and FLAG-c-Jun (C99A), crosslinker treated control samples (Table 3.1). Two biological replicates were performed, and kinases identified by at least 2 PSMs across both replicates were examined. These kinases were quantified in two ways: (1) By counting

the number of peptide spectrum matches (PSMs) in each sample[30] (2) By quantifying the relative MS1 intensity of each identified peptide.[31] In each case, the obtained value was used as a proxy for relative protein concentration, and fold changes were calculated for the phosphocysteine mutant, crosslinker treated sample versus each control. For each relative quantification method, MAPK8 (Jnk1) emerged as the top hit, with MAPK9 (Jnk2) as the second most enriched sample. These *bona fide* c-Jun kinases were the only two kinases across the dataset to exhibit two-fold enrichment over both negative control samples. These results demonstrate that PhAXA-MS is a viable method for the unbiased query of the kinome.

Protein	Average PSM Count				Fold Change (PSMs)		Fold Change (MS1 Integration)	
	C99A +	C99A -	C99A/S63C +	C99A/S63C -	Mut+/WT+	Mut+/Mut-	Mut+/WT+	Mut+/Mut-
MAPK8	5.0	0.0	28.0	1.5	5.60	18.67	5.10 +/-2.07	13.47 +/-6.84
MAPK9	22.5	1.0	30.5	14.5	1.36	2.10	2.68 +/-0.85	3.85 +/-0.98
CDK11B	1.5	3.5	1.5	1.0	1.00	1.50	1.42 (n=1)	0.84 (n=1)
NEK9	5.5	2.5	5.5	2.0	1.00	2.75	1.17 +/-0.12	2.52 +/-0.62
CDK2	11.5	0.0	7.5	0.0	0.65	N/A	1.05 +/-2.06	-
SRPK1	6.5	1.0	4.0	0.5	0.62	8.00	1.00 +/-0.08	3.61 n=1
RIO1	23.5	18.0	23.0	16.0	0.98	1.44	0.97 +/-0.24	1.35 +/-0.37
NEK1	0.5	5.0	1.0	2.5	2.00	0.40	-	-
PASK	0.0	4.5	0.5	6.0	N/A	0.08	-	-
CSNK2A1	21.0	24.5	17.5	20.0	0.83	0.88		

Table 3.1 | c-Jun Interacting Kinases Identified by PhAXA-MS. Table of all kinases identified by at least two peptides in each biological replicate following filtering of common contaminants. (See Methods) Average peptide-spectrum matches (PSMs) are from two independent biological replicates. '+' refers to samples treated with 1, while '-' refers to ATP only controls. Dashes were added for ratios that could not be calculated due to absence of any high scoring PSMs. Ratio of MS1 intensities was determined using Skyline. Fold change is represented as +/- standard deviation (n= 2 to 18).

3.4   Assay Validation using ERK2 – MEK1/2

Using the JNK-c-Jun interaction as a proof of concept for PhAXA demonstrated that this approach is amenable to profiling serine serine/threonine kinases. However, tha majority FDA approved kinase inhibitors target tyrosine kinases,[32-35] and many oncogenic activities directly or indirectly affect tyrosine phosphorylation.[32,36,37] This highlights the fact that many kinases involved in cancer progression act to regulate tyrosine residues, which makes understanding the regulation of these events incredibly important in the context ot drug discovery. Moreover, kinase-kinase signaling cascades directly regulate and

indirectly affect nearly every known cellular process.[38,39] Therefore, the application of PhAXA to a second model system involving tyrosine phosphorylation using a kinase substrate was explored.

Extracellular regulated kinase 2 (ERK2), also known as mitogen activated protein kinase 1 (MAPK1), is one the oldest known kinases involved in signal transduction, as it was first described in the early 1980s.[40-42] ERK2 is involved in phosphorylation of hundreds of substrates following activation of upstream cell receptors with mitogenic stimuli.[40,42-45] ERK2 activation is implicated in cancer progression as it positively regulates many pro-growth processes such as cell cycle[46] and protein translation,[47,48] while negatively regulating apoptosis.[49,50] Mechanistically, Erk2 is activated by phosphorylation at Thr185 and Tyr187, or the TEY motif, by the dual specific kinases MAPK2K1 and MAPK2K2 (MEK1/2).[51-54] Phosphorylation of these residues within the activation loop induces structural changes in the catalytic domain that confer full enzymatic activity.[55,56] Though this phosphorylation event has been known since the early 1990s,[51,57] the only validated kinases with activity towards Y185 are MEK1/2, making this an ideal system on which to build proof of concept for PhAXA.

The MAP kinase pathway is swiftly and strongly activated by phorbol esters[58-60]; thus, PMA was used to stimulated MEK1/2 mediated phosphorylation, and thus crosslinking, of the FLAG-Erk2 cysteine mutant probes. Importantly, the *rattus norvegicus* Erk2 open reading frame (ORF) was used as a bait for these experiments. The amino acid sequences match with over 99% homology, however Y185 is homologous to *Homo sapiens* Y187. Applying the PhAXA workflow using 3xFLAG-Erk2 (Y185C) as a bait protein resulted in robust enrichment of MEK1/2 relative to the WT Erk2 probe as determined by Western blot. (Figure 3.4A) The expected mass shift of MEK1/2 was also observed in response to treatment with crosslinker, indicating successful covalent crosslinking between the two kinases. Inhibition of MEK1/2 pulldown with trametinib was achieved at concentrations of 10nM and above, which is in line with the reported IC50 of 1nM for this compound.[53,61] (Figure 3.4B) Interestingly, as trametinib functions as a type III, or allosteric, kinase inhibitor,[62,63] pulldown inhibition is like achieved independently of crosslinker-mediated conversion of the active site lysine.
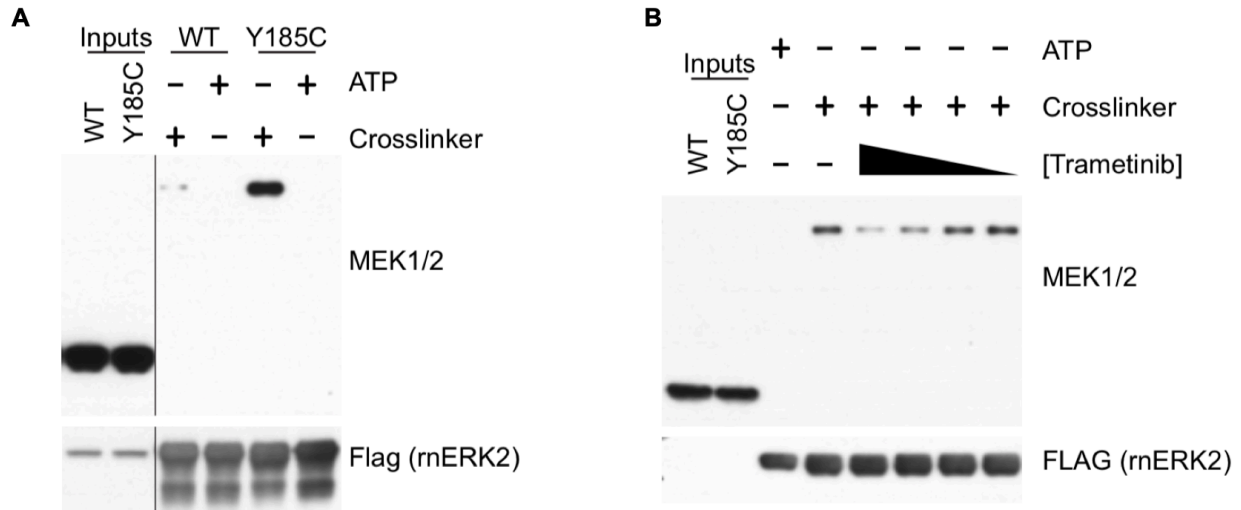
Figure 3.4 | Evaluating PhAXA Pulldown Using ERK2-MEK1/2 A) Y185C rnERK2 mutant pulls down MEK kinase. Rattus norvegicus ERK2 was used as a bait; Y185 is homologous to human Y187. **B)** Trametinib inhibition of MEK pulldown from 100 nM − 100 pM in 10-fold dilutions. Representative input samples are included in each figure to show the shift in mass upon crosslinking.

Using PhAXA-MS, the selectivity of the 3X-Flag-rnERK2 (Y185C) probe was determined. While the overall abundance was low based on spectral count, MEK2 was the only kinase exhibiting greater than 2-fold enrichment over both ATP treated control samples. (Table 3.2) The trend was maintained with both methods of fold change calculation, though S6KA5 was enriched by 1.99-fold between the Y185C and WT samples treated with crosslinker. These results still demonstrate that PhAXA-MS can be used for evaluating kinases that phosphorylate tyrosine residues with individual phosphosite resolution. Moreover, this assay is also amenable to the use of a kinase as a bait, and the possibility that using this type of protein would increase background was not realized.

Protein	Average PSM Count				Fold Change (PSMs)			Fold Change (MS1 Integration)		
	WT +	WT -	Y185C +	Y185C -	Y185C+ /WT+	Y185C+ /Y185C-	Y185C- /WT-	Y185C+/WT+	Y185C+/Y185C-	Y185C-/WT-
MEK2	1.50	0.00	4.50	0.00	3.00	-	-	2.21 +/-0.65	-	-
S6KA5	16.5	0.50	28.50	0.50	1.73	57.00	1.00	1.99 +/-0.54	-	-
S6KA6	16.5	7.00	29.00	6.00	1.76	4.83	0.86	1.70 +/-0.26	3.82 +/-0.37	0.95 +/-0.21
MAPKAP	4.00	0.50	12.50	0.00	3.13	-	-	1.55 +/-0.36	-	-
Mnk1	4.00	0.00	7.50	0.00	1.88	-	-	1.38 +/-0.46	-	-
CDK4	4.50	0.00	3.50	1.00	0.78	3.50	-	1.36 +/-0.34	3.58 +/-0.16	-
S6KA4	8.00	0.50	15.50	0.50	1.94	31.00	1.00	1.34 +/-0.38	19.16 +/-1.14	-
Mnk2	2.00	0.00	5.00	2.50	2.50	2.00	-	1.29 +/-0.49	1.78 +/-0.20	-
Rio1	2.00	0.00	5.00	0.00	2.50	-	-	1.25 +/-0.18	-	-
S6KA1	49.0	44.5	39.00	5.00	0.80	7.80	0.11	0.76 +/-0.09	17.74 +/-7.46	0.05 +/-0.03
S6KA3	89.5	113.	88.50	24.00	0.99	3.69	0.21	0.75 +/-0.13	10.45 +/-5.15	0.07 +/-0.02
MAP2K4	5.00	0.00	2.50	0.00	0.50	-	-	0.75 +/-0.22	-	-
MAP2K6	20.5	0.00	15.00	0.00	0.73	-	-	0.69 +/-0.12	-	-
MAP2K3	5.00	0.00	2.00	0.00	0.40	-	-	0.62 +/-0.004	-	-
S6KA2	4.50	8.50	4.00	2.00	0.89	2.00	0.24	0.47 +/-0.08	1.28 +/-0.33	0.27 +/-0.02

Table 3.2 | ERK2 Interacting Kinases Identified by PhAXA-MS. Table of all kinases identified by at least two peptides in each biological replicate following filtering of common contaminants. (See Methods) Average peptide-spectrum matches (PSMs) are from two independent biological replicates. '+' refers to samples treated with 1, while '-' refers to ATP only controls. Dashes were added for ratios that could not be calculated due to absence of any high scoring PSMs. Ratio of MS1 intensities was determined using Skyline. Fold change is represented as +/- standard deviation (n= 2 to 15).

3.5 Assay Validation using 4E-BP1 – mTOR

As discussed in Chapter 2, phosphorylation-mediated inactivation of 4E-BP1 by mTOR is a well-studied process. Mechanistically, 4E-BP1 is recruited to mTOR kinase by the mTORC1 subunit Raptor via interaction with the FEMDI motif at the C-terminus of 4E-BP1; this motif is absolutely critical for 4E-BP1 phosphorylation by mTOR.[64-67] Moreover, hypophosphorylated 4E-BP1 is thought to be exclusively phosphorylated while bound to eIF4E.[68] Therefore, the peptide-based approach[1] would likely not be effective for the activity-based crosslinking of mTOR-4E-BP1 using crosslinker 1.

Initial proof-of-concept using 4E-BP1 as a bait for this activity-based kinase pulldown used the 4E-BP1 (T46C) cysteine mutant probe, as this site is well validated as an mTORC1 phosphorylation site, and is thought to be constitutively phosphorylated in proliferating cells.[69] mTOR was enriched in a crosslinker-dependent manner from cell lysates expressing this probe. (Figure 3.5A) PhAXA pulldown was then performed at several other sites that are known to be phosphorylated by mTOR, as well as the poorly understood S101 site. HEK293T cells were transiently transfected with plasmids

encoding for 3xFLAG-4EBP1 wild-type (WT) or phosphosite to cysteine mutant constructs (e.g. T46C). As shown in Figure 3.5B, selective pulldown was achieved and mTOR was very clearly enriched from cells expressing the T37C and T46C 4E-BP1 mutants treated with **crosslinker 1** relative to the WT and ATP controls. Unsurprisingly, mTOR pulldown was not observed with S65C, T70C or S101C probes, as these sites are considered poor substrates of mTOR.[70]
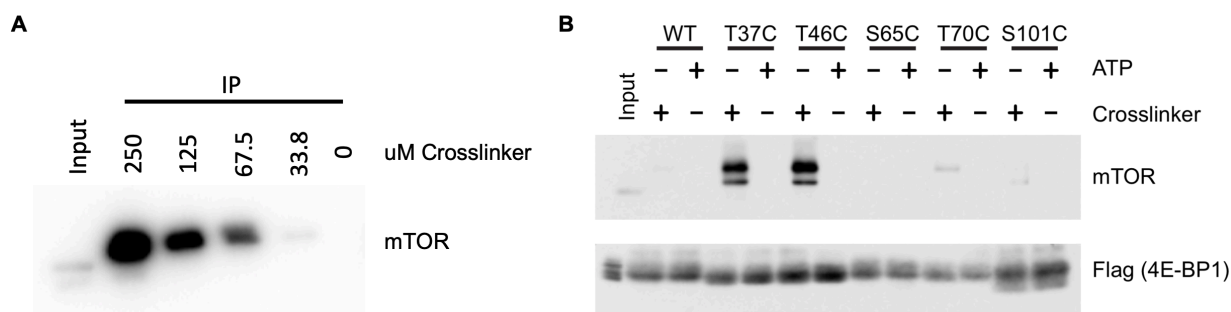
Figure 3.5 | Initial Characterization of 4E-BP1-PhAXA. A) HEK293T cells transfected with 3xFlag-4E-BP1 (T46C) were subjected to PhAXA using different concentrations of crosslinker then analyzed by Western blot. **B)** HEK293T cells transiently transfected with WT or 3XFLAG phosphosite-to-Cys mutant 4E-BP1 constructs were treated with crosslinker or ATP as a control (250 μM) then analyzed by Western blot.

Further mechanistic experiments were then performed to verify the ability of this method to serve as a proxy for mTOR activity. First, the effect of mTORC1 inhibitors on mTOR pulldown was investigated. Pre-treatment of lysate with the ATP competitive, active-site mTOR inhibitor PP242 prevented the pulldown of mTOR by Flag-4E-BP1 (T46C) probes from lysate treated with crosslinker. Inhibition was maintained at concentrations over 10nM, mirroring the reported IC50 of 8nM for this compound.[71] Specificity was further evaluated by disrupting pulldown of mTOR using rapamycin, an allosteric inhibitor. This provides evidence that inhibition of substrate docking, not just conversion of the active site lysine to an acrylamide, can inhibit kinase-substrate crosslinking.
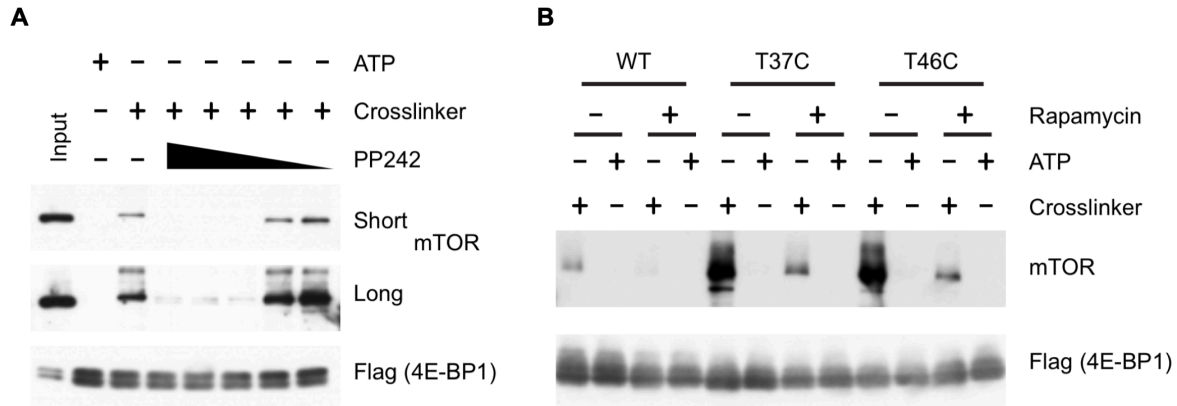
Figure 3.6 | mTORC1 Inhibitors Prevent Pulldown of mTOR by PhAXA. A) PP242 (10,000–1 nM) and B, rapamycin (100 nM) inhibit the crosslinking of mTOR to the T46C 4E-BP1 probe in the presence of crosslinker (250 µM).

As discussed previously, FEMDI motif on 4E-BP1 is required for substrate recruitment, and mutation of Phe114 to alanine decreases phosphorylation of 4E-BP1 at mTORC1-sensitive sites. (Figure 3.7A) Therefore, the effect of this mutation on mTOR pulldown was investigated. Flag-4E-BP1 (T37C) and (T46C) probes also containing a F114A mutation had almost no activity in this assay, mirroring the activity of mTORC1 towards FEMDI null substrates. (Figure 3.7A,B) Finally, the assembly of mTORC1 components is highly detergent sensitive, as mTORC1 is inactive when purified from cells lysed using most common detergents such as NP-40, Trition X100, and dodium dodecyl sulfate.[26] Given this knowledge, PhAXA pulldown was applied to cells expressing the 4E-BP1 (T46C) probe, lysed without detergent (normal conditions) or with 0.5% NP-40. mTOR was not enriched from cell lysate generated using NP-40. (Figure 3.7C)
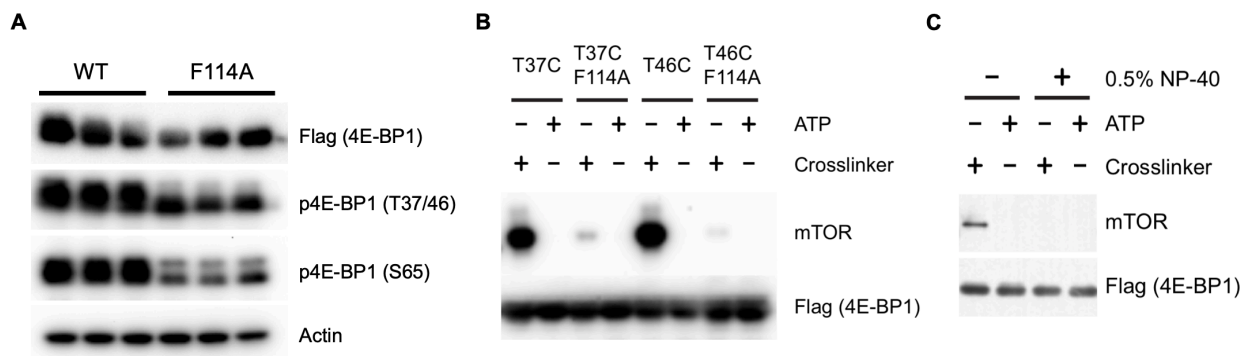
Figure 3.7 | Conditions that Inhibit mTORC1 Activity Prevent PhAXA Pulldown. A) HEK293T cells expressing WT of F114 Flag-4E-BP1 constructs were lysed and Flag-4E-BP1 phosphorylation was analyzed by Western Blot. **B)** F114 is critical for raptor-mediated recruitment of 4E-BP1 to mTOR. Mutation of this residue to alanine reduces pulldown of mTOR using the T37C and T46C probes. **C)** Non- ionic

detergents reduce mTORC1 in vitro activity. mTOR pulldown by the T46C mutant probe is inhibited when cells are lysed in buffer containing NP-40.

To investigate the ability of PhAXA-MS to identify novel 4E-BP1 kinases in HEK293T cells, the FLAG-4E-BP1 (T46C) and WT probes were used to query the kinome present in HEK293T lysate. Following LC-MS/MS analysis, significant enrichment of high-scoring mTOR peptides from the sample prepared from T46C expressing cell lysate treated with the crosslinker 1 was observed, while no mTOR peptides were identified in the ATP only negative control sample and very few were identified in the FLAG-4E-BP1 (WT), crosslinker 1 treated sample (Table 3.3). Specificity of the 3xFLAG 4E-BP1 (T46C) probe is demonstrated in Figure 3.8, which identifies mTOR as one of the most highly enriched proteins among all those identified.

Importantly, MS/MS analysis of proteins crosslinked to each cysteine probe resulted in very few kinases exhibiting significant enrichment over the WT protein. (Table 3.3) Significantly enriched kinases were considered to be those with an average of ≥2-fold enrichment in the T46C, crosslinker treated sample relative to both WT + crosslinker, and T46C + ATP controls. By this metric, two significantly enriched kinases were identified: mTOR, as would be expected, as well as CDK4, which has never been described as a 4E-BP1 kinase. This experiment provided a third example whereby PhAXA-MS identified a *bona fide* kinase as the top hit, and uncovered CDK4 as a potentially novel 4E-BP1 kinase.

| | All Kinases Identified | | | | | | | |
| | AVG PSM | | | | Fold Change (PSMs) | | Fold Change (MS1 Integration) | |
Protein	WT +	WT -	T46C +	T46C -	T46C+/WT+	T46C+/T46C-	T46C+/WT+	T46C+/T46C-
mTOR	12	0	74.5	0	6.21	----	10.8 +/-1.89	----
CDK4	5.5	2.5	11	2	2.00	5.50	2.72 +/-0.63	2.22 +/-0.04
Erk2	3	3.5	6.5	6	2.17	1.08	2.86 +/-0.69	0.80 +/-0.13

Table 3.3 | 4E-BP1 Interacting Kinases Identified by PhAXA-MS. Table of kinases identified by at least two peptides in each biological replicate following filtering of common contaminants.[72] Average peptide-spectrum matches (PSMs) are from two independent biological replicates. '+' refers to samples treated with 1; '-' refers to ATP only controls. Dashes were added for ratios that could not be calculated due to absence of any high scoring PSMs. The ratio of MS1 intensities was determined using Skyline. Fold change is represented as +/- standard deviation (n = 3−13).
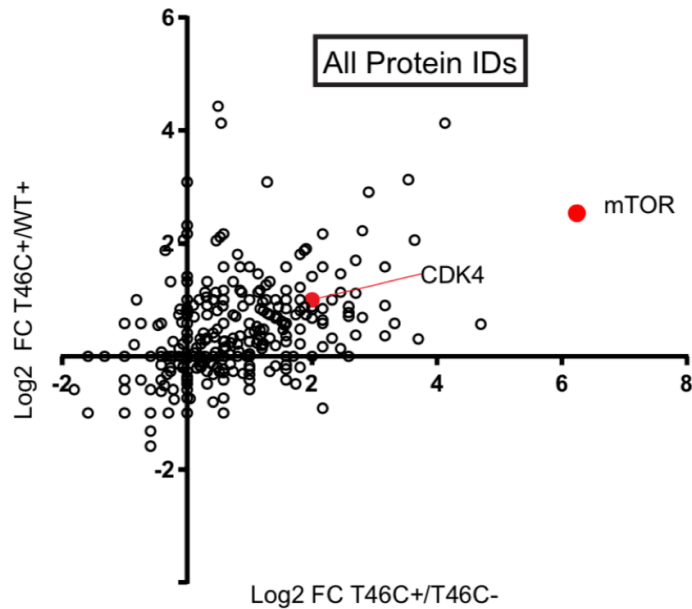
Figure 3.8 | mTOR is Highly Enriched by PhAXA-MS A scatterplot depicting all proteins identified by PhAXA-MS, Log2 fold change of spectral counts for non-filtered proteins plotted for the T46C probe relative to the appropriate controls. 1 PSM was added to each sample before averaging to enable calculation of the fold change for samples with no PSMs.

3.6 Conclusions

The development of a phosphosite accurate crosslinking assay, PhAXA, as described in this chapter represents an important step forward in kinase-targeted activity-based protein profiling. This method has been demonstrated to be broadly applicable across several different classes of bait proteins, including transcription factors, kinases, and intrinsically disordered proteins. Moreover, the phosphocysteine probes used in this assay are suitable for mimicking phosphorylation of serines, threonines and tyrosines. For each of the three examples shown here, PhAXA-MS identified only *bona fide* kinases as significantly enriched relative to control samples, making this the first reported assay capable of reliable kinase assignment in a phosphosite-specific fashion. Though this assay has been successfully implemented, several possible improvements, as well as a few clear limitations, will be discussed in Chapter 6.

3.7 Materials and Methods

Small molecule reagents

Trametinib (Selleckchem), Rapamycin (Alfa Aesar), and SP600125 (ApexBio) were dissolved in DMSO. Human recombinant insulin was purchased from Sigma, PMA (Phorbol-12-Myristate-13-Acetate) was purchased from Acros. Anisomycin was purchased from Cayman Chemical. 3XFLAG peptide was purchased from ApexBio. All reagents were used as received.

Cell Culture

HEK293T cells were grown in DMEM (Corning) supplemented with 10% FBS, glutamine, penicillin, and streptomycin (Gibco). Cells were grown at 37 °C with 5% CO_2 in a humidified incubator, passaged at least twice before use for experiments and no more than 10 times before returning to low passage stocks. All cell lines were authenticated by STR profiling, and regularly tested for mycoplasma contamination.

Plasmids

Annealed oligos corresponding to the N-terminal 3XFLAG tag were ligated into pcDNA3 at BamHI and EcoRI. 4E-BP1 cDNA was purchased from Promega in the pFN29K expression vector. HA-Erk2 (*Rattus norvegicus*) plasmid was generously shared by Dr. Diane Fingar. 4E-BP1, Erk2 and c-Jun were cloned into the pcDNA3/3XFLAG vectors. All mutations were generated by PCR mutagenesis. The sequences for all primers used have been listed in Table 3.4. All constructs were fully sequenced by Sanger sequencing.

ORF	Purpose			Sequence 5' → 3'
Tag	3x-FLAG	to 3xFLAG pcDNA3	Forward	GATCCCCACCATGGACTACAAAGACCATGACGGTGATTATAAAGATCATGACATCGATTACAAGGATGACGATGACAAGG
			Reverse	AATTCCTTGTCATCGTCATCCTTGTAATCGATGTCATGATCTTTATAATCACCGTCATGGTCTTTGTAGTCCATGGTGGG
4E-BP1	Cloning	to 3xFLAG pcDNA3	Forward	CGGAATTCATGTCCGGGGGCAGCAGCT
			Reverse	TGTTCTAGACTATTAAATGTCCATCTCAAACTGTGACTCTT
	Mutagenesis	T37C	Forward	GACTACAGCACGTGCCCCGGCGGCACG
			Reverse	CGTGCCGCCGGGGCACGTGCTGTAGTC
		T46C	Forward	GCTCTTCAGCACCTGCCCGGGAGGTACC
			Reverse	GGTACCTCCCGGGCAGGTGCTGAAGAGC
		S65C	Forward	CTGATGGAGTGTCGGAACTGTCCTGTGACCAAAACACCC
			Reverse	GGGTGTTTTGGTCACAGGACAGTTCCGACACTCCATCAG
		T70C	Forward	GAACTCACCTGTGACCAAATGTCCCCCAAGGGATCTGCCC
			Reverse	GGGCAGATCCCTTGGGGGACATTTGGTCACAGGTGAGTTC
		S101C	Forward	GCCACCTGCGCAATTGCCCAGAAGATAAGC
			Reverse	GCTTATCTTCTGGGCAATTGCGCAGGTGGC
		F114A	Forward	GCGGGCGGTGAAGAGTCACAGGCTGAGATGGACATT
			Reverse	AATGTCCATCTCAGCCTGTGACTCTTCACCGCCCGC
c-Jun	Cloning	to 3xFLAG pcDNA3	Forward	TCGGAATTCATGACTGCAAAGATGGAAACGACC
			Reverse	TGTTCTAGACTATTATCAAAATGTTTGCAACTGCTGCGTT

		C99A	Forward	CCACCCAGTTCCTGGCCCCCAAGAACGTGACAG
			Reverse	CTGTCACGTTCTTGGGGGCCAGGAACTGGGTGG
		S63C	Forward	CGGACCTCCTCACCTGCCCCGACGTGGGG
			Reverse	CCCCACGTCGGGGCAGGTGAGGAGGTCCG
		S73C	Forward	GCTCAAGCTGGCGTGCCCCGAGCTGGAGC
			Reverse	GCTCCAGCTCGGGGCACGCCAGCTTGAGC
	Mutagenesis	T91C	Forward	GGGCACATCACCACCTGTCCGACCCCCACCC
			Reverse	GGGTGGGGGTCGGACAGGTGGTGATGTGCCC
		T93C	Forward	CATCACCACCACGCCGTGCCCCACCCAGTTCC
			Reverse	GGAACTGGGTGGGGCACGGCGTGGTGGTGATG
		T95C	Forward	CCACCACGCCGACCCCCTGCCAGTTCCTGG
			Reverse	CCAGGAACTGGCAGGGGGTCGGCGTGGTGG
		D11WT	Forward	GGAAACGACCTTCTATGACGATGCCCTCAACGCC
			Reverse	GGCGTTGAGGGCATCGTCATAGAAGGTCGTTTCC
rnErk2	Cloning	to 3xFLAG pcDNA3	Forward	AATAGCGGCCGCAATACGCTAGCATGGCGGCG
			Reverse	GCTATCTAGATCAGGCCGCTTGTTAAGATCTGTA
	Mutagenesis	Y185C	Forward	CAGGGTTCTTGACAGAGTGTGTAGCCACGCGTTGG
			Reverse	CCAACGCGTGGCTACACACTCTGTCAAGAACCCTG

Table 3.4 | List of Primers Used for Cloning and Mutagenesis

Immunoblotting

Immunoprecipitates from PhAXA pulldowns, or cell lysates from HEK293T cells were resolved on 4–20% Tris-glycine gels (Invitrogen), transferred to 0.45-μm PVDF (Thermo) using Towbin's buffer (low amperage for ~4 h at 4 °C), blocked with 5% non-fat milk in TBST, then probed with primary antibodies overnight at 4 °C. Antibodies used in this study were the following: Actin-HRP (sc-47778) from Santa Cruz Biotechnology; DYKDDDK tag (14793), MEK1/2 (9122), mTOR (2972), p4E-BP1 (T37/46) (2855), p4E-BP1 (S65/101) (9451), SAPK/Jnk (9252), 4E-BP1 (9644), from Cell Signaling Technology; and FLAG-M2 (F1804) from Sigma.

PhAXA

For Western blot analysis, HEK293T cells were grown in 10-cm plates to 50% confluence and transfected with DNA (6 μg) by calcium phosphate precipitation. 18 h later, the media was changed to serum-free DMEM (4E-BP1 and rnErk2 pulldowns), or growth media (c-Jun pulldown). After 24 h, cells were stimulated as follows: 10 min with growth media containing insulin (150 nM) for 4E-BP1 pulldown, 15 min with growth media containing PMA (100 nM) for rnERK2 pulldown, or 30 min with growth media containing anisomycin (10 μg/μL) for c-Jun pulldown. Cells were then harvested in NLB buffer (1 mL; 50 mM Tris pH 8.0, 150 mM NaCl, 10 mM MgCl$_2$, 10 μg/mL aprotinin, 5 μg/mL leupeptin, 7 μg/mL pepstatin) per plate by scraping. Cells were lysed by forcefully passing through a 28.5G insulin syringe 5× consecutively on ice.

Debris was pelleted at 18,000×g for 10 min at 4 °C. Cleared lysate was split into 500 μL aliquots (×2) in 1.5-mL tubes, and **1** or ATP was added to a final concentration of 250 μM. Lysate was incubated at 30 °C for 60 min under constant agitation. FLAG-BAIT complexes were then isolated by immunoprecipitation for 12–15 h at 4 °C with end-over-end rotation. The resin was subsequently washed 3× for 15 min under constant agitation with 1× TBS containing Triton X-100 (2% v/v), then thrice with TBS for 30 s each; 1 mL was used for each wash. Proteins were eluted with 2× Laemmli buffer and resolved by SDS-PAGE.

For analysis by LC-MS/MS, the protocol is similar to that above with the following modifications: HEK293T cells were grown in 15-cm plates (×4) to 50% confluence and transfected with WT or Cys-mutant plasmid DNA (12 μg per plate) by calcium phosphate precipitation. Each plate was harvested in lysis buffer (2.5 mL), and samples were processed as above through the immunoprecipitation step. We found it critical to keep volumes at 500 μL per tube with 5 tubes per reaction condition. After overnight immunoprecipitation and following the final wash with TBS, complexes were eluted with elution buffer (250 μL; TBS, 0.1% sodium deoxycholate, 1 mg/mL 3XFLAG peptide) per tube. Elutions were carried out for 90 min at 25 °C with constant agitation on a plate shaker (120 rpm). Common eluents were pooled, tricholoracetic acid was added to a final concentration of 10% (w/v), and samples were incubated on ice for 60 min. Tubes were then centrifuged at 21,000×g for 15 min at 4 °C before discarding supernatants. Protein pellets were re-suspended in ice-cold acetone (1.5× eluate volume) for each wash using a water bath sonicator. After another 30 min on ice, the protein was again precipitated and the supernatant discarded. The acetone wash was repeated once more, and the protein pellets were re-suspended in 10 mM HEPES buffer (pH 8.0) containing 8 M urea (50 μL) and immediately frozen at -80 °C until processing by in-solution digestion.

In-solution digestion

Protein samples were treated with ammonium bicarbonate buffer (pH ~8), which was added to a final concentration of 100 mM. Cysteine residues were reduced by adding 10 mM DTT (50 μl) and incubation at 45 °C for 30 min. Samples were cooled to room temperature, and alkylation of cysteines was achieved by incubating with 2-chloroacetamide (65 mM) under darkness for 30 min at room temperature. Upon diluting the urea to a final concentration of <1 M,

overnight digestion with sequencing grade, modified trypsin (1 ug) was carried out at 37 °C. Digestion was stopped by acidification and peptides were desalted using SepPak C18 cartridges using manufacturer's protocol (Waters). Samples were completely dried using a Vacufuge concentrator (Eppendorf).

Mass spectrometry

Peptides resulting from trypsin digestion were dissolved in 0.1% formic acid/2% acetonitrile solution (9 mL). 2 mL of the resulting peptide solution were resolved on a nano-capillary reverse phase column (Acclaim PepMap C18, 2 micron, 50 cm, ThermoScientific) using a 0.1% formic acid/acetonitrile gradient at 300 nl/min over a period of 90 min (in-gel digests) or 180 min (in-solution digests). Eluent was directly introduced into a *Q Exactive HF* mass spectrometer (Thermo Scientific, San Jose CA) using an EasySpray source. MS1 scans were acquired at 60K resolution (AGC target = 3×10^6; max IT = 50 ms). Data-dependent collision-induced dissociation MS/MS spectra were acquired on the 20 most abundant ions following each MS1 scan (NCE ~28%; AGC target = 1×10^5; max IT = 45 ms).

Data analysis

The resulting raw files were converted into mzXML files and centroided using MSConvert.[73] Spectra were searched against the Swiss-Prot Human protein database (2.15.17 Download) appended with all isoforms and cRAP contaminants using the COMET[74] search engine as part of the Trans-Proteomic Pipeline (TPP) (version 5.0).[75] Peptide mass tolerance was set to 10 ppm, fragment bin tolerance to 0.02 Da, and two missed cleavages were allowed. Met oxidation (+15.9949), Ser/Thr/Tyr phosphorylation (+79.966331) and Gln/Asn deamidation (+0.98402) were included as variable modifications; carbamidomethylated Cys (+57.021464) was set as a fixed modification. The resulting pep.xml files were analyzed for peptide probability using PeptideProphet,[76] where a minimum peptide probability of 0.95 was required, with only the expect score used as a discriminant. Protein level validation was performed using ProteinProphet;[77] only proteins with a probability of >0.97 were considered.

Protein-level quantification was performed in two ways to account for the relatively low peptide-spectrum match (PSM) count of observed peptides. First, spectral counts were compiled using Abacus,[30] and the "adjusted spectral count" was used to compare relative protein

concentrations between samples. Each experiment was performed in biological duplicate, and PSMs from each duplicate sample were averaged. Second, relative quantification of proteins using MS1 intensity was accomplished using Skyline.[31] Briefly, spectral libraries were built from amino acid sequences for all kinases meeting initial refinement criteria (see below). MS1 intensities were extracted for proteotypic peptides within a mass error of 10 ppm that eluted within a 10 min window between runs. MS1 intensities were compared between samples where the corresponding peptide was positively identified by PeptideProphet with a probability >0.95. Comparisons were only made between samples that were simultaneously prepared, i.e. only within the first or second replicate, not between replicates. Between 1–15 peptides were compared for each protein depending on the number of positive identifications.

Data refinement

Initial data refinement for kinase identification was performed as follows. Only kinases found with at least 2 PSMs in both biological replicates (where applicable) were considered. These identified proteins were compared to a list of common contaminating proteins using CRAPome.[72] Briefly, a repository was built from the top 20 experiments (in terms of number of positive identified proteins) using FLAG magnetic resin and total cell lysate from HEK293 cells. Any kinase found in more than 75% of these experiments was not considered for further characterization; this removed STK38, STK38L and PRKDC.

Synthesis of Crosslinker 1
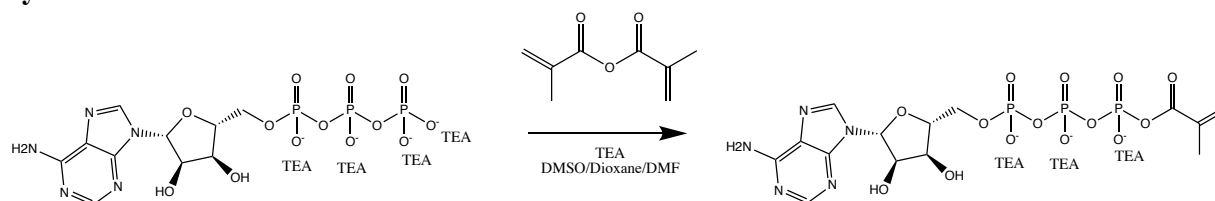
The synthesis of **1** was adapted from that reported.[1] ATP-triethylammonium salt (0.1 g, 0.11 mmol) was dissolved in anhydrous DMSO (3 mL) under nitrogen. A solution of methacrylic anyhydride (0.44 mmol), anhydrous DMSO (1 mL), dioxane (1 mL), anhydrous DMF (1 mL) was added, and the mixture was stirred at room temperature under nitrogen. After 4 d, the reaction was quenched with water (5 mL) and extracted with ethyl acetate (3 × 5 mL). The aqueous layer was collected, flash frozen and lyophilized. Crude **1** was then dissolved in water and purified by

preparative reverse-phase HPLC using an Agilent 1260 Infinity HPLC equipped with a PrepHT XDB-C18 column (21.2 × 150 mm; 5 μm) at a flow rate of 20 mL/min using 100 % water as a mobile phase and detection at 254 nm. Fractions were analyzed off-line using an Agilent Q-TOF HPLC-MS. **1**-containing fractions were pooled and lyophilized to dryness. Purified compound **1** (0.028 g) was subsequently dissolved in D_2O, and the stock concentration was determined by quantitative NMR using a 4,4-dimethyl-4-silapentane-1-sulfonic acid capillary normalized using calcium formate. Single-use aliquots (13.3 mM) were stored at -80 °C.

^{1}H NMR Spectrum of 1

DCM3164_PROTON_01
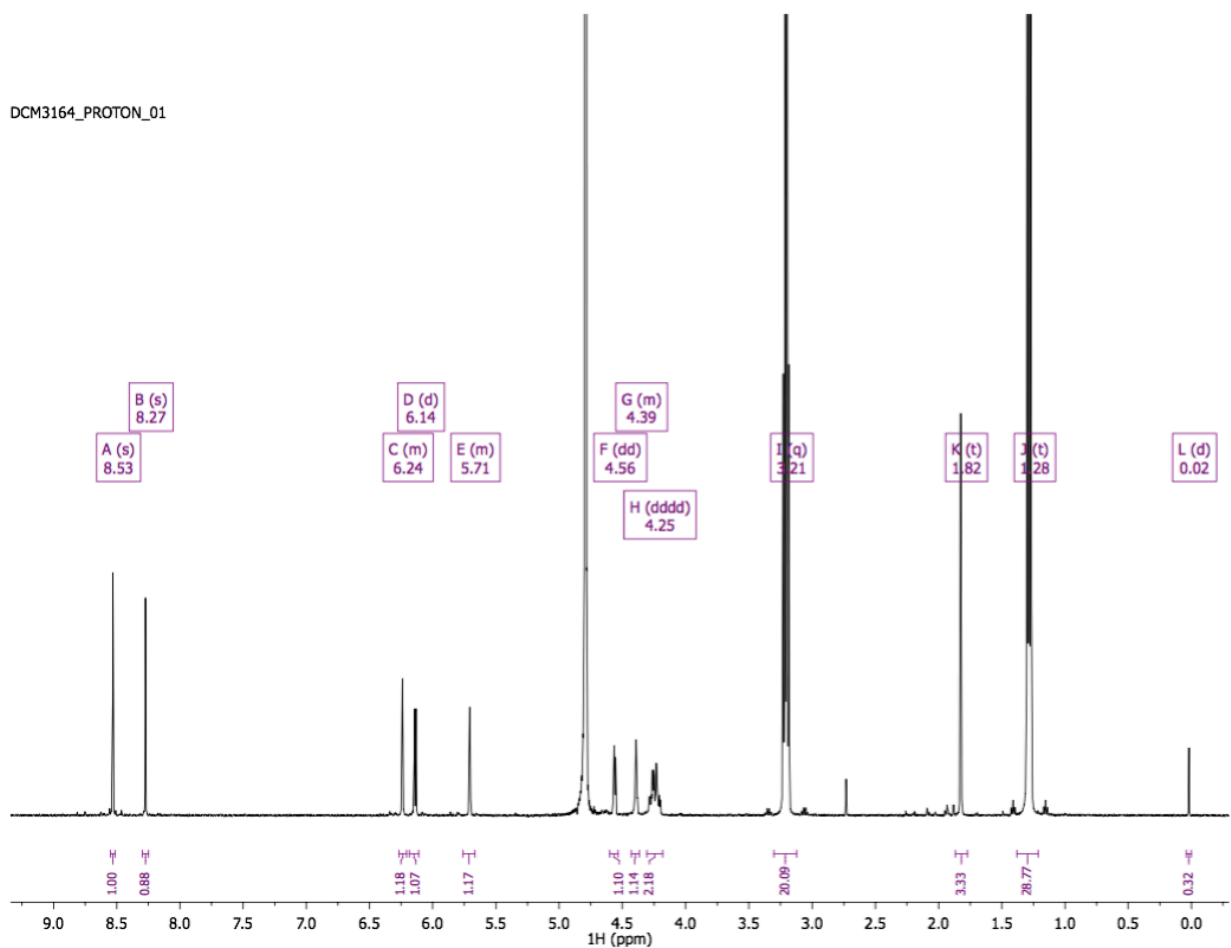
^{31}P NMR Spectrum of 1

DCM3164_PHOSPHORUS_01
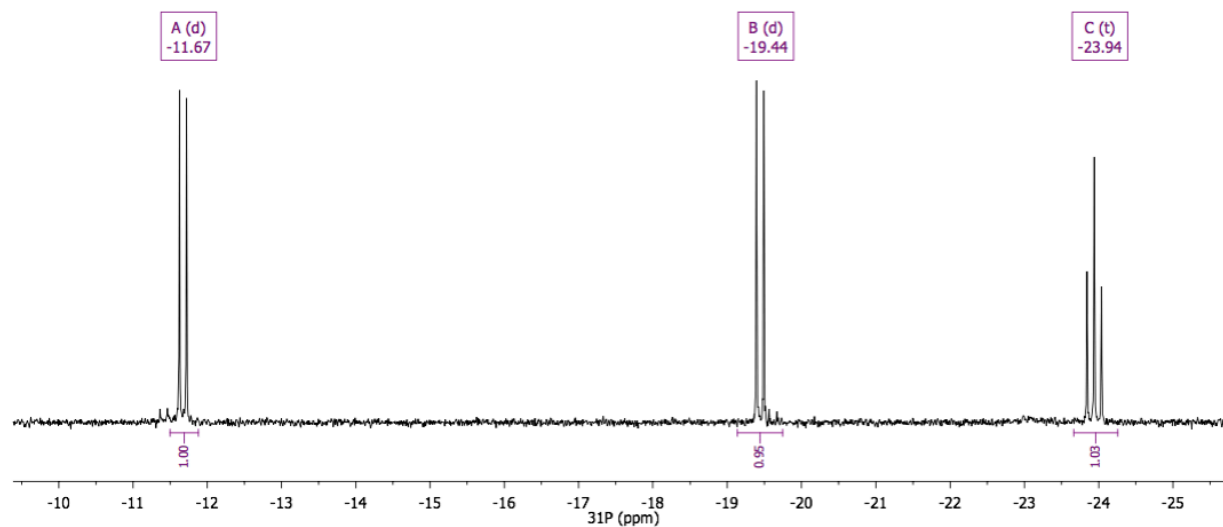
HRMS (ESI-) calcd for 574.0147, found 574.0143 [M-H]
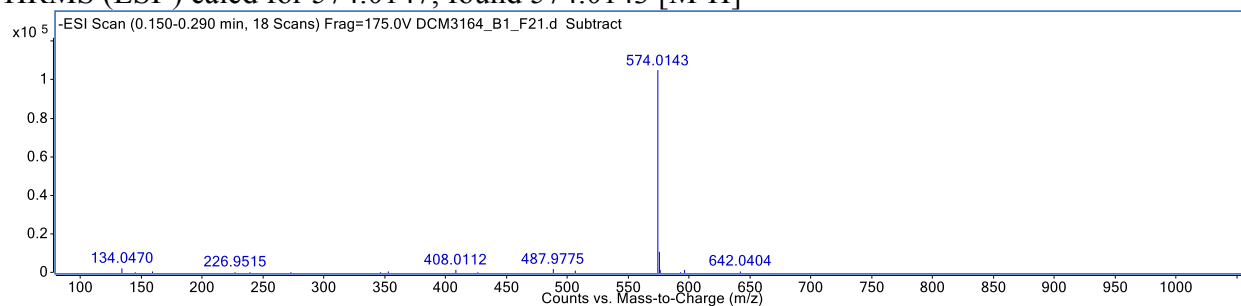
3.8 References

1   Riel-Mehan, M. M. & Shokat, K. M. A crosslinker based on a tethered electrophile for mapping kinase-substrate networks. *Chemistry & biology* **21**, 585-590, doi:10.1016/j.chembiol.2014.02.022 (2014).

2   Biondi, R. M. & Nebreda, A. R. Signalling specificity of Ser/Thr protein kinases through docking-site-mediated interactions. *Biochemical Journal* **372**, 1-13, doi:10.1042/Bj20021641 (2003).

3   Zhou, T. J., Sun, L. G., Humphreys, J. & Goldsmith, E. J. Docking interactions induce exposure of activation loop in the MAP kinase ERK2. *Structure* **14**, 1011-1019, doi:10.1016/j.str.2006.04.006 (2006).

4   Manning, G., Whyte, D. B., Martinez, R., Hunter, T. & Sudarsanam, S. The protein kinase complement of the human genome. *Science* **298**, 1912-+, doi:DOI 10.1126/science.1075762 (2002).

5   Angel, P. *et al.* Phorbol ester-inducible genes contain a common cis element recognized by a TPA-modulated trans-acting factor. *Cell* **49**, 729-739 (1987).

6   Lee, W., Mitchell, P. & Tjian, R. Purified transcription factor AP-1 interacts with TPA-inducible enhancer elements. *Cell* **49**, 741-752 (1987).

7   Aronheim, A., Zandi, E., Hennemann, H., Elledge, S. J. & Karin, M. Isolation of an AP-1 repressor by a novel method for detecting protein-protein interactions. *Molecular and cellular biology* **17**, 3094-3102 (1997).

8   Shaulian, E. & Karin, M. AP-1 in cell proliferation and survival. *Oncogene* **20**, 2390-2400, doi:10.1038/sj.onc.1204383 (2001).

9   Vleugel, M. M., Greijer, A. E., Bos, R., Van der Wall, E. & van Diest, P. J. c-Jun activation is associated with proliferation and angiogenesis in invasive breast cancer. *Hum Pathol* **37**, 668-674, doi:10.1016/j.humpath.2006.01.022 (2006).

10   Jiao, X. *et al.* c-Jun induces mammary epithelial cellular invasion and breast cancer stem cell expansion. *The Journal of biological chemistry* **285**, 8218-8226, doi:10.1074/jbc.M110.100792 (2010).

11   He, H. *et al.* c-Jun/AP-1 overexpression reprograms ERalpha signaling related to tamoxifen response in ERalpha-positive breast cancer. *Oncogene* **37**, 2586-2600, doi:10.1038/s41388-018-0165-8 (2018).

12   Maeda, S. & Karin, M. Oncogene at last - c-Jun promotes liver cancer in mice. *Cancer Cell* **3**, 102-104, doi:Doi 10.1016/S1535-6108(03)00025-4 (2003).

13   Derijard, B. *et al.* Jnk1 - a Protein-Kinase Stimulated by Uv-Light and Ha-Ras That Binds and Phosphorylates the C-Jun Activation Domain. *Cell* **76**, 1025-1037, doi:Doi 10.1016/0092-8674(94)90380-8 (1994).

14   Pulverer, B. J., Kyriakis, J. M., Avruch, J., Nikolakaki, E. & Woodgett, J. R. Phosphorylation of c-jun mediated by MAP kinases. *Nature* **353**, 670-674, doi:10.1038/353670a0 (1991).

15   Behrens, A., Sibilia, M. & Wagner, E. F. Amino-terminal phosphorylation of c-Jun regulates stress-induced apoptosis and cellular proliferation. *Nat Genet* **21**, 326-329, doi:10.1038/6854 (1999).

16   Curtin, J. F. & Cotter, T. G. Anisomycin activates JNK and sensitises DU 145 prostate carcinoma cells to Fas mediated apoptosis. *Br J Cancer* **87**, 1188-1194, doi:10.1038/sj.bjc.6600612 (2002).

17   Gaillard, P. *et al.* Design and synthesis of the first generation of novel potent, selective, and in vivo active (benzothiazol-2-yl)acetonitrile inhibitors of the c-Jun N-terminal kinase. *J Med Chem* **48**, 4596-4607, doi:10.1021/jm0310986 (2005).

18   Zhang, T. *et al.* Discovery of potent and selective covalent inhibitors of JNK. *Chemistry & biology* **19**, 140-154, doi:10.1016/j.chembiol.2011.11.010 (2012).

19   LoGrasso, P. & Kamenecka, T. Inhibitors of c-jun-N-terminal kinase (JNK). *Mini Rev Med Chem* **8**, 755-766 (2008).

20   Siddiqui, M. A. & Reddy, P. A. Small molecule JNK (c-Jun N-terminal kinase) inhibitors. *J Med Chem* **53**, 3005-3012, doi:10.1021/jm9003279 (2010).

21   Bennett, B. L. *et al.* SP600125, an anthrapyrazolone inhibitor of Jun N-terminal kinase. *Proceedings of the National Academy of Sciences of the United States of America* **98**, 13681-13686, doi:10.1073/pnas.251194298 (2001).

22   He, Y. *et al.* Synthesis and SAR of novel quinazolines as potent and brain-penetrant c-jun N-terminal kinase (JNK) inhibitors. *Bioorg Med Chem Lett* **21**, 1719-1723, doi:10.1016/j.bmcl.2011.01.079 (2011).

23   Son, Y., Kim, S., Chung, H. T. & Pae, H. O. Reactive oxygen species in the activation of MAP kinases. *Methods Enzymol* **528**, 27-48, doi:10.1016/B978-0-12-405881-1.00002-1 (2013).

24   Hibi, M., Lin, A. N., Smeal, T., Minden, A. & Karin, M. Identification of an Oncoprotein-Responsive and Uv-Responsive Protein-Kinase That Binds and Potentiates the C-Jun Activation Domain. *Genes & development* **7**, 2135-2148, doi:DOI 10.1101/gad.7.11.2135 (1993).

25   Grollman, A. P. Inhibitors of protein biosynthesis. II. Mode of action of anisomycin. *The Journal of biological chemistry* **242**, 3226-3233 (1967).

26   Kim, D. H. *et al.* MTOR interacts with Raptor to form a nutrient-sensitive complex that signals to the cell growth machinery. *Cell* **110**, 163-175, doi:Doi 10.1016/S0092-8674(02)00808-5 (2002).

27   Widmann, C., Sather, S., Oyer, R., Johnson, G. L. & Dreskin, S. C. In vitro activity of MEKK2 and MEKK3 in detergents is a function of a valine to serine difference in the catalytic domain. *Bba-Protein Struct M* **1547**, 167-173, doi:Doi 10.1016/S0167-4838(01)00183-2 (2001).

28   Reddy, C. E. *et al.* Multisite phosphorylation of c-Jun at threonine 91/93/95 triggers the onset of c-Jun pro-apoptotic activity in cerebellar granule neurons. *Cell Death Dis* **4**, e852, doi:10.1038/cddis.2013.381 (2013).

29   Morton, S., Davis, R. J., McLaren, A. & Cohen, P. A reinvestigation of the multisite phosphorylation of the transcription factor c-Jun. *EMBO J* **22**, 3876-3886, doi:10.1093/emboj/cdg388 (2003).

30   Fermin, D., Basrur, V., Yocum, A. K. & Nesvizhskii, A. I. Abacus: a computational tool for extracting and pre-processing spectral count data for label-free quantitative proteomic analysis. *Proteomics* **11**, 1340-1345, doi:10.1002/pmic.201000650 (2011).

31   MacLean, B. *et al.* Skyline: an open source document editor for creating and analyzing targeted proteomics experiments. *Bioinformatics* **26**, 966-968, doi:10.1093/bioinformatics/btq054 (2010).

32   Jiao, Q. L. *et al.* Advances in studies of tyrosine kinase inhibitors and their acquired resistance. *Molecular Cancer* **17**, doi:ARTN 36 10.1186/s12943-018-0801-5 (2018).

33   Wu, P., Nielsen, T. E. & Clausen, M. H. FDA-approved small-molecule kinase inhibitors. *Trends Pharmacol Sci* **36**, 422-439, doi:10.1016/j.tips.2015.04.005 (2015).

34   Duong-Ly, K. C. *et al.* Kinase Inhibitor Profiling Reveals Unexpected Opportunities to Inhibit Disease-Associated Mutant Kinases. *Cell Rep* **14**, 772-781, doi:10.1016/j.celrep.2015.12.080 (2016).

35   Wu, P., Nielsen, T. E. & Clausen, M. H. Small-molecule kinase inhibitors: an analysis of FDA-approved drugs. *Drug Discov Today* **21**, 5-10, doi:10.1016/j.drudis.2015.07.008 (2016).

36   Zhang, J., Yang, P. L. & Gray, N. S. Targeting cancer with small molecule kinase inhibitors. *Nature reviews. Cancer* **9**, 28-39, doi:10.1038/nrc2559 (2009).

37   Dervisis, N. & Klahn, S. Therapeutic Innovations: Tyrosine Kinase Inhibitors in Cancer. *Veterinary Sciences* **3**, 4, doi:10.3390/vetsci3010004 (2016).

38   Chang, L. & Karin, M. Mammalian MAP kinase signalling cascades. *Nature* **410**, 37-40, doi:10.1038/35065000 (2001).

39   Keshet, Y. & Seger, R. The MAP Kinase Signaling Cascades: A System of Hundreds of Components Regulates a Diverse Array of Physiological Functions. *Map Kinase Signaling Protocols, Second Edition* **661**, 3-38, doi:10.1007/978-1-60761-795-2_1 (2010).

40   Kazlauskas, A. & Cooper, J. A. Protein kinase C mediates platelet-derived growth factor-induced tyrosine phosphorylation of p42. *J Cell Biol* **106**, 1395-1402 (1988).

41   Ray, L. B. & Sturgill, T. W. Rapid Stimulation by Insulin of a Serine Threonine Kinase in 3t3-L1 Adipocytes That Phosphorylates Microtubule-Associated Protein-2 Invitro. *Proceedings of the National Academy of Sciences of the United States of America* **84**, 1502-1506, doi:DOI 10.1073/pnas.84.6.1502 (1987).

42   Cooper, J. A., Bowen-Pope, D. F., Raines, E., Ross, R. & Hunter, T. Similar effects of platelet-derived growth factor and epidermal growth factor on the phosphorylation of tyrosine in cellular proteins. *Cell* **31**, 263-273 (1982).

43   Cobb, M. H., Boulton, T. G. & Robbins, D. J. Extracellular signal-regulated kinases: ERKs in progress. *Cell Regul* **2**, 965-978, doi:10.1091/mbc.2.12.965 (1991).

44   Boulton, T. G. *et al.* An insulin-stimulated protein kinase similar to yeast kinases involved in cell cycle control. *Science* **249**, 64-67 (1990).

45   Pelech, S. L. & Sanghera, J. S. Mitogen-activated protein kinases: versatile transducers for cell signaling. *Trends in biochemical sciences* **17**, 233-238 (1992).

46   Chambard, J. C., Lefloch, R., Pouyssegur, J. & Lenormand, P. ERK implication in cell cycle regulation. *Biochim Biophys Acta* **1773**, 1299-1310, doi:10.1016/j.bbamcr.2006.11.010 (2007).

47   Monick, M. M. *et al.* Active ERK contributes to protein translation by preventing JNK-dependent inhibition of protein phosphatase 1. *J Immunol* **177**, 1636-1645 (2006).

48   Morley, S. J. & Traugh, J. A. Differential stimulation of phosphorylation of initiation factors eIF-4F, eIF-4B, eIF-3, and ribosomal protein S6 by insulin and phorbol esters. *The Journal of biological chemistry* **265**, 10611-10616 (1990).

49   Luciano, F. *et al.* Phosphorylation of Bim-EL by Erk1/2 on serine 69 promotes its degradation via the proteasome pathway and regulates its proapoptotic function. *Oncogene* **22**, 6785-6793, doi:10.1038/sj.onc.1206792 (2003).

50   McCubrey, J. A. *et al.* Roles of the Raf/MEK/ERK pathway in cell growth, malignant transformation and drug resistance. *Bba-Mol Cell Res* **1773**, 1263-1284, doi:10.1016/j.bbamcr.2006.10.001 (2007).

51   Payne, D. M. *et al.* Identification of the regulatory phosphorylation sites in pp42/mitogen-activated protein kinase (MAP kinase). *EMBO J* **10**, 885-892 (1991).

52   Butch, E. R. & Guan, K. L. Characterization of ERK1 activation site mutants and the effect on recognition by MEK1 and MEK2. *The Journal of biological chemistry* **271**, 4230-4235 (1996).

53   Caunt, C. J., Sale, M. J., Smith, P. D. & Cook, S. J. MEK1 and MEK2 inhibitors and cancer therapy: the long and winding road. *Nature reviews. Cancer* **15**, 577-592, doi:10.1038/nrc4000 (2015).

54   Shaul, Y. D. & Seger, R. The MEK/ERK cascade: from signaling specificity to diverse functions. *Biochim Biophys Acta* **1773**, 1213-1226, doi:10.1016/j.bbamcr.2006.10.005 (2007).

55   Canagarajah, B. J., Khokhlatchev, A., Cobb, M. H. & Goldsmith, E. J. Activation mechanism of the MAP kinase ERK2 by dual phosphorylation. *Cell* **90**, 859-869 (1997).

56   Zhou, B. & Zhang, Z. Y. The activity of the extracellular signal-regulated kinase 2 is regulated by differential phosphorylation in the activation loop. *Journal of Biological Chemistry* **277**, 13889-13899, doi:10.1074/jbc.M200377200 (2002).

57   Robbins, D. J. *et al.* Regulation and properties of extracellular signal-regulated protein kinases 1 and 2 in vitro. *The Journal of biological chemistry* **268**, 5097-5106 (1993).

58   Gause, K. C. *et al.* Effects of Phorbol Ester on Mitogen-Activated Protein-Kinase Kinase-Activity in Wild-Type and Phorbol Ester-Resistant El4 Thymoma Cells. *Journal of Biological Chemistry* **268**, 16124-16129 (1993).

59   Bradshaw, C. D. *et al.* Effects of phorbol ester on phospholipase D and mitogen-activated protein kinase activities in T-lymphocyte cell lines. *Immunol Lett* **53**, 69-76, doi:Doi 10.1016/S0165-2478(96)02614-4 (1996).

60   Knoepp, S. M. *et al.* Synergistic effects of insulin and phorbol ester on mitogen-activated protein kinase in rat-1 HIR cells. *Journal of Biological Chemistry* **271**, 1678-1686, doi:DOI 10.1074/jbc.271.3.1678 (1996).

61   Yamaguchi, T., Kakefuda, R., Tajima, N., Sowa, Y. & Sakai, T. Antitumor activities of JTP-74057 (GSK1120212), a novel MEK1/2 inhibitor, on colorectal cancer cell lines in vitro and in vivo. *Int J Oncol* **39**, 23-31, doi:10.3892/ijo.2011.1015 (2011).

62   Zhao, Z., Xie, L. & Bourne, P. E. Insights into the binding mode of MEK type-III inhibitors. A step towards discovering and designing allosteric kinase inhibitors across the human kinome. *PloS one* **12**, doi:ARTN e0179936 10.1371/journal.pone.0179936 (2017).

63   Hatzivassiliou, G. *et al.* Mechanism of MEK inhibition determines efficacy in mutant KRAS- versus BRAF-driven cancers. *Nature* **501**, 232-236, doi:10.1038/nature12441 (2013).

64   Coffman, K. *et al.* Characterization of the Raptor/4E-BP1 interaction by chemical cross-linking coupled with mass spectrometry analysis. *The Journal of biological chemistry* **289**, 4723-4734, doi:10.1074/jbc.M113.482067 (2014).

65   Nojima, H. *et al.* The mammalian target of rapamycin (mTOR) partner, raptor, binds the mTOR substrates p70 S6 kinase and 4E-BP1 through their TOR signaling (TOS) motif. *The Journal of biological chemistry* **278**, 15461-15464, doi:10.1074/jbc.C200665200 (2003).

66   Schalm, S. S. & Blenis, J. Identification of a conserved motif required for mTOR signaling. *Curr Biol* **12**, 632-639 (2002).

67   Schalm, S. S., Fingar, D. C., Sabatini, D. M. & Blenis, J. TOS Motif-Mediated Raptor Binding Regulates 4E-BP1 Multisite Phosphorylation and Function. *Current Biology* **13**, 797-806, doi:10.1016/s0960-9822(03)00329-4 (2003).

68   Gingras, A.-C. *et al.* Regulation of 4E-BP1 phosphorylation: a novel two-step mechanism. *Genes & development* **13**, 1422-1437 (1999).

69   Shah, O. J., Anthony, J. C., Kimball, S. R. & Jefferson, L. S. 4E-BP1 and S6K1: translational integration sites for nutritional and hormonal information in muscle. *Am J Physiol Endocrinol Metab* **279**, E715-729, doi:10.1152/ajpendo.2000.279.4.E715 (2000).

70   Kang, S. A. *et al.* mTORC1 phosphorylation sites encode their sensitivity to starvation and rapamycin. *Science* **341**, 1236566, doi:10.1126/science.1236566 (2013).

71   Apsel, B. *et al.* Targeted polypharmacology: discovery of dual inhibitors of tyrosine and phosphoinositide kinases. *Nature chemical biology* **4**, 691-699, doi:10.1038/nchembio.117 (2008).

72   Mellacheruvu, D. *et al.* The CRAPome: a contaminant repository for affinity purification-mass spectrometry data. *Nature methods* **10**, 730-736, doi:10.1038/nmeth.2557 (2013).

73   Holman, J. D., Tabb, D. L. & Mallick, P. Employing ProteoWizard to Convert Raw Mass Spectrometry Data. *Curr Protoc Bioinformatics* **46**, 13 24 11-19, doi:10.1002/0471250953.bi1324s46 (2014).

74   Eng, J. K., Jahan, T. A. & Hoopmann, M. R. Comet: an open-source MS/MS sequence database search tool. *Proteomics* **13**, 22-24, doi:10.1002/pmic.201200439 (2013).

75   Deutsch, E. W. *et al.* A guided tour of the Trans-Proteomic Pipeline. *Proteomics* **10**, 1150-1159, doi:10.1002/pmic.200900375 (2010).

76   Keller, A., Nesvizhskii, A. I., Kolker, E. & Aebersold, R. Empirical statistical model to estimate the accuracy of peptide identifications made by MS/MS and database search. *Analytical chemistry* **74**, 5383-5392, doi:10.1021/ac025747h (2002).

77   Nesvizhskii, A. I., Keller, A., Kolker, E. & Aebersold, R. A statistical model for identifying proteins by tandem mass spectrometry. *Analytical chemistry* **75**, 4646-4658, doi:10.1021/ac0341261 (2003).

Chapter 4

Validation of CDK4 as a 4E-BP1 Kinase

4.1 Abstract

PhAXA-MS analysis of 4E-BP1 kinases uncovered an interesting interaction between CDK4 and 4E-BP1 that had previously never been identified. This chapter will discuss the background of CDK4 biology, the application of CDK4 inhibitors as a cancer therapy, and the validation of CDK4 as a 4E-BP1 kinase. Through mechanistic evaluation of CDK4-4E-BP1 signaling, a new insight into the regulation of the oncogene c-Myc is uncovered, and preliminary evidence of a phosphorylation site-based biomarker for CDK4/6 inhibitors is provided. The discovery of this novel signaling axis sheds new light on the mechanisms by which CDK4/6 inhibitors control cell proliferation and constitutes the first example of successful kinase discovery using an activity-based, kinase-directed probe.

4.2 Cell Cycle Regulation and the Role of CDK4

Coordinated regulation of cell cycle progression is essential for the cell growth and proliferation. Three well-defined checkpoints exist within the several phases of the cell cycle: 1) between G1 and S phases, also known as the "restriction point;" 2) between G2 phase and mitosis; 3) the intra-mitotic checkpoint. (Figure 4.1A) Each of these transitions is regulated by signaling events that provide quality control over cellular contents, thereby preventing malignant transformation. However, dysregulation of this process is a hallmark of cancer progression, and occurs through a variety of mechanisms. One common mechanism by which cells maintain unchecked cell cycle progression is via over activity of the CDK4/6-RB1/E2F signaling axis.

CDK4 and CDK6 are homoglogous serine/threonine kinases that, in concert with the D-type cyclins, phosphorylate several substrates to drive cell cycle progression through the restriction point at the end of G1 phase.[1] The most notable CDK4/6 substrate is the retinoblastoma-associated protein (pRb), a tumor suppressor that negatively regulates of E2F, a family of master regulators that drive the cell-cycle dependent transcriptional program.[2] When hypophosphorylated, pRb sequesters E2F, preventing cell-cycle progression.[3-5] However, when pRb is hyperphosphorylated by CDK4/6-Cyclin D complexes, the interaction is disrupted, and E2F proteins facilitate the transcription of many genes that contribute to cell proliferation, including cyclin A, CDK2, thymidine kinase, cdc2, and cdc25a.[6,7] (Figure 4.1B)
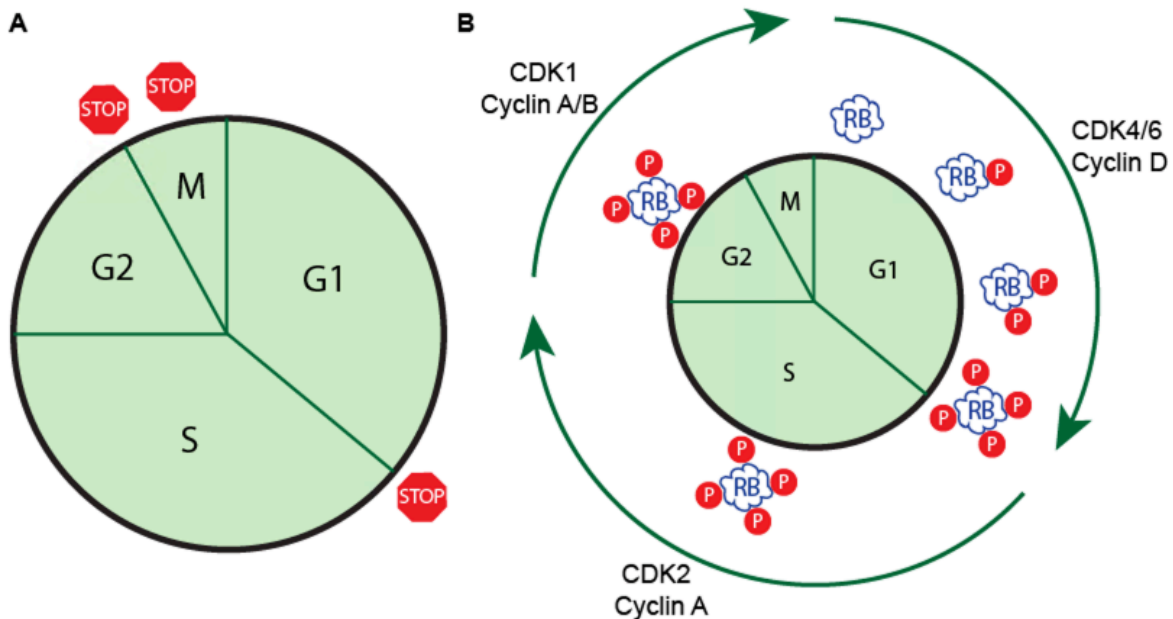
Figure 4.1 | Cell Cycle Checkpoints and the Role of CDK4 A) The three main cell cycle checkpoints are shown (red STOP signs) in relation to the main cell cycle phases: G1 – Gap 1 phase; S – Synthesis phase; G2 – Gap 2 phase; M – Mitosis **B)** A simplified scheme of the CDK-Cyclin complexes that regulate phosphorylation of pRb at during each phase of the cell cycle.

4.3 CDK4/6 Inhibitors in the Treatment of Cancers

A built-in regulatory mechanism exists with the naturally occurring CDK4/6 inhibitor p16, which normally inhibits CDK4/6-Cyclin D complexes, thus enforcing the G1→S restriction point.[8,9] However, p16 is commonly lost in cancer, giving rise to dysregulated pRb phosphorylation.[10] Restoration of p16 expression induces a G1 arrest in a number of cancer cell lines via reactivation of pRb, and sequestration of the E2F transcription factors.[11-13] These findings, in tandem with the role of CDK4/6 in driving cell proliferation

in many cancers, led to the development of several selective CDK4/6 inhibitors, including palbociclib,[14] ribociclib,[15] and abemaciclib.[16]

While CDK4/6 inhibitors have had only marginal efficacy as single-agent therapies,[17] they have achieved great success as part of combination treatments. Each of the three inhibitors has been approved for treating HR+/HER2- breast cancer in combination with endocrine therapies, which were the previous standard of care for this patient cohort.[18,19] As success with these combinations was realized, preclinical studies identified more viable combinations with CDK4/6 targeted therapies in a variety of cancer types and backgrounds. These include combinations with chemotherapy regimens,[20] radiation,[21] and with MEK inhibitors for Ras-driven cancers.[22-25] however, the most striking finding comes from several groups that have uncovered synergy between CDK4/6 and mTOR pathway inhibitors, often from unbiased inhibitor screens.[26-35] This combination has shown promising enough to move into phase I and II clinical trials.

Biomarkers that predict the efficacy of CDK4/6 inhibitors have not come easily, limiting the ultimate benefit of these drugs.[36,37] Presence of pRb seems to be necessary, but not this marker alone is not sufficient for patient stratification.[38] This may be due to a disconnect between pRb inactivation and deletion (and likewise homozygous vs heterozygous deletions), as this distinction has been shown to make a difference in progression and it might make a difference in biomarker as well.[39] Other biomarkers, such as p16, CCND1, CCND3 and CDK4 have not translated to clinical success. Therefore, given the potential of these inhibitors, more efforts need to be put into identification of suitable biomarkers by which to select the appropriate patients receiving these drugs.

4.4   4E-BP1 is a CDK4 Substrate

To validate relationship between CDK4 and 4E-BP1, the activity of CDK4 towards 4EBP1 at each well-documented 4E-BP1 phosphorylation site was investigated using PhAXA. (Figure 4.2) Indeed, CDK4 was enriched from lysate expressing the T37C, T46C, T70C, and S101C cysteine-mutant probes, though showed no increase in activity towards S65C. Of note, due to the small size of CDK4, successful crosslinking to 4E-BP1 initiates a large mass-shift on a denaturing, reducing, SDS-PAGE gel, further suggesting an on-target mode of action of these probes.
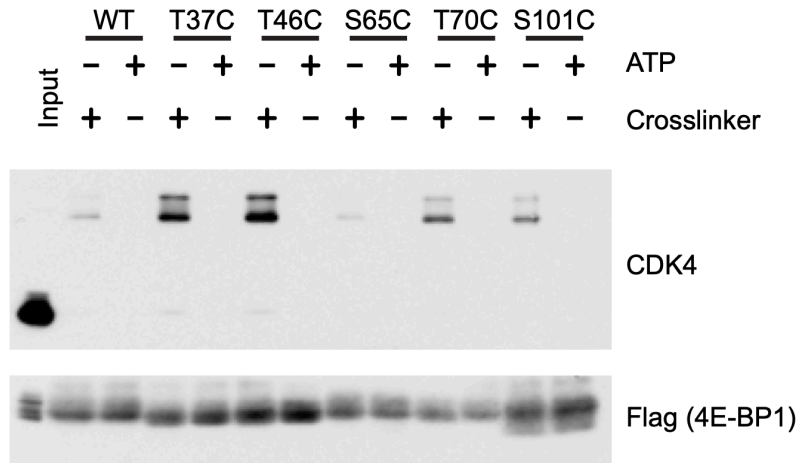
Figure 4.2 | CDK4 is Enriched by 4E-BP1 Using PhAXA CDK4 is pulled down from lysate expressing 3x-FLAG-4E-BP1 phosphosite-to-Cys mutants when treated with crosslinker. A representative input is shown to demonstrate the mass-shift of CDK4 upon crosslinking to 4E-BP1.

Each CDK associates with a specific subset of binding proteins, the cyclins, that are required for kinase activity by providing substrate specificity via recognition of a required RXL motif.[1,40] 4E-BP1 contains one RXL motif ($R^{73}DL$) in a region of the protein that is free in solution while bound to eIF4E.[41] CDK4 also demonstrates substrate specificity via recognition of the consensus sequence Ser/Thr-Pro with optimal substrates containing one or more basic amino acids downstream of this motif. 4E-BP1 has several phosphosites that fit the optimal CDK4 motif, including Thr10, Ser65, Thr70 and S101; while Thr37, Thr46 and S83 contain the minimal S/T-P motif. Moreover, 4E-BP1 can be found in the nucleus as well as the cytoplasm (Figure 4.3),[42] providing evidence that a difference in subcellular localization would not prevent CDK4 from phosphorylating 4E-BP1.[43]
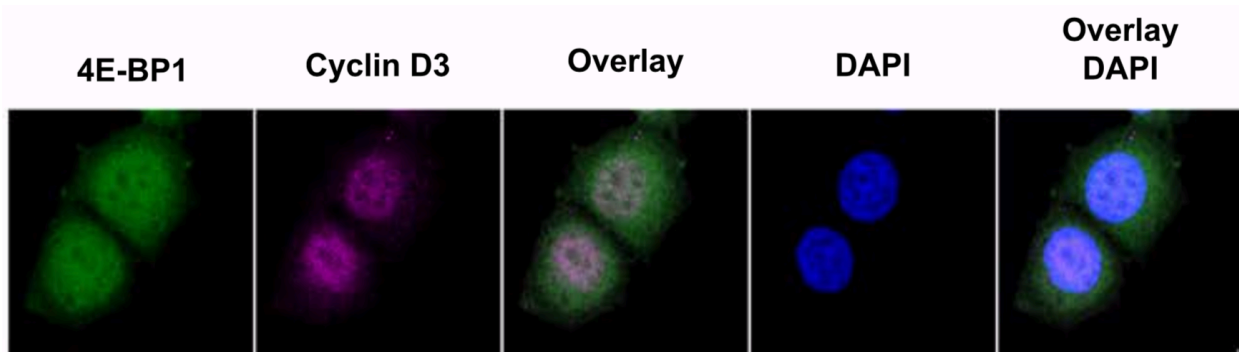
Figure 4.3 | 4E-BP1 and Cyclin D3 are Present in Common Cellular Compartments. Immunofluorescence imaging shows 4E-BP1 is present in the nucleus and cytoplasm, while cyclin D3 is mostly localized to the nucleus

CDK4 associates with cyclins D1, D2 and D3; thus, *in vitro* kinase assays were performed with each of these complexes. The presence of a D-cyclin proved necessary for CDK4 activity, and large differences in the *in vitro* activities of each CDK4−cyclin D complex were observed, with CDK4−cyclin D3 demonstrating the greatest kinase activity (Figure 4.4A). However, CDK4 appears to associate with D3 more readily than D1 or D2 so this may account for the perceived increase in activity. Nevertheless, these complexes efficiently phosphorylated 4E-BP1 at each of the canonical mTOR phosphorylation sites. No *in vitro* activity was observed with any of the three CDK6−cyclin D complexes (not shown). To verify that the activity observed was due to CDK4 and not a co-purifying kinase, the highly selective active site CDK4/6 inhibitor palbociclib[14] was used in this assay. Phosphorylation of 4E-BP1 was inhibited at concentrations between 5−50 nM, mirroring the reported *in vitro* IC_{50} value (Figure 4.4B),[14] providing additional confidence in our finding that 4E-BP1 is a CDK4 substrate.
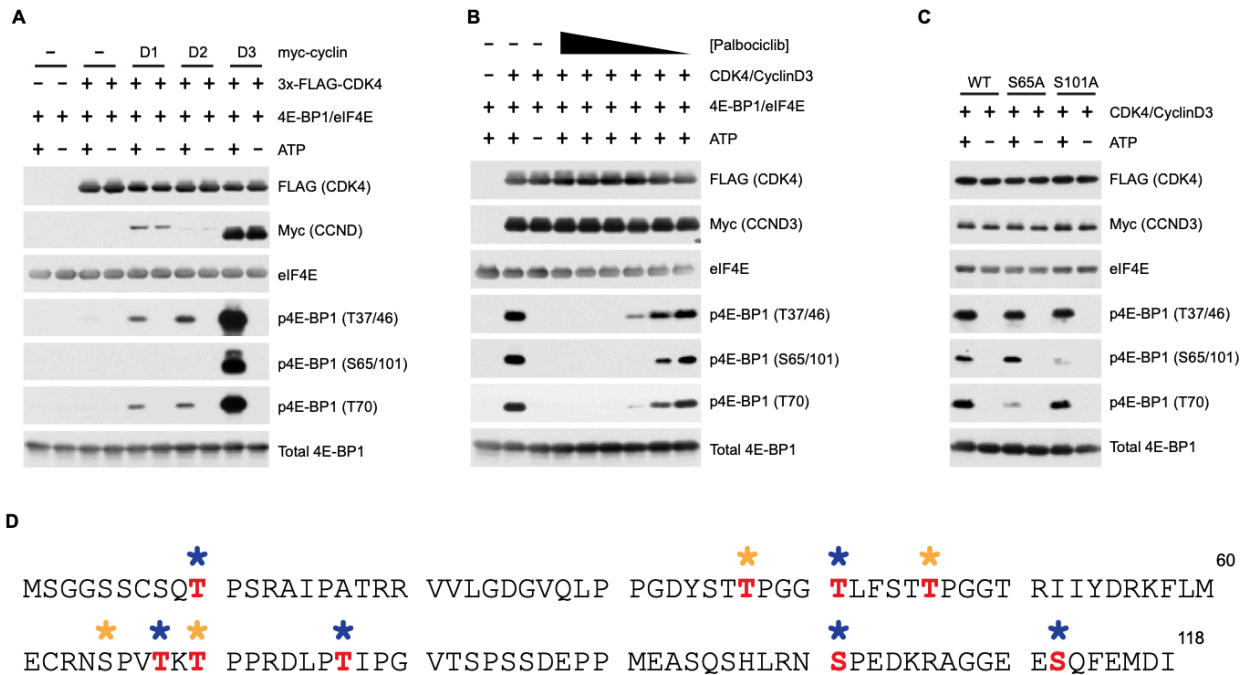
Figure 4.4 | CDK4-Cyclin D Complexes Phosphorylate 4E-BP1 *in vitro*. A) Immunopurified Flag-CDK4/myc-Cyclin D complexes phosphorylate recombinant 4E-BP1 *in vitro*. **B)** Palbociclib (50 μM – 500 pM) inhibits *in vitro* phosphorylation of 4E-BP1 by CDK4−cyclin D3. **C)** *In vitro* kinase assay using WT, S65A and S101A 4E-BP1 substrates phosphorylated by immunoprecipitated CDK4−cyclin D3 complexes. **D)** MS analysis of *in vitro* phosphorylated 4E-BP1 by cyclin D3/CDK4. Phospho-sites identified following manual curation of MS/MS assignments (See Methods) from ATP-treated sample are shown in red. No

suitable phospho-peptides were identified in the no ATP control sample. Gold asterisk = canonical mTORC1 sites, Blue asterisk = non-canonical phosphorylation sites.

S101 is a poorly studied 4E-BP1 phosphosite;[44] however, a large phosphoproteomics study observed hyperphosphorylation of this site in response to rapamycin treatment, suggesting a potential mechanism of resistance to mTORC1 inhibition.[45] Given the enrichment of CDK4 with the S101C mutant and its lack of activity with S65C (Figure 4.2), the activity of CDK4 towards S101 was explored by *in vitro* kinase assay. Due to high sequence similarity between these sites, phospho-specific antibodies recognize both phosphosites; thus, the relative contribution of each phosphorylation event was determined using Ser→Ala mutants (Figure 4.4C). Interestingly, the signal observed for phosphorylation at S65/101 was unaffected by mutation of S65; however, it was diminished with the S101A mutant. CDK4 was further validated as a S101 kinase using PhAXA, which, when analyzed by MS, identified only CDK4 and ERK2 as enriched in the S101C mutant over the controls (Table 4.1). While ERK2 is known to phosphorylate free 4E-BP1 *in vitro*, this relationship has never been validated *in vivo* or in cells.[46] CDK4−cyclin D3-mediated 4E-BP1 phosphorylation was also analyzed via phosphoproteomics, which confirmed S101 as a CDK4 substrate in addition to uncovering several potential non-canonical phosphorylation sites (Figure 4.4D). Some of the sites do not fit the CDK4 recognition motif, which may be due to STK38, a common contaminating kinase in FLAG pulldowns.[47]

Protein	AVG PSM				Fold Change (PSMs)		Fold Change (MS1 Integration)	
	WT +	WT -	S101C +	S101C -	S101C+/WT+	S101C+/S101C-	S101C+/WT+	S101C+/S101C-
CDK4	4	0	5	2	1.25	2.5	1.29	3.29
Erk2	0	0	3	2	----	1.5	----	3.99
mTOR	3	0	2	0	0.667	----	1.34	----
MAK	0	2	0	0	----	----	----	----

Table 4.1 | 4E-BP1 (S101) Kinases Identified by PhAXA-MS. Table of all kinases identified by at least two peptides in at least one sample after filtering of common contaminants. This is a single biological replicate. Ratio of MS1 intensities were determined using Skyline.

4E-BP1 is known to be phosphorylated in an ordered fashion;[48] however, the role of S101 in the hierarchy has not been established. To probe this, non-phosphorylatable

Ala mutants were expressed in HEK293T cells. A near-complete loss of signal at S65/101 in S101A transfected cells was observed, whereas S65A-transfected cells showed only a modest decrease compared to the control (Figure 4.5A). Intriguingly, S101, which is highly conserved across mammals (Figure 4.5B), has a robust effect on global 4E-BP1 function, with S101A showing marked decrease in phosphorylation at each site that was investigated. This indicates a previously unknown reliance upon S101 and its role in initiating or maintaining the inactivation of 4E-BP1.
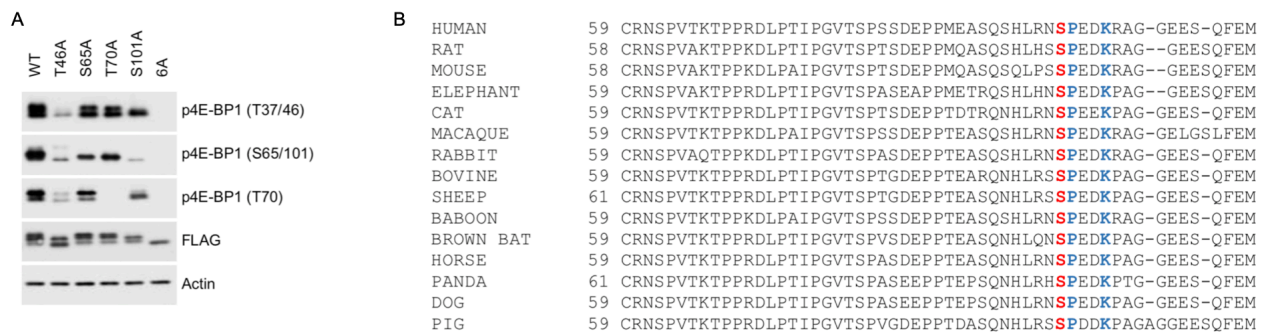
Figure 4.5 | S101 is Highly Conserved and Affects Global 4E-BP1 Phosphorylation. A)

4.5 CDK4 Promotes Rapamycin-Resistant 4E-BP1 Phosphorylation

To further characterize CDK4–cyclin D-mediated inactivation of 4E-BP1, overexpression studies were performed. HEK293T cells were transfected with FLAG-CDK4 and/or myc-Cyclin D2/D3 before stimulating with serum and insulin. Cells expressing cyclin D2 or D3 showed increased phosphorylation of 4E-BP1, an effect that became more evident in cells also treated with rapamycin (Figure 4.5A). Based on the *in vitro* kinase assay and PhAXA data shown above, this phenotype likely extends primarily to the non-canonical phosphosites such as S101, as other sites were largely unaffected.
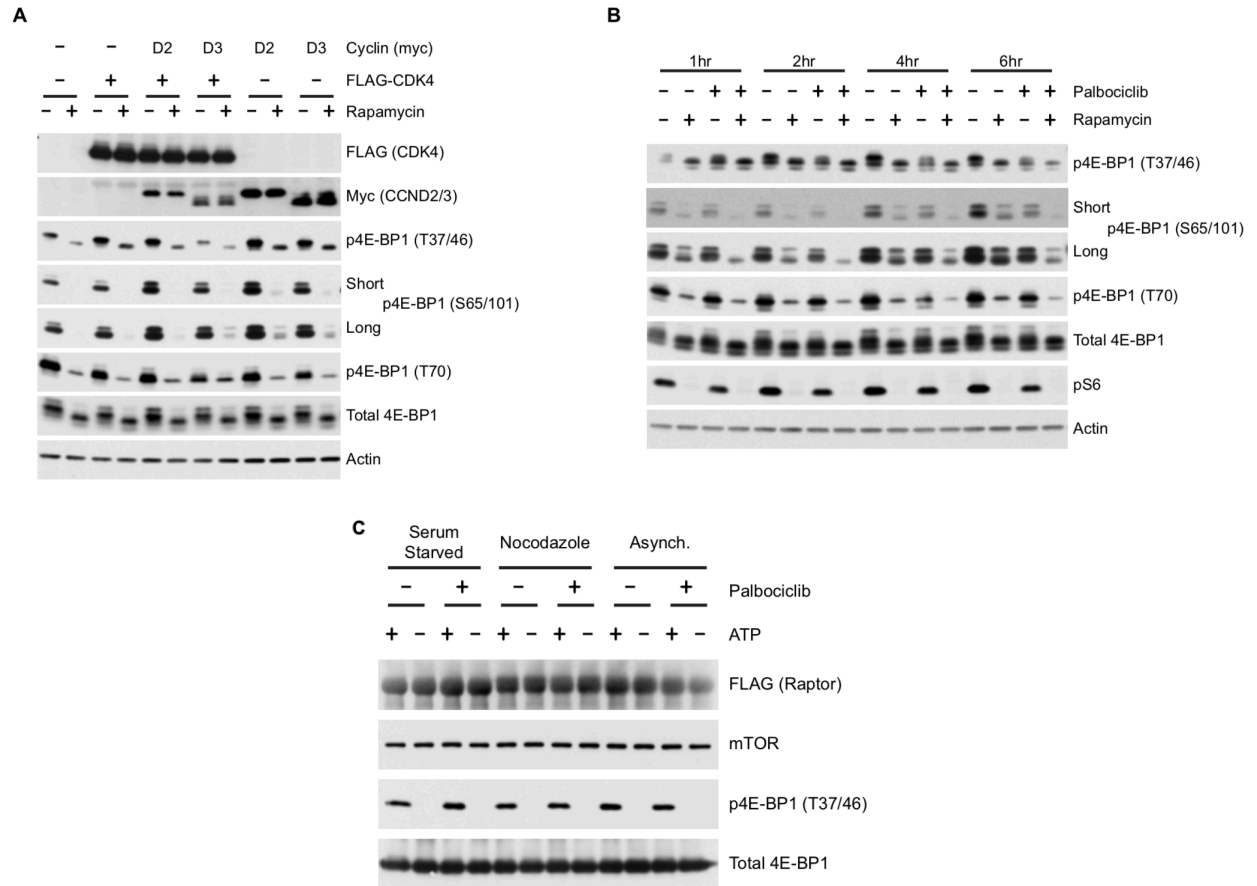
Figure 4.6 | CDK4 Promotes Rapamycin-Resistant 4E-BP1 Phosphorylation. A) Western blots of 3xFLAG-CDK4 and/or myc-D-cyclin transfected 293Ts stimulated with serum and insulin (150 nM) for 2 h with rapamycin (100 nM) or DMSO following 24-hour serum deprivation. **B)** 293Ts were deprived of serum for 24 h, followed by stimulation with media containing serum and insulin (150 nM), with or without rapamycin (100 nM) and/or palbociclib (5 μM) for the indicated duration. **C)** *In vitro* activity of immunopurified mTORC1 from serum starved, mitotic, or asynchronously 293Ts using recombinant, full length 4E-BP1 (pre-incubated with HaloTag-eIF4E) as a substrate. Palbociclib (5 μM) was included in all buffers where appropriate after treating cells for 2-hours.

Next, the role CDK4 in the previously observed, time-sensitive, rapamycin-resistant phosphorylation of 4E-BP1 was assessed.[49] HEK293T cells were treated with rapamycin and palbociclib following serum starvation, and 4E-BP1 phosphorylation was monitored over time. At 2 h post stimulation, reduced phosphorylation at S65/101 was observed, indicated by a decrease in the highly phosphorylated, slow migrating phosphoform (Figure 4.6B). 6 h post-treatment, S65/101 phosphorylation was nearly restored in cells treated with rapamycin alone; those treated with the combination, however, showed a marked decrease in phosphorylation. Interestingly, most other sites for which

phosphorylation-specific antibodies exist were only slightly affected by this co-treatment, strengthening the link between CDK4 and S101 phosphorylation (Figure 4.6B). This decrease in 4E-BP1 phosphorylation was accompanied by a decrease in cyclin D2, the translation of which has been demonstrated to be cap-dependent.[50] No changes in the phosphorylation of ribosomal protein S6 (a common readout of mTORC1 activity) were observed, verifying that palbociclib does not affect mTORC1 activity (Figure 4.6B). Additionally, the no changes were observed in the *in vitro* activity of mTORC1 isolated from palbociclib-treated cells (Figure 4.6C). These experiments clearly demonstrate that CDK4 phosphorylates 4E-BP1 in HEK293T cells under the same conditions in which PhAXA identified CDK4. Thus, these cumulative results serve as validation and strengthen the applicability of this assay to identify novel, physiologically relevant kinases.
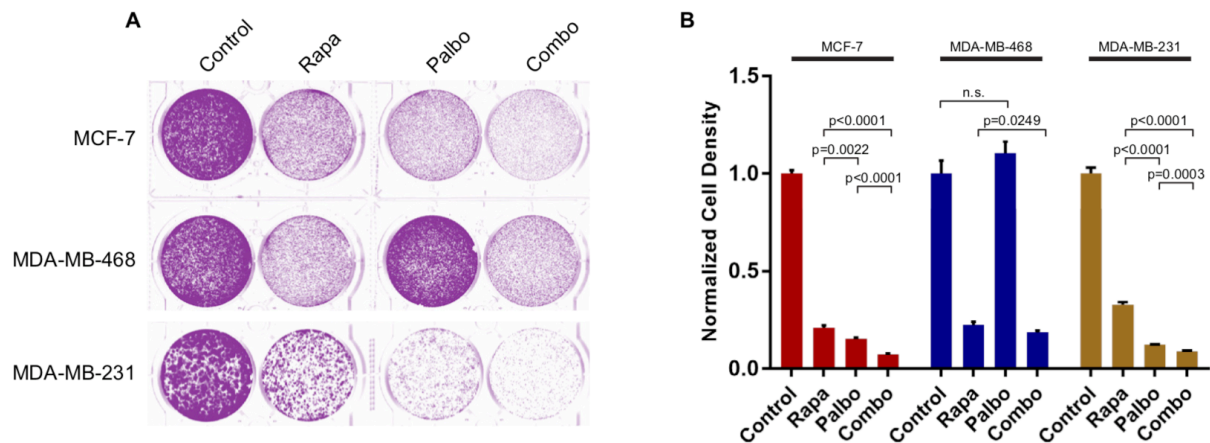
Figure 4.7 | Verification of Palbociclib and Rapamycin Sensitivity in Cell Lines. A) Colony formation of MCF-7, MDA-MB-468 and MDA-MB-231 cell lines treated with rapamycin (100 nM) and/or palbociclib (1 μM) for 10 days. **B)** Quantification of cell density from (**A**). Signal intensity is normalized relative to the no treatment control for each cell line. Error bars indicate standard deviation (n=3) for three biological replicates. Results are representative of three independent experiments.

Palbociclib has recently been approved for the treatment of HR+, HER2- breast cancers;[51] therefore, the correlation between CDK4 inhibitor sensitivity and CDK4-mediated phosphorylation of 4E-BP1 was investigated. In line with literature, the ER+ MCF-7 and triple negative MDA-MB-231 cell lines were found to be palbociclib-sensitive, and the triple-negative MDA-MB-468 cell line to be resistant (Figure 4.7A and 4.7B).[52] Inhibition of CDK4/6 resulted a decrease in 4E-BP1 phosphorylation in the MCF-7 and MDA-MB-231 cell lines; this effect is magnified in cells co-treated with rapamycin (Figure 4.9A) However, in the MDA-MB-468 cell line, palbociclib had no effect on 4E-BP1

phosphorylation. Though this cell line expresses CDK4 at levels commensurate with other cell lines, D cyclin expression is nearly undetectable at the protein level (Figure 4.8), likely contributing to palbociclib insensitivity.
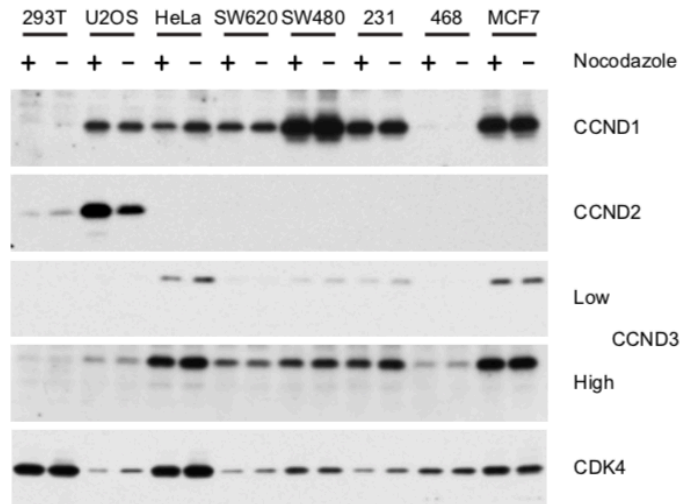
Figure 4.8 | CDK4 and D cyclin Expression Across Several Cell Lines. Western blot of CDK4 and D-cyclins in a variety of cell lines in asynchronous culture or arrested in prometaphase with nocodazole.

Next, the effect of combined inhibition of CDK4 and mTORC1 on cap-dependent translation (CDT) was investigated using cells stably expressing a bicistronic reporter construct containing *Renilla* and *Firefly* luciferase separated by the poliovirus internal ribosomal entry site (IRES).[53] With this dual-luciferase reporter assay, the combination of palbociclib and rapamycin was found to cause a functional impact by decreasing CDT in MCF-7 cells, whereas palbociclib provided no added benefit over rapamycin treatment alone in MDA-MB-468 cells. (Figure 4.9B) The current understanding of rapamycin resistance suggests mTORC1 can carry-out rapamycin-insensitive activities, thus active-site mTOR inhibitors (mTORKIs) such as INK128 are used to promote robust 4E-BP1 reactivation.[54] However, the combination of palbociclib and rapamycin was as effective as INK128 at reducing relative rates of CDT in this assay (Figure 4.9B), likely due to the significant reduction in total 4E-BP1 levels following chronic treatment with mTORKIs (Figure 4.9C). [55]
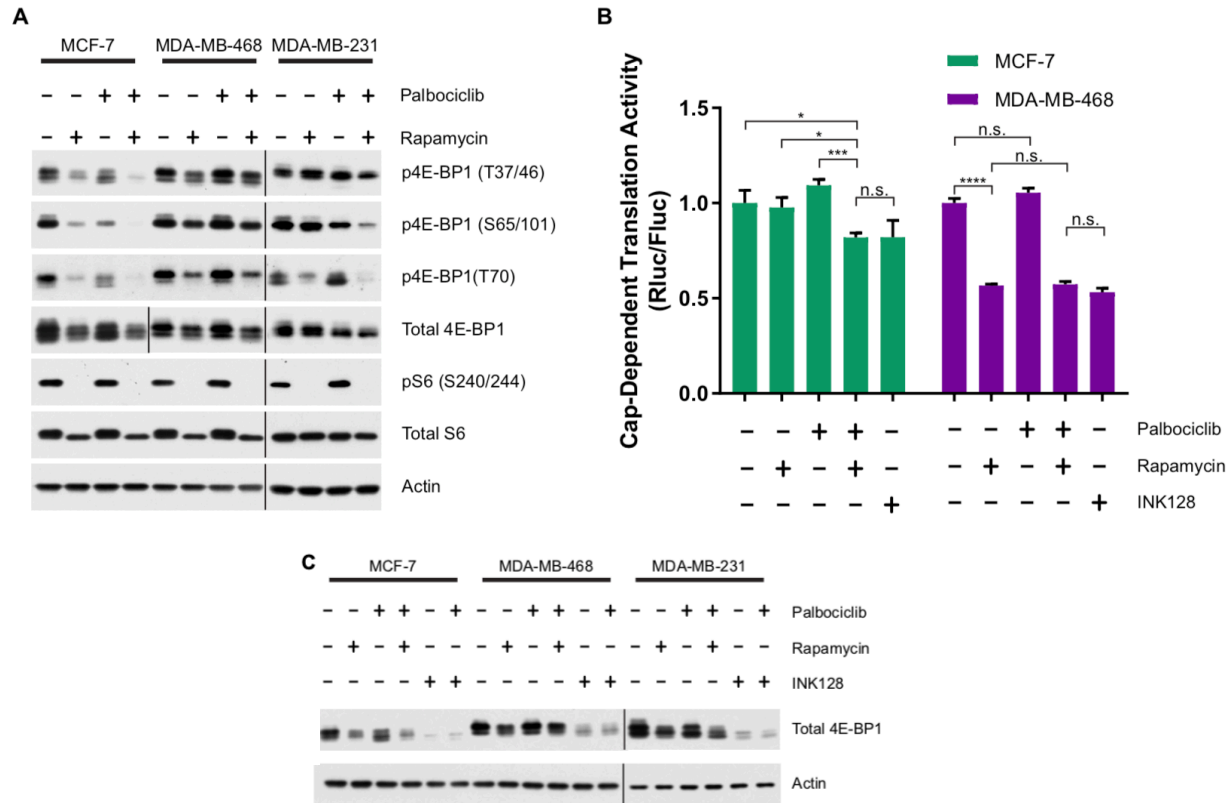
Figure 4.9 | mTORC1 and CDK4/6 cooperate to regulate cap-dependent translation. A) Western blot of MCF-7, MDA-MB-468 and MDA-MB-231 cell lines treated with rapamycin (100 nM) and/or palbociclib (1 μM) for 72 hours. Vertical bars separate samples run on separate blots or different exposures **B)** Cap-dependent dual luciferase assay of cells treated with rapamycin (100 nM) and/or palbociclib (1 μM) and/or INK128 (100 nM) for 72 hours. Normalized renilla luciferase is shown relative to the no-treatment control for each cell line. Data represented as mean +/- standard deviation (n=4), and are representative of three independent replicates. *P<0.05, **P<0.01 ***P<0.001, Statistical significance for all graphs was determined using an unpaired, two-tailed student's t-test. **C)** Wastern blot of cells treated as in **(A)**, but including INK128 (100 nM).

4.6 Inhibition of CDK4 Downregulates c-Myc via 4E-BP1

After verifying the effect of CDK4/6 and mTOR inhibition on global rates of CDT, the effect of this combination on the expression of the oncogenic transcription factor c-Myc was investigated. *MYC* mRNA is known to be translated via CDT, and is commonly used to benchmark efficacy of CDT-targeting therapies.[56] Intriguingly, c-Myc protein expression decreased in palbociclib-sensitive cells treated with the combination, while no change was observed in the resistant MDA-MB-468 cells. (Figure 4.10A) Downregulation of c-Myc expression was determined to be due to decreased rates of translation, rather than a E2F-dependent decrease in *MYC* transcription,[57] as rapamycin treatment resulted in an increase in *MYC* transcript levels in both cell lines (Figure 4.10D). mRNA expression of

several c-Myc target genes,[58] including *NPM1, EIF4E, ODC1*, and *CDK4* were then profiled to investigate the functional consequences of diminished c-Myc protein expression. In MCF-7 cells, inhibition of mTORC1 and CDK4 decreased c-Myc transcriptional activity, with the most robust decrease in activity observed in the combination treatment (Figure 4.10E). MDA-MB-468 cells showed very little change in c-Myc transcriptional activity, which is in-line with the observed response at the protein level (Figure 4.10A and 4.10E).
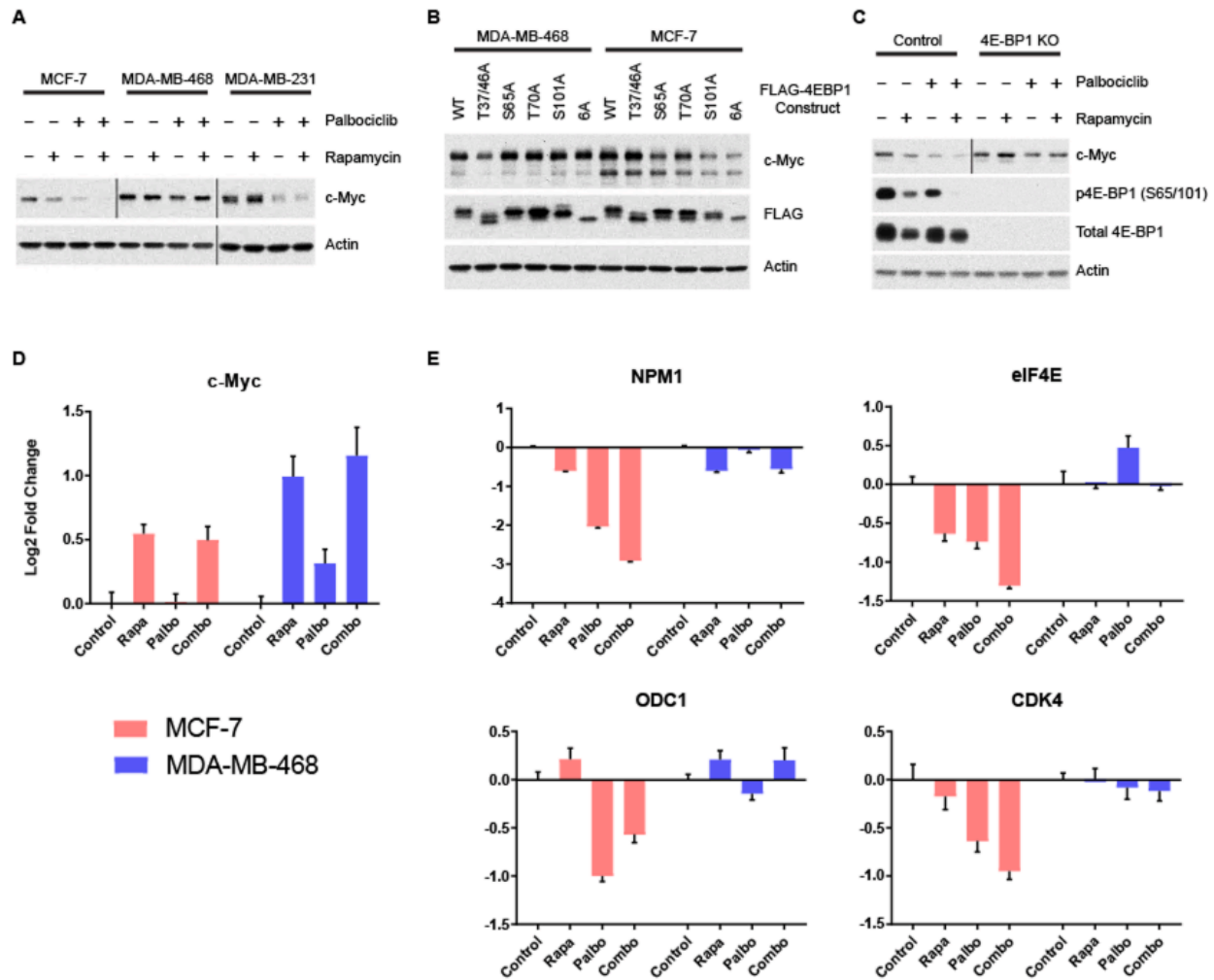
Figure 4.10 | c-Myc Expression is Dependent Upon Phosphorylation of S101. A) Western blot of c-Myc expression in MCF-7, MDA-MB-468, and MDA-MB-231 cell lines treated with rapamycin (100 nM) and/or palbociclib (1 μM) for 72 hours. **B)** Expression of c-Myc in MDA-MB-468 and MCF-7 cell lines stably expressing doxycycline inducible FLAG-4E-BP1 mutants. Sub-confluent cells were harvested 8 days after addition of 1μg/mL and 0.1μg/mL dox for MDA-MB-468 and MCF-7, respectively. 6A mutant refers to concurrent mutation of T37A, T46A, S65A, T70A, S83A, and S101A. **C)** Western blot of c-Myc expression in 4E-BP1 knockout or control cells treated as in (**A**) Vertical bars separate images obtained from separate exposures. **D-E)** Relative RNA expression of **D)** MYC and **E)** c-Myc target genes from cells treated as in (**A**). Expression is normalized to the no treatment control sample for each cell line. UBB was used as an

internal control for each gene. Error bars standard deviation (n=3). Data is representative of two independent replicates.

For further verificaiton that this phenotype is a direct result of inhibition of 4E-BP1 phosphorylation, doxycycline-inducible cell lines were generated. Importantly, these cell lines were engineered to express non-phosphorylatable forms of 4E-BP1 at near-physiological levels. c-Myc downregulation was equivalent in MCF-7 cell lines expressing the S101A mutant and the fully nonphosphorylatable, 6A (T37A, T46A, S65A, T70A, S83A, and S101A) mutant, which is a strong negative regulator of global CDT. Other mutations had minimal effect on c-Myc protein levels, whereas only the 4E-BP1 (T37/46A) expressing MDA-MB-468 cell lines showed any change. These findings correlate with the effect these 4E-BP1 mutations have on the *in vitro* proliferation of these two cell lines (Figure 4.11). Finally, to further explore the involvement of 4E-BP1 in the palbociclib-induced downregulation of c-Myc, 4E-BP1 knockout (KO) cell were generated using CRISPR Cas9. In MCF-7 cells lacking 4E-BP1, palbociclib treatment had no effect on c-Myc expression (Figure 4.10C). Alternatively, treating cells with rapamycin resulted in increased c-Myc expression, which correlated with *MYC* transcript levels. As expected, palbociclib had no effect on c-Myc expression in MDA-MB-468 cells following 4E-BP1 knockout. (Data not shown)
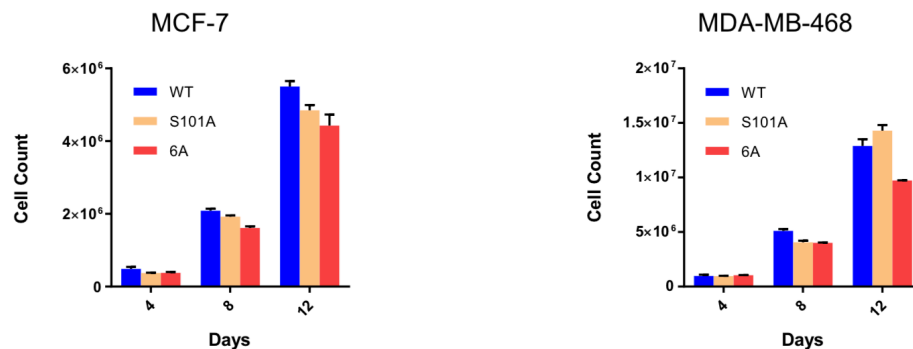
Figure 4.11 | S101 Affects Proliferation in Palbociclib-Sensitive Cells. *In vitro* proliferation of MDA-MB-468 and MCF-7 cell lines from main text Figure 5C. Cells were maintained in subconfluent culture for 12 days after plating 200,000 cells per dish. Experiment was performed in biological triplicate; data is presented as mean +/- standard deviation. 4E-BP1 expression was induced with 1μg/mL and 0.1μg/mL dox for MDA-MB-468 and MCF-7, respectively. 6A mutant refers to T37A, T46A, S65A, T70A, S83A, and S101A.

We next investigated the effects of CDK4 inhibition on cyclin D3, the translation of which is also cap-dependent.[59,60] Treatment of MCF-7 control KO cells with palbociclib resulted in a slight reduction in the expression of cyclin D3, an effect which was reversed by 4E-BP1 KO (Figure 4.12A). To further probe the effect of CDK4 mediated phosphorylation of 4E-BP1 on global regulation of CDT, 4E-BP1 KO and control cells stably expressing the dual luciferase CDT reporter construct were created. 4E-BP1 KO had very little effect on the rate of CDT in response to palbociclib treatment alone; however, treatment of 4E-BP1 KO cells with both rapamycin and palbociclib resulted in a 2.2-fold increase in CDT relative to control cells subjected to the same conditions (Figure 4.12B). These experiments provide further evidence that CDK4 and mTOR converge on 4E-BP1 to regulate CDT.
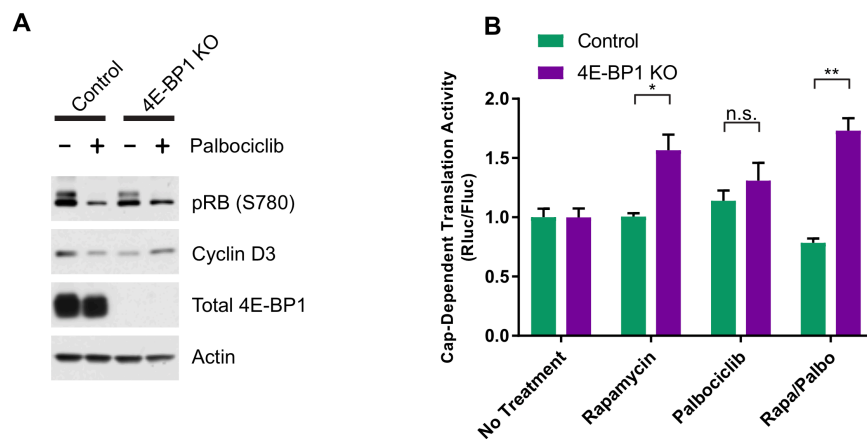
Figure 4.12 | 4E-BP1 Knockout Attenuates CDK4-driven Cap-Dependent Translation. A) Western blot of cyclin D3 expression in 4E-BP1 knockout or control cells treated +/- palbociclib (1 μM) for 72 hours **B)** Cap-dependent dual luciferase assay of cells treated with rapamycin (100 nM) and/or palbociclib (1 μM) for 72 hours. Data represented as mean +/- SEM (n=3) after normalization to no treatment control for the appropriate cell line. *P<0.05, **P<0.01 Statistical significance for all graphs was determined using an unpaired, two-tailed student's t-test.

4.7   4E-BP1 as a Biomarker for Palbociclib

CDK4/6 inhibitors are thought to function primarily by reducing phosphorylation-mediated inactivation of the RB1 tumor suppressor, thereby inducing a cell cycle arrest at the G1-S transition. While RB1 is a useful biomarker for predicting response to this class of inhibitors in cell lines and preclinical models,[14,52] the utility of RB1 as a biomarker in the clinic is controversial. [36,38,61] As it is clear that more biomarkers are needed to allow for better predictors of drug sensitivity, [37] the antiproliferative effects of palbociclib on 4E-

BP1 KO cells was investigated. These experiments were performed with the goal of gaining an understanding of the value of 4E-BP1 in regulating the response to CDK4/6 inhibition. Intriguingly, MCF-7 cells lacking 4E-BP1 were less sensitive than control cells to both palbociclib and rapamycin (Figure 4.13AA), indicating that inactivation of 4E-BP1 contributes to the global role of CDK4 as an oncogene. 4E-BP1 knockout had no effect on the sensitivity of MDA-MB-468 cells to rapamycin and palbociclib (Not Shown).
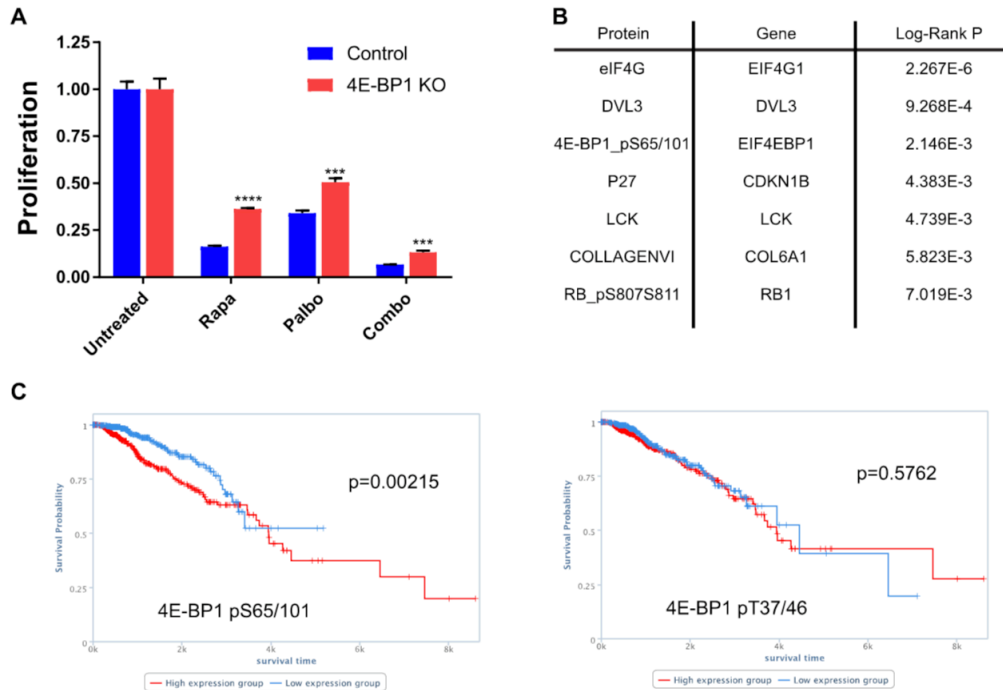
Figure 4.13 | CDK4-Mediated Phosphorylation of 4E-BP1 as a Biomarker. A) Proliferation of MCF-7 cells +/- 4E-BP1 knockout was assessed by CellTiter Glow assay. Cell proliferation was assessed after 6 days of treatment with rapamycin (100 nM) and/or palbociclib (1 μM). Treated samples are shown relative to no treatment control for that cell line. Bars represent mean +/- standard deviation (n=3) ***P<0.001, ****P<0.0001 Statistical significance for all graphs was determined using an unpaired, two-tailed student's t-test. **B)** A list of proteins/antibodies with the highest correlation to survival in the BRCA dataset from TCPA. Shown are all antibodies with a Log-Rank P value of <0.01. P-values were used as reported by TCPA. **C)** Kaplain-Meyer curves showing the total survival time for BRCA patients from the TCPA dataset with high (red) and low (blue) p4E-BP1(S65/101)

To further evaluate the impact of CDK4-mediated phosphorylation of 4E-BP1 in breast cancer patients, clinical data from the Reverse-Phase Protein Array (RPPA) Breast Invasive Carcinoma (BRCA) datasets available through The Cancer Proteome Atlas (TCPA) was mined.[62] In-depth analysis of these datasets found that phosphorylation of 4E-BP1 at S65/101 was the third most significant marker associated with overall survival across all 224 antibodies used in the array, while phosphorylation of T37/46 had no

predictive value in this dataset (Figures 4.13B and 4.13C). Analysis of protein biomarkers co-regulated with S101 phosphorylation found a strong positive correlation between phosphorylation of 4E-BP1 at S65/101 and Rb at S807/811 (Figure 4.14), indicating that these phosphorylation events are upregulated in similar patient populations. This correlation strengthens the link between, and the importance of, CDK4-mediated phosphorylation of S101 in BRCA.
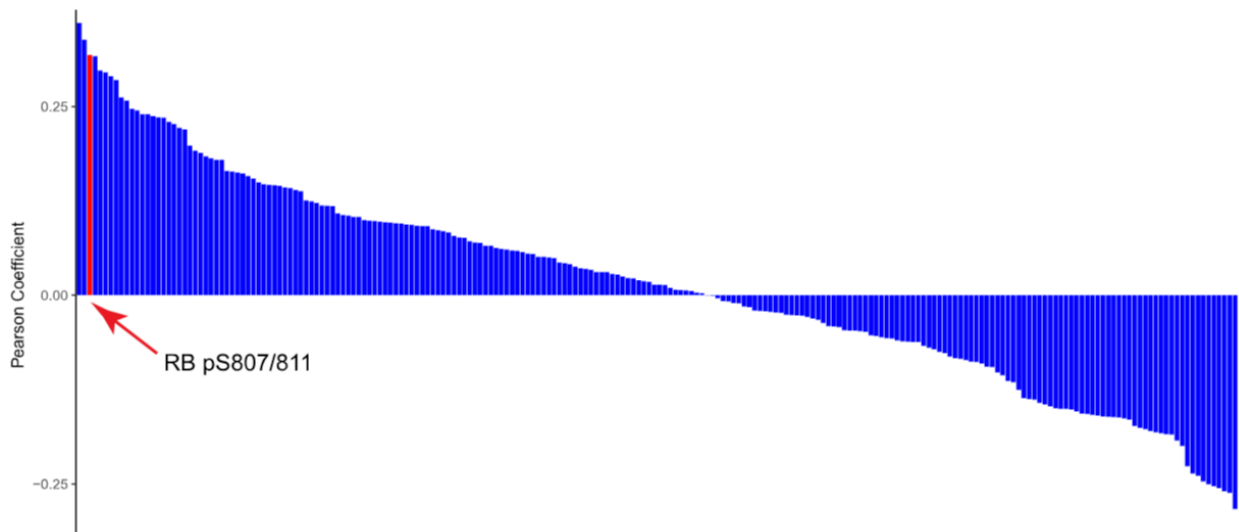
Figure 4.14 | 4E-BP1 (S65/101) Phosphorylation Mirrors pRb Phosphorylation. Histogram showing the Pearson Coefficient for pairwise regression between p4E-BP1 (S65/101) and every other antibody in the dataset. Other 4E-BP1 antibodies were excluded from the graph. See Appendix F for a full graph with labels

4.8 Conclusions

Using PhAXA-MS, a new interaction between CDK4 as a 4E-BP1 was identified. In-depth validation of this signaling axis demonstrated that CDK4 phosphorylates 4E-BP1 to maintain rapamycin-resistant cap-dependent translation. Expansion of PhAXA to other 4E-BP1 phosphorylation sites identified S101, a previously poorly understood phosphorylation site, as a *bona fide* CDK4 substrate. Mechanistic evaluation of CDK4-mediated phospohorylation of this residue uncovered the mechanism by which CDK4 promotes expression of c-Myc. However, it is currently unclear if this is strictly due to translational control, or through a combination of other mechanisms such as nuclear export, as the entirety of its function have yet to be elucidated. Finally, preliminary evidence that 4E-BP1, namely 4E-BP1 hyperphosphorylated at S101, is provided. These studies demonstrate that this phosphosite should be investigated as a biomarker for

predicting sensitivity to palbociclib and other CDK4/6 inhibitors. Unfortunately, it is impossible to differentiate between the phosphorylation of S65 and S101 by Western blot, RPPA or IHC given the promiscuity of the antibody, so targeted mass-spec based methods, such as Selected Reaction Monitoring (SRM), will need to be developed for accurate analysis of S101 as biomarker.

Given this newly discovered role of CDK4, it is likely that inhibition of this process is a previously unknown function of CDK4/6 inhibitors such as palbociclib, ribociclib and abemaciclib. Recently, several studies have reported potent *in vivo* antitumor effects by combined inhibition of mTOR and CDK4/6,[18,31-33] while a large phenotypic screen found the strongest cooperation between PI3K/mTORC1 and CDK4/6 inhibitors.[35] In addition, many ongoing clinical trials are investigating the efficacy of this combination in treating a range of cancers (Table 4.2); however, the rationale for this combination is lacking, as an in-depth understanding of the molecular mechanisms for this observed cooperativity is not understood. The data presented in this chapter promote the idea that these drugs provide an additive benefit over standalone therapies, in part, by inhibiting CDT, thereby decreasing the expression of anabolic proteins, and by altering the c-Myc transcriptional program that drives a wide range of cancers.[63] These findings support the investigation of this combination for treating cancers displaying clear hallmarks of an addiction to CDT.[64]

Identifier	Inhibitor	Combination	Phase	Condition
NCT03070301	Ribociclib	Everolimus	2	Advanced neuroendocrine tumors
NCT02732119	Ribociclib	Everolimus + Exemestane	1, 2	HR+ HER2- Breast cancer
NCT03008408	Ribociclib	Everolimus + Letrozole	2	Endometrial carcinoma
NCT02985125	Ribociclib	Everolimus	1, 2	Metastatic Pancreatic Adenocarcinoma
NCT01857193	Ribociclib	Everolimus + Exemestane	1	HR+ HER2- Breast cancer (OVER)
NCT03114527	Ribociclib	Everolimus	2	Soft Tissue Sarcoma - DDL and LMS
NCT03355794	Ribociclib	Everolimus	1	Various Gliomas
NCT03387020	Ribociclib	Everolimus	1	Malignant brain tumors (pediatric)
NCT03065387	Palbociclib	Everolimus + Neratinib	1	Adv. cancers w/ EGFR mut/amp Her2 mut/amp or Her3/4 mut
NCT02871791	Palbociclib	Everolimus + Exemestane	1	HR+ HER2- Breast cancer
NCT02057133	Abemaciclib	Everolimus + Exemestane	1	Metastatic breast cancer

Table 4.2 | US Clinical Trials Using Combination of CDK4/6 Inhibitors and Rapalogs

4.9 Materials and Methods

Small molecule reagents

Palbociclib Isethionate (Selleckchem) was dissolved in water to 10 mM. Rapamycin (Alfa Aesar), was dissolved in DMSO. Human recombinant insulin was purchased from Sigma. All reagents were used as received.

Cell Culture

HEK293T and HeLa cells were grown in DMEM (Corning) supplemented with 10% FBS, glutamine, penicillin, and streptomycin (Gibco). U2 OS cells were kindly provided by Dr. Beth Lawlor and cultured according to ATCC guidelines. MDA-MB-231 cells were a kind gift from Dr. Nouri Neamati and grown in RPMI-1640 media supplemented with 10% FBS and glutamine. MDA-MB-468 and MCF-7 cells were a kind gift from Dr. Max Wicha. MDA-MB-468 cells were grown in DMEM (Corning) supplemented with 10% FBS and glutamine. MCF-7 cells were cultured according to ATCC guidelines. Cells were grown at 37 °C with 5% CO_2 in a humidified incubator, passaged at least twice before use for experiments and no more than 10 times before returning to low passage stocks. All cell lines were authenticated by STR profiling, and regularly tested for mycoplasma contamination.

Plasmids

Annealed oligos corresponding to the C-terminal myc-tag were cloned into pcDNA3 at XbaI and ApaI. pcDNA3/Au1-mTOR and pRK5/HA-Raptor plasmids were generously shared by Dr. Diane Fingar. CDK4, CDK6, CCND1, CCND2 and CCND3 cDNA were cloned directly from A549 cDNA prepared using the Superscript III first-strand synthesis kit (Invitrogen). CDK4, CDK6, 4E-BP1, and Raptor were cloned into the pcDNA3/3XFLAG vectors. CCND1, CCND2, CCND3 were cloned into the pcDNA3/myc tag vectors. MBP-4E-BP1 (wild type and alanine mutants) was prepared by cloning into pMCSG9 (Univ. of Michigan Center for Structural Biology) using LIC cloning. HaloTag-eIF4E has been described elsewhere.[65] All mutations were generated by PCR mutagenesis. The sequences for all primers used are listed in Table 4.3. All constructs were fully sequenced by Sanger sequencing.

ORF		Purpose		Sequence 5' → 3'
Tags	c-Term Myc		Forward	CTAGAGAACAAAAACTCATCTCAGAAGAGGATCTGTGAGGGCC
			Reverse	CTCACAGATCCTCTTCTGAGATGAGTTTTTGTTCT

	PLVX	MCS Expansion	Forward	CGCGTGGATCCGAGTCTAGAG
			Reverse	AATTCTCTAGACTCGGATCCA
4E-BP1	Cloning	Into PLVX Vector	Forward	GCCCCCGGGACGCGTATGGACTACAAAGACCATGAC
			Reverse	TGTTCTAGACTATTAAATGTCCATCTCAAACTGTGACTCTT
	Mutagenesis	T37A	Forward	GACTACAGCACGGCCCCCGGCGGCACG
			Reverse	CGTGCCGCCGGGGGCCGTGCTGTAGTC
		T46A	Forward	GCTCTTCAGCACCGCCCCGGGAGGTACC
			Reverse	GGTACCTCCCGGGGCGGTGCTGAAGAGC
		S65A	Forward	CTGATGGAGTGTCGGAACGCACCTGTGACCAAAACAC
			Reverse	GTGTTTTGGTCACAGGTGCGTTCCGACACTCCATCAG
		S65A/T70A	Forward	GCACCTGTGACCAAAGCACCCCCAAGGGATCTGC
			Reverse	GCAGATCCCTTGGGGGTGCTTTGGTCACAGGTGC
		T70A	Forward	CTCACCTGTGACCAAAGCACCCCCAAGGGATCTGC
			Reverse	GCAGATCCCTTGGGGGTGCTTTGGTCACAGGTGAG
		S83A	Forward	CCGGGGGGTCACCGCCCCCTTCCAGTGATG
			Reverse	CATCACTGGAAGGGGCGGTGACCCCCGG
		S101A	Forward	GAGCCACCTGCGCAATGCCCCAGAAGATAAGCGG
			Reverse	CCGCTTATCTTCTGGGGCATTGCGCAGGTGGCTC
cDNA Cloning	CCND1	UTR	Forward	CAGCTGCCCAGGAAGAG
			Reverse	AAATGCTCCGGAGAGGAG
		Coding	Forward	AATTGAATTCATGGAACACCAGCTCCTG
			Reverse	GCTATCTAGAGATGTCCACGTCCCGCAC
	CCND2	UTR	Forward	TTCTGCTCCACCTTCTCT
			Reverse	GGATTCCCTTATGCTGTACTT
		Coding	Forward	AATTGAATTCATGGAGCTGCTGTGCCAC
			Reverse	GCTATCTAGACAGGTCGATATCCCGCAC
	CCND3	UTR	Forward	TTCCACGGTTGCTACATCG
			Reverse	TCCCTTGGGCTTTGTGAAGG
		Coding	Forward	AATTGAATTCATGGAGCTGCTGTGTTGC
			Reverse	GCTATCTAGACAGGTGTATGGCTGTGACAT
	CDK4	UTR	Forward	TCCCTTGATCTGAGAATGGCT
			Reverse	TCCATTGCTCACTCCGGATT
		Coding	Forward	AATTGAATTCATGGCTACCTCTCGATATGAG
			Reverse	GCTATCTAGATCACTCCGGATTACCTTCATC
	CDK6	UTR	Forward	GGAGCAAGTAAAGCTAGACC
			Reverse	ACAGTAAACTAGGCGGTTTC
		Coding	Forward	AATTGAATTCATGGAGAAGGACGGCCTGT
			Reverse	GCTATCTAGATCAGGCTGTATTCAGCTCCG

Table 4.3 | List of Primers Used for Cloning and Mutagenesis

Lentivirus and stable cell lines

rLuc-PolIRES-fLuc was digested out of pcDNA3 (a kind gift from Dr. Peter Bitterman) using NheI and XhoI then ligated into pLentiLoxEV (UM vector core). The multiple cloning site of PLVX-Tre3G-mCherry (Clontech) was modified to include a XbaI restriction site by ligating annealed oligos into MluI and EcoRI. 3X-FLAG-4E-BP1 constructs were cloned from pcDNA3 into MluI and XbaI. PLVX-Tet3G (Clontech) was used for making rtTA-packaging lentivirus. Lentiviruses were packaged in HEK293T cells by cotransfection of the transfer plasmid, pMD2.G (a gift from D. Trono, Addgene plasmid 12259) and psPAX2 (a gift from D. Trono, Addgene plasmid 12260) using linear PEI (3:1 ratio of PEI to DNA).

Media was changed 16 h after transfection, and viral supernatant was collected after an additional 24 and 48 h, before filtering through 0.45-μm filters and storing in aliquots at -80 ^{o}C. Titer was determined by colony formation assay where possible. Cells were infected at a MOI of <0.5 in the presence of polybrene (Santa Cruz Biotechnology) (8 μg/mL), then after 48 h, selected with geneticin (1 mg/mL) (Gibco) for 3 weeks or puromycin (2 μg/mL) (Sigma) for 6 d; no selection was used for the dual luciferase cell lines. Polyclonal cell lines were maintained in geneticin (300 μg/mL) and puromycin, 1 μg/mL for MDA-MB-231 and MDA-MB-468, and 0.25 μg/mL for MCF-7. Expression of 3X-FLAG-4E-BP1 was induced with doxycycline (Alfa Aesar), 1 μg/mL for MDA-MB-231 and MDA-MB-468 and 0.1 μg/mL for MCF-7.

CRISPR Knockouts

pSpCAS9(BB)-2A-GFP (a gift from Feng Zheng, Addgene plasmid #48138) was digested with BbsI and oligos targeting nothing (for non-target control) or exon 1 of EIF4EBP1 (designed using http://tools.genome-engineering.org) were added. $1e^6$ MCF-7 or MDA-MB-468 cells were transfected using Lipofectamine LTX with PLUS reagent according to the manufacturer's instructions, and media was changed after 18 hours. After a 48-hour recovery, GFP-positive cells were sorted and saved using a MoFlo Astrios flow cytometer. Single cell clones were then isolated in 96-well plates by limiting dilution, and knockout was confirmed by western blot and sanger sequencing. For the final cell lines used in the experiments, five clones were pooled together (knockout or non-targeting control) and all experiments were then performed within 3 passages.

Target	Orientation	Sequence 5' → 3'
Non-Target	Forward	CACCGGTAGCGAACGTGTCCGGCGT
	Reverse	AAACACGCCGGACACGTTCGCTACC
EIF4EBP1	Forward	CACCGCGCACAGGAGACCATGTCCG
	Reverse	AAACCGGACATGGTCTCCTGTGCGC

Table 4.4 | List of Primers Used for CRISPR Knockout Constructs

Kinase Assays

For CDK4/CDK6 kinase assays, HEK293T cells were grown in 10-cm plates to 60$-$70% confluence. Cells were subsequently transfected with 3XFLAG-CDK4/6 (3 μg) and myc-CCND1/2/3 or empty pcDNA3 (3 μg) using linear PEI (3:1 ratio of PEI to DNA). After 18

h, the media was changed to plain growth media. ~20 h later, cells were stimulated with insulin (150 nM) for 60 min, and then harvested by scraping into TBST (50 mM Tris pH 7.4, 150 mM NaCl, 0.1% Tween-20) with aprotinin (10 μg/mL), leupeptin (5 μg/mL), pepstatin (7 μg/mL), NaF (10 mM), sodium orthovanadate (2 mM), β-glycerophosphate (10 mM), and sodium pyrophosphate (2 mM). The cells were disrupted by pipetting up-and-down (20$\times$) and rotated end-over-end for 15 min at 4 °C. The resulting lysate was cleared by centrifugation at 18,000$\times$g for 10 min at 4 °C. CDK4/6 complexes were isolated from 1 mg of lysate (1 mL) by immunoprecipation with packed, prewashed FLAG-M2 magnetic resin (15 μL) for 90 min at 4 °C. The resin was then washed with lysis buffer (1 mL, 3$\times$), TBS with β-glycerophosphate (10 mM) (1 mL, 1$\times$), and TBS containing MgCl$_2$ (10 mM) and β-glycerophosphate (1 mM) with or without ATP (1 mM) (1 mL, 1$\times$). After washing, the resin was suspended in 1x TBS (30 μL) with 4E-BP1 (1 μM), HaloTag-eIF4E (2 μM), MgCl$_2$ (10 mM), DTT (1 mM) and β-glycerophosphate (10 mM), with or without ATP (1 mM) and palbociclib as described. The kinase reaction was incubated at 30 °C for 30 min, and subsequently quenched with 5$\times$ Laemmli buffer (7 μL).

mTOR kinase assays were performed similar to those with CDK4/6 complexes with a few notable exceptions. HEK293T cells were transfected with 3XFLAG-Raptor (4 μg) and Au1-mTOR (3 μg). Lysis was performed in HEPES buffer (pH 7.4, 20 mM) containing NaCl (100 mM), CHAPS (0.3% v/v) and protease/phosphatase inhibitors as described above. For assessing the effect of CDK4/6 inhibition on mTORC1 activity *in vitro*, palbociclib (5 μM) was included in all lysis buffers, wash buffers and assay buffers, in addition to using cells treated with palbociclib (5 μM) for 2 h before lysis.

Immunoblotting

MCF-7, MDA-MB-231, MDA-MB-468 cells were lysed directly in-well using RIPA buffer (10 mM Tris-HCl, 150 mM NaCl, 1% Triton, 1% sodium deoxycholate, 0.1% SDS, pH 7.2) supplemented with 10 μg/mL aprotinin, 5 μg/mL leupeptin, 7 μg/mL pepstatin, 10 mM NaF, 2 mM sodium orthovanadate, 10 mM β-glycerophosphate, and 2 mM sodium pyrophosphate). Lysates were then sonicated thoroughly on ice. Protein concentrations

were normalized by the BCA assay (Pierce), resolved on 4–20% Tris-glycine gels (Invitrogen), transferred to 0.45-μm PVDF (Thermo) using Towbin's buffer (low amperage for ~4 h at 4 °C), blocked with 5% non-fat milk in TBST, then probed with primary antibodies overnight at 4 °C. Antibodies used in this study were the following: Actin-HRP (sc-47778) and Myc-9E10 (sc-40) from Santa Cruz Biotechnology; CDK4 (12790), CDK6 (13331), Cyclin D2, (3741), DYKDDDK tag (14793), MEK1/2 (9122), mTOR (2972), S6 (2217), pS6 (240/244) (2215), p4E-BP1 (T37/46) (2855), p4E-BP1 (S65/101) (9451), p4E-BP1 (T70) (9455), 4E-BP1 (9644), c-Myc (13987), Rb (9313) and pRb (S780) (3590) from Cell Signaling Technology; and FLAG-M2 (F1804) from Sigma.

Protein expression and purification

MBP-tagged 4E-BP1 proteins were expressed and purified from BL21 Rosetta 2 (DE3) *E. coli*. LB media supplemented with ampicillin and chloramphenicol (500 mL) was inoculated with an overnight culture (5 mL) and grown to an OD_{600} of 0.8 before expression was induced with IPTG (1 mM) for 2 h at 37 °C. After centrifugation (15 min at 7,500×g), cell pellets were re-suspended in NiA buffer (30 mL; 50 mM sodium phosphate, 100 mM NaCl, 20 mM imidazole, 2 mM DTT) containing guanidine-HCl (6M), and then sonicated on ice for 4 min (pulse: 1sec on/1sec off at 35% amplitude). Cleared lysate (18,000×g for 20 min at 4 °C) was added to packed Ni-NTA resin (4 mL; Qiagen) by gravity filtration. The resin was washed with NiA buffer with guanidine-HCl (6M) (25 mL, 1×), NiA buffer (25 mL, 1×), and then eluted with NiB buffer (NiA buffer with 500 mM imidazole). Eluted protein was cleaved with TEV protease overnight at 4 °C and dialyzed into Tris-buffered saline (TBS) with 2mM DTT (6 L). Dialyzed protein was passed through Ni-NTA resin and pure, cleaved 4E-BP1 was collected as flow through. Purity was verified as >95% by Coomassie stain. Protein concentration was determined by absorbance at 280 nM. Single-use aliquots were stored at -80 °C. HaloTag-eIF4E was purified as described previously.[65]

qRT-PCR

Total RNA was isolated using TRIzol reagent (Invitrogen), and cDNA was subsequently prepared using the Superscript III first-strand synthesis kit (Invitrogen) according to manufacturer's instructions. For gene expression analysis, qPCR was performed using the PowerUP sybr green master mix (Applied Biosystems) on a Viia 7 thermocycler using the fast-qPCR protocol. The relative fold change was calculated using the comparative threshold cycle (C_T) method.[66] PCR amplification efficiency controls were performed for each primer set and dissociation curves verified single product amplification.

Target	Efficiency	Orientation	Sequence 5' → 3'
UBB	1.988	Forward	GCGCATAGAGGAGAAGGGAAA
		Reverse	CCTCCCGAGAGGCAGTTTAG
MYC	2.185	Forward	TGCCTTGGTTCATCTGGGTC
		Reverse	GCTTAGGAGTGCTTGGGACA
EIF4E	2.072	Forward	GACTGTCGAACCGGAAACCA
		Reverse	GCCCATCTGTTCTGTAGGGG
NPM1	2.124	Forward	TCGCGAGATCTTCAGGGTCTA
		Reverse	AGAGAAGGCGGACGGAGATA
ODC1	2.07	Forward	GCTTTCACGCTTGCAGTTAATA
		Reverse	CACTCGACTCATCTTCGTCATC
CDK4	2.11	Forward	GCTCTGCAGCACTCTTATCTAC
		Reverse	CTCAGTGTCCAGAAGGGAAATG

Table 4.5 | List of Primers Used for qRT-PCR

Dual Luciferase reporter assay

The cap-dependent translation luciferase reporter assay was performed using the dual glo luciferase assay system according to manufacturer's instructions (Promega). Briefly, polyclonal rLuc-polIRES-fLuc expressing cell lines were plated at 20,000 cells per well in 96-well, white, tissue culture-treated plates, and treated as described in the figure legends. After 72 h, media was aspirated and OptiMEM (75 μL) (Gibco) was added to each well. Cells were lysed in firefly luciferase buffer, and total (firefly luciferase) luminescence was measured after 15 min. Total luminescence (renilla luciferase) was measured within one hour after addition of Stop & Glo reagent.

In-gel digestion

TEV-cleaved 4E-BP1 (30 pmol) was used as a substrate for *in vitro* phosphorylation by cyclin D3−CDK4 complex with or without ATP (1 mM). The samples were separated by SDS-PAGE and stained with Coomassie R-250 (Bio-Rad). The protein samples were processed and analyzed at the Proteomics Resource Facility at the University of

Michigan. The gel slice corresponding to TEV-cleaved 4E-BP1 was destained with 30% methanol for 4 h. Following reduction and cysteine alkylation as described in Chapter 3, proteins were digested overnight with sequencing grade, modified trypsin (Promega) (500 ng) at 37 °C. Peptides were extracted by incubating the gel with of 50% acetonitrile/0.1% TFA (150 mL) for 30 min at room temperature. A second extraction with 100% acetonitrile/0.1% TFA (150 mL) was also performed. Both extracts were combined and dried in a Vacufuge concentrator (Eppendorf).

Mass spectrometry

Performed as described in Chapter 3

Phosphosite identification by MS/MS

To identify phosphorylation sites on 4E-BP1 following *in vitro* phosphorylation by CDK4/cyclin D3, MS/MS spectra were manually inspected after COMET search (as described above); however, a database of only cleaved 4E-BP1 was used. Only those phosphopeptides for which the phosphate could be clearly localized to one residue were considered putative CDK4 substrates. No other peptide or protein level validation was performed.

Cell Proliferation Assay

Cells were plated at a density of 2,000 cells per well in white-bottom, tissue culture treated, 96-well plates. The following day, cells were treated as stated in the figure legends; media (+/- drug) was changed every 48-hours. After 6-days, proliferation was assessed using Cell-Titer Glo (Promega). All samples were normalized to the no-treatment control.

Immunofluorescence

MCF-7 cells were grown in 24-well plates on poly-L-lysine-coated coverslips (Fisher) until ~50% confluent. Cells were washed twice with ice-cold 1× PBS, and then fixed with 4% paraformaldehyde for 15 min at room temperature. Fixed cells were washed twice with 1× PBS, permeabilized with 0.2% Triton X-100 in PBS for 30 min, blocked with 1% BSA

in PBS and 0.1% Triton X-100 for 1 h at room temperature, and then probed with primary antibody (1:500 for 4E-BP1 and CCND3) in blocking buffer overnight at 4 °C. Coverslips were washed 3× with PBS for 10 min each before probing with AlexaFluor488-conjugated donkey anti-rabbit (Invitrogen) or AlexaFluor647-conjugated goat anti-mouse secondary antibodies (1:1000 dilution for each). Cover slips were subsequently washed 3× with 1× PBS for 10 min before mounting onto glass slides with Prolong diamond antifade mountant with DAPI. Images were taken using a Nikon A1 Spectral confocal microscope with a 60x objective. All images were compared to no-primary or cross-primary controls to ensure a specific signal. Images were compiled using Adobe Photoshop (CS6).

Colony formation assay

Cells were seeded in 6-well plates at a density of 20,000 cells per well for MCF-7 and MDA-MB-468 cells, and 1,000 cells per well for MDA-MB-231 cells. The next day, cells were treated with rapamycin (100 nM), palbociclib (5 μM) or DMSO (0.001% v/v). Fresh media containing the appropriate inhibitors was added after 5 days. On day 10, cells were fixed with glutaraldehyde (6% v/v) and stained with crystal violet (0.25% w/v) for 3 hours at room temperature. After removing excess stain, plates were dried overnight before imaging and quantifying cell density using an Odyssey CLx (Licor).

TCPA dataset mining

The TCGA-L4 breast invasive carcinoma (BRCA) Reverse-Phase Protein Array (RPPA) dataset (901 samples) was downloaded from The Cancer Proteome Atlas (TCPA) on 04/08/2018. Pairwise linear regressions were run for each antibody against p4EBP1_S65, and Pearson coefficients were extracted and plotted as a histogram using R version 3.4.4.

Statistics

Two-sided t-tests were performed using Prism (v7); equal variance between samples being compared was established. Graphs show mean +/- S.E.M or +/- standard deviation as described in the figure legends.

4.10 References

1   Anders, L. *et al.* A systematic screen for CDK4/6 substrates links FOXM1 phosphorylation to senescence suppression in cancer cells. *Cancer Cell* **20**, 620-634, doi:10.1016/j.ccr.2011.10.001 (2011).

2   Weinberg, R. A. The retinoblastoma protein and cell cycle control. *Cell* **81**, 323-330 (1995).

3   Hollingsworth, R. E., Jr., Chen, P. L. & Lee, W. H. Integration of cell cycle control with transcriptional regulation by the retinoblastoma protein. *Curr Opin Cell Biol* **5**, 194-200 (1993).

4   Woitach, J. T., Zhang, M., Niu, C. H. & Thorgeirsson, S. S. A retinoblastoma-binding protein that affects cell-cycle control and confers transforming ability. *Nat Genet* **19**, 371-374, doi:10.1038/1258 (1998).

5   Burke, J. R., Hura, G. L. & Rubin, S. M. Structures of inactive retinoblastoma protein reveal multiple mechanisms for cell cycle control. *Genes & development* **26**, 1156-1166, doi:10.1101/gad.189837.112 (2012).

6   Giacinti, C. & Giordano, A. RB and cell cycle progression. *Oncogene* **25**, 5220-5227, doi:10.1038/sj.onc.1209615 (2006).

7   Ren, B. *et al.* E2F integrates cell cycle progression with DNA repair, replication, and G(2)/M checkpoints. *Genes & development* **16**, 245-256, doi:10.1101/gad.949802 (2002).

8   Hui, R. *et al.* INK4a gene expression and methylation in primary breast cancer: overexpression of p16INK4a messenger RNA is a marker of poor prognosis. *Clinical cancer research : an official journal of the American Association for Cancer Research* **6**, 2777-2787 (2000).

9   Lukas, J. *et al.* Retinoblastoma-protein-dependent cell-cycle inhibition by the tumour suppressor p16. *Nature* **375**, 503-506, doi:10.1038/375503a0 (1995).

10   Geradts, J. & Wilson, P. A. High frequency of aberrant p16(INK4A) expression in human breast cancer. *Am J Pathol* **149**, 15-20 (1996).

11   Frizelle, S. P. *et al.* Re-expression of p16INK4a in mesothelioma cells results in cell cycle arrest, cell death, tumor suppression and tumor regression. *Oncogene* **16**, 3087-3095, doi:10.1038/sj.onc.1201870 (1998).

12   Frost, S. J., Simpson, D. J., Clayton, R. N. & Farrell, W. E. Transfection of an inducible p16/CDKN2A construct mediates reversible growth inhibition and G1 arrest in the AtT20 pituitary tumor cell line. *Mol Endocrinol* **13**, 1801-1810, doi:10.1210/mend.13.11.0374 (1999).

13   Obexer, P., Hagenbuchner, J. & Ausserlechner, M.   (2011).

14   Fry, D. W. *et al.* Specific inhibition of cyclin-dependent kinase 4/6 by PD 0332991 and associated antitumor activity in human tumor xenografts. *Mol Cancer Ther* **3**, 1427-1438 (2004).

15   Infante, J. R. *et al.* A Phase I Study of the Cyclin-Dependent Kinase 4/6 Inhibitor Ribociclib (LEE011) in Patients with Advanced Solid Tumors and Lymphomas. *Clinical Cancer Research* **22**, 5696-5705, doi:10.1158/1078-0432.Ccr-16-1248 (2016).

16   Gelbert, L. M. *et al.* Preclinical characterization of the CDK4/6 inhibitor LY2835219: in-vivo cell cycle-dependent/independent anti-tumor activities alone/in combination with gemcitabine. *Invest New Drugs* **32**, 825-837, doi:10.1007/s10637-014-0120-7 (2014).

17   Schettini, F. *et al.* CDK 4/6 Inhibitors as Single Agent in Advanced Solid Tumors. *Front Oncol* **8**, doi:ARTN 608   10.3389/fonc.2018.00608 (2018).

18   Cortes, J. *et al.* The next era of treatment for hormone receptor-positive, HER2-negative advanced breast cancer: Triplet combination-based endocrine therapies. *Cancer Treat Rev* **61**, 53-60, doi:10.1016/j.ctrv.2017.09.011 (2017).

19   Finn, R. S. *et al.* The cyclin-dependent kinase 4/6 inhibitor palbociclib in combination with letrozole versus letrozole alone as first-line treatment of oestrogen receptor-positive, HER2-negative, advanced breast cancer (PALOMA-1/TRIO-18): a randomised phase 2 study. *Lancet Oncol* **16**, 25-35, doi:10.1016/S1470-2045(14)71159-3 (2015).

20   Hashizume, R. *et al.* Inhibition of DNA damage repair by the CDK4/6 inhibitor palbociclib delays irradiated intracranial atypical teratoid rhabdoid tumor and glioblastoma xenograft regrowth. *Neuro Oncol* **18**, 1519-1528, doi:10.1093/neuonc/now106 (2016).

21   Meattini, I., Desideri, I., Scotti, V., Simontacchi, G. & Livi, L. Ribociclib plus letrozole and concomitant palliative radiotherapy for metastatic breast cancer. *Breast* **42**, 1-2, doi:10.1016/j.breast.2018.08.096 (2018).

22   Hart, L. S. *et al.* Preclinical Therapeutic Synergy of MEK1/2 and CDK4/6 Inhibition in Neuroblastoma. *Clinical cancer research : an official journal of the American Association for Cancer Research* **23**, 1785-1796, doi:10.1158/1078-0432.CCR-16-1131 (2017).

23   Lee, M. S. *et al.* Efficacy of the combination of MEK and CDK4/6 inhibitors in vitro and in vivo in KRAS mutant colorectal cancer models. *Oncotarget* **7**, 39595-39608, doi:10.18632/oncotarget.9153 (2016).

24   Maust, J. D., Frankowski-McGregor, C. L., Bankhead, A., 3rd, Simeone, D. M. & Sebolt-Leopold, J. S. Cyclooxygenase-2 Influences Response to Cotargeting of MEK and CDK4/6 in a Subpopulation of Pancreatic Cancers. *Mol Cancer Ther* **17**, 2495-2506, doi:10.1158/1535-7163.MCT-18-0082 (2018).

25   Ziemke, E. K. *et al.* Sensitivity of KRAS-Mutant Colorectal Cancers to Combination Therapy That Cotargets MEK and CDK4/6. *Clinical cancer research : an official journal of the American Association for Cancer Research* **22**, 405-414, doi:10.1158/1078-0432.CCR-15-0829 (2016).

26   Bonelli, M. A. *et al.* Combined Inhibition of CDK4/6 and PI3K/AKT/mTOR Pathways Induces a Synergistic Anti-Tumor Effect in Malignant Pleural Mesothelioma Cells. *Neoplasia* **19**, 637-648, doi:10.1016/j.neo.2017.05.003 (2017).

27   Divakar, S. K. *et al.* Dual inhibition of CDK4/Rb and PI3K/AKT/mTOR pathways by ON123300 induces synthetic lethality in mantle cell lymphomas. *Leukemia* **30**, 86-93, doi:10.1038/leu.2015.185 (2016).

28   Franco, J., Balaji, U., Freinkman, E., Witkiewicz, A. K. & Knudsen, E. S. Metabolic Reprogramming of Pancreatic Cancer Mediated by CDK4/6 Inhibition Elicits Unique Vulnerabilities. *Cell Rep* **14**, 979-990, doi:10.1016/j.celrep.2015.12.094 (2016).

29   Franco, J., Witkiewicz, A. K. & Knudsen, E. S. CDK4/6 inhibitors have potent activity in combination with pathway selective therapeutic agents in models of pancreatic cancer. *Oncotarget* **5**, 6512-6525, doi:DOI 10.18632/oncotarget.2270 (2014).

30   Ku, B. M. *et al.* The CDK4/6 inhibitor LY2835219 has potent activity in combination with mTOR inhibitor in head and neck squamous cell carcinoma. *Oncotarget* **7**, 14803-14813, doi:DOI 10.18632/oncotarget.7543 (2016).

31   Michaloglou, C. *et al.* Combined inhibition of mTOR and CDK4/6 is required for optimal blockade of E2F function and long term growth inhibition in estrogen receptor positive breast cancer. *Cancer research* **78** (2018).

32   Olmez, I. *et al.* Combined CDK4/6 and mTOR Inhibition Is Synergistic against Glioblastoma via Multiple Mechanisms. *Clinical cancer research : an official journal of the American Association for Cancer Research* **23**, 6958-6968, doi:10.1158/1078-0432.CCR-17-0803 (2017).

33   Pikman, Y. *et al.* Synergistic Drug Combinations with a CDK4/6 Inhibitor in T-cell Acute Lymphoblastic Leukemia. *Clinical cancer research : an official journal of the American Association for Cancer Research* **23**, 1012-1024, doi:10.1158/1078-0432.CCR-15-2869 (2017).

34   Song, X. *et al.* Combined CDK4/6 and Pan-mTOR Inhibition Is Synergistic Against Intrahepatic Cholangiocarcinoma. *Clinical cancer research : an official journal of the American Association for Cancer Research* **25**, 403-413, doi:10.1158/1078-0432.CCR-18-0284 (2019).

35   Vora, S. R. *et al.* CDK 4/6 inhibitors sensitize PIK3CA mutant breast cancer to PI3K inhibitors. *Cancer Cell* **26**, 136-149, doi:10.1016/j.ccr.2014.05.020 (2014).

36   DeMichele, A. *et al.* CDK 4/6 inhibitor palbociclib (PD0332991) in Rb+ advanced breast cancer: phase II activity, safety, and predictive biomarker assessment. *Clinical cancer research : an official journal of the American Association for Cancer Research* **21**, 995-1001, doi:10.1158/1078-0432.CCR-14-2258 (2015).

37   Fang, H., Huang, D., Yang, F. & Guan, X. Potential biomarkers of CDK4/6 inhibitors in hormone receptor-positive advanced breast cancer. *Breast Cancer Res Treat* **168**, 287-297, doi:10.1007/s10549-017-4612-y (2018).

38   Knudsen, E. S. & Witkiewicz, A. K. The Strange Case of CDK4/6 Inhibitors: Mechanisms, Resistance, and Combination Strategies. *Trends Cancer* **3**, 39-55, doi:10.1016/j.trecan.2016.11.006 (2017).

39   McNair, C. *et al.* Differential impact of RB status on E2F1 reprogramming in human cancer. *The Journal of clinical investigation* **128**, 341-358, doi:10.1172/JCI93566 (2018).

40   Choi, Y. J. & Anders, L. Signaling through cyclin D-dependent kinases. *Oncogene* **33**, 1890-1903, doi:10.1038/onc.2013.137 (2014).

41   Peter, D. *et al.* Molecular architecture of 4E-BP translational inhibitors bound to eIF4E. *Molecular cell* **57**, 1074-1087, doi:10.1016/j.molcel.2015.01.017 (2015).

42   Rong, L. *et al.* Control of eIF4E cellular localization by eIF4E-binding proteins, 4E-BPs. *Rna* **14**, 1318-1327, doi:10.1261/rna.950608 (2008).

43   Gingras, A.-C. *et al.* Regulation of 4E-BP1 phosphorylation: a novel two-step mechanism. *Genes & development* **13**, 1422-1437 (1999).

44   Wang, X., Li, W., Parra, J.-L., Beugnet, A. & Proud, C. G. The C terminus of initiation factor 4E-binding protein 1 contains multiple regulatory features that influence its function and phosphorylation. *Mol. Cell. Biol.* **23**, 1546-1557 (2003).

45   Yu, Y. H. *et al.* Phosphoproteomic Analysis Identifies Grb10 as an mTORC1 Substrate That Negatively Regulates Insulin Signaling. *Science* **332**, 1322-1326, doi:10.1126/science.1199484 (2011).

46   Gingras, A. C. *et al.* Regulation of 4E-BP1 phosphorylation: a novel two-step mechanism. *Genes Dev.* **13**, 1422-1437 (1999).

47   Mellacheruvu, D. *et al.* The CRAPome: a contaminant repository for affinity purification-mass spectrometry data. *Nature methods* **10**, 730-736, doi:10.1038/nmeth.2557 (2013).

48   Gingras, A. C. *et al.* Hierarchical phosphorylation of the translation inhibitor 4E-BP1. *Genes Dev.* **15**, 2852-2864 (2001).

49   Choo, A. Y., Yoon, S. O., Kim, S. G., Roux, P. P. & Blenis, J. Rapamycin differentially inhibits S6Ks and 4E-BP1 to mediate cell-type-specific repression of mRNA translation. *Proceedings of the National Academy of Sciences of the United States of America* **105**, 17414-17419, doi:10.1073/pnas.0809136105 (2008).

50   Descamps, G. *et al.* The cap-translation inhibitor 4EGI-1 induces apoptosis in multiple myeloma through Noxa induction. *Br J Cancer* **106**, 1660-1667, doi:10.1038/bjc.2012.139 (2012).

51   O'Leary, B., Finn, R. S. & Turner, N. C. Treating cancer with selective CDK4/6 inhibitors. *Nat Rev Clin Oncol* **13**, 417-430, doi:10.1038/nrclinonc.2016.26 (2016).

52   Finn, R. S. *et al.* PD 0332991, a selective cyclin D kinase 4/6 inhibitor, preferentially inhibits proliferation of luminal estrogen receptor-positive human breast cancer cell lines in vitro. *Breast Cancer Res* **11**, R77 (2009).

53   Poulin, F., Gingras, A. C., Olsen, H., Chevalier, S. & Sonenberg, N. 4E-BP3, a new member of the eukaryotic initiation factor 4E-kinding protein family. *Journal of Biological Chemistry* **273**, 14002-14007, doi:DOI 10.1074/jbc.273.22.14002 (1998).

54   Thoreen, C. C. *et al.* An ATP-competitive mammalian target of rapamycin inhibitor reveals rapamycin-resistant functions of mTORC1. *The Journal of biological chemistry* **284**, 8023-8032, doi:10.1074/jbc.M900301200 (2009).

55   Wang, J. *et al.* Snail determines the therapeutic response to mTOR kinase inhibitors by transcriptional repression of 4E-BP1. *Nat Commun* **8**, 2207, doi:10.1038/s41467-017-02243-3 (2017).

56   Gera, J. F. *et al.* AKT activity determines sensitivity to mammalian target of rapamycin (mTOR) inhibitors by regulating cyclin D1 and c-myc expression. *The Journal of biological chemistry* **279**, 2737-2746 (2004).

57 Lin, C. J., Cencic, R., Mills, J. R., Robert, F. & Pelletier, J. c-Myc and eIF4F are components of a feedforward loop that links transcription and translation. *Cancer research* **68**, 5326-5334, doi:10.1158/0008-5472.Can-07-5876 (2008).

58 Schmidt, E. V. The role of c-myc in regulation of translation initiation. *Oncogene* **23**, 3217-3221 (2004).

59 Tsukumo, Y., Alain, T., Fonseca, B. D., Nadon, R. & Sonenberg, N. Translation control during prolonged mTORC1 inhibition mediated by 4E-BP3. *Nat Commun* **7**, 11776, doi:10.1038/ncomms11776 (2016).

60 Hsieh, A. C. *et al.* The translational landscape of mTOR signalling steers cancer initiation and metastasis. *Nature* **485**, 55-61, doi:10.1038/nature10912 (2012).

61 Rubio, C. *et al.* Cdk4/6-inhibitor as a novel therapeutic approach for advanced Bladder Cancer independently of RB1 status. LID - clincanres.0685.2018 [pii] LID - 10.1158/1078-0432.CCR-18-0685 [doi].

62 Li, J. *et al.* TCPA: a resource for cancer functional proteomics data. *Nature methods* **10**, 1046-1047 (2013).

63 Dang, C. V. MYC on the path to cancer. *Cell* **149**, 22-35 (2012).

64 Pelletier, J., Graff, J., Ruggero, D. & Sonenberg, N. Targeting the eIF4F translation initiation complex: a critical nexus for cancer development. *Cancer research* **75**, 250-263, doi:10.1158/0008-5472.CAN-14-2789 (2015).

65 Song, J. M., Menon, A., Mitchell, D. C., Johnson, O. T. & Garner, A. L. High-Throughput Chemical Probing of Full-Length Protein-Protein Interactions. *ACS Comb Sci* **19**, 763-769, doi:10.1021/acscombsci.7b00128 (2017).

66 Schmittgen, T. D. & Livak, K. J. Analyzing real-time PCR data by the comparative C-T method. *Nature protocols* **3**, 1101-1108, doi:10.1038/nprot.2008.73 (2008).

Chapter 5

CDK4 Regulates 4E-BP1 During Mitosis

5.1 Abstract

Chapter 4 outlined the contribution of CDK4 in the maintenance of 4E-BP1 phosphorylation under conditions of mTORC1-inhibitor resistance. In this same vein, mTORC1 inhibitors have been proven to be unable to inhibit the hyperphosphorylation of 4E-BP1, a phenotype that is a hallmark of cells undergoing mitosis. In this chapter, PhAXA-MS analysis of mitotic 4E-BP1 kinases again reveals an unexpected role of CDK4. Mechanistic evaluation of this signaling event uncovers a controversial finding linking CDK4 to the progression of cells from metaphase, through cytokinesis, and into the G1 phase of the cell cycle. Finally, a speculative model is suggested that incorporates these findings into those linking CDK1 activity to both mitotic progression and 4E-BP1 phosphorylation.

5.2 Mitosis and the M→G1 Transition

Mitosis and cytokinesis ultimately result in the formation of two daughter cells and represent the culmination of the eukaryotic cell cycle. This process, consisting of prophase, metaphase, anaphase and telophase, is responsible for the orderly dissemination of genetic material to a new generation. Dysregulation of mitosis can lead to improper chromosomal distribution, or aneuploidy, which can lead to birth defects and cancers.[1,2] Therefore, progression through mitosis is highly regulated by a number of important pathways, including by many kinases.[3] However, the kinase that is generally recognized as being responsible for progression into cytokinesis is CDK1. CDK1

positively regulates most aspects of mitosis, including mitotic entry, chromosome condensation, spindle assembly and breakdown of the nuclear envelope.[4] Upon bipolar spindle assembly, the E3 ligase anaphase-promoting complex or cyclosome (APC/C) promotes inactivation of CDK1 via degradation of Cyclin B1, pushing cells into anaphase.[5]
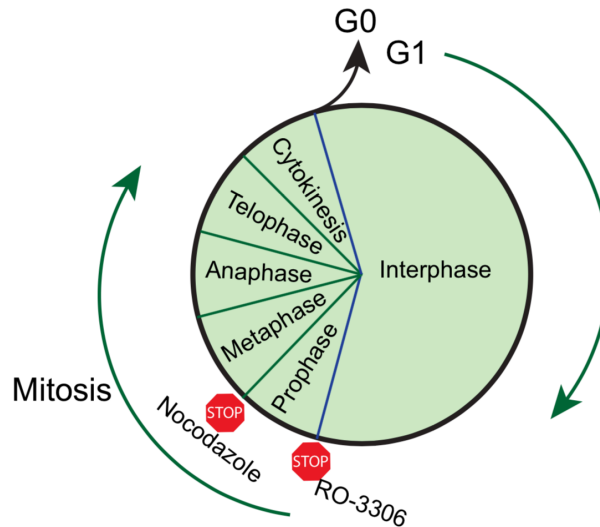
Figure 5.1 | Phases of Mitosis with Arresting Agents. The phases of mitosis are shown in the context of the beginning of G1-phase (interphase). Nocodazole and RO-3306 are shown with respect to the specific point at which these agents induce cell cycle arrest.

One difficulty with studying discrete, mitosis-specific signaling events is the relative complexity of each step and the dearth of tools available with which to isolate cells in each phase. Some of these tools include the non-specific CDK1 inhibitor RO-3306, which arrests cells at the G2/M border, and nocodazole, which arrests cells in prometaphase. (Figure 5.1) Few other tools, aside from microscopy, exist to study signaling events within each discrete phase of mitosis. This, coupled with the promiscuity of CDK1[6] and the lack of CDK1 activity after metaphase,[5] leaves open the possibility of undiscovered biology within the context of the M→G1 transition.

5.3   Phosphorylation of 4E-BP1 in Mitosis

One hallmark of mitosis is the hyperphosphorylation of 4E-BP1 (Figure 5.2), though it is well-validated that this phenotype is maintained independent of mTOR activity.[7-9]
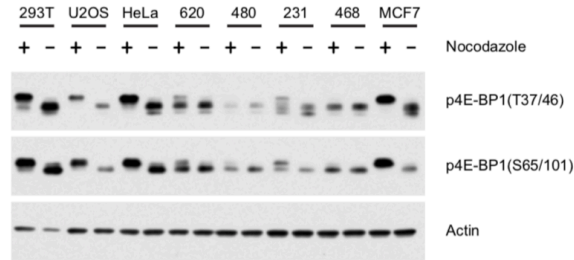
Figure 5.2 | Cells Arrested in Mitosis Exhibit Hyperphosphorylation of 4E-BP1. Western blot of phosphorylated 4E-BP1 from cell lines growing asynchronously, or treated +/- 500 nM nocodazole for 20 hours to induce a prometaphase arrest.

The ramifications of 4E-BP1 phosphorylation during this phase of the cell cycle are not well understood, as most reports agree that cap-dependent translation (CDT) is reduced during mitosis.[10-14] However, these findings are controversial, as other groups have found that most mitotic protein synthesis is cap-dependent, and driven by CDK1/Cyclin B1-mediated phosphorylation of 4E-BP1.[8] Further evaluation of mitosis-specific 4E-BP1 phosphorylation sites in the context of the optimal CDK1 recognition motif yielded the identification of S83 as a novel CDK1 phosphorylation site.[9] While this phosphorylation event has no effect on CDT, S83-phosphorylated 4E-BP1 reportedly associates with centrosomes upon chromatin condensation, hinting at a function of mitotic 4E-BP1 that is independent of translational control. However, the studies implicating CDK1 in the phosphorylation of 4E-BP1 relied heavily on the highly non-specific CDK1 inhibitor RO-3308. As this molecule is typically used as a tool compound for inducing a mitotic arrest at the precipice of prophase, these studies provide only a snapshot of the regulation of 4E-BP1 during a very narrow window of mitosis. Moreover, the promiscuity of this inhibitor at the high concentration that was used (9 μM) makes assessment of these findings quite difficult.

5.4   CDK4 Regulation of Mitotic 4E-BP1

Given the relative lack of information regarding 4E-BP1 phosphorylation in mitosis, and the knowledge that this process is mTOR independent, PhAXA-MS was used to identify candidate 4E-BP1 kinases. Using the microtubule inhibitor nocodazole, HEK293T cells were arrested in prometaphase, and released into medium containing insulin for 1 hour before harvesting and proceeding with PhAXA-MS analysis. Four kinases were

enriched in the T46C sample treated with crosslinker relative to the controls. (Table 5.1) CDK4 was again identified as a top hit, though this was unexpected given the relative lack of information linking CDK4 to regulation of mitosis and/or cytokinesis.

Protein	AVG PSM				Fold Change (PSMs)	
	WT +	WT -	T46C +	T46C -	T46C+/WT+	T46C+/T46C-
mTOR	7	0	45	0	6.43	----
CDK4	1	0	6	0	6.00	----
Erk2	0	1	3	1	----	3.00
TP53RK	0	0	2	1	----	2.00

Table 5.1 | Mitosis-Specific 4E-BP1 Kinases Identified by PhAXA-MS. 4E-BP1 (T46) kinases from nocodazole-arrested HEK293T cells. Table consists of all kinases identified by at least two peptides in at least one sample after filtering of common contaminants. This is a single biological replicate. Relative quantification of protein levels using MS1 intensity is not shown due to a lack of shared peptides between samples. '+' refers to samples treated with 1, while '-' refers to ATP only controls

However, given the role of CDK4 in regulating rapamycin resistant 4E-BP1 phosphorylation, as discussed in Chapter 4, this same signaling event was again investigated, but in the context of mitosis. To assess mitosis-specific CDK4-mediated phosphorylation of 4E-BP1, a variety of cell lines were arrested in prometaphase, and released into medium containing insulin with or without rapamycin and/or palbociclib. (Figure 5.3) As expected, rapamycin has no effect on the mitotic phosphorylation of 4E-BP1. However, cells released from nocodazole arrest in medium containing palbociclib show a marked decrease in phosphorylation, as demonstrated by the disappearance of the β, and γ bands. This effect is markedly increased in cells treated with both rapamycin and palbociclib, indicating that mTOR and CDK4 act in concert to regulate 4E-BP1 phosphorylation following release from prometaphase arrest.
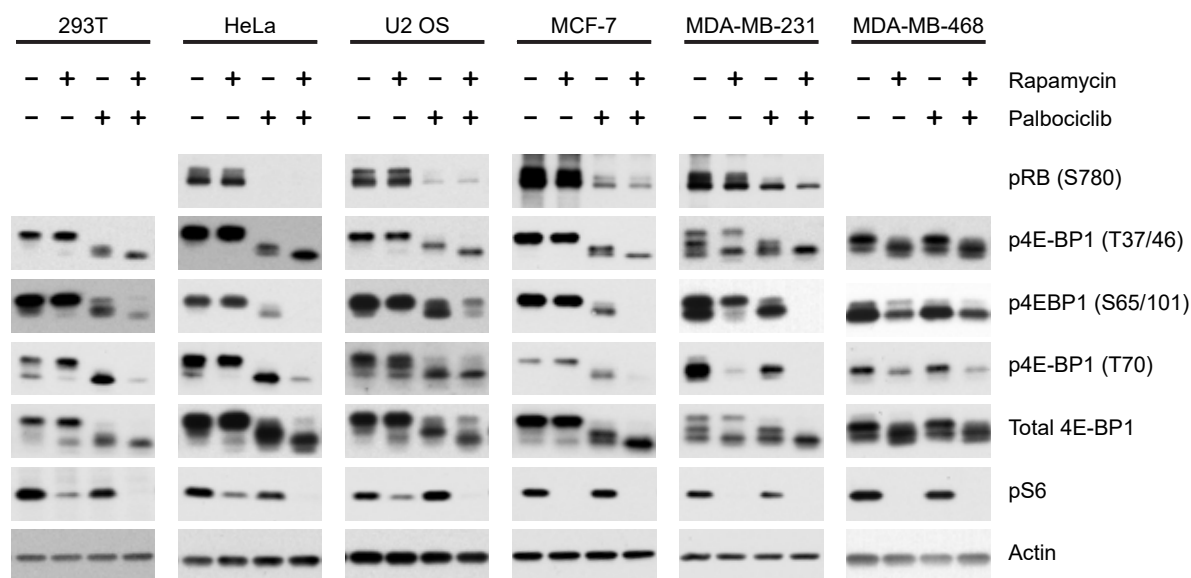
Figure 5.3 | Mitotic Phosphorylation of 4E-BP1 is Palbociclib-Sensitive. Nocodazole-arrested cells were treated with rapamycin (100 nM) and/or palbociclib (5 μM) in fresh media containing insulin (150 nM) for 2 h. Blots for pRb in HEK293T and MDA-MB-468 cells are not shown as they are Rb inactive and null, respectively.

Palbociclib has recently been approved for treatment of HR+, HER2- breast cancers; therefore, a correlation between CDK4 inhibitor sensitivity and CDK4-mediated mitotic phosphorylation of 4E-BP1 was investigated. Three commonly used breast cancer cell lines, for which palbociclib sensitivity has been previously established using an *in vitro* cell proliferation assay, were further evaluated.[15] Using MCF-7, MDA-MB-231 and MDA-MB-468 cell lines, which show high, intermediate, and low sensitivity to palbociclib, respectively, a striking correlation was uncovered in relation to the mitotic 4E-BP1 phosphorylation in response to palbociclib treatment. CDK4 inhibition almost completely abrogated mitotic phosphorylation of 4E-BP1 in the ER+ MCF-7 cell line, whereas no effect was observed in the triple-negative MDA-MB-468 cell line even when treated in combination with rapamycin. A slight response was also observed in the MDA-MB-231 cell line, which correlates to the previously reported, intermediate sensitivity to palbociclib.[15]

To verify that the palbociclib treatment was on-target, the phosphorylation state of 4E-BP1 phosphorylation was compared to that of Rb at S780, the canonical CDK4 phosphorylation site (Figure 5.4A) Interestingly, a broad range of sensitivity to palbociclib

across cell lines was observed, ranging from <330nM in U2 OS, to ~1.25uM in HeLa cells. However, the effective concentration of palbociclib required to inhibit both 4E-BP1 and Rb phosphorylation at S780 correlated with the relative expression of CDK4 in each cell line. (Figure 5.4B) A similar effect is seen with 293Ts, which require a concentration of ~2.5uM to fully inhibit 4E-BP1 phosphorylation and have the highest relative expression of CDK4 at the protein level. (Not shown) While there are clearly other factors that affect CDK4 inhibitor sensitivity, including Rb status and D-cyclin expression levels, among others, this correlation was noteworthy.
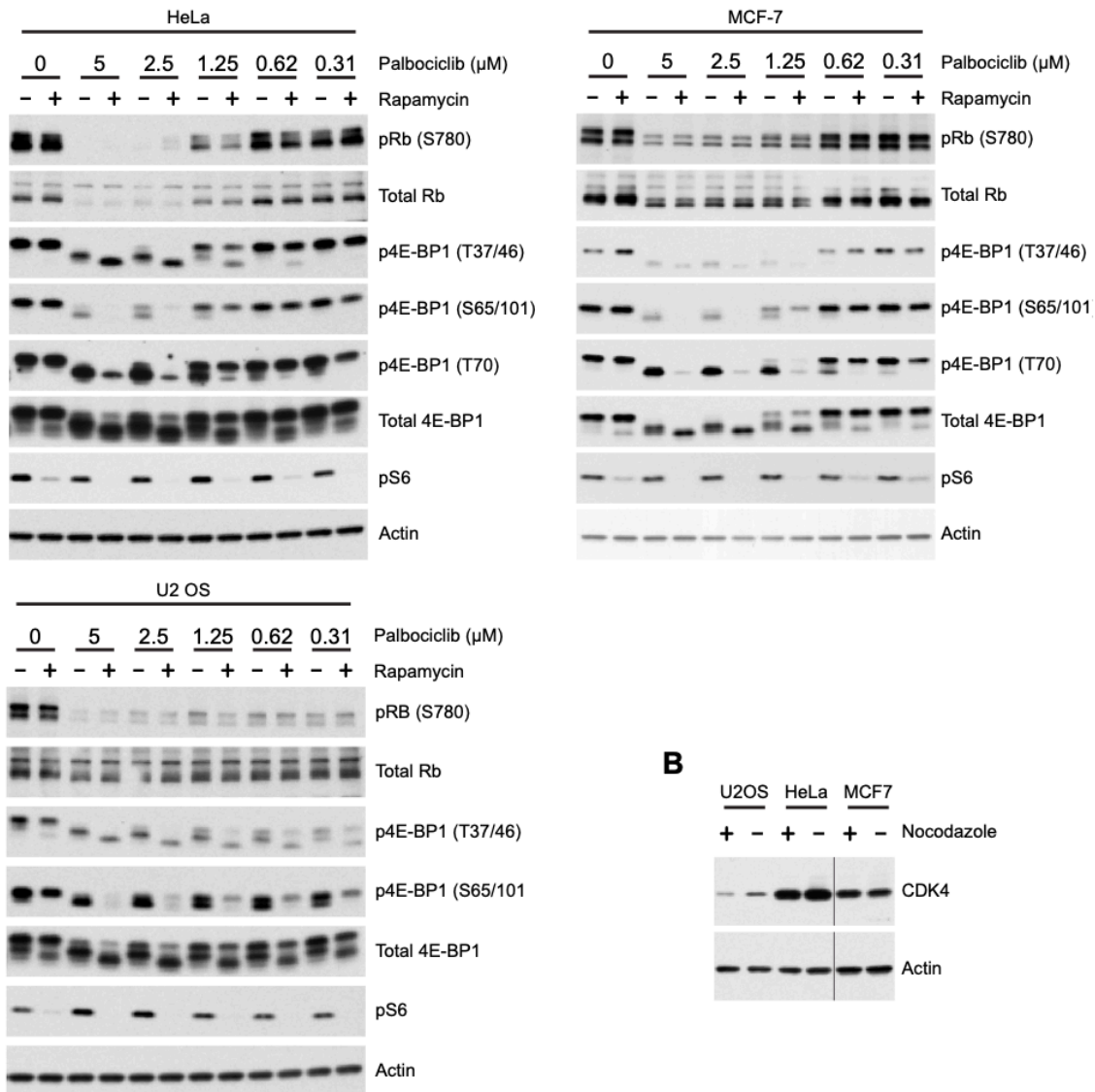
Figure 5.4 | 4E-BP1 phosphorylation mirrors pRb dose-dependently. A) Nocodazole arrested cells were treated with rapamycin (100 nM) and/or palbociclib (5 μM – 313 nM) in fresh media containing insulin

(150 nM) for 2 h. **B)** Western blot of relative CDK4 expression in cell lines used in **(A).** Samples were run on the same gel and are from the same exposure.

5.5 Palbociclib and Mitotic Cap-Dependent Translation

CDK4 inhibition results in reduced mitotic phosphorylation of 4E-BP1; however, it was unclear whether this directly affects rates of cap-dependent translation. To measure assembly of the eIF4F translation initiation complex, the 7-methyl guanosine (m7G) cap binding assay was used. Mitotic MCF-7 cells treated with rapamycin showed a marginal increase in 4E-BP1, and a corresponding slight decrease in eIF4G, associated with cap-bound eIF4E (Figure 5.5A). Similar results were observed in palbociclib treated cells; however, mitotic MCF-7s treated with the combination showed a robust increase in m7G associated 4E-BP1, and a large decrease in eIF4G. This benefit was only observed in MCF-7 cells recently release from nocodazole arrest, as palbociclib had very little effect eIF4F complex association in asynchronous cells. As expected, MDA-MB-468 cells did not respond to CDK4 inhibition, but displayed a predictable response to rapamycin.

The m7G cap affinity assay is a robust way of analyzing the ratio of 4E-BP1- and eIF4G-bound eIF4E, however it is performed in lysate, thus rendering any intricacies in sub-cellular localization of these proteins indeterminable. Therefore, a split-nanoluciferase-based assay was developed to quantify the eIF4E-4E-BP1 interaction in live cells. (Figure 5.6) Using this assay, CDK4 inhibition was found to cause a large increase in this interaction in live cells; the effect is compounded by tandem inhibition of mTORC1 with rapamycin. Attempts to use this assay for measuring the eIF4E-eIF4G interaction were unsuccessful, as no signal was observed under any conditions. This is likely due to the large size of eIF4G (220kDa) and the relative orientation of the two protein's N- and C-termini.
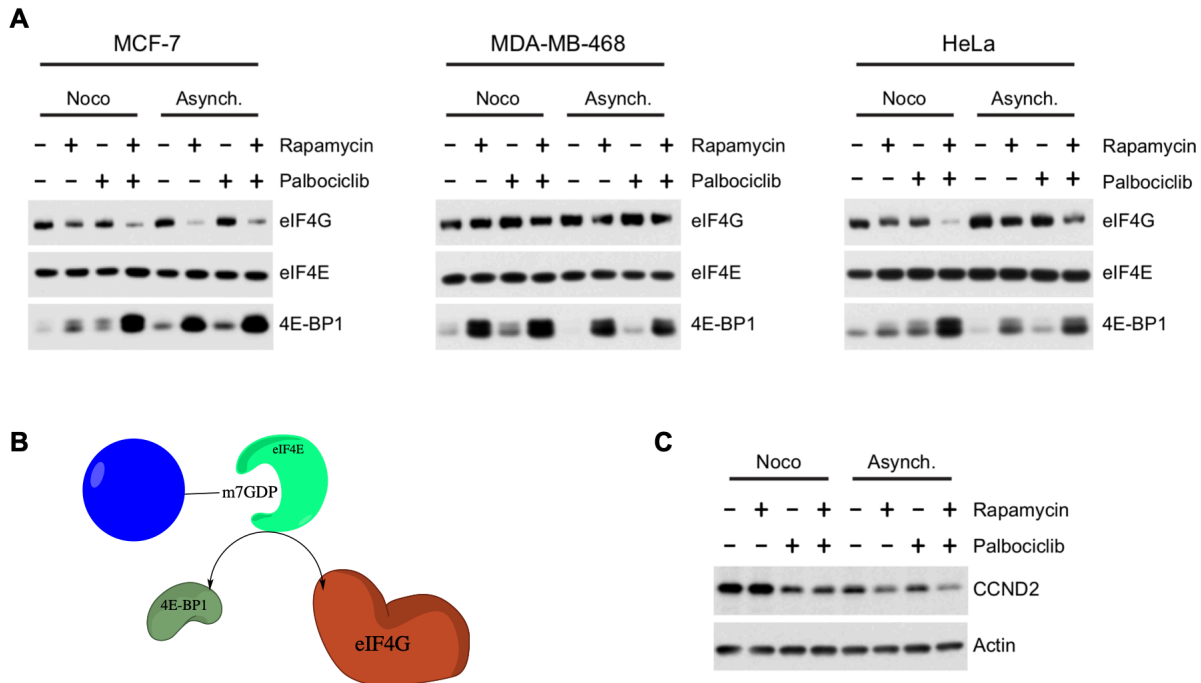
Figure 5.5 | mTOR and CDK4 Co-regulate Mitotic Cap-Dependent Translation. a, m′G cap affinity assay. Palbociclib and rapamycin synergize to increase eIF4E−4E-BP1 association and decrease eIF4E−eIF4G association in Palbociclib-sensitive cells. **B)** Schematic for the cap-affinity assay. **C)** Palbociclib results in the reduction of cap-dependent translation of Cyclin D2 in nocodazole-arrested U2 OS cells. All experiments were performed in biological triplicate; representative images are shown.

Though it was clearly established that CDK4 inhibition during mitosis increased eIF4E association with 4E-BP1, and decreased eIF4E association with eIF4G, it was still unclear of the effects this had on the expression of cap-dependent transcripts at the protein level. Therefore, the expression of cyclin D2, a *bona fide* cap-dependent transcript, was analyzed in both mitotic and asynchronous cells treated with palbociclib and/or rapamycin. In asynchronous U2 OS cells, palbociclib had no effect on cyclin D2 levels, whereas rapamycin markedly reduced the levels of this protein. Conversely, in cells recently released from a prometaphase block, rapamycin had very little effect, while inhibition of CDK4 resulted in a drastic reduction of cyclin D2 at the protein level. (Figure 5.5C) Moreover, Cyclin D2 expression was found to be higher in nocodazole arrested cells than in asynchronous cells, alluding to a requirement for CDK4/6 activity post-metaphase.
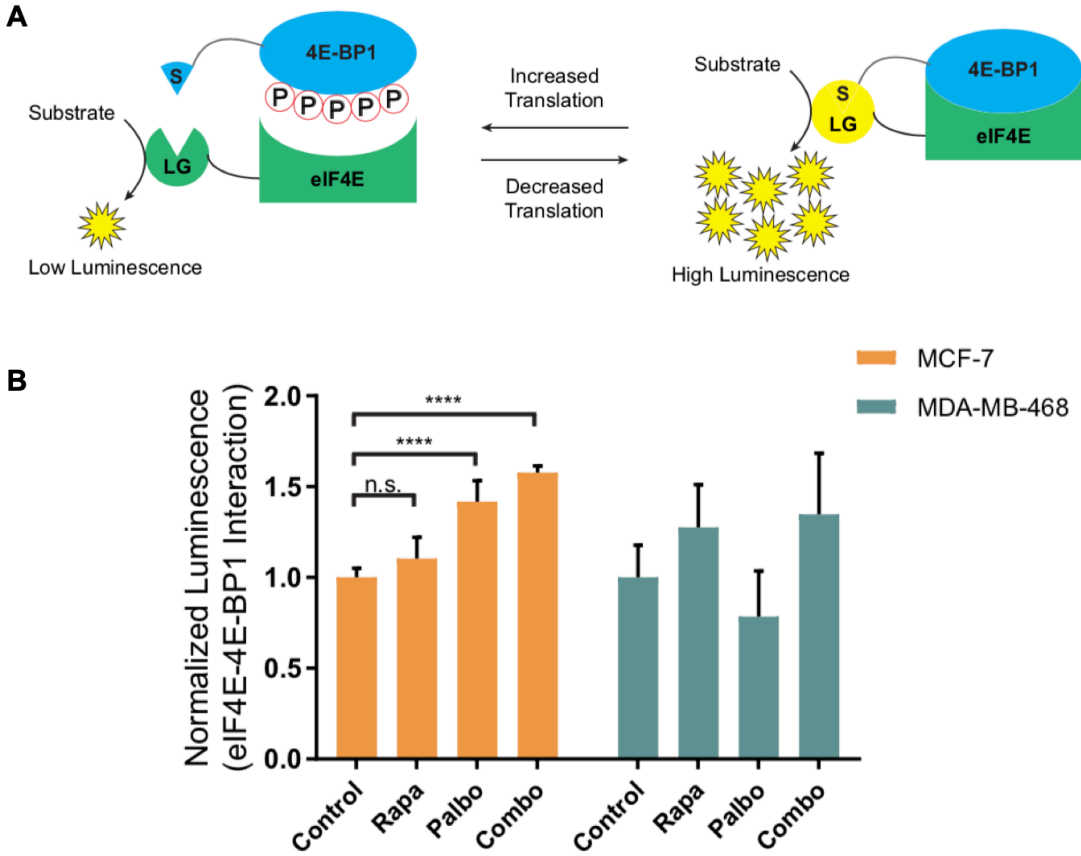
Figure 5.6 | mTOR and CDK4 Regulate eIF4E-4E-BP1 Association in Mitotic Cells. A) Schematic for the nanoluciferase assay monitoring the eIF4E–4E-BP1 interaction in live cells. S=SmBit, LG=LargeBit. Data shown in panel **B)** Error is plotted as +/- SEM, n = 5.

5.6 CDK4 Controls the M→G1 Transition

To characterize the effect of CDK4 inhibition on progression through mitosis into G1, the cell cycle distribution was analyzed at several time points following release from a prometaphase arrest. MCF-7 cells treated with palbociclib showed a profound G2 block, relative to control cells, as they were unable to transition into G1. (Figure 5.7A and 5.7B) However, in the CDK4 inhibitor resistant MDA-MB-468 cell line, palbociclib had very little effect after an initial G2 delay. As expected, the MDA-MB-231 cell line showed an intermediate G2 block compared to these other two cell lines. These results were not influenced by a change in polyploidy. (Figure 5.7C)
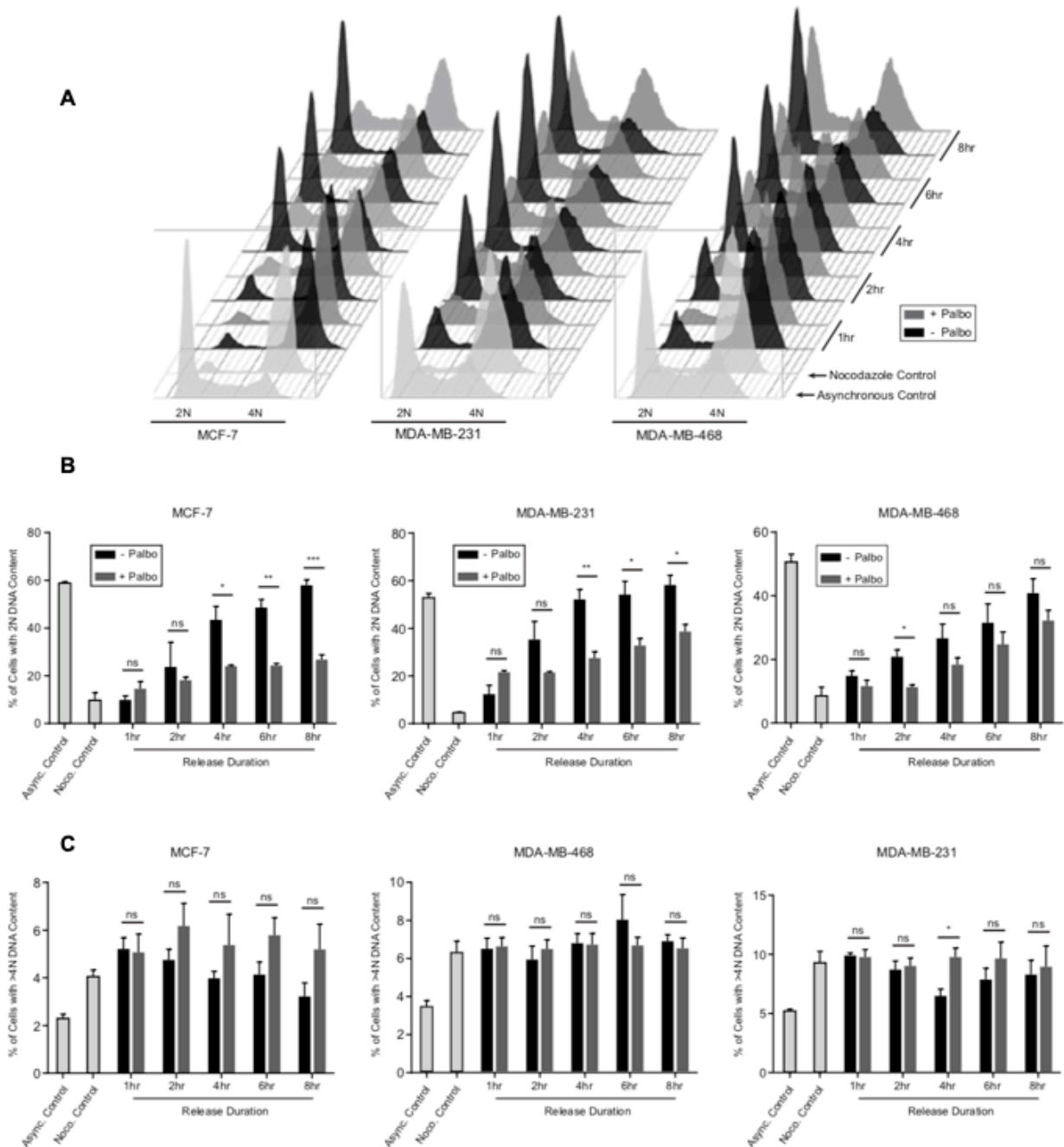
Figure 5.7 | CDK4 Inhibition Results in a G2-Block in Palbociclib-Sensitive cells. A) Full cell-cycle profiles of cells arrested with nocodazole, and then released into media with or without palbociclib (5 μM) for the indicated time points. **B)** Quantification of the percentage of cells from a with 2N DNA content from **(A)**. **C)** Quantification of the percentage of cells from a with >4N DNA content from **(A)** Data are represented as the mean +/- standard deviation of three biological replicates.

These results are quite interesting in the context of the canonical role of CDK4, as it is primarily responsible for controlling the checkpoint at the G1→S transition. However, it

has previously been demonstrated that Cyclin D3/CDK4 activity is essential for progression through G2, and that ionizing radiation activates p16 causing CDK4 inhibition leading to a G2 phase delay.[16] Additionally, analysis of pRb phosphorylation at S780, showed an increase in CDK4 activity in cells released from a prometaphase arrest across a panel of cell lines. (Figure 5.8) These data support the essential role of CDK4/Cyclin D3 in progression into G1 from G2/M, and provides evidence that pharmacological inhibition can result in a G2 block even in p16 null cancer cell lines, such as MCF 7.[17] However, the exact mechanism of this G2 delay is not fully understood. It is possible that inhibition of Rb phosphorylation is the primary factor, though an inability to translate critical anabolic proteins, due to inhibited cap-dependent translation, may also play a role. However, the fact that palbociclib treatment slows G1 entry in Rb-null MDA-MB-468 cells at early time points following release, suggests that other CDK4/6 activity is important for regulation of this transition. This could be due to an altered transcriptional program induced by inhibition of phosphorylation of FOXM1, a master transcription factor that regulates expression of genes essential for mitosis.[18] Moreover, it is unclear at what stage of the cell cycle these cells are being blocked, whether in later stages of mitosis or simply a failure to undergo cytokinesis. However, it is clear that a post-mitotic checkpoint is in part regulated by CDK4, and gaining a better understanding of the mechanism behind this warrants further consideration.
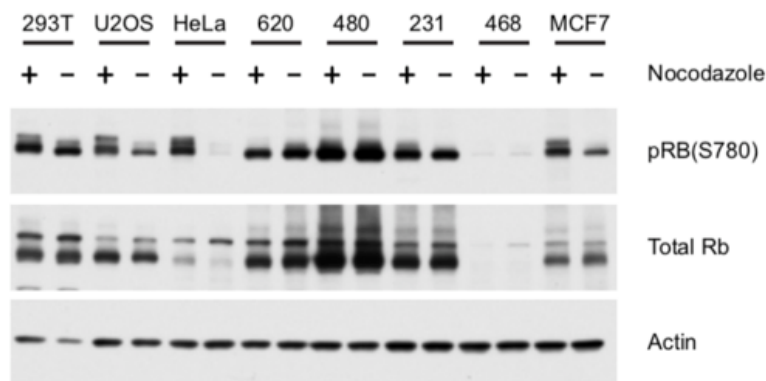
Figure 5.8 | Cells Arrested in Mitosis Exhibit Increased CDK4 Activity. Western blot of phosphorylated pRb from cell lines growing asynchronously, or treated +/- 500 nM nocodazole for 20 hours to induce a prometaphase arrest.

5.7 Conclusions

In this chapter, evidence was presented suggesting that CDK4 phosphorylates 4E-BP1 during mitosis, maintaining cap-dependent translation. Given this newly discovered role, it is likely that inhibition of this process is a previously unknown function of CDK4 inhibitors such as palbociclib. However, it is important to point out a discrepancy between our findings and previous studies that have investigated the mechanism of action of CDK4/6 inhibitors. It is well established that long-term inhibition of CDK4/6 activity results in a robust G1 arrest. However, these findings have demonstrated that inhibition of CDK4 during mitosis results in an arrest at the M→G1 transition. It is likely that cells that escape mitosis and transit into G1 do so with lower levels of important proteins that would otherwise contribute to the G1→S transition, such as the D-type cyclins, thereby increasing the propensity for a G1 arrest. Moreover, those cells that do not escape CDK4 inhibitor induced G2 arrest may, after an extended period, undergo apoptosis or necrosis. Though this has not been observed at time points up to 8 hours, (data not shown) longer time points may yield a better understanding of these discrepancies.

It is important to try to reconcile these observations with those previously observed that report CDK1 as the kinase that phosphorylates 4E-BP1 during mitosis.[8,9] It is possible that, given the differences in experimental design between this report and those of Shuda et. al, CDK1 phosphorylates 4E-BP1 in prometaphase, but in later stages of mitosis and/or cytokinesis (following degradation of cyclin B1), CDK4 assumes that role. (Figure 5.9) It is also possible that S101 phosphorylation is strictly CDK4 dependent (See Chapter 4), but the effect it has on global phosphorylation of 4E-BP1, renders CDK1 effectively null towards the reported CDK1 sites. Therefore, it is possible that mTOR, CDK1 and CDK4 all act in concert to regulate cap-dependent translation during mitosis and the transition into G1.
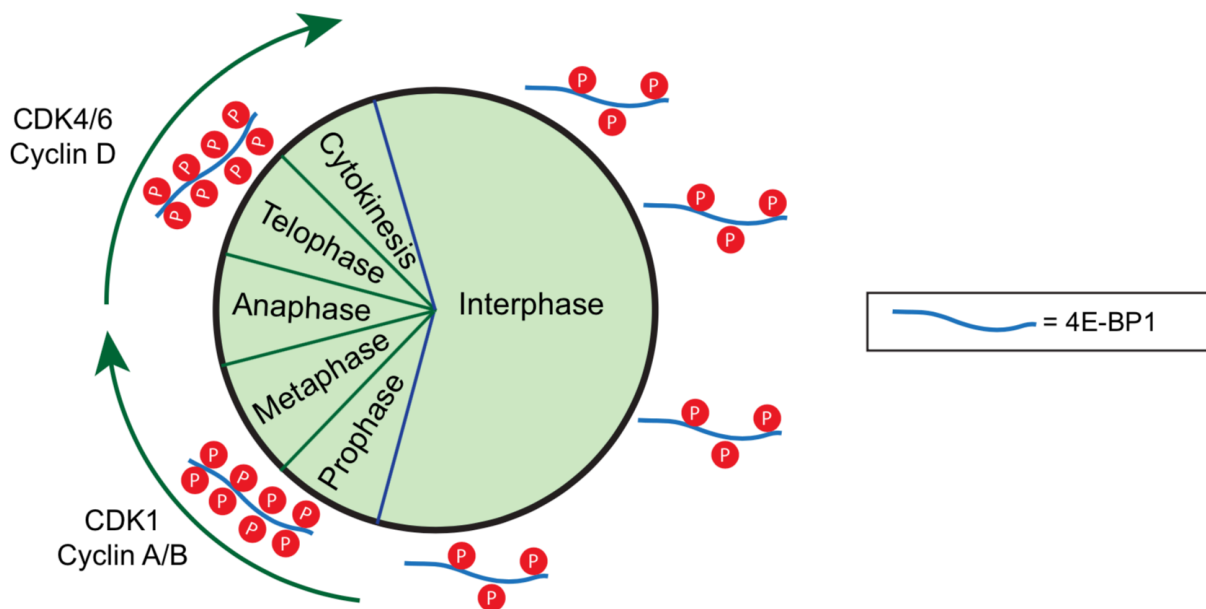
Figure 5.9 | Proposed Scheme for Regulation of Mitotic 4E-BP1 Phosphorylation. In this scheme, 4E-BP1 phosphorylation is maintained at medium levels during interphase (G1, S, G2), but induction of CDK1 activity in prophase induces hyperphosphorylation. This phenotype is maintained by Cyclin D-CDK4 complexes through cytokinesis after degradation of Cyclin B1 to start Anaphase.

5.8   Materials and Methods

Small molecule reagents

Palbociclib Isethionate (Selleckchem) was dissolved in water to 10 mM. Rapamycin (Alfa Aesar), and SP600125 (ApexBio) were dissolved in DMSO. Human recombinant insulin was purchased from Sigma. Nocodazole and 3XFLAG peptide were purchased from ApexBio. All reagents were used as received.

Cell Culture

HEK293T and HeLa cells were grown in DMEM (Corning) supplemented with 10% FBS, glutamine, penicillin, and streptomycin (Gibco). U2 OS cells were kindly provided by Dr. Beth Lawlor and cultured according to ATCC guidelines. MDA-MB-231 cells were a kind gift from Dr. Nouri Neamati and grown in RPMI-1640 media supplemented with 10% FBS and glutamine. MDA-MB-468 and MCF-7 cells were a kind gift from Dr. Max Wicha. MDA-MB-468 cells were grown in DMEM (Corning) supplemented with 10% FBS and glutamine. MCF-7 cells were cultured according to ATCC guidelines. Cells were grown at

37 °C with 5% CO_2 in a humidified incubator, passaged at least twice before use for experiments and no more than 10 times before returning to low passage stocks. All cell lines were authenticated by STR profiling, and regularly tested for mycoplasma contamination.

Preparation of m⁷GDP resin

 m⁷GDP resin synthesis was adapted from that reported.[19] m⁷GDP sodium salt (2.3 mg; Sigma) was dissolved in water (500 μL), and a solution of sodium periodate (1.1 mg) in sodium acetate buffer (100 μL; 0.1M, pH 6) was added. The resulting mixture was agitated at room temperature for 30 min protected from light. Adipic acid dihydrazide agarose (1 mL packed; Sigma) was washed with water (1× 20 mL) followed by sodium acetate buffer (1× 20mL), and then re-suspended in sodium acetate buffer (2 mL). To this slurry was added with aniline (10 μL) and the oxidized m⁷GDP solution. The resin mixture was then shaken at room temperature for 45 min before adding sodium cyanoborohydride (5 mg) and agitated overnight at 4 °C. The resin was washed with NaCl (1M; 5× 5 mL), equilibrated in buffer A (5 mL; 50 mM HEPES, pH 7, 200 mM KCl), and stored at 4 °C.

m7G cap affinity assay

Cap pull-down assay was carried out as previously described[20]. Briefly, cells were lysed in cap pull-down buffer (50 mM HEPES-KOH pH 7.5, 150 mM KCl, 1 mM EDTA, 2 mM DTT and 0.1% Tween 20) containing protease and phosphatase inhibitors and freeze-thawed thrice. Cell lysate was centrifuged at 20,000×g for 25 min. Supernatant was then incubated for 2 h at 4 °C with m⁷GDP-agarose resin. Resin was washed with cap pull-down buffer (3×) followed by TBS and water. Proteins were then eluted by boiling in 2× LDS sample buffer (10 min at 70 °C) and analyzed by Western blotting.

Nanobit/split luciferase assay

pFN33K LgBiT-eIF4E and pFN35K SmBiT-4EBP1 (50 ng each) were reverse-transfected into MCF-7 and MDA-MB-468 cells in a 96-well white opaque plate using Lipfectamine LTX with PLUS reagent. After 16 h, cells were arrested with nocodazole (500 nM). 20 h

later, cells were treated with rapamycin (100 nM) and/or palbociclib (5 μM). After 2 h incubation, Nano-Glo Live cell reagent (Promega #N2011; 25 μL) was added and total luminescence was read within 40 min on a BioTek Cytation 3 reader.

DNA constructs

eIF4E was digested out of HaloTag-eIF4E using SgfI and PmeI, and then ligated into pFN33K (Promega) to obtain the LargeBit-eIF4E construct. 4E-BP1 was cloned into pFN35K (Promega) using the same method to obtain the SmallBit-4E-BP1 construct. HaloTag-4E-BP1 and -eIF4E have been described elsewhere.[21]

Flow cytometry

Cells were harvested with trypsin, washed once with ice-cold 1$\times$ PBS, re-suspended in ice cold 1$\times$ PBS, and then 100% ice-cold ethanol was added dropwise to a final concentration of 70%. Cells were fixed at -20 °C for 4 h, and then stored at 4 °C for 18–96 h. Fixed cells were washed twice with ice-cold 1$\times$ PBS, re-suspended in 1$\times$ PBS containing propidium iodide (50 μg/mL; Sigma) and RNase A (100 μg/mL, Fisher), and incubated at 37 °C for 30 min. Cells were then filtered and analyzed using a Cytoflex flow cytometer (Beckman). Cell cycle distributions were analyzed using FlowJo (v10).

Statistics

Two-sided t-tests were performed using Prism (v7); equal variance between samples being compared was established. Graphs show mean +/- S.E.M or +/- standard deviation as described in the figure legends.

Immunoblotting and PhAXA-MS

Performed as described in Chapters 3 and 4.

5.9   References

1   Chen, E. *et al.* Dysregulated expression of mitotic regulators is associated with B-cell lymphomagenesis in HOX11-transgenic mice. *Oncogene* **25**, 2575-2587, doi:10.1038/sj.onc.1209285 (2006).

2   Urzua, U., Ampuero, S., Roby, K. F., Owens, G. A. & Munroe, D. J. Dysregulation of mitotic machinery genes precedes genome instability during spontaneous pre-malignant transformation of mouse ovarian surface epithelial cells. *BMC Genomics* **17**, 728, doi:10.1186/s12864-016-3068-5 (2016).

3   Salaun, P., Rannou, Y. & Prigent, C. Cdk1, Plks, Auroras, and Neks: the mitotic bodyguards. *Adv Exp Med Biol* **617**, 41-56 (2008).

4   van Leuken, R., Clijsters, L. & Wolthuis, R. To cell cycle, swing the APC/C. *Biochim Biophys Acta* **1786**, 49-59, doi:10.1016/j.bbcan.2008.05.002 (2008).

5   Chang, D. C., Xu, N. H. & Luo, K. Q. Degradation of cyclin B is required for the onset of anaphase in mammalian cells. *Journal of Biological Chemistry* **278**, 37865-37873, doi:10.1074/jbc.M306376200 (2003).

6   Petrone, A., Adamo, M. E., Cheng, C. & Kettenbach, A. N. Identification of Candidate Cyclin-dependent kinase 1 (Cdk1) Substrates in Mitosis by Quantitative Phosphoproteomics. *Molecular & cellular proteomics : MCP* **15**, 2448-2461, doi:10.1074/mcp.M116.059394 (2016).

7   Heesom, K. J., Gampel, A., Mellor, H. & Denton, R. M. Cell cycle-dependent phosphorylation of the translational repressor eIF-4E binding protein-1 (4E-BP1). *Curr Biol* **11**, 1374-1379 (2001).

8   Shuda, M. *et al.* CDK1 substitutes for mTOR kinase to activate mitotic cap-dependent protein translation. *Proceedings of the National Academy of Sciences of the United States of America* **112**, 5875-5882, doi:10.1073/pnas.1505787112 (2015).

9   Velasquez, C. *et al.* Mitotic protein kinase CDK1 phosphorylation of mRNA translation regulator 4E-BP1 Ser83 may contribute to cell transformation. *Proceedings of the National Academy of Sciences of the United States of America* **113**, 8466-8471, doi:10.1073/pnas.1607768113 (2016).

10   Marash, L. *et al.* DAP5 promotes cap-independent translation of Bcl-2 and CDK1 to facilitate cell survival during mitosis. *Molecular cell* **30**, 447-459, doi:10.1016/j.molcel.2008.03.018 (2008).

11   Pyronnet, S., Dostie, J. & Sonenberg, N. Suppression of cap-dependent translation in mitosis. *Genes & development* **15**, 2083-2093, doi:10.1101/gad.889201 (2001).

12   Qin, X. & Sarnow, P. Preferential translation of internal ribosome entry site-containing mRNAs during the mitotic cycle in mammalian cells. *The Journal of biological chemistry* **279**, 13721-13728, doi:10.1074/jbc.M312854200 (2004).

13   Wilker, E. W. *et al.* 14-3-3sigma controls mitotic translation to facilitate cytokinesis. *Nature* **446**, 329-332, doi:10.1038/nature05584 (2007).

14   Tanenbaum, M. E., Stern-Ginossar, N., Weissman, J. S. & Vale, R. D. Regulation of mRNA translation during mitosis. *Elife* **4**, doi:10.7554/eLife.07957 (2015).

15   Finn, R. S. *et al.* PD 0332991, a selective cyclin D kinase 4/6 inhibitor, preferentially inhibits proliferation of luminal estrogen receptor-positive human breast cancer cell lines in vitro. *Breast Cancer Res* **11**, R77 (2009).

16   Gabrielli, B. G. *et al.* A cyclin D-Cdk4 activity required for G2 phase cell cycle progression is inhibited in ultraviolet radiation-induced G2 phase delay. *The Journal of biological chemistry* **274**, 13961-13969 (1999).

17   Hui, R. *et al.* INK4a gene expression and methylation in primary breast cancer: overexpression of p16INK4a messenger RNA is a marker of poor prognosis. *Clinical cancer research : an official journal of the American Association for Cancer Research* **6**, 2777-2787 (2000).

18   Anders, L. *et al.* A systematic screen for CDK4/6 substrates links FOXM1 phosphorylation to senescence suppression in cancer cells. *Cancer Cell* **20**, 620-634, doi:10.1016/j.ccr.2011.10.001 (2011).

19   Edery, I., Altmann, M. & Sonenberg, N. High-level synthesis in Escherichia coli of functional cap-binding eukaryotic initiation factor eIF-4E and affinity purification using a simplified cap-analog resin. *Gene* **74**, 517-525 (1988).

20   Yanagiya, A. *et al.* Translational homeostasis via the mRNA cap-binding protein, eIF4E. *Molecular cell* **46**, 847-858, doi:10.1016/j.molcel.2012.04.004 (2012).

21   Song, J. M., Menon, A., Mitchell, D. C., Johnson, O. T. & Garner, A. L. High-Throughput Chemical Probing of Full-Length Protein-Protein Interactions. *ACS Comb Sci* **19**, 763-769, doi:10.1021/acscombsci.7b00128 (2017).

Chapter 6

Conclusions and Future Directions

6.1 PhAXA: Limitations and Further Optimization

The development of activity-based probes for kinase discovery has been an active area of interest for over 15 years. Yet, the tools that have so far been developed have not reached the desired goal of reliably identifying novel kinase-substrate interactions. This work has demonstrated the ability of PhAXA to fill this unmet need, constituting the first reported successful kinase discovery using an activity-based probe. PhAXA was proven to be broadly applicable relative to the desired bait protein, as it performed well using three distinct classes of substrate proteins (4E-BP1, c-Jun and Erk2). Moreover, this method has been deemed amenable to using serine, threonine, and tyrosine to cysteine mutants as phosphosite mimetics. However, it is important to emphasize that the work-flow for this assay will need to be optimized for each bait protein of interest. Each bait system described here utilized the exact same assay conditions with respect to buffers, additives, detergents, lysis methods and cell lines. It is possible that, with further optimization of these assay parameters, PhAXA can provide more robust enrichment of the appropriate kinase or kinases. However, the conditions outlined in this report provide a starting point for pursuing other kinase-substrate systems of interest, and serve as a testament to the robust nature of this chemoproteomic approach.

The largest limitation of this assay is the need to perform the pulldown in lysate, rather than with intact cells, as subcellular localization is known to significantly contribute to kinase activity.[1,2] Moreover, a positive identification may arise from a kinase that is normally localized to a compartment that would preclude an interaction with the bait of interest. This hypothetical scenario highlights the importance of thoroughly validating any

118

identified relationships in a more physiological setting. Some groups have attempted to make cell permeable, kinase-directed probes to circumvent the issue of cell permeability.[3,4] While the goal of cell permeability can be achieved, these probes lose affinity to kinases, resulting in under-sampling the available kinome relative to the non-cell permeable probes used in lysate. Thus, it is clear that this is a balancing act between achieving increased target engagement vs increased physiological relevance. It seems the most prudent course would be to couple PhAXA for an unbiased query of the available kinome, with a proximity labeling technique that maintains cellular integrity. Implementation of this type of orthogonal approach would yield very high-confidence interactions, but would also substantially increase the amount of work required for answering a biological question.

Another potentially useful adaptation to PhAXA would be to incorporate ADP-based methacrylate crosslinkers into the workflow, as the conserved active-site lysine targeted by these probes can be shifted towards the beta-phosphate in some kinases. This modified crosslinker would likely improve kinome coverage, as a similar finding was observed with the nucleotide acyl phosphate probes discussed in Chapter 1.[5] Finally, to achieve a more accurate and sensitive quantification between samples, an approach utilizing isobaric tags[6] should be used. When coupled with Real-Time Searching (RTS) and MS3 analysis of reporter ions,[7] this method can provide more accurate peptide/protein quantitation and significantly reduced acquisition time relative to label free methods.[8]

6.2 4E-BP1 as a Biomarker for CDK4/6 Inhibitors

The lack of biomarkers that predict the efficacy of CDK4/6 inhibitors has significantly limited the clinical success of these drugs.[9,10]. Biomarker such as RB1, p16, CCND1, CCND3 and CDK4 have not translated to clinical success, likely due to an incomplete understanding of the mechanism by which these drugs ultimately work.[11,12] However, implementation of PhAXA for identifying kinases capable of mTOR-independent phosphorylation of 4E-BP1 identified a novel function of CDK4, and CDK4/6 inhibitors by extension. The finding that CDK4 phosphorylates 4E-BP1, thereby

maintaining cap-dependent translation under conditions of mTOR inhibition is a critical insight into how CDK4/6 inhibitors regulate cell proliferation in cancers.

The identification of S101, a previously poorly understood phosphorylation site, as a *bona fide* CDK4 substrate has far-reaching applications. Data presented in Chapter 4 shows S65/101 phosphorylation can predict overall survival of patients with breast cancer, while T37/46 provide no prognostic value. As Ser65, Thr37, and Thr46 are all canonical mTORC1 substrates, while Ser101 is not, it is possible that S101 phosphorylation could provide the majority of predictive value in this patient cohort. Unfortunately, it is impossible to differentiate between the phosphorylation of S65 and S101 by Western blot, RPPA or IHC given the promiscuity of the antibody, so targeted mass-spec based methods, such as Selected Reaction Monitoring (SRM), will need to be developed for accurate analysis of S101 as biomarker. However, given that phosphorylation of this residue promotes expression of c-Myc, an oncogene that strongly promotes malignant transformation, successful adaptation of S101 as a clinical biomarker could open up a new patient population that may benefit from CDK4/6 inhibitors.

6.3   Palbociclib and Rapalog Therapy in the Clinic

CDK4/6 inhibitors are largely ineffective as standalone therapies for cancer, likely due their properties as cytostatic, rather than cytotoxic, drugs.[13] However, as field of leveraging kinase inhibitors as cancer therapeutics moves in the direction of double or triple agent therapies,[14,15] the future of CDK4/6 inhibitors lies in two realms. First, in the field of immunotherapeutics, CDK4/6 inhibitors have been shown to cooperate with anti-PD-L1 antibodies to modulate the immune response, thereby increasing infiltration of tumors by cytotoxic T-cells.[16] This has been shown to occur via upregulation of the PD-L1 protein in response to CDK4/6 inhibition.[17] Second, several studies have reported potent *in vivo* antitumor effects by combined inhibition of mTOR and CDK4/6, [18-21] while a large phenotypic screen found the strongest synergy between PI3K/mTORC1 and CDK4/6 inhibitors.[22] In addition, many ongoing clinical trials are investigating the efficacy of this combination in treating a range of cancers (Table 4.2). However, the rationale for this combination is lacking, as an in-depth understanding of the molecular mechanisms for this observed cooperativity is not understood.

Findings presented in Chapter 4 clearly demonstrate that these drugs provide an additive benefit over standalone therapies, in part, by inhibiting CDT, thereby decreasing the expression of anabolic proteins, and by altering the c-Myc transcriptional program that drives a wide range of cancers.[23] These findings support the investigation of this combination for treating cancers displaying clear hallmarks of an addiction to CDT.[24] Finally, investigations should be made into this using this combination as a therapy for KRAS driven cancers. Tumors harboring activated KRAS are the most resistant to mTOR inhibitors, and CDK4/6 inhibition can partially downregulate the KRAS-associated gene signature.[25-28]

6.4 Concluding Remarks

As our knowledge of the human phosphoproteome expands, development of tools for confidently assigning kinases to these tens of thousands of orphan phosphorylation sites is paramount. By filling in these gaps of knowledge, scientists can uncover signaling intermediates and biomarkers important for more effective treatment of cancers and other diseases. Despite the potential for improvements, wide-spread application of the existing PhAXA platform will help achieve this result. Leveraging these new findings will uncover novel drug targets, while maximizing the clinical benefit of existing inhibitors through a better understanding of cancer-specific signal transduction.

6.5 References

1   Menon, S. *et al.* Spatial control of the TSC complex integrates insulin and nutrient regulation of mTORC1 at the lysosome. *Cell* **156**, 771-785, doi:10.1016/j.cell.2013.11.049 (2014).
2   Wang, S. Y. *et al.* Lysosomal amino acid transporter SLC38A9 signals arginine sufficiency to mTORC1. *Science* **347**, 188-194, doi:10.1126/science.1257132 (2015).
3   Fouda, A. E. & Pflum, M. K. A Cell-Permeable ATP Analogue for Kinase-Catalyzed Biotinylation. *Angewandte Chemie* **54**, 9618-9621, doi:10.1002/anie.201503041 (2015).
4   Zhao, Q. *et al.* Broad-Spectrum Kinase Profiling in Live Cells with Lysine-Targeted Sulfonyl Fluoride Probes. *Journal of the American Chemical Society* **139**, 680-685, doi:10.1021/jacs.6b08536 (2017).
5   Patricelli, M. P. *et al.* Functional interrogation of the kinome using nucleotide acyl phosphates. *Biochemistry* **46**, 350-358, doi:DOI 10.1021/bi062142x (2007).

6 Thompson, A. *et al.* Tandem mass tags: a novel quantification strategy for comparative analysis of complex protein mixtures by MS/MS. *Analytical chemistry* **75**, 1895-1904 (2003).

7 Erickson, B. K. *et al.* Active instrument engagement combined with a real-time database search for improved performance of sample multiplexing workflows. *J Proteome Res*, doi:10.1021/acs.jproteome.8b00899 (2019).

8 O'Connell, J. D., Paulo, J. A., O'Brien, J. J. & Gygi, S. P. Proteome-Wide Evaluation of Two Common Protein Quantification Methods. *J Proteome Res* **17**, 1934-1942, doi:10.1021/acs.jproteome.8b00016 (2018).

9 DeMichele, A. *et al.* CDK 4/6 inhibitor palbociclib (PD0332991) in Rb+ advanced breast cancer: phase II activity, safety, and predictive biomarker assessment. *Clinical cancer research : an official journal of the American Association for Cancer Research* **21**, 995-1001, doi:10.1158/1078-0432.CCR-14-2258 (2015).

10 Fang, H., Huang, D., Yang, F. & Guan, X. Potential biomarkers of CDK4/6 inhibitors in hormone receptor-positive advanced breast cancer. *Breast Cancer Res Treat* **168**, 287-297, doi:10.1007/s10549-017-4612-y (2018).

11 Knudsen, E. S. & Witkiewicz, A. K. The Strange Case of CDK4/6 Inhibitors: Mechanisms, Resistance, and Combination Strategies. *Trends Cancer* **3**, 39-55, doi:10.1016/j.trecan.2016.11.006 (2017).

12 McNair, C. *et al.* Differential impact of RB status on E2F1 reprogramming in human cancer. *The Journal of clinical investigation* **128**, 341-358, doi:10.1172/JCI93566 (2018).

13 Hamilton, E. & Infante, J. R. Targeting CDK4/6 in patients with cancer. *Cancer Treat Rev* **45**, 129-138, doi:10.1016/j.ctrv.2016.03.002 (2016).

14 Apsel, B. *et al.* Targeted polypharmacology: discovery of dual inhibitors of tyrosine and phosphoinositide kinases. *Nature chemical biology* **4**, 691-699, doi:10.1038/nchembio.117 (2008).

15 Ma, X. D., Lv, X. Q. & Zhang, J. K. Exploiting polypharmacology for improving therapeutic outcome of kinase inhibitors (KIs): An update of recent medicinal chemistry efforts. *Eur J Med Chem* **143**, 449-463, doi:10.1016/j.ejmech.2017.11.049 (2018).

16 Schaer, D. A. *et al.* The CDK4/6 Inhibitor Abemaciclib Induces a T Cell Inflamed Tumor Microenvironment and Enhances the Efficacy of PD-L1 Checkpoint Blockade. *Cell Rep* **22**, 2978-2994, doi:10.1016/j.celrep.2018.02.053 (2018).

17 Zhang, J. *et al.* Cyclin D-CDK4 kinase destabilizes PD-L1 via cullin 3-SPOP to control cancer immune surveillance. *Nature* **553**, 91-95, doi:10.1038/nature25015 (2018).

18 Michaloglou, C. *et al.* Combined inhibition of mTOR and CDK4/6 is required for optimal blockade of E2F function and long term growth inhibition in estrogen receptor positive breast cancer. *Cancer research* **78** (2018).

19 Cortes, J. *et al.* The next era of treatment for hormone receptor-positive, HER2-negative advanced breast cancer: triplet combination-based endocrine therapies. *Cancer Treat. Rev.* **61**, 53-60 (2017).

20 Pikman, Y. *et al.* Synergistic drug combinations with a CDK4/6 inhibitor in T-cell acute lymphoblastic leukemia. *Clin. Cancer Res.* **23**, 1012-1024 (2016).

21 Olmez, I. *et al.* Combined CDK4/6 and mTOR inhibition is synergistic against glioblastoma via multiple mechanisms. *Clin. Cancer Res.* **23**, 6958-6968 (2017).

22   Vora, S. R. *et al.* CDK 4/6 inhibitors sensitize PIK3CA mutant breast cancer to PI3K inhibitors. *Cancer Cell* **26**, 136-149, doi:10.1016/j.ccr.2014.05.020 (2014).

23   Dang, C. V. MYC on the path to cancer. *Cell* **149**, 22-35 (2012).

24   Pelletier, J., Graff, J., Ruggero, D. & Sonenberg, N. Targeting the eIF4F translation initiation complex: a critical nexus for cancer development. *Cancer Res.* **75**, 250-263 (2015).

25   Lee, M. S. *et al.* Efficacy of the combination of MEK and CDK4/6 inhibitors in vitro and in vivo in KRAS mutant colorectal cancer models. *Oncotarget* **7**, 39595-39608, doi:10.18632/oncotarget.9153 (2016).

26   Ziemke, E. K. *et al.* Sensitivity of KRAS-Mutant Colorectal Cancers to Combination Therapy That Cotargets MEK and CDK4/6. *Clinical cancer research : an official journal of the American Association for Cancer Research* **22**, 405-414, doi:10.1158/1078-0432.CCR-15-0829 (2016).

27   Hart, L. S. *et al.* Preclinical Therapeutic Synergy of MEK1/2 and CDK4/6 Inhibition in Neuroblastoma. *Clinical cancer research : an official journal of the American Association for Cancer Research* **23**, 1785-1796, doi:10.1158/1078-0432.CCR-16-1131 (2017).

28   Pek, M. *et al.* Oncogenic KRAS-associated gene signature defines co-targeting of CDK4/6 and MEK as a viable therapeutic strategy in colorectal cancer. *Oncogene* **36**, 4975-4986, doi:10.1038/onc.2017.120 (2017).

APPENDICES

Appendix A

All Protein IDs from PhAXA-MS with c-Jun as Bait

	Replicate 1 PSMs				Replicate 2 PSMs				Average PSMs			
PROTID	c-Jun (C99A) + **1**	c-Jun (C99A) ATP ctl	c-Jun (C99A/S63C) + **1**	c-Jun (C99A/S63C) ATP ctl	c-Jun (C99A) + **1**	c-Jun (C99A) ATP ctl	c-Jun (C99A/S63C) + **1**	c-Jun (C99A/S63C) ATP ctl	c-Jun (C99A) + **1**	c-Jun (C99A) ATP ctl	c-Jun (C99A/S63C) + **1**	c-Jun (C99A/S63C) ATP ctl
P05412	541	634	481	499	1546	1537	1260	1235	1043.5	1085.5	870.5	867
P30153	96	41	104	49	275	106	324	132	185.5	73.5	214	90.5
P06748	135	156	133	137	248	337	271	335	191.5	246.5	202	236
O14744	167	177	151	176	210	207	252	246	188.5	192	201.5	211
P63151	92	29	88	36	194	62	253	74	143	45.5	170.5	55
Q9BQA1	190	201	158	193	159	145	161	172	174.5	173	159.5	182.5
TRYP_PIG	126	129	108	100	211	210	206	240	168.5	169.5	157	170
A0A087X2H	115	14	105	18	119	31	137	30	117	22.5	121	24
P78347	122	123	106	111	120	152	124	142	121	137.5	115	126.5
O95373	93	99	78	88	128	68	152	118	110.5	83.5	115	103
H0YIV4	55	126	58	98	198	259	151	248	126.5	192.5	104.5	173
P67775	42	25	44	26	109	37	153	36	75.5	31	98.5	31
O15397	61	46	74	38	95	13	105	21	78	29.5	89.5	29.5
P07437	80	66	85	60	42	38	68	54	61	52	76.5	57
P23588	0	87	138	93	5	4	6	5	2.5	45.5	72	49
Q99733-2	33	64	45	63	103	138	77	152	68	101	61	107.5
A0A0A0MF	105	87	113	91	6	5	7	11	55.5	46	60	51
P55072	105	122	117	125	2	1	1	1	53.5	61.5	59	63
P50990	65	74	72	74	35	31	44	34	50	52.5	58	54
P68363	36	9	72	47	44	42	38	41	40	25.5	55	44
Q16531	57	42	41	39	79	55	68	31	68	48.5	54.5	35
O75643	88	76	68	65	24	7	30	12	56	41.5	49	38.5
P78371	53	76	60	69	29	29	37	35	41	52.5	48.5	52
P26641	41	45	47	43	51	34	50	15	46	39.5	48.5	29
P17987	53	62	58	60	25	34	36	29	39	48	47	44.5
P11142	47	45	59	46	39	29	33	24	43	37	46	35
P48643	51	67	55	61	29	31	34	37	40	49	44.5	49
Q9Y5B9	79	78	84	90	0	2	2	1	39.5	40	43	45.5
Q66LE6	21	5	28	5	42	7	51	12	31.5	6	39.5	8.5
P78527	92	93	73	83	3	1	6	2	47.5	47	39.5	42.5
Q6P2Q9	56	58	54	51	12	9	25	7	34	33.5	39.5	29
Q01105-2	19	32	17	28	87	98	60	70	53	65	38.5	49
Q15393	33	33	40	36	34	35	37	26	33.5	34	38.5	31
O43719	55	42	57	39	24	12	15	16	39.5	27	36	27.5
P54105	51	61	51	46	13	11	20	11	32	36	35.5	28.5
P17544-6	38	34	28	37	46	57	42	65	42	45.5	35	51
P21333	73	61	66	58	3	3	4	3	38	32	35	30.5
B8ZZU6	25	48	35	40	29	37	34	46	27	42.5	34.5	43
O15355	41	20	28	23	66	27	41	31	53.5	23.5	34.5	27
Q14204	77	71	61	73	5	5	7	11	41	38	34	42
A0A0G2JIW	52	50	44	37	24	18	24	17	38	34	34	27
Q99832	41	63	41	52	20	27	26	27	30.5	45	33.5	39.5
P04264	89	61	47	80	45	39	19	17	67	50	33	48.5
G5E9A6	0	7	21	21	2	9	45	38	1	8	33	29.5
P68104	53	54	39	46	26	18	24	18	39.5	36	31.5	32
Q8NHY2	28	24	28	23	36	40	35	21	32	32	31.5	22
P04075	50	65	62	74	0	0	0	0	25	32.5	31	37
Q9C0C9	37	41	26	36	46	66	35	55	41.5	53.5	30.5	45.5
O75533	37	38	36	32	24	22	25	30	30.5	30	30.5	31
P45984	15	1	11	9	30	1	50	20	22.5	1	30.5	14.5
P62714	22	3	19	5	48	14	41	21	35	8.5	30	13
P40227	31	56	37	41	16	19	23	24	23.5	37.5	30	32.5

P11021	40	36	35	27	26	23	25	15	33	29.5	30	21
Q92688	36	42	35	32	38	41	23	43	37	41.5	29	37.5
P50991	45	55	43	43	8	14	14	16	26.5	34.5	28.5	29.5
P45983-3	4	0	21	0	6	0	35	3	5	0	28	1.5
P13645	64	50	46	49	46	42	9	25	55	46	27.5	37
Q01105	56	68	50	56	23	18	4	24	39.5	43	27	40
Q15208	31	40	28	32	20	20	26	23	25.5	30	27	27.5
P09651-2	47	36	45	40	4	6	9	7	25.5	21	27	23.5
Q9BT78	31	2	18	2	40	3	36	2	35.5	2.5	27	2
Q13200	34	37	32	41	22	10	19	16	28	23.5	25.5	28.5
Q02930	21	38	28	28	15	24	22	34	18	31	25	31
P49368	40	47	39	52	6	10	11	7	23	28.5	25	29.5
P13489	17	7	16	10	44	31	33	26	30.5	19	24.5	18
P05455	23	30	23	19	16	26	25	31	19.5	28	24	25
Q15029	32	34	31	28	14	7	17	11	23	20.5	24	19.5
Q9BRS2	42	32	41	29	5	4	5	3	23.5	18	23	16
Q15750	45	43	43	50	0	0	1	1	22.5	21.5	22	25.5
Q7KZF4	45	50	44	57	0	0	0	0	22.5	25	22	28.5
E9PRY8	31	28	27	19	17	13	17	4	24	20.5	22	11.5
Q12899	19	18	17	22	39	34	26	37	29	26	21.5	29.5
Q9BUA3	36	44	41	35	0	1	1	1	18	22.5	21	18
P24534	20	18	23	16	12	13	19	4	16	15.5	21	10
Q9BQE3	50	40	13	15	18	0	28	0	34	20	20.5	7.5
P35908	41	44	34	44	0	0	7	8	20.5	22	20.5	26
Q99613	40	40	35	36	6	7	6	10	23	23.5	20.5	23
Q08945	39	37	41	41	0	0	0	0	19.5	18.5	20.5	20.5
P07900	34	41	40	41	1	0	0	2	17.5	20.5	20	21.5
Q99460	37	40	34	41	9	5	6	4	23	22.5	20	22.5
P35527	55	36	24	54	26	11	15	20	40.5	23.5	19.5	37
Q9Y4B6	16	16	16	11	29	36	23	26	22.5	26	19.5	18.5
B0QY89	31	26	24	24	13	14	15	15	22	20	19.5	19.5
P61201	22	6	16	4	32	2	23	0	27	4	19.5	2
A0A0J9YXJ8	0	19	19	17	0	0	19	0	0	9.5	19	8.5
P17980	27	31	30	28	8	4	8	7	17.5	17.5	19	17.5
P09874	40	29	38	36	0	0	0	1	20	14.5	19	18.5
P26640	33	32	37	24	2	1	1	0	17.5	16.5	19	12
P36578	18	18	19	17	21	31	18	22	19.5	24.5	18.5	19.5
P04406	37	42	36	40	0	0	0	0	18.5	21	18	20
Q14152	31	33	36	33	1	0	0	0	16	16.5	18	16.5
Q96EB6	10	11	13	13	23	43	22	38	16.5	27	17.5	25.5
Q8WWY3	38	32	30	28	7	8	5	5	22.5	20	17.5	16.5
E7EU96	14	17	11	15	28	32	24	25	21	24.5	17.5	20
P60228	25	21	24	23	12	11	11	17	18.5	16	17.5	20
J3QLE5	15	16	17	17	15	15	18	15	15	15.5	17.5	16
P18847	10	9	8	7	21	19	26	21	15.5	14	17	14
P62191	19	23	26	14	9	10	8	9	14	16.5	17	11.5
Q9Y4X5	20	5	13	5	38	5	21	2	29	5	17	3.5
Q02878	20	20	16	14	13	24	17	23	16.5	22	16.5	18.5
P35998	22	22	24	21	10	6	8	7	16	14	16	14
C9JEH3	19	0	8	0	49	0	24	0	34	0	16	0
P39687	30	22	26	18	6	8	5	5	18	15	15.5	11.5
P61978	30	23	21	25	8	5	10	7	19	14	15.5	16
P11940	8	8	9	9	20	33	22	31	14	20.5	15.5	20
Q08211	22	18	23	20	8	16	8	12	15	17	15.5	16
P53621	29	32	31	23	0	0	0	0	14.5	16	15.5	11.5
A0A087WU	17	13	22	13	14	5	9	2	15.5	9	15.5	7.5
P49902	31	3	25	2	2	0	6	2	16.5	1.5	15.5	2
P19338	18	19	16	22	21	30	14	31	19.5	24.5	15	26.5
P35580	30	29	30	35	0	0	0	0	15	14.5	15	17.5
P52272	19	21	26	14	2	11	4	11	10.5	16	15	12.5
P46060	11	17	23	21	3	1	7	4	7	9	15	12.5

A0A087X2I	22	25	24	23	5	6	5	3	13.5	15.5	14.5	13
Q09028	13	16	18	15	6	7	11	8	9.5	11.5	14.5	11.5
A0A0U1RQ	20	21	28	20	0	0	1	0	10	10.5	14.5	10
Q12906	9	9	10	9	17	17	18	25	13	13	14	17
B3KS98	22	22	21	17	5	5	7	8	13.5	13.5	14	12.5
Q92598	17	5	12	8	17	5	16	7	17	5	14	7.5
Q9UNF1	10	13	20	12	6	5	8	6	8	9	14	9
C9JFE4	17	1	10	3	27	1	18	0	22	1	14	1.5
Q14974	13	6	16	6	14	3	12	5	13.5	4.5	14	5.5
P22626	29	30	25	26	0	1	2	0	14.5	15.5	13.5	13
O00231	26	24	23	24	6	4	4	5	16	14	13.5	14.5
Q14011	12	21	20	13	6	6	7	7	9	13.5	13.5	10
P53618	28	29	26	26	0	1	1	1	14	15	13.5	13.5
Q9Y657	15	20	22	18	6	6	5	6	10.5	13	13.5	12
Q9Y230	20	20	21	15	2	3	6	2	11	11.5	13.5	8.5
P23396	8	7	13	7	11	9	14	4	9.5	8	13.5	5.5
Q92973	8	1	13	2	8	0	14	0	8	0.5	13.5	1
P17535	8	14	10	6	20	17	16	16	14	15.5	13	11
P08238	19	19	22	23	0	0	4	2	9.5	9.5	13	12.5
ALBU_BOV	25	22	16	23	16	11	10	13	20.5	16.5	13	18
P55884	26	23	25	21	1	0	1	0	13.5	11.5	13	10.5
Q9UMS4	11	17	20	17	6	4	6	10	8.5	10.5	13	13.5
P51991	16	16	24	19	0	0	2	0	8	8	13	9.5
P62316	13	10	18	11	6	7	8	7	9.5	8.5	13	9
G8JLB6	23	14	17	16	15	11	8	9	19	12.5	12.5	12.5
P62195	20	19	19	19	7	6	6	12	13.5	12.5	12.5	15.5
Q9Y678	26	30	24	21	1	2	1	1	13.5	16	12.5	11
P60709	16	14	20	15	10	5	5	12	13	9.5	12.5	13.5
O75688	20	11	17	15	7	4	8	6	13.5	7.5	12.5	10.5
Q9Y6Y0	27	35	20	30	2	0	4	1	14.5	17.5	12	15.5
Q9P2R3	24	24	24	30	0	0	0	0	12	12	12	15
O43242	19	24	19	24	4	5	5	2	11.5	14.5	12	13
Q9Y4E8	15	19	21	21	1	3	3	0	8	11	12	10.5
O95905	15	6	9	3	21	0	15	0	18	3	12	1.5
P30154	7	0	4	0	10	0	19	1	8.5	0	11.5	0.5
P39023	24	24	18	24	9	15	5	11	16.5	19.5	11.5	17.5
O00303	19	16	16	20	8	9	7	12	13.5	12.5	11.5	16
P43686	20	22	20	20	4	4	3	5	12	13	11.5	12.5
P53396	15	25	23	20	0	0	0	0	7.5	12.5	11.5	10
A0A087WV	9	12	14	16	9	8	9	9	9	10	11.5	12.5
PRDX1_HU	5	5	12	8	10	6	11	10	7.5	5.5	11.5	9
Q2TAY7	19	16	23	12	0	0	0	0	9.5	8	11.5	6
Q92905	13	1	7	2	21	2	16	1	17	1.5	11.5	1.5
Q14103	15	18	23	9	0	0	0	0	7.5	9	11.5	4.5
P13010	27	26	22	25	2	11	0	15	14.5	18.5	11	20
P12956	19	25	19	23	1	12	3	22	10	18.5	11	22.5
Q00839	26	20	18	15	7	10	4	5	16.5	15	11	10
Q15057	26	34	22	27	0	0	0	0	13	17	11	13.5
O75607	7	9	7	6	16	23	15	25	11.5	16	11	15.5
Q13347	21	16	20	16	3	6	2	3	12	11	11	9.5
Q9NYJ8	23	19	22	19	0	0	0	0	11.5	9.5	11	9.5
B4DY09	7	7	10	7	15	17	12	16	11	12	11	11.5
Q14008	28	20	22	15	0	0	0	0	14	10	11	7.5
H3BLZ8	16	15	22	17	1	0	0	2	8.5	7.5	11	9.5
Q8N5C8	21	16	22	15	0	0	0	0	10.5	8	11	7.5
H0Y8C6	15	13	12	8	8	0	10	3	11.5	6.5	11	5.5
B1AKJ5	14	34	13	26	9	32	8	29	11.5	33	10.5	27.5
P61247	15	9	11	10	17	26	10	20	16	17.5	10.5	15
P62424	15	16	15	15	16	14	6	10	15.5	15	10.5	12.5
Q7L2H7	14	15	13	14	3	4	8	5	8.5	9.5	10.5	9.5
P61163	12	17	16	16	3	2	5	3	7.5	9.5	10.5	9.5

Q14566	17	16	21	17	0	0	0	0	8.5	8	10.5	8.5
O75694	11	0	13	0	3	0	8	0	7	0	10.5	0
E9PDP5	22	4	15	1	32	4	5	8	27	4	10	4.5
P35606	30	30	20	25	0	0	0	0	15	15	10	12.5
O43318-2	24	23	20	20	0	0	0	1	12	11.5	10	10.5
P25205	22	22	20	20	0	0	0	0	11	11	10	10
Q13263	24	19	19	14	1	0	1	0	12.5	9.5	10	7
O60506-3	13	13	17	17	7	1	3	4	10	7	10	10.5
Q15233	13	12	17	16	0	1	3	1	6.5	6.5	10	8.5
P55036	9	11	16	13	4	3	4	7	6.5	7	10	10
E7EM64	13	2	6	0	27	0	14	0	20	1	10	0
Q9BTY7	5	0	5	1	6	0	15	0	5.5	0	10	0.5
Q71U36	5	27	0	4	19	21	19	21	12	24	9.5	12.5
A0A0J9YVP	25	0	0	17	21	15	19	20	23	7.5	9.5	18.5
Q15365	16	11	8	12	9	7	11	16	12.5	9	9.5	14
Q13561	22	14	15	10	4	2	4	2	13	8	9.5	6
P33993	20	22	19	18	0	0	0	0	10	11	9.5	9
P23246	18	18	18	10	1	0	1	0	9.5	9	9.5	5
P49736	15	20	19	21	0	0	0	0	7.5	10	9.5	10.5
P31689	16	11	18	13	1	0	1	1	8.5	5.5	9.5	7
Q4G0J3	7	8	6	10	17	16	12	20	12	12	9	15
P61353	8	7	7	6	15	14	11	14	11.5	10.5	9	10
Q13435	10	18	13	13	7	8	5	6	8.5	13	9	9.5
Q07021	1	4	0	4	12	19	18	25	6.5	11.5	9	14.5
Q9BTT0	9	18	17	13	6	9	1	9	7.5	13.5	9	11
P62979	10	4	7	6	9	13	11	7	9.5	8.5	9	6.5
P62701	12	10	10	7	8	11	8	10	10	10.5	9	8.5
O00203	11	16	17	11	1	1	1	0	6	8.5	9	5.5
Q9UNS2	11	0	7	1	16	0	11	0	13.5	0	9	0.5
Q8TEB1	6	1	6	0	13	0	12	0	9.5	0.5	9	0
P06753-2	13	0	12	1	0	0	6	0	6.5	0	9	0.5
Q13185	2	5	9	4	1	0	9	1	1.5	2.5	9	2.5
O00232	20	25	15	17	0	4	2	2	10	14.5	8.5	9.5
A0A0C4DG	24	22	17	16	0	0	0	0	12	11	8.5	8
B0YIW6	17	16	16	22	0	0	1	1	8.5	8	8.5	11.5
P15880	5	4	7	5	14	14	10	13	9.5	9	8.5	9
Q9Y265	13	15	15	15	0	3	2	3	6.5	9	8.5	9
Q16875	20	11	14	9	1	1	3	0	10.5	6	8.5	4.5
O43143	13	6	15	7	2	2	2	1	7.5	4	8.5	4
Q93008	12	7	15	8	1	0	2	0	6.5	3.5	8.5	4
P68371	7	3	6	4	30	25	10	12	18.5	14	8	8
P61978-3	0	23	6	0	8	5	10	7	4	14	8	3.5
P62241	6	11	6	6	10	12	10	12	8	11.5	8	9
P62906	6	9	6	9	15	20	10	17	10.5	14.5	8	13
Q9Y2H1	16	15	13	18	3	2	3	1	9.5	8.5	8	9.5
O95347	24	25	16	20	1	0	0	0	12.5	12.5	8	10
P09661	12	10	12	12	8	4	4	7	10	7	8	9.5
O15371	11	13	15	7	0	0	1	0	5.5	6.5	8	3.5
Q9UPN9-2	10	5	16	4	2	1	0	0	6	3	8	2
Q9BUF5	14	9	15	3	0	1	0	2	7	5	7.5	2.5
Q9NTJ3	22	19	15	21	0	2	0	2	11	10.5	7.5	11.5
J3QQ67	10	11	7	6	9	12	8	15	9.5	11.5	7.5	10.5
Q9NP73	19	17	15	9	0	0	0	0	9.5	8.5	7.5	4.5
P35637	11	17	13	14	1	1	2	0	6	9	7.5	7
Q15020	13	10	14	10	2	1	1	0	7.5	5.5	7.5	5
O60825	15	5	15	5	0	0	0	0	7.5	2.5	7.5	2.5
Q9Y383	10	7	13	6	3	2	2	1	6.5	4.5	7.5	3.5
G3V5T9	7	0	5	0	16	0	10	0	11.5	0	7.5	0
Q8TEX9	4	1	6	1	11	1	9	1	7.5	1	7.5	1
H0Y4R1	5	3	9	2	0	0	6	0	2.5	1.5	7.5	1
H0YM23	4	0	5	5	25	12	9	8	14.5	6	7	6.5

E9PB61	6	5	5	6	13	12	9	12	9.5	8.5	7	9
Q14683	23	21	14	14	0	0	0	0	11.5	10.5	7	7
P46777	14	17	14	16	3	5	0	0	8.5	11	7	8
Q14498	8	7	8	7	8	8	6	8	8	7.5	7	7.5
Q15021	17	16	14	12	0	0	0	0	8.5	8	7	6
Q9NSD9	13	15	14	15	0	0	0	0	6.5	7.5	7	7.5
P49321	17	12	13	12	1	0	1	0	9	6	7	6
Q0VDG4	4	6	8	10	2	4	6	13	3	5	7	11.5
Q92499	7	11	14	12	0	0	0	0	3.5	5.5	7	6
O76071	5	1	4	1	12	1	10	0	8.5	1	7	0.5
P02533	9	8	11	10	2	8	2	0	5.5	8	6.5	5
Q7Z6Z7	23	12	9	13	8	5	4	6	15.5	8.5	6.5	9.5
P33991	15	19	13	14	0	0	0	0	7.5	9.5	6.5	7
O43390	6	3	6	5	3	5	7	8	4.5	4	6.5	6.5
P26368	12	10	9	8	5	1	4	0	8.5	5.5	6.5	4
B2R5W2	2	4	3	3	11	12	10	12	6.5	8	6.5	7.5
P25398	5	7	5	5	8	7	8	9	6.5	7	6.5	7
Q9UQ80	14	12	13	15	0	0	0	0	7	6	6.5	7.5
P52907	8	5	8	5	8	3	5	4	8	4	6.5	4.5
G3V5Z7	12	13	13	14	0	0	0	0	6	6.5	6.5	7
O60256	9	14	13	11	0	0	0	1	4.5	7	6.5	6
Q6PD62	7	8	9	3	4	7	4	5	5.5	7.5	6.5	4
Q93009	13	7	10	4	4	1	3	2	8.5	4	6.5	3
O95376	7	0	6	0	14	0	7	0	10.5	0	6.5	0
P35579	16	21	12	17	0	0	0	0	8	10.5	6	8.5
E7EV71	5	17	7	12	2	6	5	8	3.5	11.5	6	10
P26599	21	16	10	13	1	2	2	1	11	9	6	7
Q15008	16	17	11	13	4	2	1	1	10	9.5	6	7
P23284	18	19	11	16	0	1	1	1	9	10	6	8.5
P62318	10	9	9	8	6	4	3	4	8	6.5	6	6
C9J2Y9	17	22	12	11	0	0	0	0	8.5	11	6	5.5
P62917	10	9	6	6	6	12	6	8	8	10.5	6	7
P52597	5	6	6	8	3	0	6	1	4	3	6	4.5
P67870	5	5	5	6	6	12	7	12	5.5	8.5	6	9
P84090	6	5	3	4	7	8	9	9	6.5	6.5	6	6.5
O95218	9	10	10	8	5	6	2	4	7	8	6	6
P24928	14	14	12	12	0	0	0	0	7	7	6	6
O94776	12	14	12	10	0	0	0	0	6	7	6	5
P18077	3	7	4	5	6	10	8	7	4.5	8.5	6	6
F8VPD4	10	13	12	10	0	0	0	1	5	6.5	6	5.5
C9JNW5	6	5	6	5	5	9	6	6	5.5	7	6	5.5
M0QXS5	9	10	11	9	0	0	1	0	4.5	5	6	4.5
G8JLA2	6	11	12	8	1	0	0	1	3.5	5.5	6	4.5
E9PGT6	3	0	4	0	12	1	8	0	7.5	0.5	6	0
P17544	0	0	0	0	0	0	11	0	0	0	5.5	0
P19784	11	7	6	6	11	8	5	6	11	7.5	5.5	6
P55795	2	3	6	1	0	0	5	0	1	1.5	5.5	0.5
O00487	9	13	9	11	3	2	2	4	6	7.5	5.5	7.5
P62753	6	3	4	4	7	11	7	9	6.5	7	5.5	6.5
A0A024R4N	7	3	3	3	12	8	8	6	9.5	5.5	5.5	4.5
P67809	3	10	8	9	5	7	3	4	4	8.5	5.5	6.5
P62314	7	4	5	5	8	6	6	5	7.5	5	5.5	5
A0A087WX	4	6	5	4	6	6	6	6	5	6	5.5	5
Q13162	9	6	5	6	0	0	6	4	4.5	3	5.5	5
P62888	8	7	7	7	4	5	4	3	6	6	5.5	5
Q9BPX3	10	13	10	9	0	0	1	1	5	6.5	5.5	5
A0A075B6S	4	4	5	5	5	5	6	7	4.5	4.5	5.5	6
O76094	6	7	9	6	1	1	2	1	3.5	4	5.5	3.5
Q8TD19	7	3	6	3	4	2	5	1	5.5	2.5	5.5	2
Q9Y6A5	5	6	11	9	0	0	0	0	2.5	3	5.5	4.5
P62937	2	5	6	2	1	2	5	5	1.5	3.5	5.5	3.5

129

Q15170-2	0	0	5	4	1	2	6	7	0.5	1	5.5	5.5
P20248	2	0	3	0	9	0	8	0	5.5	0	5.5	0
P60891	11	26	10	14	0	0	0	1	5.5	13	5	7.5
O75487	9	9	6	11	6	10	4	7	7.5	9.5	5	9
P11908	0	7	10	7	0	0	0	1	0	3.5	5	4
Q9UQE7	20	13	10	15	0	0	0	0	10	6.5	5	7.5
P05387	4	4	4	3	7	11	6	14	5.5	7.5	5	8.5
P26373	6	7	7	7	4	8	3	2	5	7.5	5	4.5
Q9UNM6	7	14	9	14	1	0	1	0	4	7	5	7
P33992	15	11	10	15	0	0	0	0	7.5	5.5	5	7.5
P51665	11	9	8	12	0	2	2	2	5.5	5.5	5	7
P07814	11	14	10	10	0	0	0	0	5.5	7	5	5
P62829	6	3	4	5	5	8	6	7	5.5	5.5	5	6
P98179	8	8	8	8	3	3	2	3	5.5	5.5	5	5.5
O43823	11	9	10	8	0	0	0	0	5.5	4.5	5	4
P18754	11	12	10	6	0	0	0	0	5.5	6	5	3
E9PLL6	3	8	7	5	1	6	3	5	2	7	5	5
E7EX90	8	10	10	8	0	0	0	0	4	5	5	4
Q7RTV0	3	1	3	6	6	4	7	5	4.5	2.5	5	5.5
O14617	8	8	10	8	0	0	0	0	4	4	5	4
P08579	6	5	6	0	3	2	4	3	4.5	3.5	5	1.5
Q8WUA2	6	7	10	6	0	0	0	0	3	3.5	5	3
P15408	2	4	6	4	2	1	4	1	2	2.5	5	2.5
Q15459	6	3	10	3	0	0	0	0	3	1.5	5	1.5
Q13885	9	4	3	11	5	1	6	0	7	2.5	4.5	5.5
Q9BVA1	0	4	3	0	5	1	6	0	2.5	2.5	4.5	0
P41091	17	14	9	18	0	0	0	0	8.5	7	4.5	9
F6VRR5	4	4	2	1	8	10	7	5	6	7	4.5	3
Q9UPN9	0	5	0	4	2	1	9	0	1	3	4.5	2
P10155	3	5	4	6	8	9	5	5	5.5	7	4.5	5.5
E5RJR5	8	7	3	6	5	3	6	5	6.5	5	4.5	5.5
O75821	8	9	9	5	1	1	0	1	4.5	5	4.5	3
A0A024RA!	5	8	9	12	0	0	0	1	2.5	4	4.5	6.5
Q6GMV2	5	3	2	2	11	4	7	3	8	3.5	4.5	2.5
Q7L2J0	4	4	4	3	5	5	5	3	4.5	4.5	4.5	3
Q9Y3I0	12	8	9	8	0	0	0	0	6	4	4.5	4
A0A087WL	3	1	3	1	6	7	6	9	4.5	4	4.5	5
P62750	6	3	3	4	4	4	6	5	5	3.5	4.5	4.5
Q01804	6	10	9	7	0	0	0	0	3	5	4.5	3.5
Q8N7H5	4	5	6	1	4	3	3	2	4	4	4.5	1.5
Q9Y3B4	7	3	7	5	2	2	2	1	4.5	2.5	4.5	3
B0YJC4	9	2	8	8	0	0	1	0	4.5	1	4.5	4
E7EVA0	7	6	9	5	0	0	0	0	3.5	3	4.5	2.5
Q6PEV8	3	3	5	3	2	0	4	4	2.5	1.5	4.5	3.5
P27694	0	2	1	2	2	5	8	6	1	3.5	4.5	4
Q712K3	4	1	2	0	11	1	7	0	7.5	1	4.5	0
P40222	6	4	9	3	0	0	0	0	3	2	4.5	1.5
Q9UBW8	4	0	2	0	11	0	7	1	7.5	0	4.5	0.5
O60763	7	5	9	3	0	0	0	0	3.5	2.5	4.5	1.5
Q9UHB9	5	5	9	3	0	0	0	0	2.5	2.5	4.5	1.5
Q9UJX3	1	1	5	1	0	0	4	0	0.5	0.5	4.5	0.5
Q9HAV4	1	0	2	0	0	0	7	0	0.5	0	4.5	0
P04350	4	9	5	10	0	0	3	0	2	4.5	4	5
Q16576	5	7	4	6	8	1	4	3	6.5	4	4	4.5
P19474	9	13	7	4	2	2	1	1	5.5	7.5	4	2.5
A0A0A0MF	3	5	1	2	6	9	7	10	4.5	7	4	6
P53539	2	3	8	7	0	7	0	0	1	5	4	3.5
P05388	0	3	1	3	8	13	7	10	4	8	4	6.5
P42356	11	13	8	13	0	0	0	0	5.5	6.5	4	6.5
M0QYS1	6	7	6	3	5	7	2	8	5.5	7	4	5.5
Q99729-3	9	13	8	10	0	0	0	0	4.5	6.5	4	5

130

P46778	6	9	5	5	4	6	3	4	5	7.5	4	4.5
Q12874	11	7	6	10	1	1	2	1	6	4	4	5.5
M0QXB4	7	8	8	12	0	0	0	0	3.5	4	4	6
Q96JK2	6	6	5	3	4	6	3	4	5	6	4	3.5
P20618	6	13	8	10	0	0	0	0	3	6.5	4	5
P62280	4	3	4	3	5	8	4	5	4.5	5.5	4	4
B1AK87	5	5	5	4	5	2	3	4	5	3.5	4	4
Q9Y237	5	7	7	9	1	0	1	1	3	3.5	4	5
P14618	9	9	7	6	1	0	1	2	5	4.5	4	4
A0A087WZ	5	4	5	5	1	2	3	1	3	3	4	3
P35244	1	2	0	1	5	4	8	6	3	3	4	3.5
Q92616	6	6	8	10	0	0	0	0	3	3	4	5
P13639	5	6	6	5	0	1	2	0	2.5	3.5	4	2.5
H3BLV9	9	2	5	1	4	0	3	0	6.5	1	4	0.5
O14818	5	10	8	6	0	0	0	0	2.5	5	4	3
P63173	3	2	3	2	5	2	5	5	4	2	4	3.5
O00505	5	0	3	1	11	2	5	0	8	1	4	0.5
I3L397	3	0	2	1	5	2	6	3	4	1	4	2
P14625	5	2	8	2	0	0	0	0	2.5	1	4	1
P62258	2	3	3	1	3	1	5	0	2.5	2	4	0.5
P30041	4	4	5	3	0	1	3	4	2	2.5	4	3.5
A0A087WV	6	6	7	3	0	0	1	0	3	3	4	1.5
Q92922	6	3	8	6	0	0	0	0	3	1.5	4	3
Q9BQ67	3	5	3	1	4	0	5	0	3.5	2.5	4	0.5
A0A087WS	6	1	6	0	4	0	2	0	5	0.5	4	0
A0A087X0N	7	1	8	3	0	0	0	0	3.5	0.5	4	1.5
Q9Y2X3	3	2	4	0	4	0	4	1	3.5	1	4	0.5
Q9UHW5	2	0	3	1	4	0	5	0	3	0	4	0.5
Q5THR1	1	1	1	0	2	2	7	0	1.5	1.5	4	0
J3QRG6	1	0	2	0	1	0	6	2	1	0	4	1
K22E_HUM	8	0	0	0	34	33	7	8	21	16.5	3.5	4
P09972	13	6	7	9	0	0	0	0	6.5	3	3.5	4.5
O43164	5	4	4	8	3	13	3	14	4	8.5	3.5	11
Q14558	9	26	7	20	0	0	0	1	4.5	13	3.5	10.5
P18124	8	7	4	11	8	11	3	9	8	9	3.5	10
P68133	2	2	2	2	0	0	5	1	1	1	3.5	1.5
J3KTA4	7	5	7	4	1	0	0	2	4	2.5	3.5	3
P27635	6	8	6	8	4	9	1	8	5	8.5	3.5	8
P61313	8	7	3	8	4	7	4	7	6	7	3.5	7.5
Q9UBF2	6	10	6	9	0	0	1	1	3	5	3.5	5
P09132	5	2	1	2	5	9	6	6	5	5.5	3.5	4
Q13045	14	10	7	9	0	0	0	0	7	5	3.5	4.5
Q9Y3U8	5	4	4	3	4	7	3	7	4.5	5.5	3.5	5
Q13547	7	10	7	9	0	1	0	1	3.5	5.5	3.5	5
A0A0D9SF5	2	6	7	4	0	0	0	0	1	3	3.5	2
Q9BVP2	7	5	6	4	2	3	1	2	4.5	4	3.5	3
Q9NR30	6	3	6	3	4	8	1	2	5	5.5	3.5	2.5
Q9UMZ2	8	9	7	9	0	0	0	0	4	4.5	3.5	4.5
P26358	8	7	7	9	0	0	0	0	4	3.5	3.5	4.5
P49207	3	4	3	3	3	5	4	5	3	4.5	3.5	4
A0A0C4DG	7	6	7	6	0	0	0	0	3.5	3	3.5	3
Q9H2U1	5	8	7	8	0	0	0	0	2.5	4	3.5	4
A0A0R4J2E	2	5	3	4	1	5	4	5	1.5	5	3.5	4.5
P28074	5	8	7	9	0	0	0	0	2.5	4	3.5	4.5
Q86YM7	7	6	7	7	0	0	0	1	3.5	3	3.5	4
J3KTE4	5	2	5	3	2	5	2	4	3.5	3.5	3.5	3.5
Q9NPA8	1	2	0	3	4	5	7	5	2.5	3.5	3.5	4
Q9Y2T2	5	5	7	6	0	0	0	0	2.5	2.5	3.5	3
Q8WXF1	4	9	6	5	1	0	1	0	2.5	4.5	3.5	2.5
Q13409-2	7	6	6	5	0	0	1	0	3.5	3	3.5	2.5
Q9NU22	8	4	7	6	0	0	0	0	4	2	3.5	3

P47813	5	5	5	2	3	1	2	1	4	3	3.5	1.5
Q14257	5	6	6	6	0	0	1	0	2.5	3	3.5	3
P0DN76	7	3	6	2	2	1	1	0	4.5	2	3.5	1
Q9Y224	5	6	7	2	0	0	0	1	2.5	3	3.5	1.5
P62249	3	1	4	1	2	4	3	2	2.5	2.5	3.5	1.5
Q99459	4	3	4	2	1	1	3	1	2.5	2	3.5	1.5
J3KQ34	3	0	1	0	9	0	6	0	6	0	3.5	0
Q9NSB8	2	3	7	1	0	0	0	0	1	1.5	3.5	0.5
E7EX17	134	87	0	93	5	4	6	5	69.5	45.5	3	49
M0R117	7	4	4	5	5	11	2	5	6	7.5	3	5
P52756	4	7	6	7	0	0	0	0	2	3.5	3	3.5
O95163	13	14	6	9	0	0	0	0	6.5	7	3	4.5
P50914	5	7	4	7	5	6	2	5	5	6.5	3	6
A0A087WL	13	5	6	7	0	0	0	0	6.5	2.5	3	3.5
K7ERF1	8	7	3	6	2	4	3	5	5	5.5	3	5.5
E9PHA2	7	12	6	10	0	0	0	0	3.5	6	3	5
P62244	4	1	3	3	4	3	3	6	4	2	3	4.5
A0A0A0MS	3	0	1	3	5	7	5	4	4	3.5	3	3.5
P30050	4	3	3	3	2	7	3	7	3	5	3	5
P46940	9	12	6	3	0	0	0	0	4.5	6	3	1.5
Q5W0B1	6	9	6	7	0	0	0	0	3	4.5	3	3.5
P62266	4	1	2	2	5	4	4	5	4.5	2.5	3	3.5
C9JFV4	3	3	0	3	3	6	6	3	3	4.5	3	3
P28072	4	9	6	5	0	0	0	0	2	4.5	3	2.5
P27348	2	0	5	1	7	1	1	0	4.5	0.5	3	0.5
E7ESY4	2	2	6	5	0	0	0	0	1	1	3	2.5
TRY1_BOVI	1	3	3	5	3	3	3	3	2	3	3	4
O95400	7	5	5	5	1	0	1	0	4	2.5	3	2.5
Q05519	7	5	5	4	2	0	1	0	4.5	2.5	3	2
G3V3M6	5	7	6	3	0	0	0	0	2.5	3.5	3	1.5
Q969G3	4	6	6	5	0	0	0	0	2	3	3	2.5
O60271	7	4	6	5	0	0	0	0	3.5	2	3	2.5
O60884	8	3	5	3	1	0	1	0	4.5	1.5	3	1.5
J3QT28	3	6	6	6	0	0	0	0	1.5	3	3	3
O94906	10	3	6	2	0	0	0	0	5	1.5	3	1
P25788	3	5	6	6	0	0	0	1	1.5	2.5	3	3.5
A8MWD9	1	2	3	2	4	1	3	5	2.5	1.5	3	3.5
P62913	1	2	2	2	2	4	4	3	1.5	3	3	2.5
Q9UER7	6	2	5	2	0	1	1	0	3	1.5	3	1
Q9Y2L1	3	6	6	5	0	0	0	0	1.5	3	3	2.5
J3KR24	4	5	6	5	0	0	0	0	2	2.5	3	2.5
Q9P258	3	4	5	6	1	0	1	0	2	2	3	3
Q9NZI8	6	2	5	3	0	1	1	1	3	1.5	3	2
H0YGW7	7	2	6	3	0	0	0	0	3.5	1	3	1.5
J3QRS3	5	2	3	1	1	2	3	0	3	2	3	0.5
O14776	5	2	6	4	0	0	0	0	2.5	1	3	2
P08621	4	2	6	5	0	0	0	0	2	1	3	2.5
Q8IWV8-4	0	0	0	0	5	4	6	1	2.5	2	3	0.5
P08708	1	0	3	1	2	3	3	2	1.5	1.5	3	1.5
P46736	1	3	2	1	1	0	4	0	1	1.5	3	0.5
Q6ULP2	2	1	6	2	0	0	0	0	1	0.5	3	1
O14929	1	1	2	0	0	0	4	0	0.5	0.5	3	0
P13647	20	9	5	8	1	3	0	0	10.5	6	2.5	4
D6RHC4	1	4	0	1	4	0	5	0	2.5	2	2.5	0.5
P60510	1	3	5	2	0	0	0	0	0.5	1.5	2.5	1
P48556	8	6	4	9	3	1	1	1	5.5	3.5	2.5	5
P62140	2	6	5	6	0	8	0	3	1	7	2.5	4.5
B2WTI3	4	5	3	2	4	7	2	3	4	6	2.5	2.5
Q92769	4	6	4	4	1	1	1	1	2.5	3.5	2.5	2.5
A0A024QZI	4	3	5	7	0	0	0	0	2	1.5	2.5	3.5
P05198	10	10	5	7	0	0	0	0	5	5	2.5	3.5

O14646	8	3	4	2	1	6	1	2	4.5	4.5	2.5	2
P25786	5	9	5	10	0	0	0	0	2.5	4.5	2.5	5
P78332	6	0	5	3	0	0	0	0	3	0	2.5	1.5
P62304	6	5	3	5	2	1	2	3	4	3	2.5	4
Q9UG63	6	4	5	7	1	1	0	2	3.5	2.5	2.5	4.5
Q9BWJ5	6	1	2	3	4	2	3	5	5	1.5	2.5	4
O60814	3	0	3	0	2	5	2	7	2.5	2.5	2.5	3.5
P42285	8	6	5	5	0	0	0	0	4	3	2.5	2.5
B1AJY7	5	3	3	4	2	2	2	2	3.5	2.5	2.5	3
Q32MZ4	6	6	5	6	0	0	0	0	3	3	2.5	3
Q4J6C6	4	0	1	0	13	0	4	0	8.5	0	2.5	0
P05386	3	2	4	1	3	4	1	3	3	3	2.5	2
F5H2F4	4	6	5	6	0	0	0	0	2	3	2.5	3
B8ZZU8	5	2	4	4	3	0	1	2	4	1	2.5	3
P62854	1	2	3	1	0	6	2	5	0.5	4	2.5	3
C9JR56	3	5	5	5	0	0	0	0	1.5	2.5	2.5	2.5
Q96DI7	6	2	5	4	0	0	0	0	3	1	2.5	2
Q13464	1	5	5	7	0	0	0	0	0.5	2.5	2.5	3.5
O43865	2	0	1	1	2	4	4	3	2	2	2.5	2
Q8N8S7	4	4	5	4	0	0	0	0	2	2	2.5	2
P35268	3	4	4	2	0	0	1	2	1.5	2	2.5	2
H0Y6I0	0	0	1	0	0	0	4	3	0	0	2.5	1.5
O75934	1	0	3	1	1	2	2	1	1	1	2.5	1
O43776	3	4	5	3	0	0	0	0	1.5	2	2.5	1.5
Q9NWU2	1	4	4	3	0	0	1	2	0.5	2	2.5	2.5
A0A087WT	4	3	5	3	0	0	0	0	2	1.5	2.5	1.5
O95273	0	0	1	0	4	0	4	0	2	0	2.5	0
P11802	0	0	1	0	0	0	4	0	0	0	2.5	0
Q9UHV9	2	3	4	3	0	0	1	1	1	1.5	2.5	2
Q06481	4	1	3	1	1	0	2	1	2.5	0.5	2.5	1
E7ESD2	4	2	5	2	0	0	0	0	2	1	2.5	1
B4DKA4	4	2	5	2	0	0	0	0	2	1	2.5	1
Q15717	2	4	5	1	0	0	0	0	1	2	2.5	0.5
Q7Z7L7	0	0	0	0	6	1	5	0	3	0.5	2.5	0
Q96PK6	3	3	5	1	0	0	0	0	1.5	1.5	2.5	0.5
Q9BUQ8	3	0	4	2	0	0	1	0	1.5	0	2.5	1
P32119	1	1	1	2	3	2	3	6	2	1.5	2	4
D3YTB1	6	6	3	4	3	7	1	1	4.5	6.5	2	2.5
P11387	5	1	2	4	2	5	2	6	3.5	3	2	5
P11047	8	4	4	3	1	3	0	0	4.5	3.5	2	1.5
Q9GZS3	5	4	3	3	3	3	1	4	4	3.5	2	3.5
P49721	4	9	4	7	0	0	0	0	2	4.5	2	3.5
O14654	11	4	4	3	0	0	0	0	5.5	2	2	1.5
A0A087WL	3	5	4	2	0	0	0	0	1.5	2.5	2	1
P28070	5	6	4	3	0	0	0	0	2.5	3	2	1.5
P23458	8	7	4	4	0	0	0	0	4	3.5	2	2
P62269	2	0	2	2	2	5	2	7	2	2.5	2	4.5
P46779	7	5	4	4	0	1	0	1	3.5	3	2	2.5
Q09161	3	4	3	5	1	1	1	4	2	2.5	2	4.5
P49458	2	3	1	2	3	4	3	4	2.5	3.5	2	3
O75909	0	1	0	0	4	7	4	5	2	4	2	2.5
P25789	3	8	4	6	0	0	0	0	1.5	4	2	3
Q9BPZ2	4	3	4	4	0	0	0	0	2	1.5	2	2
Q9H7D7	5	5	3	4	0	1	1	1	2.5	3	2	2.5
Q07666	5	4	3	3	3	0	1	0	4	2	2	1.5
Q9HD40	3	8	4	1	0	0	0	0	1.5	4	2	0.5
P37108	4	4	3	2	1	1	1	3	2.5	2.5	2	2.5
O75937	5	5	4	4	0	0	0	0	2.5	2.5	2	2
P52294	1	1	4	6	0	0	0	0	0.5	0.5	2	3
Q15007	5	4	4	5	0	0	0	0	2.5	2	2	2.5
Q96HR8	0	1	1	3	3	3	3	3	1.5	2	2	3

O60684	4	6	4	2	0	0	0	0	2	3	2	1
F8VVA7	4	5	4	2	0	0	0	0	2	2.5	2	1
Q13033	5	3	4	1	0	0	0	0	2.5	1.5	2	0.5
Q86YP4	2	6	4	3	0	0	0	0	1	3	2	1.5
B5MCP9	1	2	2	1	3	1	2	4	2	1.5	2	2.5
J3KN16	4	4	4	4	0	0	0	0	2	2	2	2
P40937	2	3	4	2	0	2	0	1	1	2.5	2	1.5
Q99575	6	5	4	1	0	0	0	0	3	2.5	2	0.5
Q96AV8	6	4	4	2	0	0	0	0	3	2	2	1
E7EQU1	2	1	3	2	1	1	1	0	1.5	1	2	1
Q00688	4	3	4	4	0	0	0	0	2	1.5	2	2
O43290	5	4	4	2	0	0	0	0	2.5	2	2	1
P10644	2	2	3	3	0	0	1	0	1	1	2	1.5
P36954	2	4	3	2	1	0	1	1	1.5	2	2	1.5
O43251-6	5	2	4	3	0	0	0	0	2.5	1	2	1.5
K7EK33	4	5	4	1	0	0	0	0	2	2.5	2	0.5
A2A2Q9	3	5	4	2	0	0	0	0	1.5	2.5	2	1
Q16659	4	3	4	3	0	0	0	0	2	1.5	2	1.5
P05204	3	3	4	2	0	1	0	0	1.5	2	2	1
O94888	3	0	1	0	5	0	3	0	4	0	2	0
P39019	4	2	4	2	0	0	0	1	2	1	2	1.5
Q16186	3	3	4	3	0	0	0	0	1.5	1.5	2	1.5
Q9NY27	2	5	4	2	0	0	0	0	1	2.5	2	1
Q15427	1	0	2	2	1	2	2	1	1	1	2	1.5
Q12788	2	4	4	3	0	0	0	0	1	2	2	1.5
Q8N3U4	3	3	4	2	0	0	0	0	1.5	1.5	2	1
O14519	2	2	3	2	0	0	1	0	1	1	2	1
E5RHG8	3	2	1	3	0	0	3	0	1.5	1	2	1.5
Q8ND56	3	2	4	1	0	0	0	0	1.5	1	2	0.5
Q96PU8	4	0	2	0	2	0	2	0	3	0	2	0
Q9NR55	0	3	3	1	1	1	1	1	0.5	2	2	1
Q8N163	4	1	4	2	0	0	0	0	2	0.5	2	1
H0YCK3	2	2	4	3	0	0	0	0	1	1	2	1.5
Q6IN85	4	2	4	1	0	0	0	0	2	1	2	0.5
P10599	1	0	1	1	1	1	3	3	1	0.5	2	2
Q9H5V9	2	1	4	4	0	0	0	0	1	0.5	2	2
P25685	3	2	4	1	0	0	0	0	1.5	1	2	0.5
Q9NUQ3	1	3	4	1	0	0	0	0	0.5	1.5	2	0.5
P46783	2	0	3	0	0	1	1	1	1	0.5	2	0.5
Q96N67	3	1	4	0	0	0	0	0	1.5	0.5	2	0
P49792	2	1	4	1	0	0	0	0	1	0.5	2	0.5
E9PJM3	1	1	3	1	0	0	1	1	0.5	0.5	2	1
Q13112	0	1	3	1	0	0	1	0	0	0.5	2	0.5
K7ER96	1	0	2	0	1	0	2	0	1	0	2	0
Q8WVC0	1	0	3	1	0	0	1	0	0.5	0	2	0.5
P08779	9	0	1	1	2	0	2	5	5.5	0	1.5	3
B1ANR0	1	1	0	0	3	2	3	2	2	1.5	1.5	1
F8VZX2	0	1	3	3	0	0	0	0	0	0.5	1.5	1.5
O00468-6	2	8	1	4	5	8	2	4	3.5	8	1.5	4
P10412	1	2	3	1	5	9	0	12	3	5.5	1.5	6.5
P28066	7	4	3	6	0	0	0	0	3.5	2	1.5	3
A0A024R4E	8	5	3	5	0	0	0	0	4	2.5	1.5	2.5
Q08499-12	2	1	1	3	3	5	2	4	2.5	3	1.5	3.5
P0C0S8	1	1	2	0	4	5	1	6	2.5	3	1.5	3
P61254	3	5	3	3	1	2	0	1	2	3.5	1.5	2
H0YK48	0	0	1	0	0	0	2	0	0	0	1.5	0
E9PKP7	0	0	0	0	5	3	3	7	2.5	1.5	1.5	3.5
Q9Y608	3	4	3	6	0	0	0	0	1.5	2	1.5	3
A0A0D9SET	1	1	2	0	0	0	1	0	0.5	0.5	1.5	0
E7EWR4	4	4	3	5	0	0	0	0	2	2	1.5	2.5
A0A0D9SEI	3	5	2	2	0	2	1	0	1.5	3.5	1.5	1

Q92734	5	4	3	3	0	0	0	0	2.5	2	1.5	1.5
Q9UKF6	4	4	3	3	0	0	0	0	2	2	1.5	1.5
Q8WV44	5	0	3	1	5	0	0	0	5	0	1.5	0.5
A0A087WV	2	3	2	3	0	1	1	2	1	2	1.5	2.5
H0Y6E7	2	4	3	1	2	0	0	2	2	2	1.5	1.5
G3V3G9	3	3	3	5	0	0	0	0	1.5	1.5	1.5	2.5
P46063	4	4	3	1	0	0	0	0	2	2	1.5	0.5
Q92878	3	4	3	3	0	0	0	0	1.5	2	1.5	1.5
O15160	4	4	3	2	0	0	0	0	2	2	1.5	1
B4E0T2	4	3	3	3	0	0	0	0	2	1.5	1.5	1.5
Q5BIX2	0	0	0	0	4	2	3	3	2	1	1.5	1.5
Q52LJ0	4	3	3	3	0	0	0	0	2	1.5	1.5	1.5
P06576	2	4	3	3	0	0	0	0	1	2	1.5	1.5
O75935	3	3	2	2	0	0	1	1	1.5	1.5	1.5	1.5
Q9UJW0	1	3	3	2	0	0	0	0	0.5	1.5	1.5	1
P09429	3	2	3	3	0	0	0	1	1.5	1	1.5	2
E7EMB3	2	4	2	3	0	0	1	0	1	2	1.5	1.5
Q15046	3	4	3	2	0	0	0	0	1.5	2	1.5	1
Q8WUM0	4	2	3	3	0	0	0	0	2	1	1.5	1.5
Q8NC51	4	2	3	1	1	1	0	0	2.5	1.5	1.5	0.5
Q2NL82	3	3	3	3	0	0	0	0	1.5	1.5	1.5	1.5
O14530	2	3	3	4	0	0	0	0	1	1.5	1.5	2
P14868	3	4	3	1	0	0	0	0	1.5	2	1.5	0.5
Q5VTR2	2	4	3	1	0	0	0	0	1	2	1.5	0.5
E9PCY5	4	2	3	2	0	0	0	0	2	1	1.5	1
F8WJN3	3	3	3	2	0	0	0	0	1.5	1.5	1.5	1
Q6P1J9	0	4	3	2	0	0	0	2	0	2	1.5	2
Q9Y5B6	0	1	2	2	0	0	1	1	0	0.5	1.5	1.5
Q99436	1	3	3	4	0	0	0	0	0.5	1.5	1.5	2
P62306	2	2	1	1	1	1	2	1	1.5	1.5	1.5	1
O95777	2	2	2	2	0	1	1	1	1	1.5	1.5	1.5
O95782	2	4	3	0	0	0	0	0	1	2	1.5	0
P17858	2	4	3	1	0	0	0	0	1	2	1.5	0.5
Q8IX12	3	3	3	1	0	0	0	0	1.5	1.5	1.5	0.5
P63167	2	1	2	2	1	1	1	0	1.5	1	1.5	1
M0R2B7	1	2	3	4	0	0	0	0	0.5	1	1.5	2
B7Z4C8	1	2	2	1	1	1	1	1	1	1.5	1.5	1
Q96J01	2	3	2	2	0	0	1	0	1	1.5	1.5	1
Q9UPQ9	3	3	3	1	0	0	0	0	1.5	1.5	1.5	0.5
P54136	3	2	3	1	0	0	0	0	1.5	1	1.5	0.5
Q9Y5Q8	5	0	3	1	0	0	0	0	2.5	0	1.5	0.5
A0A024RCF	1	1	3	4	0	0	0	0	0.5	0.5	1.5	2
C9JLU1	3	2	3	1	0	0	0	0	1.5	1	1.5	0.5
D3DQV9	2	2	3	2	0	0	0	0	1	1	1.5	1
A0A087WX	2	1	1	0	1	1	2	1	1.5	1	1.5	0.5
E9PEB5	1	2	3	3	0	0	0	0	0.5	1	1.5	1.5
A0A075B6F	0	0	0	1	0	0	3	5	0	0	1.5	3
A6NCC9	2	2	3	2	0	0	0	0	1	1	1.5	1
Q9UHI6	2	1	3	3	0	0	0	0	1	0.5	1.5	1.5
O60518	1	0	1	0	2	0	2	0	1.5	0	1.5	0
Q8N2I9	4	0	3	2	0	0	0	0	2	0	1.5	1
O00743	3	2	2	0	1	0	1	0	2	1	1.5	0
D6R9A6	1	2	3	0	0	0	0	1	0.5	1	1.5	0.5
F8W7U8	2	2	3	1	0	0	0	0	1	1	1.5	0.5
A8MQB8	4	0	3	1	0	0	0	0	2	0	1.5	0.5
Q96ST3	2	2	3	1	0	0	0	0	1	1	1.5	0.5
Q3YEC7	1	3	3	1	0	0	0	0	0.5	1.5	1.5	0.5
P35249	4	1	3	0	0	0	0	0	2	0.5	1.5	0
E7EQI7	2	1	3	1	0	0	0	0	1	0.5	1.5	0.5
D6RER5	1	2	3	1	0	0	0	0	0.5	1	1.5	0.5
P22102	0	2	2	0	1	0	1	1	0.5	1	1.5	0.5

P08243	1	1	1	1	0	0	2	0	0.5	0.5	1.5	0.5
Q5T4S7	1	1	2	0	0	0	1	1	0.5	0.5	1.5	0.5
P30419	1	1	3	1	0	0	0	0	0.5	0.5	1.5	0.5
P00492	0	0	0	1	1	1	3	0	0.5	0.5	1.5	0.5
A0A0A0MT	2	0	3	1	0	0	0	0	1	0	1.5	0.5
E9PH82	3	0	3	0	0	0	0	0	1.5	0	1.5	0
Q96C92-4	2	0	2	0	1	0	1	0	1.5	0	1.5	0
A0A087WY	2	0	3	1	0	0	0	0	1	0	1.5	0.5
F5H1Y4	3	0	3	0	0	0	0	0	1.5	0	1.5	0
Q8NFH3	0	1	3	2	0	0	0	0	0	0.5	1.5	1
O15294	1	1	3	1	0	0	0	0	0.5	0.5	1.5	0.5
P40938	0	1	3	1	0	0	0	0	0	0.5	1.5	0.5
Q9Y5K6	0	1	3	0	0	0	0	0	0	0.5	1.5	0
P52292	1	0	2	0	0	0	1	0	0.5	0	1.5	0
O43663	1	0	3	0	0	0	0	0	0.5	0	1.5	0
P31153	1	0	2	0	0	0	1	0	0.5	0	1.5	0
P22314	1	0	2	0	0	0	1	0	0.5	0	1.5	0
C9J4Z3	0	0	3	0	0	0	0	0	0	0	1.5	0
H0YHQ5	0	0	1	0	0	0	2	0	0	0	1.5	0
B7Z9C2	3	6	1	7	2	23	1	26	2.5	14.5	1	16.5
Q13509	0	0	2	0	1	0	0	0	0.5	0	1	0
P29692-3	11	3	2	10	0	0	0	4	5.5	1.5	1	7
Q05639	7	5	2	3	0	0	0	0	3.5	2.5	1	1.5
A0A075B73	8	9	2	9	0	0	0	0	4	4.5	1	4.5
Q5JUX0	0	1	2	1	0	0	0	0	0	0.5	1	0.5
E9PKG1	7	9	2	7	0	0	0	0	3.5	4.5	1	3.5
P06899	0	2	0	2	2	0	2	0	1	1	1	1
B0QYK0	9	5	2	5	0	0	0	0	4.5	2.5	1	2.5
G3V529	2	5	1	4	0	5	1	2	1	5	1	3
O43818	4	4	1	3	2	3	1	2	3	3.5	1	2.5
Q9Y625	1	0	0	1	1	1	2	1	1	0.5	1	1
Q96PY6	0	4	2	3	1	6	0	2	0.5	5	1	2.5
J3KMX5	2	2	1	2	2	3	1	4	2	2.5	1	3
Q14978-3	2	2	2	2	0	6	0	3	1	4	1	2.5
ALBU_HUM	0	0	2	1	0	0	0	0	0	0	1	0.5
P62851	3	2	2	2	2	2	0	3	2.5	2	1	2.5
A6NEM2	4	4	2	6	0	0	0	0	2	2	1	3
Q13107	1	0	0	0	0	0	2	0	0.5	0	1	0
Q12996	3	7	2	3	0	0	0	0	1.5	3.5	1	1.5
P12081	3	4	2	6	0	0	0	0	1.5	2	1	3
P49354	1	4	1	4	2	1	1	1	1.5	2.5	1	2.5
K7ER00	3	2	2	5	0	0	0	0	1.5	1	1	2.5
Q05048	3	4	2	4	0	0	0	0	1.5	2	1	2
E7EQ64	0	0	0	2	0	0	2	3	0	0	1	2.5
A0A087X2I	1	2	1	1	1	2	1	1	1	2	1	1
A0A0A0M0	1	1	1	1	2	2	1	2	1.5	1.5	1	1.5
Q92900	3	6	2	2	0	0	0	0	1.5	3	1	1
Q96F63	4	2	2	4	0	0	0	0	2	1	1	2
P81605	3	2	1	1	2	1	1	1	2.5	1.5	1	1
Q13868	2	3	2	5	0	0	0	0	1	1.5	1	2.5
B9ZVN9	3	4	2	2	0	0	0	0	1.5	2	1	1
P35250	3	3	2	3	0	0	0	0	1.5	1.5	1	1.5
Q9UBB9	4	3	2	1	0	0	0	1	2	1.5	1	1
O43172	4	2	2	1	1	0	0	1	2.5	1	1	1
P47914	2	2	2	2	0	1	0	1	1	1.5	1	1.5
Q92572	1	3	2	3	0	0	0	1	0.5	1.5	1	2
Q9H9Y6	1	4	2	3	0	0	0	0	0.5	2	1	1.5
P19387	1	3	2	4	0	0	0	0	0.5	1.5	1	2
D6RAN4	3	2	2	3	0	0	0	0	1.5	1	1	1.5
P26196	4	2	2	2	0	0	0	0	2	1	1	1
P31151	2	2	2	4	0	0	0	0	1	1	1	2

Q96S59	3	3	2	2	0	0	0	0	1.5	1.5	1	1
O43815	1	1	2	0	0	0	0	0	0.5	0.5	1	0
P62310	2	2	2	2	1	0	0	1	1.5	1	1	1.5
Q96DG6	1	3	2	3	0	0	0	0	0.5	1.5	1	1.5
Q9Y5Q9	2	3	2	2	0	0	0	0	1	1.5	1	1
M0QXL5	4	2	1	0	1	0	1	0	2.5	1	1	0
E5RHU3	2	1	2	2	0	1	0	1	1	1	1	1.5
J3KQN4	2	1	1	0	2	2	1	0	2	1.5	1	0
B1AKR6	2	2	2	0	1	1	0	1	1.5	1.5	1	0.5
Q96T76	4	0	0	0	3	0	2	0	3.5	0	1	0
P15927	1	1	1	1	0	1	1	3	0.5	1	1	2
CASB_BOV	0	3	2	2	0	0	0	0	0	1.5	1	1
Q9Y4C2	1	3	2	3	0	0	0	0	0.5	1.5	1	1.5
P23381	2	2	2	1	0	0	0	0	1	1	1	0.5
O96019	2	2	2	2	0	0	0	0	1	1	1	1
Q8TEQ6	3	1	2	2	0	0	0	0	1.5	0.5	1	1
H0YEB6	0	2	2	4	0	0	0	0	0	1	1	2
J3QT87	1	3	2	2	0	0	0	0	0.5	1.5	1	1
P06702	3	1	2	2	0	0	0	0	1.5	0.5	1	1
Q00577	0	0	1	0	0	3	1	3	0	1.5	1	1.5
P49427	3	0	2	0	3	0	0	0	3	0	1	0
A0A0B4J2E	3	1	2	2	0	0	0	0	1.5	0.5	1	1
P52701	2	1	2	2	0	0	0	0	1	0.5	1	1
Q6IA86	1	1	2	3	0	0	0	0	0.5	0.5	1	1.5
Q9NV70	1	1	2	1	0	0	0	0	0.5	0.5	1	0.5
Q12789	3	2	2	0	0	0	0	0	1.5	1	1	0
Q7Z4Q2	1	1	1	0	3	0	1	0	2	0.5	1	0
A0A0C4DFI	1	1	2	0	0	0	0	0	0.5	0.5	1	0
B3KQ25	1	3	2	1	0	0	0	0	0.5	1.5	1	0.5
E9PLA9	2	1	2	2	0	0	0	0	1	0.5	1	1
A0A0X1KG	1	3	2	0	0	0	0	1	0.5	1.5	1	0.5
A0A087WS	2	2	2	1	0	0	0	0	1	1	1	0.5
F8W733	2	1	2	2	0	0	0	0	1	0.5	1	1
F5GX77	2	1	1	1	0	0	1	1	1	0.5	1	1
A0A087X2I	0	1	1	0	0	1	1	1	0	1	1	0.5
O75449	2	1	2	2	0	0	0	0	1	0.5	1	1
Q9BVG4	2	2	2	1	0	0	0	0	1	1	1	0.5
P60866	0	2	2	2	0	0	0	0	0	1	1	1
P42677	3	0	2	1	0	0	0	0	1.5	0	1	0.5
P62857	2	1	1	0	0	0	1	1	1	0.5	1	0.5
Q9H2P0	1	2	2	1	0	0	0	0	0.5	1	1	0.5
Q9Y6D5	1	1	2	2	0	0	0	0	0.5	0.5	1	1
Q15018	0	3	2	1	0	0	0	0	0	1.5	1	0.5
Q8WXC6	1	0	1	0	2	0	1	1	1.5	0	1	0.5
Q9Y295	1	2	2	1	0	0	0	0	0.5	1	1	0.5
Q9UKN8	2	1	2	1	0	0	0	0	1	0.5	1	0.5
F2Z2W6	1	2	2	1	0	0	0	0	0.5	1	1	0.5
H3BR35	0	1	1	1	0	1	1	1	0	1	1	1
E7EQR4	0	3	2	1	0	0	0	0	0	1.5	1	0.5
M0R0F0	0	0	1	2	0	1	1	1	0	0.5	1	1.5
A0A087X25	1	1	2	1	1	0	0	0	1	0.5	1	0.5
P20774	1	2	2	1	0	0	0	0	0.5	1	1	0.5
P52298	1	1	1	1	0	0	1	1	0.5	0.5	1	1
Q15637	1	1	2	2	0	0	0	0	0.5	0.5	1	1
P83369	1	2	2	1	0	0	0	0	0.5	1	1	0.5
Q9NT62	1	1	1	1	1	0	1	0	1	0.5	1	0.5
Q6NZY4	1	2	2	1	0	0	0	0	0.5	1	1	0.5
Q9H0D6	2	0	2	1	0	0	0	0	1	0	1	0.5
O95816	2	0	1	1	0	0	1	0	1	0	1	0.5
Q9Y3Y2	0	0	1	0	1	1	1	1	0.5	0.5	1	0.5
P49916	1	1	2	1	0	0	0	0	0.5	0.5	1	0.5

Q8WXX5	0	0	0	0	1	2	2	0	0.5	1	1	0
Q9NS91	1	0	1	0	1	0	1	1	1	0	1	0.5
Q9UKB1	2	0	2	0	1	0	0	0	1.5	0	1	0
Q13151	1	0	2	2	0	0	0	0	0.5	0	1	1
B4DXZ6	2	0	2	0	0	0	0	0	1	0	1	0
B1AHD1	0	0	0	0	0	0	2	3	0	0	1	1.5
A0A087WY	2	0	0	0	1	0	2	0	1.5	0	1	0
E7ER68	0	2	2	1	0	0	0	0	0	1	1	0.5
C9JHW1	2	0	2	1	0	0	0	0	1	0	1	0.5
A0A0A0MS	1	0	1	0	2	0	1	0	1.5	0	1	0
Q8N108	1	1	2	1	0	0	0	0	0.5	0.5	1	0.5
Q15785	0	2	2	1	0	0	0	0	0	1	1	0.5
P26038	1	0	2	1	0	0	0	0	0.5	0	1	0.5
P57740	1	1	2	1	0	0	0	0	0.5	0.5	1	0.5
O00567	1	0	1	0	0	1	1	1	0.5	0.5	1	0.5
Q8NB46	1	1	1	0	1	0	1	0	1	0.5	1	0
CAS1_BOVI	0	2	1	0	0	1	1	0	0	1.5	1	0
Q7KZ85	2	0	2	1	0	0	0	0	1	0	1	0.5
Q9Y333	1	1	2	0	1	0	0	0	1	0.5	1	0
A2RU37	0	0	1	1	0	0	1	0	0	0	1	0.5
P54727	0	1	2	2	0	0	0	0	0	0.5	1	1
Q96RL7	1	0	1	0	2	0	1	0	1.5	0	1	0
P61964	2	0	2	1	0	0	0	0	1	0	1	0.5
Q96CT7	1	0	2	1	0	0	0	0	0.5	0	1	0.5
P38432	1	0	2	1	0	0	0	0	0.5	0	1	0.5
P50570	0	1	2	1	0	0	0	0	0	0.5	1	0.5
Q9Y450	2	0	2	0	0	0	0	0	1	0	1	0
A0A0A0MR	0	1	2	1	0	0	0	0	0	0.5	1	0.5
B4DEH8	1	0	2	1	0	0	0	0	0.5	0	1	0.5
Q9HCD5	1	0	2	1	0	0	0	0	0.5	0	1	0.5
Q9Y3F4	1	0	2	1	0	0	0	0	0.5	0	1	0.5
HBA_HUMA	1	1	2	0	0	0	0	0	0.5	0.5	1	0
Q7L5Y6	1	0	2	0	0	0	0	0	0.5	0	1	0
Q99871	0	1	2	0	0	0	0	0	0	0.5	1	0
J3QRS9	1	0	2	0	0	0	0	0	0.5	0	1	0
E9PK25	0	1	2	0	0	0	0	0	0	0.5	1	0
F8W726	1	0	2	0	0	0	0	0	0.5	0	1	0
C4B7M2	0	0	2	1	0	0	0	0	0	0	1	0.5
C9J494	0	0	0	0	1	0	2	0	0.5	0	1	0
Q66K74	1	0	2	0	0	0	0	0	0.5	0	1	0
O43805	0	0	2	0	0	0	0	0	0	0	1	0
Q709C8	0	0	2	0	1	0	0	0	0.5	0	1	0
Q9P1U0	0	0	2	0	0	0	0	0	0	0	1	0
O00479	0	0	0	0	0	0	2	0	0	0	1	0
H0YEL5	0	0	2	0	0	0	0	0	0	0	1	0
A0A140T8Y	0	0	1	0	0	0	1	0	0	0	1	0
K7EQA9	0	0	2	0	0	0	0	0	0	0	1	0
Q9NYK1	0	0	1	0	0	0	1	0	0	0	1	0
H0Y711	0	0	0	0	0	0	1	1	0	0	0.5	0.5
C9JZI7	0	0	0	0	1	1	1	1	0.5	0.5	0.5	0.5
M0QZM1	0	0	1	1	0	0	0	0	0	0	0.5	0.5
O60825-2	1	0	1	0	0	0	0	0	0.5	0	0.5	0
Q7Z3Y7	0	0	0	0	0	0	1	1	0	0	0.5	0.5
P42025	0	0	1	1	0	0	0	0	0	0	0.5	0.5
P09012	2	1	1	4	3	0	0	3	2.5	0.5	0.5	3.5
P35052	2	3	1	3	1	5	0	3	1.5	4	0.5	3
P62805	2	0	1	0	2	8	0	9	2	4	0.5	4.5
Q96RG2	0	3	1	4	0	6	0	8	0	4.5	0.5	6
Q58FF6	2	0	0	0	0	0	1	1	1	0	0.5	0.5
K7ER90	0	0	1	0	1	0	0	0	0.5	0	0.5	0
P15924	8	1	1	2	0	1	0	1	4	1	0.5	1.5

Q99767	0	1	1	3	1	3	0	5	0.5	2	0.5	4
Q9Y6G9	5	7	1	3	0	0	0	0	2.5	3.5	0.5	1.5
E7EX29	2	0	1	1	0	1	0	0	1	0.5	0.5	0.5
A0A0U1RR	6	2	1	5	0	0	0	0	3	1	0.5	2.5
Q9NQ29	0	1	1	1	0	0	0	0	0	0.5	0.5	0.5
Q96B23-2	2	0	1	1	4	2	0	3	3	1	0.5	2
J3KPP4	4	5	1	4	0	0	0	0	2	2.5	0.5	2
P23258	5	3	1	1	0	0	0	0	2.5	1.5	0.5	0.5
Q9P1Y5	2	5	1	5	0	0	0	0	1	2.5	0.5	2.5
Q14315	0	0	1	0	0	0	0	0	0	0	0.5	0
O95983	4	6	1	2	0	0	0	0	2	3	0.5	1
Q9H814	2	2	0	2	2	2	1	2	2	2	0.5	2
Q86YZ3	6	0	1	5	0	0	0	0	3	0	0.5	2.5
P42166	2	4	1	5	0	0	0	0	1	2	0.5	2.5
Q92804	4	1	1	0	0	0	0	0	2	0.5	0.5	0
O60216	4	4	1	2	0	0	0	0	2	2	0.5	1
P31942	1	0	1	0	0	0	0	0	0.5	0	0.5	0
A0A0B4J2B	1	1	1	1	0	1	0	1	0.5	1	0.5	1
A0A0D9SG	2	5	1	2	0	1	0	0	1	3	0.5	1
Q9BW61	1	1	0	2	2	2	1	1	1.5	1.5	0.5	1.5
P12273	4	3	1	2	0	0	0	0	2	1.5	0.5	1
Q9H0A0	2	2	1	3	0	2	0	0	1	2	0.5	1.5
Q9P2P6	2	2	1	1	2	1	0	1	2	1.5	0.5	1
O94973	2	1	1	2	0	0	0	0	1	0.5	0.5	1
Q96I24	1	0	1	1	0	0	0	0	0.5	0	0.5	0.5
P15407	2	3	1	0	1	0	0	0	1.5	1.5	0.5	0
F8VZN8	0	1	1	1	0	3	0	3	0	2	0.5	2
A0A087WL	0	6	1	2	0	0	0	0	0	3	0.5	1
P49591	1	3	1	4	0	0	0	0	0.5	1.5	0.5	2
Q86TV6	2	3	1	3	0	0	0	0	1	1.5	0.5	1.5
P08237	3	1	1	2	0	0	0	0	1.5	0.5	0.5	1
P53567	1	1	1	1	0	0	0	0	0.5	0.5	0.5	0.5
B4DL54	2	0	1	3	1	0	0	1	1.5	0	0.5	2
P60842	1	0	1	1	3	1	0	1	2	0.5	0.5	1
K7EM18	2	2	1	3	0	0	0	0	1	1	0.5	1.5
F5H039	1	4	1	2	0	0	0	0	0.5	2	0.5	1
P78346	1	3	1	3	0	0	0	0	0.5	1.5	0.5	1.5
P49756	4	2	1	1	0	0	0	0	2	1	0.5	0.5
P31431	1	1	0	0	2	2	1	1	1.5	1.5	0.5	0.5
Q9Y5A9	3	2	1	2	0	0	0	0	1.5	1	0.5	1
P11388	0	2	1	2	0	0	0	0	0	1	0.5	1
P63172	2	1	1	2	0	0	0	1	1	0.5	0.5	1.5
P01859	1	1	0	1	1	1	1	1	1	1	0.5	1
O00629	0	0	1	0	0	0	0	0	0	0	0.5	0
O15131	0	0	0	0	0	0	1	0	0	0	0.5	0
H0YIE9	1	1	1	1	0	0	0	0	0.5	0.5	0.5	0.5
D6RJ96	0	0	0	0	0	0	1	0	0	0	0.5	0
H0YKE4	2	1	0	2	0	0	1	1	1	0.5	0.5	1.5
O60341	2	2	1	2	0	0	0	0	1	1	0.5	1
Q13242	1	3	1	2	0	0	0	0	0.5	1.5	0.5	1
TRY2_BOVI	1	1	1	0	1	0	0	0	1	0.5	0.5	0
Q9P013	3	2	0	0	1	0	1	0	2	1	0.5	0
Q14232	1	3	1	2	0	0	0	0	0.5	1.5	0.5	1
Q9NR50	1	2	1	3	0	0	0	0	0.5	1	0.5	1.5
Q9Y4Z0	4	1	1	1	0	0	0	0	2	0.5	0.5	0.5
Q70CQ2	0	0	0	0	1	3	1	2	0.5	1.5	0.5	1
A5YKK6	1	2	1	2	0	0	0	0	0.5	1	0.5	1
Q9NQ92	2	1	1	2	0	0	0	0	1	0.5	0.5	1
P49643	2	2	1	1	0	0	0	0	1	1	0.5	0.5
Q6P2E9	2	2	1	1	0	0	0	0	1	1	0.5	0.5
O60306	2	2	1	1	0	0	0	0	1	1	0.5	0.5

I3L3U9	0	1	1	0	0	2	0	2	0	1.5	0.5	1
D6RBW1	3	1	1	1	0	0	0	0	1.5	0.5	0.5	0.5
E9PKF6	0	2	1	1	0	0	0	1	0	1	0.5	1
G3V1S7	1	1	0	1	0	1	1	1	0.5	1	0.5	1
A0A087WV	1	4	1	0	0	0	0	0	0.5	2	0.5	0
B5MBZ0	2	2	1	1	0	0	0	0	1	1	0.5	0.5
J3KNS1	2	1	1	2	0	0	0	0	1	0.5	0.5	1
Q5T749	3	0	1	2	0	0	0	0	1.5	0	0.5	1
O76041	0	2	0	0	3	0	1	0	1.5	1	0.5	0
P53350	2	1	1	2	0	0	0	0	1	0.5	0.5	1
O95721	2	2	1	1	0	0	0	0	1	1	0.5	0.5
Q9UPU7	0	1	0	0	0	1	1	0	0	1	0.5	0
Q9NXF1	1	1	1	0	1	1	0	1	1	1	0.5	0.5
Q08J23	0	1	1	2	0	0	0	0	0	0.5	0.5	1
Q01813	0	1	1	1	0	0	0	0	0	0.5	0.5	0.5
Q9NR09	1	0	1	2	0	1	0	0	0.5	0.5	0.5	1
O95239	1	2	1	1	0	0	0	0	0.5	1	0.5	0.5
P00742	0	0	0	0	1	2	1	1	0.5	1	0.5	0.5
Q9Y3Z3	3	1	1	0	0	0	0	0	1.5	0.5	0.5	0
P53803	1	1	1	1	1	0	0	0	1	0.5	0.5	0.5
Q14258	1	2	1	1	0	0	0	0	0.5	1	0.5	0.5
Q9NQT4	1	1	1	2	0	0	0	0	0.5	0.5	0.5	1
P51654	0	1	0	0	0	1	1	2	0	1	0.5	1
Q9NY12	1	1	1	2	0	0	0	0	0.5	0.5	0.5	1
Q9P2D3	2	1	1	1	0	0	0	0	1	0.5	0.5	0.5
O60337-5	1	0	0	1	1	1	1	0	1	0.5	0.5	0.5
A0A0U1RQ	1	2	1	1	0	0	0	0	0.5	1	0.5	0.5
A0A087WV	2	1	1	1	0	0	0	0	1	0.5	0.5	0.5
K7EMK7	0	1	1	1	1	0	0	0	0.5	0.5	0.5	0.5
A0A0D9SES	2	1	1	1	0	0	0	0	1	0.5	0.5	0.5
D6RIY6	1	2	1	1	0	0	0	0	0.5	1	0.5	0.5
A0A087WU	2	1	1	1	0	0	0	0	1	0.5	0.5	0.5
J3KNN5	1	2	1	1	0	0	0	0	0.5	1	0.5	0.5
Q15773	2	1	1	1	0	0	0	0	1	0.5	0.5	0.5
Q9BZE4	1	1	1	1	1	0	0	0	1	0.5	0.5	0.5
Q13610	0	0	1	0	1	1	0	2	0.5	0.5	0.5	1
P35659	0	3	1	1	0	0	0	0	0	1.5	0.5	0.5
O15084	3	0	1	1	0	0	0	0	1.5	0	0.5	0.5
O00268	1	1	1	2	0	0	0	0	0.5	0.5	0.5	1
P49770	1	3	1	0	0	0	0	0	0.5	1.5	0.5	0
Q7Z2T5	0	1	1	3	0	0	0	0	0	0.5	0.5	1.5
Q2TAM9	1	1	1	1	0	1	0	0	0.5	1	0.5	0.5
P42766	1	0	1	0	0	1	0	1	0.5	0.5	0.5	0.5
P02765	2	0	1	0	0	0	0	1	1	0	0.5	0.5
Q9UJX2	1	1	1	1	0	0	0	0	0.5	0.5	0.5	0.5
Q9P2I0	2	1	1	0	0	0	0	0	1	0.5	0.5	0
O43175	1	1	1	0	0	0	0	1	0.5	0.5	0.5	0.5
Q8IYD1	0	1	0	0	0	1	1	1	0	1	0.5	0.5
Q9NPD3	1	1	1	1	0	0	0	0	0.5	0.5	0.5	0.5
P82970	1	1	1	1	0	0	0	0	0.5	0.5	0.5	0.5
Q7Z353	3	0	1	0	0	0	0	0	1.5	0	0.5	0
O95861-2	0	1	1	0	0	0	0	0	0	0.5	0.5	0
A0A087WT	1	0	1	0	0	0	0	0	0.5	0	0.5	0
H7C3P6	1	1	1	1	0	0	0	0	0.5	0.5	0.5	0.5
B1AQK6	0	1	1	0	0	0	0	0	0	0.5	0.5	0
F8WA39	0	0	1	3	0	0	0	0	0	0	0.5	1.5
A0A0A0MT	1	2	1	0	0	0	0	0	0.5	1	0.5	0
B1ALD9	0	1	1	0	0	0	0	0	0	0.5	0.5	0
A0A0G2JRX	1	1	1	1	0	0	0	0	0.5	0.5	0.5	0.5
A0A087X1E	1	1	1	1	0	0	0	0	0.5	0.5	0.5	0.5
A0A087WT	1	1	1	1	0	0	0	0	0.5	0.5	0.5	0.5

A0A0B4J21	1	0	0	0	0	0	1	2	0.5	0	0.5	1
H3BM60	1	1	1	1	0	0	0	0	0.5	0.5	0.5	0.5
Q8WXA9-2	1	1	0	0	0	0	1	1	0.5	0.5	0.5	0.5
E5RFF9	1	1	0	0	1	0	1	0	1	0.5	0.5	0
B4DDH2	0	1	1	0	0	0	0	0	0	0.5	0.5	0
A6NIZ0	1	1	1	0	0	1	0	0	0.5	1	0.5	0
J3QQJ0	1	1	1	1	0	0	0	0	0.5	0.5	0.5	0.5
B1AMU3	1	1	1	1	0	0	0	0	0.5	0.5	0.5	0.5
J3KQR7	1	1	1	0	0	0	0	1	0.5	0.5	0.5	0.5
O75037	1	1	1	1	0	0	0	0	0.5	0.5	0.5	0.5
Q9P2J5	1	1	1	1	0	0	0	0	0.5	0.5	0.5	0.5
O75400	1	1	1	1	0	0	0	0	0.5	0.5	0.5	0.5
Q6PI26	0	0	0	0	2	0	1	1	1	0	0.5	0.5
Q15428	2	0	1	1	0	0	0	0	1	0	0.5	0.5
P17028	2	1	1	0	0	0	0	0	1	0.5	0.5	0
Q06203	1	1	1	0	0	0	0	0	0.5	0.5	0.5	0
Q8NHZ8	0	1	1	1	0	0	0	0	0	0.5	0.5	0.5
P32121	0	1	1	1	0	0	0	0	0	0.5	0.5	0.5
Q9NWV8	0	1	1	1	0	0	0	0	0	0.5	0.5	0.5
Q8WTR2	1	1	0	0	0	0	1	0	0.5	0.5	0.5	0
Q92538	1	0	1	1	0	0	0	0	0.5	0	0.5	0.5
Q9HCN4	1	0	1	0	1	0	0	0	1	0	0.5	0
P17096	0	2	1	0	0	0	0	0	0	1	0.5	0
Q09472	1	1	1	0	0	0	0	0	0.5	0.5	0.5	0
P20719	2	0	1	0	0	0	0	0	1	0	0.5	0
E9PM92	1	0	1	0	1	0	0	0	1	0	0.5	0
B3KXD6	0	1	1	1	0	0	0	0	0	0.5	0.5	0.5
F5H2E5	1	1	1	0	0	0	0	0	0.5	0.5	0.5	0
J3KNV1	1	0	1	0	0	0	0	1	0.5	0	0.5	0.5
E2QRF9	0	0	0	0	1	1	1	0	0.5	0.5	0.5	0
A8MX94	0	0	1	0	0	0	0	2	0	0	0.5	1
D6REM4	0	1	1	1	0	0	0	0	0	0.5	0.5	0.5
A8MU27	0	1	1	1	0	0	0	0	0	0.5	0.5	0.5
A0A0A0MC	0	1	1	1	0	0	0	0	0	0.5	0.5	0.5
A0A024R7\	1	0	1	0	0	0	0	0	0.5	0	0.5	0
F2Z2W7	2	0	1	0	0	0	0	0	1	0	0.5	0
H7C466	1	1	1	0	0	0	0	0	0.5	0.5	0.5	0
D6RFW3	0	1	1	1	0	0	0	0	0	0.5	0.5	0.5
D6RJ98	1	1	1	0	0	0	0	0	0.5	0.5	0.5	0
Q5TDF0	1	0	1	1	0	0	0	0	0.5	0	0.5	0.5
F2Z2B9	0	1	1	1	0	0	0	0	0	0.5	0.5	0.5
E9PHH9	0	1	1	1	0	0	0	0	0	0.5	0.5	0.5
H7C5M7	0	0	0	0	1	0	1	1	0.5	0	0.5	0.5
A0A0R4J2F	0	1	1	1	0	0	0	0	0	0.5	0.5	0.5
P33176	2	0	1	0	0	0	0	0	1	0	0.5	0
Q12756	1	0	1	0	0	0	0	0	0.5	0	0.5	0
O00139	2	0	1	0	0	0	0	0	1	0	0.5	0
Q14114	1	1	0	0	0	0	1	0	0.5	0.5	0.5	0
Q8WW12	0	1	1	1	0	0	0	0	0	0.5	0.5	0.5
Q13371	0	1	1	1	0	0	0	0	0	0.5	0.5	0.5
Q9UNQ2	0	0	1	2	0	0	0	0	0	0	0.5	1
Q5VTE6	1	1	1	0	0	0	0	0	0.5	0.5	0.5	0
A8MVW0	0	1	1	0	0	0	0	1	0	0.5	0.5	0.5
A0A0A6YYF	1	0	1	0	1	0	0	0	1	0	0.5	0
Q9NRJ7	0	1	1	0	1	0	0	0	0.5	0.5	0.5	0
Q5T280	0	0	1	1	0	1	0	0	0	0.5	0.5	0.5
A6NDX5	0	0	1	1	0	1	0	0	0	0.5	0.5	0.5
Q13283	1	0	1	1	0	0	0	0	0.5	0	0.5	0.5
Q8N5L8	0	1	1	1	0	0	0	0	0	0.5	0.5	0.5
Q9H6T3	0	2	1	0	0	0	0	0	0	1	0.5	0
O43347	1	0	1	1	0	0	0	0	0.5	0	0.5	0.5

CASK_BOVI	0	1	1	1	0	0	0	0	0	0.5	0.5	0.5
Q13838	2	0	1	0	0	0	0	0	1	0	0.5	0
Q5VSL9	1	0	1	1	0	0	0	0	0.5	0	0.5	0.5
Q86W42	1	1	1	0	0	0	0	0	0.5	0.5	0.5	0
A0A0A0MF	0	1	0	0	0	0	1	1	0	0.5	0.5	0.5
P17275	0	0	1	1	0	0	0	0	0	0	0.5	0.5
Q8WUH2	1	1	1	0	0	0	0	0	0.5	0.5	0.5	0
Q969L4	0	1	1	1	0	0	0	0	0	0.5	0.5	0.5
A0A0B4J20	1	0	1	1	0	0	0	0	0.5	0	0.5	0.5
Q9H269	1	1	1	0	0	0	0	0	0.5	0.5	0.5	0
Q8TAF3	0	1	1	1	0	0	0	0	0	0.5	0.5	0.5
Q6UXN9	0	0	1	1	0	0	0	1	0	0	0.5	1
Q8N3C0	0	1	1	0	0	0	0	0	0	0.5	0.5	0
P49588	0	1	1	0	0	0	0	0	0	0.5	0.5	0
Q96S55	0	1	1	0	0	0	0	0	0	0.5	0.5	0
Q4LE39	1	0	1	0	0	0	0	0	0.5	0	0.5	0
Q6PJG6	0	0	0	0	1	0	1	0	0.5	0	0.5	0
Q15417	0	0	0	0	1	0	1	0	0.5	0	0.5	0
O43852	0	0	1	1	0	0	0	0	0	0	0.5	0.5
P45973	0	0	0	0	0	0	1	0	0	0	0.5	0
Q6P1N0	0	1	1	0	0	0	0	0	0	0.5	0.5	0
C9J1V9	0	0	1	1	0	0	0	0	0	0	0.5	0.5
Q9NQT5	0	0	1	1	0	0	0	0	0	0	0.5	0.5
Q75N90	0	1	1	0	0	0	0	0	0	0.5	0.5	0
Q5JY77	0	1	1	0	0	0	0	0	0	0.5	0.5	0
Q9NX24	0	0	1	0	0	0	0	1	0	0	0.5	0.5
Q9NX55	0	0	0	0	1	0	1	0	0.5	0	0.5	0
A0A096LNV	0	0	0	1	0	0	1	0	0	0	0.5	0.5
K7EKT4	0	0	1	1	0	0	0	0	0	0	0.5	0.5
A0A087X0X	0	0	1	0	0	1	0	0	0	0.5	0.5	0
H0Y9A0	1	0	1	0	0	0	0	0	0.5	0	0.5	0
E7EMW7	0	1	1	0	0	0	0	0	0	0.5	0.5	0
E7EWD9	0	0	1	1	0	0	0	0	0	0	0.5	0.5
K7EM90	1	0	1	0	0	0	0	0	0.5	0	0.5	0
A8MW50	0	0	0	0	0	0	1	1	0	0	0.5	0.5
E9PR30	0	1	0	0	0	0	1	0	0	0.5	0.5	0
H0YIQ2	0	0	1	0	0	1	0	0	0	0.5	0.5	0
A8K878	1	0	1	0	0	0	0	0	0.5	0	0.5	0
B4DWR3	1	0	1	0	0	0	0	0	0.5	0	0.5	0
D6RG19	0	1	1	0	0	0	0	0	0	0.5	0.5	0
E9PQ57	0	0	0	1	0	0	1	0	0	0	0.5	0.5
A0A0A0MT	1	0	1	0	0	0	0	0	0.5	0	0.5	0
H7C072	0	1	1	0	0	0	0	0	0	0.5	0.5	0
B1AL79	0	1	1	0	0	0	0	0	0	0.5	0.5	0
Q5VU13-2	1	0	1	0	0	0	0	0	0.5	0	0.5	0
B7ZLT2	1	0	1	0	0	0	0	0	0.5	0	0.5	0
H3BRX1	1	0	1	0	0	0	0	0	0.5	0	0.5	0
A0A0A0MS	1	0	1	0	0	0	0	0	0.5	0	0.5	0
H3BSW0	0	0	0	0	0	1	1	0	0	0.5	0.5	0
E9PQ73	1	0	0	0	0	0	1	0	0.5	0	0.5	0
A0A087WY	0	0	0	0	0	0	1	1	0	0	0.5	0.5
E9PMG1	0	1	1	0	0	0	0	0	0	0.5	0.5	0
B8ZZ47	1	0	1	0	0	0	0	0	0.5	0	0.5	0
K7ELS0	1	0	1	0	0	0	0	0	0.5	0	0.5	0
C9IZE1	1	0	1	0	0	0	0	0	0.5	0	0.5	0
F8WA32	1	0	1	0	0	0	0	0	0.5	0	0.5	0
A0A0C4DFZ	0	1	0	0	0	0	1	0	0	0.5	0.5	0
Q5JR04	0	0	0	0	1	0	1	0	0.5	0	0.5	0
H0YIH0	0	1	1	0	0	0	0	0	0	0.5	0.5	0
A0A087WT	1	0	1	0	0	0	0	0	0.5	0	0.5	0
C9J7E8	1	0	1	0	0	0	0	0	0.5	0	0.5	0

B1ANM7	0	0	0	0	1	0	1	0	0.5	0	0.5	0
B4DM50	0	0	1	1	0	0	0	0	0	0	0.5	0.5
Q9BRS8	0	1	1	0	0	0	0	0	0	0.5	0.5	0
P55081	1	0	1	0	0	0	0	0	0.5	0	0.5	0
O60830	0	0	1	0	0	0	0	1	0	0	0.5	0.5
Q99558	0	0	1	0	0	0	0	1	0	0	0.5	0.5
Q9NXX6	1	0	1	0	0	0	0	0	0.5	0	0.5	0
Q9H4L5	0	0	0	0	0	1	1	0	0	0.5	0.5	0
Q5VUB5	1	0	1	0	0	0	0	0	0.5	0	0.5	0
Q8TF72	1	0	1	0	0	0	0	0	0.5	0	0.5	0
P0C860	0	0	1	1	0	0	0	0	0	0	0.5	0.5
P34896	1	0	1	0	0	0	0	0	0.5	0	0.5	0
CAS2_BOVI	0	1	1	0	0	0	0	0	0	0.5	0.5	0
Q96GM8	0	1	1	0	0	0	0	0	0	0.5	0.5	0
Q7L0X0	0	1	1	0	0	0	0	0	0	0.5	0.5	0
O75896	0	0	0	0	1	0	1	0	0.5	0	0.5	0
Q9Y4Y9	0	1	1	0	0	0	0	0	0	0.5	0.5	0
H7C155	0	0	1	0	0	0	0	0	0	0	0.5	0
G3V461	0	0	1	0	0	0	0	0	0	0	0.5	0
A6NIT2	0	0	1	0	0	0	0	0	0	0	0.5	0
C9J1X3	0	0	0	0	0	0	1	0	0	0	0.5	0
B7ZA25	0	0	1	0	0	0	0	0	0	0	0.5	0
E9PIX7	0	0	0	0	0	0	1	0	0	0	0.5	0
M0QYT7	0	0	1	0	0	0	0	0	0	0	0.5	0
P28482	0	0	1	0	0	0	0	0	0	0	0.5	0
P42345	0	0	1	0	0	0	0	0	0	0	0.5	0
P06748-3	7	0	0	2	0	0	0	0	3.5	0	0	1
F8VVB5	0	3	0	3	0	4	0	4	0	3.5	0	3.5
Q3ZCM7	2	2	0	0	0	0	0	0	1	1	0	0
H0YJP0	1	0	0	0	0	0	0	0	0.5	0	0	0
P02538	0	1	0	2	0	0	0	0	0	0.5	0	1
F6SS63	2	0	0	0	0	0	0	0	1	0	0	0
Q58FF7	0	0	0	0	0	0	0	1	0	0	0	0.5
Q8TDI0	1	1	0	1	0	0	0	0	0.5	0.5	0	0.5
Q58FG1	1	0	0	0	0	0	0	0	0.5	0	0	0
J3KN67	1	0	0	1	7	0	0	0	4	0	0	0.5
P62136	2	6	0	1	0	0	0	0	1	3	0	0.5
F8VYE8	1	0	0	0	0	0	0	0	0.5	0	0	0
P16989	0	1	0	0	0	0	0	0	0	0.5	0	0
P15408-2	2	1	0	0	2	1	0	0	2	1	0	0
Q562R1	0	1	0	0	0	0	0	0	0	0.5	0	0
Q58FG0	0	0	0	0	0	0	0	1	0	0	0	0.5
P62263	4	1	0	3	0	2	0	2	2	1.5	0	2.5
O75531	0	1	0	5	0	4	0	7	0	2.5	0	6
Q8NB90	0	0	0	2	0	0	0	0	0	0	0	1
P61981	1	1	0	0	0	1	0	0	0.5	1	0	0
F8VZY9	0	0	0	0	1	0	0	0	0.5	0	0	0
Q9UKA9	1	0	0	0	0	0	0	0	0.5	0	0	0
Q5JZB7	1	0	0	0	0	0	0	1	0.5	0	0	0.5
E7EQY4	1	0	0	2	0	0	0	0	0.5	0	0	1
O14556	0	1	0	0	0	0	0	0	0	0.5	0	0
Q96SI9	1	1	0	0	0	0	0	0	0.5	0.5	0	0
B5MD17	0	1	0	0	1	0	0	0	0.5	0.5	0	0
F5GYK2	4	0	0	0	0	0	0	0	2	0	0	0
Q14004	0	0	0	0	0	0	0	2	0	0	0	1
F5H6Z0	0	0	0	0	0	2	0	0	0	1	0	0
E7ETY2	0	1	0	2	1	2	0	3	0.5	1.5	0	2.5
E7ERS3	0	0	0	0	2	3	0	4	1	1.5	0	2
F8VXC8	1	1	0	0	0	0	0	0	0.5	0.5	0	0
Q13615	1	5	0	1	0	0	0	2	0.5	2.5	0	1.5
P20794	0	0	0	1	0	0	0	0	0	0	0	0.5

Q5TAH2	1	0	0	0	1	0	0	1	1	0	0	0.5
Q15024	1	5	0	2	0	0	0	0	0.5	2.5	0	1
P31948	0	7	0	1	0	0	0	0	0	3.5	0	0.5
Q01826	0	0	0	1	0	0	0	0	0	0	0	0.5
A0A087X1A	1	1	0	0	0	2	0	3	0.5	1.5	0	1.5
J3QR65	0	0	0	1	1	3	0	0	0.5	1.5	0	0.5
P61221	2	3	0	1	0	0	0	0	1	1.5	0	0.5
P17812	1	2	0	1	1	0	0	1	1	1	0	1
Q8IWV7	0	4	0	2	0	0	0	0	0	2	0	1
H3BP71	2	0	0	3	0	0	0	0	1	0	0	1.5
I3L2C7	2	3	0	1	0	0	0	0	1	1.5	0	0.5
A0A087WV	0	1	0	0	0	0	0	0	0	0.5	0	0
H0YGK9	0	0	0	0	1	0	0	0	0.5	0	0	0
P46821	2	2	0	2	0	0	0	0	1	1	0	1
P46087	1	2	0	1	0	1	0	1	0.5	1.5	0	1
Q9UKV8	3	2	0	1	0	0	0	0	1.5	1	0	0.5
Q6ZU15	1	2	0	1	0	0	0	0	0.5	1	0	0.5
P11172	1	0	0	0	2	3	0	0	1.5	1.5	0	0
Q15147	0	0	0	2	0	0	0	1	0	0	0	1.5
Q5RKV6	2	2	0	1	0	0	0	0	1	1	0	0.5
O00425	0	0	0	0	0	1	0	1	0	0.5	0	0.5
P19525	1	2	0	0	0	1	0	1	0.5	1.5	0	0.5
Q96PK6-5	1	0	0	1	0	0	0	0	0.5	0	0	0.5
Q8N1N4	2	0	0	0	0	0	0	0	1	0	0	0
Q92620	0	3	0	2	0	0	0	0	0	1.5	0	1
Q8IX18	1	3	0	1	0	0	0	0	0.5	1.5	0	0.5
Q9NTI5	1	2	0	2	0	0	0	0	0.5	1	0	1
P07996	0	2	0	3	0	0	0	0	0	1	0	1.5
Q96QR8	0	0	0	0	0	1	0	2	0	0.5	0	1
Q69YN2	0	3	0	1	0	0	0	0	0	1.5	0	0.5
P51116	2	0	0	0	0	0	0	0	1	0	0	0
E7EUU4	1	2	0	1	0	0	0	0	0.5	1	0	0.5
A0A0A0MS	0	0	0	0	1	1	0	0	0.5	0.5	0	0
Q5JVF3-4	0	1	0	0	1	0	0	0	0.5	0.5	0	0
F5GY73	1	0	0	1	0	0	0	0	0.5	0	0	0.5
A0A075B74	0	1	0	1	0	0	0	0	0	0.5	0	0.5
Q8N9N2-2	1	3	0	0	0	0	0	0	0.5	1.5	0	0
F5H0F9	1	1	0	2	0	0	0	0	0.5	0.5	0	1
Q04721	0	1	0	2	0	1	0	0	0	1	0	1
Q5SY16	3	0	0	0	0	1	0	0	1.5	0.5	0	0
Q9H6S0	0	0	0	0	1	1	0	2	0.5	0.5	0	1
Q06323	1	2	0	1	0	0	0	0	0.5	1	0	0.5
Q9C005	0	1	0	1	1	0	0	1	0.5	0.5	0	1
Q13123	2	1	0	0	0	1	0	0	1	1	0	0
P05109	1	0	0	0	0	1	0	0	0.5	0.5	0	0
Q6ZS86	0	0	0	0	0	1	0	1	0	0.5	0	0.5
Q99986	0	1	0	3	0	0	0	0	0	0.5	0	1.5
Q9H0U9	0	3	0	1	0	0	0	0	0	1.5	0	0.5
Q49AR2	0	0	0	0	3	0	0	1	1.5	0	0	0.5
Q9BZH6	0	2	0	2	0	0	0	0	0	1	0	1
O15060	0	2	0	2	0	0	0	0	0	1	0	1
Q9HB71	1	1	0	1	0	0	0	0	0.5	0.5	0	0.5
Q9NX58	1	0	0	0	0	0	0	2	0.5	0	0	1
Q08554	2	0	0	1	0	0	0	0	1	0	0	0.5
P62875	1	1	0	1	0	0	0	0	0.5	0.5	0	0.5
Q99543	2	0	0	1	0	0	0	0	1	0	0	0.5
Q96B26	2	0	0	1	0	0	0	0	1	0	0	0.5
P0C2W1	1	1	0	1	0	0	0	0	0.5	0.5	0	0.5
Q5D862	1	1	0	1	0	0	0	0	0.5	0.5	0	0.5
Q8WUA4	2	1	0	0	0	0	0	0	1	0.5	0	0
Q9H3P7	2	0	0	0	1	0	0	0	1.5	0	0	0

A0A0G2JM	2	1	0	0	0	0	0	0	1	0.5	0	0
A0A087WV	1	1	0	0	0	0	0	0	0.5	0.5	0	0
A0A0A0MF	1	1	0	1	0	0	0	0	0.5	0.5	0	0.5
F8WE71	0	0	0	0	0	0	0	1	0	0	0	0.5
B5MDF5	2	1	0	0	0	0	0	0	1	0.5	0	0
A0A0A0MF	3	0	0	0	0	0	0	0	1.5	0	0	0
J3KSD8	1	1	0	1	0	0	0	0	0.5	0.5	0	0.5
F5H658	0	0	0	1	0	0	0	0	0	0	0	0.5
A0A0D9SEl	0	0	0	1	0	0	0	0	0	0	0	0.5
C9J6P4	0	2	0	1	0	0	0	0	0	1	0	0.5
A0A087WY	2	0	0	0	0	0	0	1	1	0	0	0.5
M0R2U7	0	0	0	0	0	1	0	0	0	0.5	0	0
B4E3S0	2	1	0	0	0	0	0	0	1	0.5	0	0
P14923	1	1	0	1	0	0	0	0	0.5	0.5	0	0.5
Q9GZU2	2	0	0	1	0	0	0	0	1	0	0	0.5
Q9H0S4	2	1	0	0	0	0	0	0	1	0.5	0	0
Q9H871	1	1	0	1	0	0	0	0	0.5	0.5	0	0.5
Q15291	1	0	0	0	2	0	0	0	1.5	0	0	0
P57772	1	0	0	2	0	0	0	0	0.5	0	0	1
Q9UPN7	2	1	0	0	0	0	0	0	1	0.5	0	0
A6NHR9	1	0	0	2	0	0	0	0	0.5	0	0	1
O95620	0	0	0	0	0	1	0	2	0	0.5	0	1
O94763	1	2	0	0	0	0	0	0	0.5	1	0	0
Q9NZ32	1	1	0	0	0	0	0	0	0.5	0.5	0	0
Q9BR61	0	0	0	0	0	1	0	1	0	0.5	0	0.5
Q9UKA4	0	2	0	0	0	0	0	0	0	1	0	0
Q02952	0	2	0	0	0	0	0	0	0	1	0	0
Q13155	2	0	0	0	0	0	0	0	1	0	0	0
P25705	0	1	0	1	0	0	0	0	0	0.5	0	0.5
Q8N4T0	0	2	0	0	0	0	0	0	0	1	0	0
P39060	0	1	0	0	0	1	0	0	0	1	0	0
P42695	0	1	0	1	0	0	0	0	0	0.5	0	0.5
Q13618	2	0	0	0	0	0	0	0	1	0	0	0
Q14999	0	2	0	0	0	0	0	0	0	1	1	0
Q02413	1	0	0	1	0	0	0	0	0.5	0	0	0.5
Q969P6	0	0	0	0	1	0	0	0	0.5	0	0	0
Q8TD57	0	1	0	0	0	0	0	1	0	0.5	0	0.5
O60869	0	1	0	1	0	0	0	0	0	0.5	0	0.5
P20042	1	0	0	1	0	0	0	0	0.5	0	0	0.5
Q9BYI3	0	0	0	2	0	0	0	0	0	0	0	1
Q4G0P3	0	1	0	0	0	0	0	1	0	0.5	0	0.5
Q8IV63	0	0	0	2	0	0	0	0	0	0	0	1
H0YHK5	1	0	0	1	0	0	0	0	0.5	0	0	0.5
H0YAN8	1	0	0	1	0	0	0	0	0.5	0	0	0.5
H7C2Q2	0	0	0	0	1	1	0	0	0.5	0.5	0	0
E9PQG0	0	0	0	0	1	0	0	1	0.5	0	0	0.5
A0A087WZ	1	0	0	1	0	0	0	0	0.5	0	0	0.5
H0YKL9	0	1	0	1	0	0	0	0	0	0.5	0	0.5
H3BP07	1	0	0	1	0	0	0	0	0.5	0	0	0.5
E9PHH3	0	0	0	0	1	1	0	0	0.5	0.5	0	0
A2IDA3	2	0	0	0	0	0	0	0	1	0	0	0
A0A096LNl	1	0	0	0	1	0	0	0	1	0	0	0
A0A0C4DG	2	0	0	0	0	0	0	0	1	0	0	0
E9PP40	1	0	0	0	0	1	0	0	0.5	0.5	0	0
G8JLG2	1	0	0	1	0	0	0	0	0.5	0	0	0.5
A0A0B4J1Z	1	0	0	0	0	1	0	0	0.5	0.5	0	0
A0A087WV	0	2	0	0	0	0	0	0	0	1	0	0
E7EPB1	0	1	0	0	1	0	0	0	0.5	0.5	0	0
E9PG32	0	1	0	0	0	1	0	0	0	1	0	0
H0Y9L8	1	0	0	1	0	0	0	0	0.5	0	0	0.5
E7ESC9	1	0	0	1	0	0	0	0	0.5	0	0	0.5

A0A1B0GV	2	0	0	0	0	0	0	0	1	0	0	0
A0A0C4DG	0	2	0	0	0	0	0	0	0	1	0	0
F5H0C4	0	2	0	0	0	0	0	0	0	1	0	0
F5H0W7	0	1	0	1	0	0	0	0	0	0.5	0	0.5
J9JIC5	1	0	0	1	0	0	0	0	0.5	0	0	0.5
E7ESG2	0	0	0	0	0	1	0	1	0	0.5	0	0.5
D6RAP6	1	1	0	0	0	0	0	0	0.5	0.5	0	0
A0A0A0MF	0	0	0	1	1	0	0	0	0.5	0	0	0.5
M0QY97	0	2	0	0	0	0	0	0	0	1	0	0
F8W0Q0	0	1	0	0	0	1	0	0	0	1	0	0
J3KSL8	0	1	0	1	0	0	0	0	0	0.5	0	0.5
E5RHR6	1	0	0	1	0	0	0	0	0.5	0	0	0.5
E7EW58	0	0	0	0	1	0	0	1	0.5	0	0	0.5
Q8IW41	1	1	0	0	0	0	0	0	0.5	0.5	0	0
Q96PG2	1	1	0	0	0	0	0	0	0.5	0.5	0	0
A6NFA1	0	1	0	1	0	0	0	0	0	0.5	0	0.5
Q15014	1	1	0	0	0	0	0	0	0.5	0.5	0	0
Q8WVJ2	1	0	0	1	0	0	0	0	0.5	0	0	0.5
Q9UBD5	2	0	0	0	0	0	0	0	1	0	0	0
Q9Y3Q4	1	0	0	0	1	0	0	0	1	0	0	0
Q5VTL8	1	1	0	0	0	0	0	0	0.5	0.5	0	0
Q9ULR0	0	1	0	1	0	0	0	0	0	0.5	0	0.5
Q9NUL7	1	1	0	0	0	0	0	0	0.5	0.5	0	0
Q15751	1	0	0	0	0	0	0	1	0.5	0	0	0.5
Q8NBJ5	1	1	0	0	0	0	0	0	0.5	0.5	0	0
Q9BRP1	1	0	0	0	1	0	0	0	1	0	0	0
Q8IVF2	0	0	0	1	1	0	0	0	0.5	0	0	0.5
Q08174	0	1	0	1	0	0	0	0	0	0.5	0	0.5
Q6ZN68	0	0	0	0	0	1	0	1	0	0.5	0	0.5
Q8IXW5	1	1	0	0	0	0	0	0	0.5	0.5	0	0
Q15042	2	0	0	0	0	0	0	0	1	0	0	0
Q9NZL6	0	0	0	1	0	1	0	0	0	0.5	0	0.5
Q9P227	0	0	0	1	0	0	0	0	0	0	0	0.5
Q9NRR4	1	0	0	1	0	0	0	0	0.5	0	0	0.5
Q9Y4W2	1	1	0	0	0	0	0	0	0.5	0.5	0	0
P21817	1	1	0	0	0	0	0	0	0.5	0.5	0	0
A0A087X0F	0	0	0	0	1	1	0	0	0.5	0.5	0	0
O75170	2	0	0	0	0	0	0	0	1	0	0	0
Q562F6	1	1	0	0	0	0	0	0	0.5	0.5	0	0
Q16650	1	1	0	0	0	0	0	0	0.5	0.5	0	0
Q99614	0	0	0	1	0	1	0	0	0	0.5	0	0.5
O60779	0	0	0	0	1	0	0	1	0.5	0	0	0.5
Q13144	0	2	0	0	0	0	0	0	0	1	0	0
Q9Y2S6	0	1	0	1	0	0	0	0	0	0.5	0	0.5
P60174	0	1	0	1	0	0	0	0	0	0.5	0	0.5
Q9UPU5	1	0	0	0	1	0	0	0	1	0	0	0
H3BMM5	1	0	0	1	0	0	0	0	0.5	0	0	0.5
Q9UNX4	1	1	0	0	0	0	0	0	0.5	0.5	0	0
Q9Y2I7	0	0	0	0	1	0	0	0	0.5	0	0	0
J3KR82	0	0	0	0	1	0	0	0	0.5	0	0	0
D6RCP9	0	1	0	0	0	0	0	0	0	0.5	0	0
H0YJF2	0	0	0	1	0	0	0	0	0	0	0	0.5
I3L112	0	0	0	0	1	0	0	0	0.5	0	0	0
A0A087WZ	0	0	0	0	1	0	0	0	0.5	0	0	0
H0YDJ3	0	0	0	0	0	1	0	0	0	0.5	0	0
H0Y9K2	0	0	0	1	0	0	0	0	0	0	0	0.5
A0A0C4DG	1	0	0	0	0	0	0	0	0.5	0	0	0
A0A087WV	1	0	0	0	0	0	0	0	0.5	0	0	0
J3KT82	0	1	0	0	0	0	0	0	0	0.5	0	0
A8MYT4	0	1	0	0	0	0	0	0	0	0.5	0	0
A0A0C4DG	0	1	0	0	0	0	0	0	0	0.5	0	0

K7ELH3	0	0	0	0	0	0	0	1	0	0	0	0.5
O94806	0	1	0	0	0	0	0	0	0	0.5	0	0
Q9UL54	0	0	0	0	0	1	0	0	0	0.5	0	0
Q15772	0	0	0	0	0	1	0	0	0	0.5	0	0
Q9ULD0	0	0	0	0	0	0	1	0				
P49189	0	0	1	0	0	0	0	0				
Q8WXS8	0	0	0	0	1	0	0	0				
Q8IZT6	0	0	0	1	0	0	0	0				
Q9NUB1	0	0	0	0	0	0	0	1				
Q8WYK0	0	0	1	0	0	0	0	0				
Q01518	0	0	1	0	0	0	0	0				
Q86V24	0	0	0	0	0	0	0	1				
Q66PJ3	0	0	0	0	0	0	0	1				
P03973	0	0	0	0	0	0	0	1				
P02647	0	1	0	0	0	0	0	0				
Q9HCS5	0	1	0	0	0	0	0	0				
Q68DE3	0	0	0	0	1	0	0	0				
P22914	1	0	0	0	0	0	0	0				
Q9NRL2	1	0	0	0	0	0	0	0				
Q96CX2	0	1	0	0	0	0	0	0				
Q9NXV2	0	0	0	1	0	0	0	0				
O75844	1	0	0	0	0	0	0	0				
Q8WUQ7	0	1	0	0	0	0	0	0				
P17655	0	0	0	0	1	0	0	0				
Q9NRB3	0	0	0	0	1	0	0	0				
P16152	0	1	0	0	0	0	0	0				
P50416	0	1	0	0	0	0	0	0				
Q9H8G2	0	1	0	0	0	0	0	0				
Q9H7T0	0	0	1	0	0	0	0	0				
Q00587	1	0	0	0	0	0	0	0				
Q92674	0	0	1	0	0	0	0	0				
Q9C0F1	0	0	0	0	0	0	1	0				
P35523	1	0	0	0	0	0	0	0				
Q8NCU4	0	0	0	0	0	1	0	0				
P25940	0	0	0	0	0	0	0	1				
A6NMZ7	0	0	0	1	0	0	0	0				
Q9UP83	0	1	0	0	0	0	0	0				
P83436	0	0	0	0	0	0	1	0				
Q9P232	0	0	0	0	0	1	0	0				
Q9HCH3	1	0	0	0	0	0	0	0				
P18846	0	0	0	1	0	0	0	0				
O60583	0	0	1	0	0	0	0	0				
Q8N1N5	0	0	1	0	0	0	0	0				
Q9P021	0	0	1	0	0	0	0	0				
P35462	0	0	1	0	0	0	0	0				
P0C7V8	0	1	0	0	0	0	0	0				
Q96BY6	0	1	0	0	0	0	0	0				
Q6PJP8	0	0	0	0	1	0	0	0				
Q9NRF9	1	0	0	0	0	0	0	0				
O15446	1	0	0	0	0	0	0	0				
Q8IXB1	0	0	1	0	0	0	0	0				
A8MYV0	0	0	0	0	1	0	0	0				
Q9P225	0	0	0	1	0	0	0	0				
Q9Y508	0	0	0	1	0	0	0	0				
Q9Y252	0	0	1	0	0	0	0	0				
Q96EB1	0	0	0	1	0	0	0	0				
P60507	1	0	0	0	0	0	0	0				
Q14511	0	1	0	0	0	0	0	0				
A8K979	1	0	0	0	0	0	0	0				
O14980	0	0	1	0	0	0	0	0				
O15360	0	0	0	0	1	0	0	0				

Q8N4B4	0	0	0	0	0	0	1	0
A9Z1Z3	1	0	0	0	0	0	0	0
Q9C0D6	0	0	0	0	0	0	0	1
Q86WI1	0	0	1	0	0	0	0	0
Q5SZK8	1	0	0	0	0	0	0	0
P48169	0	0	0	1	0	0	0	0
O76003	0	0	0	1	0	0	0	0
O75311	0	0	0	0	0	1	0	0
P54840	0	0	1	0	0	0	0	0
Q96MS3	0	0	0	0	0	0	1	0
P51810	0	0	0	0	0	0	1	0
Q8WXG9	0	0	0	0	0	0	0	1
P54826	0	0	1	0	0	0	0	0
O00178	0	0	1	0	0	0	0	0
Q9BT25	0	0	0	0	1	0	0	0
Q0VDF9	1	0	0	0	0	0	0	0
Q92522	0	0	0	0	0	1	0	0
P01860	0	0	0	0	0	0	1	0
A0A0C4DH	0	0	0	1	0	0	0	0
A0A075B6S	0	0	0	0	0	0	1	0
A6NCW7	0	0	0	0	0	1	0	0
Q01968	0	0	1	0	0	0	0	0
P20592	0	0	0	0	0	0	1	0
Q13325	0	0	0	1	0	0	0	0
A0A096LNI	1	0	0	0	0	0	0	0
A0A1B0GTI	0	0	1	0	0	0	0	0
A0A024QY\	0	0	0	0	0	0	1	0
A0A087X0T	0	0	1	0	0	0	0	0
H0Y6I8	0	1	0	0	0	0	0	0
A0A087WT	1	0	0	0	0	0	0	0
M0R2X1	0	0	0	1	0	0	0	0
F8W785	0	0	0	0	0	0	0	1
B4DHN5	0	0	1	0	0	0	0	0
A0A1B0GU	0	1	0	0	0	0	0	0
G3V331	0	0	0	1	0	0	0	0
A0A075B7I	0	0	0	0	1	0	0	0
C9JZD1	0	0	0	1	0	0	0	0
H3BRW4	0	0	0	0	0	0	1	0
H3BUM4	0	1	0	0	0	0	0	0
A0A087WV	1	0	0	0	0	0	0	0
H3BND3	1	0	0	0	0	0	0	0
H7BXZ5	0	0	1	0	0	0	0	0
G3V4D9	0	0	0	1	0	0	0	0
B8ZZL3	0	0	0	1	0	0	0	0
E5RGS4	0	0	1	0	0	0	0	0
O75061-2	0	0	1	0	0	0	0	0
A0A096LPI	0	1	0	0	0	0	0	0
A0A088AW	0	1	0	0	0	0	0	0
E9PLT0	1	0	0	0	0	0	0	0
A0A1B0GV	0	1	0	0	0	0	0	0
A0A0G2JP7	1	0	0	0	0	0	0	0
A0A075B6I	0	0	0	0	0	0	1	0
E9PC87	0	0	0	0	0	1	0	0
A0A0C4DG	0	0	0	0	1	0	0	0
A0A0J9YX6	0	1	0	0	0	0	0	0
A0A0A0MC	0	0	0	1	0	0	0	0
B3KWA8	0	1	0	0	0	0	0	0
O95803-2	0	0	0	1	0	0	0	0
A0A087WX	0	0	0	0	0	0	1	0
A8MUF7	0	0	0	0	0	0	0	1
F8W943	0	0	1	0	0	0	0	0

C9J3N8	1	0	0	0	0	0	0	0
F2Z3K5	0	1	0	0	0	0	0	0
B8ZZA1	0	0	1	0	0	0	0	0
A0A087WT	0	0	1	0	0	0	0	0
A0A087WT	1	0	0	0	0	0	0	0
F5GZD9	1	0	0	0	0	0	0	0
A0A0A0MS	0	0	1	0	0	0	0	0
A8MUH2	1	0	0	0	0	0	0	0
K7EL89	0	0	1	0	0	0	0	0
E7EV59	0	0	1	0	0	0	0	0
J3KPD9	0	0	0	0	1	0	0	0
D3YTI2	0	0	0	0	0	0	0	1
B7Z2B6	0	0	1	0	0	0	0	0
E9PAQ1	0	0	0	0	1	0	0	0
J3KRV2	0	0	0	1	0	0	0	0
H0YGD4	0	0	0	0	0	1	0	0
C9J0J7	1	0	0	0	0	0	0	0
H0Y8U4	0	0	0	0	0	0	0	1
E7ES19	0	0	0	0	0	0	1	0
M0QXN5	0	0	0	0	0	0	1	0
I3L3E9	1	0	0	0	0	0	0	0
K7EIF9	0	1	0	0	0	0	0	0
A0A0A0MS	0	0	0	0	0	0	0	1
A0A0D9SFl	0	0	0	1	0	0	0	0
A0A0U1RQ	1	0	0	0	0	0	0	0
A0A1B0GTI	0	0	0	1	0	0	0	0
H3BMQ0	1	0	0	0	0	0	0	0
B1AKY9	0	0	0	0	0	0	1	0
H3BQ95	0	0	0	1	0	0	0	0
H0YE37	0	0	0	0	0	0	0	1
P51800-3	0	0	0	1	0	0	0	0
A8MZF9	0	0	0	0	0	1	0	0
A8MQ02	0	0	1	0	0	0	0	0
H7C3V3	0	0	0	0	0	0	1	0
A0A1B0GU	0	0	0	0	1	0	0	0
I3L1E7	0	0	0	0	0	0	0	1
E7ER26	0	0	0	1	0	0	0	0
H0YDB7	0	0	0	0	1	0	0	0
M0R2W9	0	0	0	0	0	0	1	0
A0A024R7E	0	1	0	0	0	0	0	0
H0YDL5	0	0	0	0	1	0	0	0
A0A0D9SG	1	0	0	0	0	0	0	0
F5GYI5	0	0	0	0	0	1	0	0
F8WF45	1	0	0	0	0	0	0	0
F5GZB0	0	0	0	0	0	1	0	0
A0A087X0F	0	0	0	0	1	0	0	0
A0A0A0MF	1	0	0	0	0	0	0	0
D6RAT2	0	1	0	0	0	0	0	0
H0Y8R3	1	0	0	0	0	0	0	0
Q07444-2	0	0	0	0	0	1	0	0
F5H1D6	0	1	0	0	0	0	0	0
J3KSR8	1	0	0	0	0	0	0	0
Q0GE19-5	0	0	1	0	0	0	0	0
F8VS81	0	0	0	0	0	0	1	0
F8VWL0	0	1	0	0	0	0	0	0
A0A0A0MF	0	0	0	1	0	0	0	0
H7C101	0	0	0	0	0	0	0	1
F8VVF8	1	0	0	0	0	0	0	0
K7EN45	0	0	0	0	0	0	1	0
F5GXJ9	1	0	0	0	0	0	0	0
B1ALK7	1	0	0	0	0	0	0	0

B7Z5R6	0	1	0	0	0	0	0	0
A0A087WY	0	0	0	0	1	0	0	0
F8WBH5	0	0	0	1	0	0	0	0
B5MCX3	0	0	1	0	0	0	0	0
C9JXD7	0	1	0	0	0	0	0	0
A0A0A0MT	1	0	0	0	0	0	0	0
A0A0D9SFS	0	0	0	1	0	0	0	0
G3V4Q5	0	0	1	0	0	0	0	0
B7Z5N5	1	0	0	0	0	0	0	0
F8W7U0	0	0	0	0	0	0	1	0
A0A0A0MC	0	0	0	0	0	0	0	1
F5H7S1	0	0	0	0	0	1	0	0
F8WCH7	0	0	0	0	1	0	0	0
K7N7D6	0	0	0	1	0	0	0	0
G3V3G0	0	0	0	0	0	1	0	0
A0A1B0GU	0	0	0	0	0	0	0	1
K7ELG9	1	0	0	0	0	0	0	0
F5H435	0	0	1	0	0	0	0	0
C9JPQ4	1	0	0	0	0	0	0	0
A8MUM1	0	0	0	1	0	0	0	0
A0A0J9YXN	0	0	0	0	1	0	0	0
G3V2W9	0	1	0	0	0	0	0	0
H7BY83	1	0	0	0	0	0	0	0
B1AQM6	0	0	0	0	1	0	0	0
A0A0A0MT	0	0	1	0	0	0	0	0
H0Y904	1	0	0	0	0	0	0	0
E7ES50	0	0	1	0	0	0	0	0
F6VX93	0	0	0	1	0	0	0	0
Q5VUA4-2	0	0	0	0	0	0	0	1
Q68CQ7-2	1	0	0	0	0	0	0	0
A0A087WV	0	0	0	0	1	0	0	0
A0A1B0GU	1	0	0	0	0	0	0	0
A0A087WZ	0	0	0	0	0	1	0	0
A0A087WU	0	0	0	0	0	0	1	0
C9JYQ9	0	0	0	0	0	0	1	0
Q6SZW1-2	0	0	0	0	1	0	0	0
C9JMQ9	0	0	0	0	0	0	1	0
D6REK3	1	0	0	0	0	0	0	0
E9PB18	0	0	0	0	0	0	1	0
B4DX60	0	0	0	0	0	0	0	1
H0Y2S9	0	0	0	1	0	0	0	0
G3V218	0	0	0	0	0	0	1	0
Q6ZMY3-4	0	0	1	0	0	0	0	0
B4DQT1	1	0	0	0	0	0	0	0
X6R717	1	0	0	0	0	0	0	0
F8W6G5	1	0	0	0	0	0	0	0
E5RHG5	0	0	1	0	0	0	0	0
E9PRC5	0	0	0	0	0	0	1	0
E9PGH5	0	0	1	0	0	0	0	0
F8WA11	0	1	0	0	0	0	0	0
K7ERA4	0	0	0	0	1	0	0	0
A0A087X1S	0	0	1	0	0	0	0	0
A0A0A0MS	0	0	0	1	0	0	0	0
K7EM46	0	0	0	0	0	1	0	0
A0A087X1F	1	0	0	0	0	0	0	0
C9JEH4	0	0	0	0	0	0	0	1
F2Z2E2	0	1	0	0	0	0	0	0
C9J7J4	0	1	0	0	0	0	0	0
A0A0C4DG	0	0	0	0	1	0	0	0
J3KRD0	0	0	1	0	0	0	0	0
Q86W56-4	0	0	0	0	1	0	0	0

H0YFE4	0	0	0	0	1	0	0	0
F8WE06	1	0	0	0	0	0	0	0
Q86Y39-2	0	0	1	0	0	0	0	0
K7EQF1	0	1	0	0	0	0	0	0
J3KR22	1	0	0	0	0	0	0	0
A0A088AW	0	1	0	0	0	0	0	0
H3BU53	1	0	0	0	0	0	0	0
H0UI80	0	0	0	0	0	0	0	1
J3KRG7	0	0	0	0	0	1	0	0
A0A087X0(	0	0	0	0	0	0	1	0
C9IZ46	0	0	0	0	0	0	0	1
J3KNJ7	0	0	0	0	1	0	0	0
A0A087WX	0	1	0	0	0	0	0	0
E9PCJ7	1	0	0	0	0	0	0	0
Q5TA05	0	0	0	0	0	0	0	1
H0YMU7	0	0	0	0	0	0	0	1
F8W925	0	0	0	0	0	0	0	1
B7Z2D2	0	0	0	1	0	0	0	0
H0Y3Y7	0	0	0	0	0	0	1	0
A0A087WT	0	0	0	0	1	0	0	0
H0YEB0	0	0	0	0	0	0	0	1
J3KRU1	1	0	0	0	0	0	0	0
A0A087WV	1	0	0	0	0	0	0	0
A0A087WZ	1	0	0	0	0	0	0	0
B8ZZ98	0	0	1	0	0	0	0	0
C9JDE6	0	0	1	0	0	0	0	0
U3KQE6	0	0	0	0	0	0	0	1
C9JSD5	0	1	0	0	0	0	0	0
C9JE27	1	0	0	0	0	0	0	0
H0Y448	0	0	0	0	1	0	0	0
A0A087WV	0	0	1	0	0	0	0	0
A0A0J9YWl	0	1	0	0	0	0	0	0
H7C0W4	0	0	0	0	0	0	0	1
K7EQS2	1	0	0	0	0	0	0	0
K7EJA9	0	1	0	0	0	0	0	0
B4DHE8	1	0	0	0	0	0	0	0
M0QYI9	0	0	1	0	0	0	0	0
H0Y9X1	1	0	0	0	0	0	0	0
K7ELQ6	0	0	0	0	0	0	0	1
H3BM29	0	0	0	0	0	1	0	0
H0YIS8	1	0	0	0	0	0	0	0
K7ESB7	0	0	0	1	0	0	0	0
E9PD99	1	0	0	0	0	0	0	0
G3V4L6	0	0	1	0	0	0	0	0
A0A087WL	0	0	1	0	0	0	0	0
H0Y7Q2	0	0	0	0	0	0	0	1
H0Y8W1	0	1	0	0	0	0	0	0
Q96KV7-3	0	0	1	0	0	0	0	0
A0A1B0GTl	0	0	0	0	1	0	0	0
E5RGX6	0	0	0	1	0	0	0	0
A0A087WT	1	0	0	0	0	0	0	0
H0Y853	0	0	0	0	0	0	0	1
E7ESL9	0	0	0	0	1	0	0	0
H0YLN8	0	0	0	1	0	0	0	0
A0A0A0M(	0	0	0	0	1	0	0	0
A0A087WV	1	0	0	0	0	0	0	0
A0A1B0GW	1	0	0	0	0	0	0	0
H3BPF6	0	0	0	0	0	0	1	0
F8W6K1	0	0	0	1	0	0	0	0
K7EIH8	0	0	1	0	0	0	0	0
F5GXW5	0	0	1	0	0	0	0	0

F5H492	0	0	1	0	0	0	0	0
A0A0A0MS	0	0	1	0	0	0	0	0
K7EIN2	0	0	1	0	0	0	0	0
A0A087WT	1	0	0	0	0	0	0	0
I3NI31	0	0	0	0	0	0	1	0
H0YCH4	0	0	1	0	0	0	0	0
A0A087WT	1	0	0	0	0	0	0	0
A0A087WV	0	0	1	0	0	0	0	0
A2A2L6	0	0	1	0	0	0	0	0
B1AQT4	1	0	0	0	0	0	0	0
A0A0D9SF2	0	1	0	0	0	0	0	0
A0A087WT	0	0	1	0	0	0	0	0
H0YL62	0	0	1	0	0	0	0	0
A0A024QZ3	1	0	0	0	0	0	0	0
A0A0B4J2F	0	0	1	0	0	0	0	0
I6L9I8	0	0	0	0	0	0	1	0
A0A087WX	0	1	0	0	0	0	0	0
B3KVZ3	1	0	0	0	0	0	0	0
A0A024R57	1	0	0	0	0	0	0	0
H3BS42	1	0	0	0	0	0	0	0
B4DHR0	1	0	0	0	0	0	0	0
A6NGY7	0	0	0	1	0	0	0	0
G3V541	0	1	0	0	0	0	0	0
A0A075B6I	0	0	0	0	1	0	0	0
A0A0A0MS	1	0	0	0	0	0	0	0
F5H3T4	0	0	0	1	0	0	0	0
A0A1B0GU	0	1	0	0	0	0	0	0
F8VUA2	0	0	0	1	0	0	0	0
Q9NPA1-5	0	0	0	0	0	1	0	0
K7ENT1	0	0	0	0	0	1	0	0
Q5T911	0	0	0	1	0	0	0	0
A0A087X2I	0	0	0	0	0	1	0	0
F8WBJ6	0	1	0	0	0	0	0	0
Q9NS73-5	1	0	0	0	0	0	0	0
A0A0B4J22	1	0	0	0	0	0	0	0
F8W7R3	0	0	1	0	0	0	0	0
H3BNW0	1	0	0	0	0	0	0	0
E9PJA7	0	1	0	0	0	0	0	0
H7BXP1	1	0	0	0	0	0	0	0
A0A087WV	0	0	1	0	0	0	0	0
A0A0G2JLV	0	0	0	1	0	0	0	0
B5ME80	0	0	0	0	0	0	0	1
H7C254	0	0	0	0	0	0	0	1
K7EK91	0	0	1	0	0	0	0	0
F5GZ56	0	1	0	0	0	0	0	0
E7EMB1	0	0	0	0	0	1	0	0
E9PGN6	0	0	0	0	0	0	0	1
Q6B8I1-3	0	0	0	0	1	0	0	0
Q5QPL9	0	0	0	0	1	0	0	0
Q9UKZ4-2	0	0	0	0	0	1	0	0
A0A087X12	0	1	0	0	0	0	0	0
A0A0C4DG	1	0	0	0	0	0	0	0
A0A087WY	0	0	0	0	0	0	0	1
A0A0J9YW	0	1	0	0	0	0	0	0
A0A0A0MF	0	0	0	1	0	0	0	0
A0A0A0MS	0	0	0	1	0	0	0	0
E7EMX0	1	0	0	0	0	0	0	0
E9PCD7	1	0	0	0	0	0	0	0
A0A0J9YYL	0	0	1	0	0	0	0	0
A0A087X12	0	1	0	0	0	0	0	0
F5H5G4	0	1	0	0	0	0	0	0

H3BNV7	0	0	0	0	0	0	1	0
D6R8Y9	0	0	0	0	0	1	0	0
A0A0U1RQ	0	0	0	0	0	0	1	0
F8VWT9	0	0	0	1	0	0	0	0
G3XAE9	0	0	0	0	1	0	0	0
C9J014	0	0	1	0	0	0	0	0
J3KPG9	0	0	0	0	0	0	1	0
E5RJA8	0	0	0	0	0	0	0	1
H3BRH0	1	0	0	0	0	0	0	0
F8VVR0	0	0	0	0	0	0	0	1
Q9HDC5	0	0	1	0	0	0	0	0
Q86V97	0	0	0	0	1	0	0	0
P59990	0	0	0	0	1	0	0	0
Q99661	0	0	0	1	0	0	0	0
P55268	1	0	0	0	0	0	0	0
Q13753	0	0	0	1	0	0	0	0
Q6P5Q4	0	0	0	0	0	1	0	0
Q5VUJ6	0	0	1	0	0	0	0	0
Q5T7N2	0	0	0	0	0	1	0	0
Q9Y4C4	0	0	0	0	0	0	0	1
Q14676	0	1	0	0	0	0	0	0
Q13255	0	0	1	0	0	0	0	0
Q6ZN28	0	0	1	0	0	0	0	0
Q8TE76	1	0	0	0	0	0	0	0
Q7Z5P9	0	0	0	0	1	0	0	0
Q9BU76	0	0	0	0	1	0	0	0
P05164	1	0	0	0	0	0	0	0
P54296	0	0	0	0	0	0	0	1
P12883	0	0	0	0	0	0	0	1
P46531	0	1	0	0	0	0	0	0
Q7Z3B1	0	0	0	0	1	0	0	0
P56730	0	0	0	1	0	0	0	0
Q96F24	0	0	1	0	0	0	0	0
Q02818	0	1	0	0	0	0	0	0
Q5C9Z4	0	0	1	0	0	0	0	0
Q7Z3B4	0	0	0	0	0	0	1	0
Q8NGR8	0	0	1	0	0	0	0	0
Q8NGI6	0	0	0	0	0	0	0	1
Q6IF36	0	0	0	0	0	0	1	0
Q13416	0	0	1	0	0	0	0	0
O43913	0	0	1	0	0	0	0	0
Q9BXB5	0	0	1	0	0	0	0	0
Q9NUG6	0	0	0	1	0	0	0	0
Q86YC2	0	1	0	0	0	0	0	0
O60346	0	0	0	1	0	0	0	0
O14939	0	0	1	0	0	0	0	0
Q3KR16	0	0	0	1	0	0	0	0
Q9BWT3	0	0	0	0	1	0	0	0
Q12837	0	0	0	1	0	0	0	0
Q495C1	1	0	0	0	0	0	0	0
O75388	0	0	0	0	1	0	0	0
Q7Z333	0	0	0	0	0	0	0	1
Q13395	0	0	1	0	0	0	0	0
O43861	0	0	0	0	1	0	0	0
Q9NY28	0	0	1	0	0	0	0	0
Q96B36	0	0	0	0	0	0	1	0
P55197	0	0	1	0	0	0	0	0
A0A0A6YYI	0	0	0	1	0	0	0	0
O43439	1	0	0	0	0	0	0	0
Q9NSV4	0	0	1	0	0	0	0	0
Q96F81	1	0	0	0	0	0	0	0

P13667	1	0	0	0	0	0	0	0
Q5QGS0	0	0	0	1	0	0	0	0
Q8NG48	0	0	0	0	0	1	0	0
P48634	0	0	1	0	0	0	0	0
Q5JSZ5	0	0	0	0	0	0	1	0
Q8N2C7	0	0	0	0	0	0	1	0
Q9GZT5	0	0	0	1	0	0	0	0
Q495N2	0	0	0	0	0	0	1	0
A6NDZ8	0	0	0	0	0	0	1	0
Q6P2S7	0	0	0	0	1	0	0	0
Q1A5X7	0	0	0	1	0	0	0	0
Q9H2M9	1	0	0	0	0	0	0	0
Q5TD94	0	0	0	0	0	1	0	0
Q9UL26	0	0	0	0	1	0	0	0
Q8NC24	0	1	0	0	0	0	0	0
Q7Z5J4	1	0	0	0	0	0	0	0
Q9C0H5	0	0	0	1	0	0	0	0
Q14684	0	0	0	0	0	1	0	0
Q14137	0	0	0	0	1	0	0	0
Q9ULX3	0	0	1	0	0	0	0	0
Q15424	1	0	0	0	0	0	0	0
P83105	0	0	0	0	0	0	0	1
Q9UQ35	0	0	0	1	0	0	0	0
O75494	1	0	0	0	0	0	0	0
Q9Y6J8	0	0	0	1	0	0	0	0
P36952	0	1	0	0	0	0	0	0
Q8IX30	0	0	0	0	1	0	0	0
Q9NRQ5	0	0	0	1	0	0	0	0
Q96PX8	0	0	1	0	0	0	0	0
O43147	0	0	0	1	0	0	0	0
Q9BQI6	1	0	0	0	0	0	0	0
Q5SXM2	0	0	1	0	0	0	0	0
Q9Y675	0	0	0	1	0	0	0	0
Q8WWX8	0	0	1	0	0	0	0	0
Q86YT5	0	0	0	0	0	0	1	0
P78524	0	0	0	1	0	0	0	0
O75159	0	0	0	0	0	1	0	0
O75940	0	1	0	0	0	0	0	0
Q9Y4R8	0	0	1	0	0	0	0	0
Q9P273	0	0	1	0	0	0	0	0
Q9BZG2	0	0	0	0	0	0	0	1
P37173	0	0	0	0	0	1	0	0
Q96EK4	1	0	0	0	0	0	0	0
Q86XW9	1	0	0	0	0	0	0	0
P30048	0	1	0	0	0	0	0	0
Q9P016	0	0	1	0	0	0	0	0
O95049	1	0	0	0	0	0	0	0
O15050	0	0	0	0	0	1	0	0
Q96RI8	0	0	0	0	0	1	0	0
P23193	1	0	0	0	0	0	0	0
O15525	0	0	1	0	0	0	0	0
O60675	0	0	1	0	0	0	0	0
P08047	1	0	0	0	0	0	0	0
P62995	0	1	0	0	0	0	0	0
Q9BX84	0	0	0	0	1	0	0	0
P17152	0	0	0	0	0	0	0	1
A2RUT3	0	0	1	0	0	0	0	0
P54577	0	0	0	1	0	0	0	0
Q96K76	0	0	0	1	0	0	0	0
Q92890	0	0	0	1	0	0	0	0
Q9UGI0	0	1	0	0	0	0	0	0

Q14CS0	0	0	0	0	1	0	0	0
P22310	0	0	1	0	0	0	0	0
A0A0U1RQ	0	1	0	0	0	0	0	0
Q6NUN7	0	0	0	0	0	0	1	0
Q8NEP4	0	1	0	0	0	0	0	0
Q8NBC4	0	0	1	0	0	0	0	0
H3BNL8	0	0	0	0	0	0	1	0
K7ENM7	0	0	0	1	0	0	0	0
B0I1T2	0	0	1	0	0	0	0	0
Q9BUW7	0	0	0	0	1	0	0	0
A8MWY0	0	0	0	0	0	0	1	0
Q9P253	1	0	0	0	0	0	0	0
Q9UID3	0	0	1	0	0	0	0	0
Q8N1B4	0	0	1	0	0	0	0	0
O75396	0	0	0	0	1	0	0	0
Q96A05	0	0	1	0	0	0	0	0
A4D1P6	0	1	0	0	0	0	0	0
Q6P2C0	0	0	0	0	0	1	0	0
O95389	0	1	0	0	0	0	0	0
Q2TBF2	0	0	0	0	0	0	1	0
Q05516	0	0	0	0	0	1	0	0
Q5SVQ8	0	0	0	0	0	1	0	0
Q68DK2	0	0	0	0	0	0	0	1
O95405	0	1	0	0	0	0	0	0
Q9UL59	0	0	0	0	0	0	1	0
P59817	0	1	0	0	0	0	0	0
Q8IYI8	0	0	0	0	1	0	0	0
Q76KX8	0	0	0	0	0	1	0	0
Q5T7W0	0	1	0	0	0	0	0	0
P17098	1	0	0	0	0	0	0	0
Q86V15	0	0	0	0	1	0	0	0
O95409	0	0	0	1	0	0	0	0
Q9UPR6	0	1	0	0	0	0	0	0
A7E2V4	1	0	0	0	0	0	0	0
Q8TAD4	0	1	0	0	0	0	0	0
Q8TCW7	0	0	0	0	0	0	0	1

Appendix B

All Protein IDs from PhAXA-MS with ERK2 as Bait

PROTID	rnERK2 (WT) + 1	rnERK2 (WT) ATP ctl	rnERK2 (Y185C) + 1	rnERK2 (Y185C) ATP ctl	rnERK2 (WT) + 1	rnERK2 (WT) ATP ctl	rnERK2 (Y185C) + 1	rnERK2 (Y185C) ATP ctl	rnERK2 (WT) + 1	rnERK2 (WT) ATP ctl	rnERK2 (Y185C) + 1	rnERK2 (Y185C) ATP ctl
P28482	633	624	536	529	1951	2145	1499	1507	1292	1384.5	1017.5	1018
O14744	63	58	64	63	258	295	243	264	160.5	176.5	153.5	163.5
Q9BQA1	51	58	56	66	161	189	178	211	106	123.5	117	138.5
P78347	67	55	62	51	129	141	150	143	98	98	106	97
TRYP_PIG	46	48	43	45	153	179	158	167	99.5	113.5	100.5	106
P51812	38	36	33	8	141	190	144	40	89.5	113	88.5	24
P68363	30	17	43	19	103	85	131	61	66.5	51	87	40
P07437	25	18	20	20	92	84	130	85	58.5	51	75	52.5
P68104	11	6	18	8	80	70	111	68	45.5	38	64.5	38
Q99956	16	3	25	2	82	23	94	27	49	13	59.5	14.5
P49327	9	1	21	3	31	11	74	17	20	6	47.5	10
P12268	21	0	17	0	88	0	67	0	54.5	0	42	0
G8JLB6	10	0	17	7	33	23	66	16	21.5	11.5	41.5	11.5
E9PGT3	16	19	18	0	82	70	60	10	49	44.5	39	5
Q15208	4	6	12	8	60	68	65	60	32	37	38.5	34
P61978	4	5	10	1	39	22	67	22	21.5	13.5	38.5	11.5
P50990	23	19	18	18	57	63	58	57	40	41	38	37.5
P48643	18	12	15	10	48	56	61	62	33	34	38	36
P78371	15	9	14	7	61	62	61	50	38	35.5	37.5	28.5
P17987	18	13	20	16	53	51	54	45	35.5	32	37	30.5
P52597	6	2	13	2	29	14	49	6	17.5	8	31	4
P04264	30	20	22	30	51	28	38	45	40.5	24	30	37.5
Q99832	15	10	15	5	46	41	45	52	30.5	25.5	30	28.5
Q9UK32	3	2	5	6	30	12	53	6	16.5	7	29	6
O75582	7	0	17	0	26	1	40	1	16.5	0.5	28.5	0.5
P11142	5	2	8	6	39	18	44	18	22	10	26	12
H3BLZ8	0	1	1	1	34	2	48	2	17	1.5	24.5	1.5
Q15393	13	12	12	9	33	33	36	40	23	22.5	24	24.5
P78527	16	4	12	0	60	23	35	20	38	13.5	23.5	10
Q13162	8	8	10	12	41	57	36	63	24.5	32.5	23	37.5
A0A0J9YVP	12	5	9	5	21	23	35	19	16.5	14	22	12
P13645	23	13	21	28	44	10	19	19	33.5	11.5	20	23.5
P68371	0	0	0	0	70	45	39	8	35	22.5	19.5	4
P40227	7	3	4	6	36	36	35	28	21.5	19.5	19.5	17
P49368	9	7	8	6	27	23	31	24	18	15	19.5	15
Q16531	11	5	9	6	19	11	29	12	15	8	19	9
P13639	8	6	9	5	22	10	29	7	15	8	19	6
Q7Z3B4	1	0	1	0	13	0	37	0	7	0	19	0
P54886	0	0	11	0	0	0	27	0	0	0	19	0
Q9BVA1	1	0	5	3	18	14	32	10	9.5	7	18.5	6.5
Q13435	5	2	4	2	20	15	33	20	12.5	8.5	18.5	11
P60709	11	3	10	1	23	15	26	9	17	9	18	5
ALBU_BOV	21	21	17	20	13	15	18	9	17	18	17.5	14.5
Q15365	4	2	9	4	20	27	26	17	12	14.5	17.5	10.5
Q14204	14	13	13	15	21	36	21	32	17.5	24.5	17	23.5
Q9BYB4	9	0	10	0	27	0	24	0	18	0	17	0
Q9BQE3	7	5	2	5	37	16	31	25	22	10.5	16.5	15
P50991	2	2	3	2	22	17	30	24	12	9.5	16.5	13
Q9UJ70	8	0	7	0	42	0	26	0	25	0	16.5	0
Q15029	8	1	11	5	16	7	22	9	12	4	16.5	7
A0A0G2JIW	6	0	6	2	21	3	26	8	13.5	1.5	16	5
Q07666	0	0	3	0	8	0	29	0	4	0	16	0
A0A087WT	1	1	5	0	14	3	26	2	7.5	2	15.5	1

O75676	2	0	4	0	14	1	27	1	8	0.5	15.5	0.5
A0A0A0MF	11	9	4	5	23	27	26	50	17	18	15	27.5
P21333	0	1	0	0	23	22	30	33	11.5	11.5	15	16.5
P52564	6	0	5	0	35	0	25	0	20.5	0	15	0
Q15637-6	0	0	3	0	17	13	27	10	8.5	6.5	15	5
A0A087WT	2	1	4	2	17	8	26	6	9.5	4.5	15	4
PRDX1_HU	7	8	8	11	13	20	21	36	10	14	14.5	23.5
O75643	1	0	3	0	27	17	26	9	14	8.5	14.5	4.5
Q6P2Q9	8	6	10	5	18	7	19	7	13	6.5	14.5	6
P55072	12	10	10	6	29	24	18	27	20.5	17	14	16.5
Q0VDG4	4	4	3	4	21	26	25	23	12.5	15	14	13.5
P50548	1	0	6	0	12	7	22	3	6.5	3.5	14	1.5
P08238	9	3	9	3	11	3	18	5	10	3	13.5	4
Q9P258	2	0	5	0	4	0	22	0	3	0	13.5	0
E9PB61	2	3	3	3	29	27	23	23	15.5	15	13	13
P35527	9	15	14	7	13	11	12	17	11	13	13	12
H3BSW6	7	0	4	0	23	0	22	0	15	0	13	0
F6VRR5	0	0	2	1	22	30	23	35	11	15	12.5	18
O60701	2	0	3	0	10	0	22	0	6	0	12.5	0
P49137	1	1	4	0	7	0	21	0	4	0.5	12.5	0
Q15121	0	0	4	0	6	0	20	0	3	0	12	0
P55795	0	5	8	0	4	3	15	0	2	4	11.5	0
B0QY89	5	7	6	6	17	20	17	19	11	13.5	11.5	12.5
Q9UMS4	8	3	3	2	18	16	20	15	13	9.5	11.5	8.5
O75533	2	1	1	0	18	13	22	22	10	7	11.5	11
H7BYF2	0	0	1	0	9	0	22	0	4.5	0	11.5	0
P04350	3	7	15	0	0	0	7	8	1.5	3.5	11	4
F5H2F4	5	1	8	1	12	1	14	1	8.5	1	11	1
P09874	0	0	1	0	21	0	21	0	10.5	0	11	0
Q8WUA2	0	0	5	0	2	0	17	0	1	0	11	0
Q15366-2	0	0	4	0	11	2	17	3	5.5	1	10.5	1.5
Q15233	3	0	1	0	28	8	19	4	15.5	4	10	2
F8VPD4	2	1	5	1	11	9	15	2	6.5	5	10	1.5
Q13263	2	3	8	0	4	0	12	1	3	1.5	10	0.5
P35908	12	10	13	31	24	2	6	8	18	6	9.5	19.5
P60228	7	5	5	5	16	14	14	15	11.5	9.5	9.5	10
A0A087WV	3	8	7	6	15	16	12	15	9	12	9.5	10.5
Q16829	0	0	4	0	6	1	15	1	3	0.5	9.5	0.5
E7EX17	7	2	5	1	14	11	14	11	10.5	6.5	9.5	6
Q15750	3	4	6	2	13	10	12	7	8	7	9	4.5
F8W6I7	4	1	1	1	17	11	17	9	10.5	6	9	5
Q8WWY3	1	0	3	0	10	9	15	12	5.5	4.5	9	6
P04406	4	1	4	0	13	5	14	4	8.5	3	9	2
Q96K76	2	0	6	0	8	0	12	0	5	0	9	0
Q8NC51	2	0	4	0	6	0	14	1	4	0	9	0.5
O00303	4	3	5	5	12	10	12	11	8	6.5	8.5	8
A0A087WV	6	7	9	5	6	8	8	10	6	7.5	8.5	7.5
P30041	6	4	5	6	12	10	11	25	9	7	8	15.5
P84090	3	1	5	1	13	13	11	9	8	7	8	5
Q13200	3	1	5	2	12	9	11	10	7.5	5	8	6
O43143	1	0	1	0	12	8	15	6	6.5	4	8	3
P67775	2	0	5	1	5	0	11	0	3.5	0	8	0.5
A0A0U1RR	1	0	4	0	4	0	12	0	2.5	0	8	0
O43823	0	1	4	1	4	1	12	0	2	1	8	0.5
A0A0R4J2E	2	0	5	0	2	0	11	0	2	0	8	0
P07900	7	0	3	3	7	4	12	5	7	2	7.5	4
B5ME19	8	1	5	3	11	8	10	14	9.5	4.5	7.5	8.5
P61163	4	2	4	1	10	7	11	12	7	4.5	7.5	6.5
H0Y8C6	8	1	4	0	21	2	11	2	14.5	1.5	7.5	1
E9PM69	2	2	3	2	13	5	12	8	7.5	3.5	7.5	5
P11021	1	2	0	1	12	10	15	7	6.5	6	7.5	4

J3KTA4	2	1	4	1	4	0	11	0	3	0.5	7.5	0.5
P22102	0	0	2	1	7	2	13	2	3.5	1	7.5	1.5
O15371	2	0	5	0	0	2	10	3	1	1	7.5	1.5
Q9BUB5	0	0	2	0	8	0	13	0	4	0	7.5	0
E9PMI6	6	1	4	4	12	10	10	12	9	5.5	7	8
A0A075B6S	4	3	2	2	12	10	12	11	8	6.5	7	6.5
Q13347	5	5	6	1	7	7	8	8	6	6	7	4.5
Q14011	2	2	6	5	7	9	8	11	4.5	5.5	7	8
Q9NQW7-3	5	0	2	0	31	0	12	0	18	0	7	0
P35998	3	1	4	1	6	7	10	7	4.5	4	7	4
M0QXS5	4	0	5	0	9	1	9	1	6.5	0.5	7	0.5
C9JIR6	3	0	3	1	3	4	11	1	3	2	7	1
P37198	0	0	1	0	6	0	13	0	3	0	7	0
P52272	0	0	3	0	6	0	11	0	3	0	7	0
Q09028	0	2	0	3	13	13	13	16	6.5	7.5	6.5	9.5
P43686	1	2	2	2	10	9	11	10	5.5	5.5	6.5	6
Q9Y657	3	2	3	2	8	8	10	9	5.5	5	6.5	5.5
A0A087X2I	2	1	2	0	11	7	11	10	6.5	4	6.5	5
Q12874	2	3	5	3	6	9	8	5	4	6	6.5	4
H0YEN5	5	0	4	0	4	1	9	3	4.5	0.5	6.5	1.5
P22626	3	0	3	1	12	3	9	0	7.5	1.5	6	0.5
P30153	4	1	2	0	8	0	10	0	6	0.5	6	0
P15170-2	4	0	5	1	4	0	7	0	4	0	6	0.5
P25205	4	0	4	0	6	0	8	1	5	0	6	0.5
Q8WUM4	1	0	1	0	5	0	11	0	3	0	6	0
Q8IWX8	0	0	0	0	4	0	12	0	2	0	6	0
Q5T7U1	1	0	5	0	2	0	7	0	1.5	0	6	0
Q5QPM7	0	0	4	0	2	0	8	0	1	0	6	0
P62937	6	2	3	5	8	8	8	9	7	5	5.5	7
E9PBS1	6	1	3	0	3	1	8	1	4.5	1	5.5	0.5
A0A0A0MS	3	0	4	0	6	1	7	0	4.5	0.5	5.5	0
K9J957	1	0	2	0	2	0	9	0	1.5	0	5.5	0
A0A0D9SF5	2	0	2	0	0	0	9	0	1	0	5.5	0
Q96I24	0	0	1	0	6	0	10	0	3	0	5.5	0
O15042	0	0	0	0	1	0	11	0	0.5	0	5.5	0
E9PC52	4	2	3	3	4	4	7	2	4	3	5	2.5
A0A087WZ	1	2	3	2	13	8	7	5	7	5	5	3.5
P23284	0	0	0	0	10	11	10	9	5	5.5	5	4.5
P62316	2	3	2	2	6	4	8	8	4	3.5	5	5
O60506	2	1	2	1	16	2	8	0	9	1.5	5	0.5
D6RG13	4	1	2	2	4	4	8	5	4	2.5	5	3.5
P98179	2	2	4	2	4	3	6	3	3	2.5	5	2.5
Q9HBH9	0	0	2	0	4	0	8	5	2	0	5	2.5
P49643	2	0	3	0	3	0	7	0	2.5	0	5	0
P63151	0	0	1	0	5	0	9	0	2.5	0	5	0
Q9BRS2	2	0	4	0	2	0	6	0	2	0	5	0
Q12906	0	0	0	0	4	0	10	0	2	0	5	0
Q15417	1	0	3	0	2	0	7	1	1.5	0	5	0.5
F8W726	0	0	0	0	3	0	10	0	1.5	0	5	0
Q9Y5X1	0	0	4	0	0	0	6	0	0	0	5	0
Q9BUF5	0	0	1	0	2	0	8	5	1	0	4.5	2.5
A0A0J9YXJ	0	5	9	5	21	23	0	19	10.5	14	4.5	12
P62195	3	1	2	2	14	12	7	11	8.5	6.5	4.5	6.5
Q9Y2H1	1	0	0	0	7	2	9	7	4	1	4.5	3.5
Q7L2H7	3	5	2	3	7	8	7	7	5	6.5	4.5	5
Q01804	1	0	0	0	4	9	9	18	2.5	4.5	4.5	9
J3QLE5	3	1	1	0	8	11	8	6	5.5	6	4.5	3
P55884	0	1	1	0	7	9	8	12	3.5	5	4.5	6
Q7RTV0	3	3	3	2	8	5	6	5	5.5	4	4.5	3.5
Q9Y230	3	2	5	2	6	4	4	4	4.5	3	4.5	3
P62318	1	2	3	3	5	5	6	4	3	3.5	4.5	3.5

P23246	1	0	0	0	13	2	9	1	7	1	4.5	0.5
P53618	1	1	1	1	6	3	8	5	3.5	2	4.5	3
Q00839	4	0	2	0	5	3	7	5	4.5	1.5	4.5	2.5
P10599	3	2	2	1	7	1	7	2	5	1.5	4.5	1.5
A0A087WT	1	0	2	0	6	5	7	4	3.5	2.5	4.5	2
Q96GM8	0	0	1	0	16	0	8	0	8	0	4.5	0
Q5THR1	7	1	8	1	3	2	1	2	5	1.5	4.5	1.5
O00487	1	2	5	1	4	1	4	2	2.5	1.5	4.5	1.5
F5H4R6	1	0	0	1	5	2	9	3	3	1	4.5	2
P19338	1	0	2	0	5	2	7	2	3	1	4.5	1
P53396	2	0	2	0	6	0	7	0	4	0	4.5	0
P61962	0	0	1	1	4	1	8	2	2	0.5	4.5	1.5
P41162	0	0	2	0	3	0	7	0	1.5	0	4.5	0
P36507	1	0	3	0	2	0	6	0	1.5	0	4.5	0
Q14247	0	0	0	0	0	0	9	0	0	0	4.5	0
O14613	0	0	1	0	0	0	8	0	0	0	4.5	0
F2Z2J1	1	5	6	2	8	12	2	2	4.5	8.5	4	2
Q13561	2	2	1	1	9	10	7	11	5.5	6	4	6
P62191	2	3	2	2	7	9	6	5	4.5	6	4	3.5
Q9BUA3	3	2	3	3	6	7	5	5	4.5	4.5	4	4
B1ALA9	0	0	2	0	1	6	6	11	0.5	3	4	5.5
P25398	3	1	1	1	3	3	7	3	3	2	4	2
A0A087WZ	1	1	4	2	4	3	4	3	2.5	2	4	2.5
E9PL09	2	1	2	0	6	3	6	1	4	2	4	0.5
Q86X55	4	0	5	0	4	0	3	0	4	0	4	0
J3QRG6	1	0	2	1	4	0	6	1	2.5	0	4	1
B8ZZU8	1	1	4	0	3	2	4	0	2	1.5	4	0
P31689	1	0	2	0	4	1	6	0	2.5	0.5	4	0
Q14974	0	0	2	1	4	0	6	1	2	0	4	1
Q92598	3	0	4	0	1	0	4	0	2	0	4	0
Q9NP73	1	0	4	2	2	0	4	0	1.5	0	4	1
A2RQR6	1	0	2	0	3	0	6	0	2	0	4	0
I3L2N2	0	0	2	0	3	0	6	0	1.5	0	4	0
Q96HA7	0	0	2	1	0	0	6	2	0	0	4	1.5
P55265	0	0	2	0	2	0	6	0	1	0	4	0
C9J0I9	0	0	3	0	0	0	5	0	0	0	4	0
P49366	13	4	2	7	36	43	5	32	24.5	23.5	3.5	19.5
P11802	5	0	4	2	4	0	3	0	4.5	0	3.5	1
Q13547	2	5	5	4	3	3	2	2	2.5	4	3.5	3
P09661	1	1	1	3	5	3	6	6	3	2	3.5	4.5
O00231	5	2	4	0	4	3	3	4	4.5	2.5	3.5	2
E5RJR5	4	2	3	1	4	3	4	3	4	2.5	3.5	2
H3BNT7	1	1	2	1	6	3	5	4	3.5	2	3.5	2.5
Q9BWJ5	0	1	3	1	4	4	4	3	2	2.5	3.5	2
E9PK25	2	1	3	3	3	2	4	1	2.5	1.5	3.5	2
P62979	2	0	2	0	3	3	5	3	2.5	1.5	3.5	1.5
Q16644	1	1	0	0	8	0	7	0	4.5	0.5	3.5	0
Q96J01	2	1	3	2	2	1	4	1	2	1	3.5	1.5
P13010	1	0	2	0	5	1	5	1	3	0.5	3.5	0.5
O14654	0	0	0	0	3	2	7	0	1.5	1	3.5	0
P05412	0	0	1	0	4	0	6	0	2	0	3.5	0
O00743	0	0	2	0	3	0	5	0	1.5	0	3.5	0
E7EPP6	0	0	0	0	2	0	7	0	1	0	3.5	0
Q9ULX6	0	0	1	0	0	0	6	0	0	0	3.5	0
P27694	2	0	0	0	7	8	6	7	4.5	4	3	3.5
Q9NPA8	2	1	1	2	9	5	5	4	5.5	3	3	3
P35244	2	2	1	1	6	5	5	6	4	3.5	3	3.5
K7ERF1	3	2	3	1	6	3	3	4	4.5	2.5	3	2.5
J3QLI9	1	0	0	0	7	4	6	6	4	2	3	3
Q9Y265	1	1	1	0	6	5	5	3	3.5	3	3	1.5
P55036	1	0	2	0	4	4	4	6	2.5	2	3	3

B7Z6Z4	1	1	3	1	5	3	3	3	3	2	3	2
P63167	0	0	0	1	6	3	6	2	3	1.5	3	1.5
E9PD53	0	0	0	0	2	3	6	6	1	1.5	3	3
P06748	3	0	1	0	5	1	5	1	4	0.5	3	0.5
P17858	2	0	3	0	3	1	3	0	2.5	0.5	3	0
Q9C0B7	3	0	3	0	6	0	3	0	4.5	0	3	0
E9PKG1	2	1	1	0	3	1	5	2	2.5	1	3	1
P62701	0	0	1	1	3	2	5	2	1.5	1	3	1.5
Q86XN8	1	0	1	0	5	2	5	0	3	1	3	0
P14618	4	1	2	1	1	0	4	0	2.5	0.5	3	0.5
Q5JVS0	1	0	1	0	5	0	5	0	3	0	3	0
Q7Z7A3	0	0	0	0	5	0	6	0	2.5	0	3	0
E5RHG8	0	0	0	0	4	0	6	0	2	0	3	0
B1AHB1	1	0	3	1	0	0	3	1	0.5	0	3	1
Q96D09	0	0	0	0	2	0	6	0	1	0	3	0
Q9ULW0	0	0	0	0	1	0	6	0	0.5	0	3	0
P11413	0	0	4	0	1	0	2	0	0.5	0	3	0
H3BR83	0	0	1	0	1	0	5	0	0.5	0	3	0
Q9P215	0	0	1	0	1	0	5	0	0.5	0	3	0
O60678	0	0	1	0	0	0	5	0	0	0	3	0
A0A087WV	0	0	2	0	0	0	4	0	0	0	3	0
Q14008	0	0	0	0	0	0	6	0	0	0	3	0
E9PKF6	0	0	0	0	0	0	6	0	0	0	3	0
Q14152	1	0	0	1	3	5	5	9	2	2.5	2.5	5
P49458	2	2	2	1	4	3	3	4	3	2.5	2.5	2.5
Q9Y6Y0	2	2	4	3	1	4	1	3	1.5	3	2.5	3
P48556	1	2	2	0	3	4	3	2	2	3	2.5	1
J3KT73	0	1	0	0	2	5	5	4	1	3	2.5	2
Q15008	1	0	1	1	3	4	4	2	2	2	2.5	1.5
P06733	2	1	0	1	2	1	5	3	2	1	2.5	2
P45985	3	0	1	0	7	0	4	0	5	0	2.5	0
P63241	1	2	0	0	3	2	5	2	2	2	2.5	1
F2Z2I2	5	0	3	0	4	0	2	1	4.5	0	2.5	0.5
O95163	0	0	0	0	8	0	5	0	4	0	2.5	0
O43318	0	0	0	0	2	2	5	1	1	1	2.5	0.5
A0A0U1RQ	0	0	1	0	2	1	4	4	1	0.5	2.5	2
P12277	2	1	1	1	1	0	4	1	1.5	0.5	2.5	1
P00492	2	1	3	0	1	1	2	0	1.5	1	2.5	0
B1AHC9	1	0	2	0	2	1	3	1	1.5	0.5	2.5	0.5
P46109	1	0	3	0	4	0	2	0	2.5	0	2.5	0
Q93008	1	0	2	0	4	0	3	0	2.5	0	2.5	0
Q96DI7	0	0	0	0	2	3	5	0	1	1.5	2.5	0
P43246	0	0	0	0	3	0	5	0	1.5	0	2.5	0
Q9Y4E8	0	0	4	0	1	0	1	0	0.5	0	2.5	0
B4DY09	0	0	2	0	2	0	3	1	1	0	2.5	0.5
A0A0X1KG	1	0	1	0	1	0	4	0	1	0	2.5	0
P60174	0	0	1	0	0	0	4	1	0	0	2.5	0.5
E7EU96	0	0	0	0	1	0	5	0	0.5	0	2.5	0
Q08J23	1	0	1	0	0	0	4	0	0.5	0	2.5	0
E9PM92	0	0	1	0	0	0	4	0	0	0	2.5	0
F8W7U8	0	0	0	0	0	0	5	0	0	0	2.5	0
Q96F86	0	0	1	0	0	0	4	0	0	0	2.5	0
Q96I25	0	0	0	0	0	0	5	0	0	0	2.5	0
Q9BWF3	0	0	2	0	0	0	3	0	0	0	2.5	0
Q9H2U1	0	0	0	1	11	26	4	23	5.5	13	2	12
Q92576	1	0	0	0	8	16	4	9	4.5	8	2	4.5
P32119	3	2	2	3	4	5	2	17	3.5	3.5	2	10
O43242	3	3	1	4	3	4	3	8	3	3.5	2	6
P46734	2	0	1	0	8	0	3	0	5	0	2	0
Q92616	9	0	1	0	14	0	3	0	11.5	0	2	0
O60307	0	0	1	0	0	4	3	0	0	2	2	0

O95347	1	0	0	1	5	7	4	4	3	3.5	2	2.5
Q9Y3B4	1	1	0	2	3	6	4	4	2	3.5	2	3
P47813	0	0	0	1	6	6	4	4	3	3	2	2.5
J3QRS3	3	3	2	1	4	2	2	3	3.5	2.5	2	2
Q92769	1	0	0	1	0	0	4	2	0.5	0	2	1.5
P24666	4	6	3	4	0	1	1	0	2	3.5	2	2
P62304	0	0	1	0	4	4	3	3	2	2	2	1.5
P15927	0	0	1	1	4	4	3	3	2	2	2	2
A8MWD9	0	1	1	1	2	3	3	1	1	2	2	1
O43809	0	0	0	0	8	0	4	0	4	0	2	0
P62913	1	1	0	0	2	2	4	2	1.5	1.5	2	1
O00232	1	0	0	1	1	1	4	3	1	0.5	2	2
Q14562	0	0	1	0	1	0	3	0	0.5	0	2	0
Q9UBB9	2	1	3	0	0	0	1	3	1	0.5	2	1.5
P62310	1	0	1	1	2	1	3	1	1.5	0.5	2	1
Q92900	0	0	1	0	1	0	3	0	0.5	0	2	0
Q9BQ67	3	0	3	0	1	0	1	0	2	0	2	0
G5E9A6	0	0	1	0	3	0	3	0	1.5	0	2	0
O14929	1	0	0	0	2	0	4	0	1.5	0	2	0
O15294	0	0	1	1	0	0	3	2	0	0	2	1.5
P22314	1	0	2	1	1	0	2	0	1	0	2	0.5
Q6PJG6	1	0	1	0	2	0	3	0	1.5	0	2	0
A0A1C7CYX	0	0	0	0	1	1	4	1	0.5	0.5	2	0.5
P26368	1	0	3	0	1	0	1	0	1	0	2	0
P0DN76	0	0	1	0	2	0	3	0	1	0	2	0
P26641	2	0	2	0	0	0	2	0	1	0	2	0
H0Y8G5	0	0	0	0	2	0	4	0	1	0	2	0
I1E4Y6	0	0	0	0	2	0	4	0	1	0	2	0
Q9NPD3	0	0	2	0	2	0	2	0	1	0	2	0
Q04864	0	1	1	0	1	0	3	0	0.5	0.5	2	0
P19623	1	0	1	0	0	0	3	0	0.5	0	2	0
A0A087WV	0	0	2	0	1	0	2	0	0.5	0	2	0
P17482	0	0	0	0	1	0	4	0	0.5	0	2	0
P28562	0	0	1	0	1	0	3	0	0.5	0	2	0
Q13868	1	0	1	0	0	0	3	0	0.5	0	2	0
A0A087X28	0	0	1	0	1	0	3	0	0.5	0	2	0
K7EP90	0	0	1	0	1	0	3	0	0.5	0	2	0
Q9Y3F4	1	0	2	0	0	0	2	0	0.5	0	2	0
O15355	0	0	2	0	1	0	2	0	0.5	0	2	0
Q96HR8	0	0	2	0	1	0	2	0	0.5	0	2	0
P49757	0	0	0	0	0	0	4	0	0	0	2	0
Q93009	0	0	1	0	0	0	3	0	0	0	2	0
P08779	9	3	0	3	2	0	3	1	5.5	1.5	1.5	2
P02533	3	3	0	3	2	0	3	1	2.5	1.5	1.5	2
TRY1_BOVI	1	1	1	2	4	4	2	3	2.5	2.5	1.5	2.5
B0YIW6	0	0	0	0	4	4	3	4	2	2	1.5	2
P05204	0	0	0	0	3	4	3	2	1.5	2	1.5	1
B1AKR6	0	0	0	0	4	4	3	1	2	2	1.5	0.5
H0Y720	0	0	0	0	1	5	3	3	0.5	2.5	1.5	1.5
P01859	1	0	1	1	2	2	2	2	1.5	1	1.5	1.5
P20839	2	0	1	0	6	0	2	0	4	0	1.5	0
E7EW58	1	0	0	0	0	3	3	3	0.5	1.5	1.5	1.5
Q13409	0	0	1	1	2	2	2	2	1	1	1.5	1.5
A0A0A0MS	0	0	1	1	1	3	2	2	0.5	1.5	1.5	1.5
G5E9W3	2	0	1	0	2	1	2	1	2	0.5	1.5	0.5
B0YJC4	1	0	1	1	2	1	2	1	1.5	0.5	1.5	1
P35606	1	2	0	1	0	0	3	2	0.5	1	1.5	1.5
P63104	2	0	0	0	0	0	3	1	1	0	1.5	0.5
F5GX77	0	1	1	0	1	2	2	2	0.5	1.5	1.5	1
H7C0N4	0	0	0	0	2	3	3	1	1	1.5	1.5	0.5
P81605	0	1	1	1	2	1	2	1	1	1	1.5	1

GSTP1_HUI	0	1	2	0	0	2	1	2	0	1.5	1.5	1
P05387	2	1	1	0	1	1	2	0	1.5	1	1.5	0
E7ERL0	3	0	3	0	1	1	0	0	2	0.5	1.5	0
A0A024QZI	0	0	1	0	0	0	2	0	0	0	1.5	0
P49642	0	0	1	1	4	0	2	0	2	0	1.5	0.5
A1L020	1	0	1	0	2	0	2	0	1.5	0	1.5	0
O43175	1	0	2	0	2	1	1	0	1.5	0.5	1.5	0
O43719	0	0	1	0	2	1	2	1	1	0.5	1.5	0.5
J3KNN5	2	0	2	0	0	1	1	0	1	0.5	1.5	0
Q9Y3I0	0	0	0	0	2	1	3	0	1	0.5	1.5	0
O60884	0	0	1	0	1	0	2	0	0.5	0	1.5	0
D6RBW1	1	1	2	0	0	1	1	0	0.5	1	1.5	0
P08237	0	0	0	0	1	0	3	0	0.5	0	1.5	0
J3KT12	1	0	1	0	2	0	2	0	1.5	0	1.5	0
Q9H7S9	1	0	0	0	1	1	3	0	1	0.5	1.5	0
J3KQ32	1	1	2	1	0	0	1	0	0.5	0.5	1.5	0.5
A0A087X2I	0	0	1	0	1	1	2	1	0.5	0.5	1.5	0.5
P42285	0	0	0	0	1	1	3	0	0.5	0.5	1.5	0
P85037	1	0	0	0	1	0	3	0	1	0	1.5	0
Q5T6F2	0	0	0	0	1	1	3	0	0.5	0.5	1.5	0
Q8ND56	0	0	1	0	2	0	2	0	1	0	1.5	0
J3KR97	0	0	0	0	2	0	3	0	1	0	1.5	0
P62241	0	0	0	0	0	1	3	1	0	0.5	1.5	0.5
Q9HAV4	0	0	1	0	1	0	2	0	0.5	0	1.5	0
P08243	0	0	0	0	1	0	3	0	0.5	0	1.5	0
Q01813	0	0	3	0	0	0	0	0	0	0	1.5	0
A0A0A0MF	0	0	0	0	1	0	3	0	0.5	0	1.5	0
P26196	0	0	0	0	1	0	3	0	0.5	0	1.5	0
Q6P2H3	0	0	1	0	1	0	2	0	0.5	0	1.5	0
Q96PK6	0	0	0	0	1	0	3	0	0.5	0	1.5	0
D6R9Z6	0	1	0	0	0	0	3	0	0	0.5	1.5	0
O75792	0	0	0	0	0	0	3	0	0	0	1.5	0
A0A0A0MT	0	0	0	0	0	0	3	0	0	0	1.5	0
P23921	0	0	0	0	0	0	3	0	0	0	1.5	0
E7EVA0	0	0	0	0	0	0	3	0	0	0	1.5	0
A0A087WL	0	0	0	0	0	0	3	0	0	0	1.5	0
P42166	0	0	0	0	0	0	3	0	0	0	1.5	0
D3YTB5	0	0	0	0	0	0	3	0	0	0	1.5	0
Q6P158	0	0	1	0	0	0	2	0	0	0	1.5	0
E9PQA6	0	0	0	0	0	0	3	0	0	0	1.5	0
F5H442	0	0	1	0	0	0	2	0	0	0	1.5	0
Q9BRP1	0	0	1	0	0	0	2	0	0	0	1.5	0
E9PN81	0	0	0	0	0	0	3	0	0	0	1.5	0
H0YDQ8	0	0	0	0	0	0	3	0	0	0	1.5	0
Q96RG2	0	0	0	0	0	0	3	0	0	0	1.5	0
P68032	1	3	1	1	1	1	1	1	1	2	1	1
P13647	3	1	2	2	2	0	0	1	2.5	0.5	1	1.5
O43390	2	0	0	1	0	2	2	2	1	1	1	1.5
Q96GX5	0	0	0	0	2	1	2	1	1	0.5	1	0.5
P01033	0	0	0	0	3	5	2	3	1.5	2.5	1	1.5
P19474	4	1	2	1	1	2	0	1	2.5	1.5	1	1
Q15427	0	0	0	0	3	4	2	3	1.5	2	1	1.5
A0A087WL	1	0	1	1	3	3	1	2	2	1.5	1	1.5
O60814	2	0	0	0	0	1	2	1	1	0.5	1	0.5
Q08499-12	1	0	0	0	1	3	2	4	1	1.5	1	2
O94952	1	1	2	3	0	0	0	0	0.5	0.5	1	1.5
Q5H9B5	0	0	0	0	0	0	2	3	0	0	1	1.5
Q9H6R7	0	1	0	0	1	4	2	1	0.5	2.5	1	0.5
Q9Y383	2	0	0	1	1	2	2	1	1.5	1	1	1
P52907	1	0	0	2	3	0	2	0	2	0	1	1
Q15428	0	0	0	0	2	2	2	2	1	1	1	1

P14174	0	1	0	0	2	2	2	1	1	1.5	1	0.5
Q9P2P6	0	0	0	0	2	2	2	2	1	1	1	1
Q8NBS9	0	0	0	0	1	1	2	4	0.5	0.5	1	2
A0A024RA5	0	0	0	0	2	3	2	0	1	1.5	1	0
Q99459	0	0	0	0	2	1	2	2	1	0.5	1	1
P35813	0	0	2	1	0	0	0	0	0	0	1	0.5
A0A0U1RR	0	1	0	0	1	1	2	1	0.5	1	1	0.5
P31153	0	0	0	1	3	0	2	0	1.5	0	1	0.5
C9JD84	0	0	0	0	1	1	2	2	0.5	0.5	1	1
O60573	1	0	0	0	2	0	2	0	1.5	0	1	0
B8ZZA1	2	1	1	0	0	0	1	0	1	0.5	1	0
P49902	0	0	1	0	3	0	1	0	1.5	0	1	0
P67809	1	1	1	0	0	1	1	0	0.5	1	1	0
F5H6X6	1	0	0	0	1	0	2	1	1	0	1	0.5
Q15021	0	0	0	0	1	0	2	2	0.5	0	1	1
Q8N684	0	0	1	0	3	0	1	0	1.5	0	1	0
P56545	1	0	1	0	2	0	1	0	1.5	0	1	0
H0YN81	0	0	2	0	1	1	0	1	0.5	0.5	1	0.5
Q8WTR2	0	0	0	0	1	0	2	1	0.5	0	1	0.5
Q9UHV9	0	0	0	0	0	1	2	1	0	0.5	1	0.5
F2Z2W6	0	0	0	0	1	1	2	0	0.5	0.5	1	0
H7BYH4	1	0	0	0	0	1	2	0	0.5	0.5	1	0
P0DN79	0	0	0	0	1	1	2	0	0.5	0.5	1	0
E9PMD7	0	0	2	0	2	0	0	0	1	0	1	0
P12004	1	0	0	0	1	0	2	0	1	0	1	0
Q02878	2	0	0	0	0	0	2	0	1	0	1	0
A0A024QZX	1	0	0	0	1	0	2	0	1	0	1	0
Q15717	1	1	1	0	0	0	1	0	0.5	0.5	1	0
P04080	1	0	0	0	1	0	2	0	1	0	1	0
C9JLI6	0	0	0	0	1	1	2	0	0.5	0.5	1	0
K7ELS0	0	0	1	0	1	1	1	0	0.5	0.5	1	0
Q96CX2	0	0	0	0	2	0	2	0	1	0	1	0
P39900	0	0	0	0	0	2	2	0	0	1	1	0
H7C3G1	0	0	1	0	1	0	1	0	0.5	0	1	0
O75934	0	0	1	0	0	1	1	0	0	0.5	1	0
A0A087WZ	0	0	0	0	1	0	2	0	0.5	0	1	0
P05386	0	0	0	0	1	0	2	0	0.5	0	1	0
P17028	1	0	2	0	0	0	0	0	0.5	0	1	0
P30307	0	0	0	0	0	1	2	0	0	0.5	1	0
P48634	0	0	0	0	0	1	2	0	0	0.5	1	0
P67870	0	0	1	0	1	0	1	0	0.5	0	1	0
G3V198	0	0	0	0	0	1	2	0	0	0.5	1	0
Q14331	0	0	0	0	1	0	2	0	0.5	0	1	0
A0A087WY	0	0	2	0	0	1	0	0	0	0.5	1	0
E9PM04	0	0	1	0	1	0	1	0	0.5	0	1	0
D6RC52	0	0	1	0	1	0	1	0	0.5	0	1	0
Q9Y3Z3	0	0	0	0	1	0	2	0	0.5	0	1	0
A6NDF3	0	1	2	0	0	0	0	0	0	0.5	1	0
P62906	0	0	0	0	0	1	2	0	0	0.5	1	0
P78318	0	0	0	0	1	0	2	0	0.5	0	1	0
Q06587	0	0	1	0	1	0	1	0	0.5	0	1	0
C9J470	1	0	0	0	0	0	2	0	0.5	0	1	0
F2Z2R5	0	0	0	0	0	1	2	0	0	0.5	1	0
H3BN98	1	0	1	0	0	0	1	0	0.5	0	1	0
K7EP06	0	0	0	0	0	0	2	0	0	0	1	0
Q9BPU6	0	0	0	0	0	0	2	0	0	0	1	0
A0A087WY	0	0	0	0	0	0	2	0	0	0	1	0
A1A564	0	0	0	0	0	0	2	0	0	0	1	0
P24534	0	0	1	0	0	0	1	0	0	0	1	0
Q9H3P7	0	0	0	0	0	0	2	0	0	0	1	0
Q9HB71	0	0	1	0	0	0	1	0	0	0	1	0

H0YKU1	0	0	0	0	0	0	2	0	0	0	1	0
O43290	0	0	0	0	0	0	2	0	0	0	1	0
F5GXS2	0	0	0	0	0	0	2	0	0	0	1	0
H7C3X0	0	0	0	0	0	0	2	0	0	0	1	0
C9IYT0	0	0	0	0	0	0	2	0	0	0	1	0
O75534	0	0	0	0	0	0	2	0	0	0	1	0
P31260	0	0	0	0	0	0	2	0	0	0	1	0
P36578	0	0	1	0	0	0	1	0	0	0	1	0
H7C422	0	0	0	0	0	0	2	0	0	0	1	0
P56192	0	0	0	0	0	0	2	0	0	0	1	0
Q12948	0	0	0	0	0	0	2	0	0	0	1	0
A0A0G2JN2	0	0	0	0	0	0	2	0	0	0	1	0
Q16342	0	0	0	0	0	0	2	0	0	0	1	0
A0A087WV	0	0	1	0	0	0	1	0	0	0	1	0
Q6UUV7	0	0	0	0	0	0	2	0	0	0	1	0
Q8N163	0	0	1	0	0	0	1	0	0	0	1	0
Q8TD19	0	0	0	0	0	0	2	0	0	0	1	0
F5GXS8	0	0	0	0	0	0	2	0	0	0	1	0
Q9P2E3	0	0	1	0	0	0	1	0	0	0	1	0
Q9Y3I1	0	0	0	0	0	0	2	0	0	0	1	0
Q9Y3R0	0	0	0	0	0	0	2	0	0	0	1	0
O15084	0	0	0	0	0	0	2	0	0	0	1	0
Q8WU90	0	0	0	0	0	0	2	0	0	0	1	0
Q96S90	0	0	0	0	0	0	2	0	0	0	1	0
Q70JA7	0	0	1	0	0	0	1	0	0	0	1	0
J3QT28	0	0	0	0	0	0	2	0	0	0	1	0
J3KS31	0	0	0	0	0	0	2	0	0	0	1	0
E7EQZ7	0	0	0	0	0	0	2	0	0	0	1	0
Q8N1G4	0	0	0	0	0	0	2	0	0	0	1	0
E9PFL1	0	0	0	0	0	0	2	0	0	0	1	0
D6RA57	0	0	0	0	0	0	2	0	0	0	1	0
H3BUR4	0	0	1	0	0	0	1	0	0	0	1	0
H0Y873	0	0	0	0	0	0	2	0	0	0	1	0
Q96RS6	0	0	1	0	0	0	1	0	0	0	1	0
Q13509	3	0	0	3	0	0	1	0	1.5	0	0.5	1.5
E9PI65	0	0	0	0	0	0	1	0	0	0	0.5	0
A0A0C4DG	2	1	1	1	0	0	0	0	1	0.5	0.5	0.5
CAS1_BOV	7	3	0	0	1	0	1	1	4	1.5	0.5	0.5
Q15459	0	0	0	0	3	3	1	6	1.5	1.5	0.5	3
Q8IYD1	0	0	0	0	0	0	1	0	0	0	0.5	0
K7EQL0	0	0	0	0	0	0	1	0	0	0	0.5	0
Q8N5C6	1	0	0	0	4	3	1	2	2.5	1.5	0.5	1
P62258	2	2	1	0	0	2	0	1	1	2	0.5	0.5
Q08174	0	1	0	0	2	2	1	4	1	1.5	0.5	2
B1ANR0	1	0	0	0	2	0	1	0	1.5	0	0.5	0
P08579	1	0	0	1	2	2	1	1	1.5	1	0.5	1
A0A0A0MS	0	0	0	0	1	2	1	1	0.5	1	0.5	0.5
Q9H496	0	0	0	0	6	0	1	0	3	0	0.5	0
P61221	0	0	0	0	4	1	1	1	2	0.5	0.5	0.5
Q1L5Z9	2	0	1	0	4	0	0	0	3	0	0.5	0
G8JLD5	0	0	0	0	5	0	1	0	2.5	0	0.5	0
Q8IZL9	0	0	0	0	0	0	1	0	0	0	0.5	0
Q02750	1	0	0	0	0	0	1	0	0.5	0	0.5	0
P53621	0	0	0	1	2	2	1	0	1	1	0.5	0.5
A0A087WV	0	1	0	0	0	2	1	2	0	1.5	0.5	1
Q96DG6	0	0	0	0	2	2	1	1	1	1	0.5	0.5
O15160	0	0	0	0	2	2	1	0	1	1	0.5	0
O43660	0	0	0	0	1	1	1	0	0.5	0.5	0.5	0
O75449	0	0	0	0	3	1	1	0	1.5	0.5	0.5	0
P23258	1	0	1	0	1	1	0	1	1	0.5	0.5	0.5
E9PGM9	0	0	0	0	0	0	1	0	0	0	0.5	0

B4DP31	0	0	1	0	1	2	0	1	0.5	1	0.5	0.5
P62306	1	1	0	0	2	0	1	0	1.5	0.5	0.5	0
Q9Y6G9	0	0	0	0	0	2	1	2	0	1	0.5	1
Q13395	1	0	1	0	3	0	0	0	2	0	0.5	0
Q7Z2Z2	1	0	1	0	1	0	0	0	1	0	0.5	0
Q9UJ68	1	1	1	0	1	0	0	1	1	0.5	0.5	0.5
REF_HEVBF	0	3	0	0	0	0	1	0	0	1.5	0.5	0
O00429-7	0	0	0	0	0	0	1	0	0	0	0.5	0
O75909	0	0	0	1	1	1	1	0	0.5	0.5	0.5	0.5
P05455	0	0	0	0	2	1	1	0	1	0.5	0.5	0
A0A0A0MF	1	0	0	0	1	0	1	1	1	0	0.5	0.5
CAS2_BOVI	3	0	1	0	0	0	0	0	1.5	0	0.5	0
Q08211	0	0	0	0	3	0	1	0	1.5	0	0.5	0
A0A087WX	0	0	0	0	2	1	1	0	1	0.5	0.5	0
P35372-13	0	0	0	0	1	0	1	0	0.5	0	0.5	0
Q86U70	0	0	0	0	1	0	1	2	0.5	0	0.5	1
A0A087WT	0	0	1	0	0	0	0	0	0	0	0.5	0
B5MCP9	0	0	0	0	1	1	1	1	0.5	0.5	0.5	0.5
Q9NYJ8	0	0	0	0	2	1	1	0	1	0.5	0.5	0
H7C4I3	0	0	1	0	0	0	0	0	0	0	0.5	0
P62269	0	0	0	0	1	1	1	1	0.5	0.5	0.5	0.5
O00401	0	0	0	0	1	1	1	1	0.5	0.5	0.5	0.5
P25705	1	1	1	1	0	0	0	0	0.5	0.5	0.5	0.5
P54296	0	0	0	0	1	2	1	0	0.5	1	0.5	0
F8VVA7	0	0	0	0	1	1	1	1	0.5	0.5	0.5	0.5
A0A087WX	0	0	0	0	3	0	1	0	1.5	0	0.5	0
K7EIH8	1	0	1	1	0	0	0	0	0.5	0	0.5	0.5
Q16650	0	0	0	0	1	1	1	0	0.5	0.5	0.5	0
O43172	0	0	0	0	2	0	1	0	1	0	0.5	0
A0A0G2JJZ	0	0	0	0	1	0	1	1	0.5	0	0.5	0.5
O95400	1	1	0	0	0	0	1	0	0.5	0.5	0.5	0
P10644	0	0	0	0	0	1	1	1	0	0.5	0.5	0.5
P17812	1	0	0	0	1	0	1	0	1	0	0.5	0
A0A087WV	1	1	0	0	0	0	1	0	0.5	0.5	0.5	0
P37108	0	0	0	0	2	0	1	0	1	0	0.5	0
A0A024R4N	1	0	0	0	0	0	1	1	0.5	0	0.5	0.5
P54136	1	0	0	0	1	0	1	0	1	0	0.5	0
A8MXH2	0	0	0	0	0	0	1	0	0	0	0.5	0
Q15020	0	0	0	0	0	0	1	2	0	0	0.5	1
Q29RF7	0	0	0	0	1	1	1	0	0.5	0.5	0.5	0
Q2TAY7	0	0	0	1	1	0	1	0	0.5	0	0.5	0.5
Q7Z2T5	1	0	1	0	1	0	0	0	1	0	0.5	0
Q96N67	0	0	0	0	2	0	1	0	1	0	0.5	0
Q9BPX3	0	0	0	0	1	0	1	1	0.5	0	0.5	0.5
Q9UMX1	0	0	1	0	2	0	0	0	1	0	0.5	0
Q13185	1	0	1	0	0	1	0	0	0.5	0.5	0.5	0
P62805	2	0	1	0	0	0	0	0	1	0	0.5	0
A0A0B4J2B	0	0	0	0	2	0	1	0	1	0	0.5	0
F5GWN5	1	0	0	0	0	1	1	0	0.5	0.5	0.5	0
E7EMB3	0	0	1	1	0	1	0	0	0	0.5	0.5	0.5
A0A087X1F	1	1	1	0	0	0	0	0	0.5	0.5	0.5	0
A0A087X2I	1	0	0	0	0	1	1	0	0.5	0.5	0.5	0
Q96F63	1	0	1	0	1	0	0	0	1	0	0.5	0
P28072	1	1	1	0	0	0	0	0	0.5	0.5	0.5	0
A0A0A0MF	1	0	0	0	0	0	1	0	0.5	0	0.5	0
P38432	0	0	0	0	1	0	1	0	0.5	0	0.5	0
H7C0F4	0	0	0	0	1	0	1	0	0.5	0	0.5	0
Q9H0D6	0	0	0	0	1	0	1	0	0.5	0	0.5	0
A0A087WU	0	0	0	0	1	0	1	0	0.5	0	0.5	0
P30050	0	0	0	0	0	0	1	1	0	0	0.5	0.5
Q9UNS1	1	0	1	0	0	0	0	0	0.5	0	0.5	0

O75925	0	0	1	0	1	0	0	0	0.5	0	0.5	0
O95239	0	0	0	0	1	0	1	0	0.5	0	0.5	0
O95487	0	0	0	0	1	0	1	0	0.5	0	0.5	0
P19784	0	0	0	0	0	0	1	0	0	0	0.5	0
F5GWX5	0	1	1	0	0	0	0	0	0	0.5	0.5	0
Q5T280	0	0	0	0	0	1	1	0	0	0.5	0.5	0
Q9UER7	0	0	1	0	1	0	0	0	0.5	0	0.5	0
Q9Y295	0	0	0	0	1	0	1	0	0.5	0	0.5	0
Q7Z3Z4	1	0	1	0	0	0	0	0	0.5	0	0.5	0
P07737	0	0	0	0	1	0	1	0	0.5	0	0.5	0
P33993	0	0	0	0	1	0	1	0	0.5	0	0.5	0
Q9UJX5	0	1	1	0	0	0	0	0	0	0.5	0.5	0
F5H0Y3	0	0	0	0	1	0	1	0	0.5	0	0.5	0
Q8NCM8	0	0	1	0	0	1	0	0	0	0.5	0.5	0
F5H303	0	0	1	0	1	0	0	0	0.5	0	0.5	0
P98088	0	1	0	0	0	0	1	0	0	0.5	0.5	0
O60346	0	0	0	0	1	0	1	0	0.5	0	0.5	0
C9JIZ0	0	0	0	0	1	0	1	0	0.5	0	0.5	0
P02765	1	0	1	0	0	0	0	0	0.5	0	0.5	0
C9J896	0	0	0	0	1	0	1	0	0.5	0	0.5	0
P23458	0	0	0	0	0	0	1	1	0	0	0.5	0.5
P23526	1	0	0	0	0	0	1	0	0.5	0	0.5	0
P25788	0	0	0	0	1	0	1	0	0.5	0	0.5	0
P30520	0	0	1	0	1	0	0	0	0.5	0	0.5	0
P33981	0	0	0	0	1	0	1	0	0.5	0	0.5	0
M0QZN2	0	0	0	0	0	0	1	1	0	0	0.5	0.5
C9JL85	1	0	1	0	0	0	0	0	0.5	0	0.5	0
A0A087WL	0	0	0	0	1	0	1	0	0.5	0	0.5	0
G5E953	1	0	0	0	0	0	1	0	0.5	0	0.5	0
A0A0A0MC	1	0	1	0	0	0	0	0	0.5	0	0.5	0
Q8IXB1	0	0	0	0	1	0	1	0	0.5	0	0.5	0
B5MDQ0	0	0	1	0	1	0	0	0	0.5	0	0.5	0
K7EK33	0	0	0	0	1	0	1	0	0.5	0	0.5	0
Q9GZN8	1	0	1	0	0	0	0	0	0.5	0	0.5	0
Q9UBV8	0	0	0	0	1	0	1	0	0.5	0	0.5	0
A0A075B6F	0	0	0	0	1	0	1	0	0.5	0	0.5	0
A0A0A0MS	0	0	0	0	1	0	1	0	0.5	0	0.5	0
A0A0D9SES	0	0	0	0	1	0	1	0	0.5	0	0.5	0
Q92922	0	0	0	0	1	0	1	0	0.5	0	0.5	0
P0C2W1	0	0	0	0	0	1	1	0	0	0.5	0.5	0
P62857	1	0	0	0	0	0	1	0	0.5	0	0.5	0
Q9UPN7	0	0	0	0	0	0	1	0	0	0	0.5	0
H0YEH2	0	0	0	0	0	0	1	0	0	0	0.5	0
F2Z356	0	0	1	0	0	0	0	0	0	0	0.5	0
P28715	0	0	0	0	0	0	1	0	0	0	0.5	0
J3KRL6	0	0	0	0	0	0	1	0	0	0	0.5	0
A0A0C4DG	0	0	1	0	0	0	0	0	0	0	0.5	0
B4DTN4	0	0	0	0	0	0	1	0	0	0	0.5	0
Q96SY0-3	0	0	1	0	0	0	0	0	0	0	0.5	0
A6NFU8	0	0	0	0	0	0	1	0	0	0	0.5	0
Q5SZ59	0	0	0	0	0	0	1	0	0	0	0.5	0
Q8IZF0	0	0	1	0	0	0	0	0	0	0	0.5	0
Q9UPM8	0	0	0	0	0	0	1	0	0	0	0.5	0
H3BM45	0	0	1	0	0	0	0	0	0	0	0.5	0
A0A0U1RQ	0	0	0	0	0	0	1	0	0	0	0.5	0
Q96S55	0	0	0	0	0	0	1	0	0	0	0.5	0
D6RAX7	0	0	1	0	0	0	0	0	0	0	0.5	0
Q9H9A6	0	0	1	0	0	0	0	0	0	0	0.5	0
A0A024QZ3	0	0	0	0	0	0	1	0	0	0	0.5	0
F8WB94	0	0	0	0	0	0	1	0	0	0	0.5	0
Q9HD33	0	0	0	0	0	0	1	0	0	0	0.5	0

H7BXY3	0	0	0	0	0	0	1	0	0	0	0.5	0
J3KNE8	0	0	0	0	0	0	1	0	0	0	0.5	0
Q9UNN8	0	0	0	0	0	0	1	0	0	0	0.5	0
Q6STE5	0	0	1	0	0	0	0	0	0	0	0.5	0
H0YJ14	0	0	1	0	0	0	0	0	0	0	0.5	0
Q8N967	0	0	0	0	0	0	1	0	0	0	0.5	0
Q92731	0	0	0	0	0	0	1	0	0	0	0.5	0
Q15772	0	0	1	0	0	0	0	0	0	0	0.5	0
A0A087WV	0	0	1	0	0	0	0	0	0	0	0.5	0
Q9NZM1-2	0	0	0	0	0	0	1	0	0	0	0.5	0
Q02930	0	0	1	0	0	0	0	0	0	0	0.5	0
J3KS22	0	0	0	0	0	0	1	0	0	0	0.5	0
Q8TC57	0	0	0	0	0	0	1	0	0	0	0.5	0
C9JLW8	0	0	0	0	0	0	1	0	0	0	0.5	0
A0A087X0	0	0	0	0	0	0	1	0	0	0	0.5	0
H0YKE6	0	0	1	0	0	0	0	0	0	0	0.5	0
A7MCY6	0	0	1	0	0	0	0	0	0	0	0.5	0
H3BTW3	0	0	0	0	0	0	1	0	0	0	0.5	0
P62312	0	0	1	0	0	0	0	0	0	0	0.5	0
A8MYT4	0	0	1	0	0	0	0	0	0	0	0.5	0
Q96K49	0	0	1	0	0	0	0	0	0	0	0.5	0
Q16384	0	0	1	0	0	0	0	0	0	0	0.5	0
E7EPG1	0	0	0	0	0	0	1	0	0	0	0.5	0
A0A087WZ	0	0	1	0	0	0	0	0	0	0	0.5	0
Q9UNS2	0	0	0	0	0	0	1	0	0	0	0.5	0
D6RG18	0	0	1	0	0	0	0	0	0	0	0.5	0
Q5TDE7	0	0	1	0	0	0	0	0	0	0	0.5	0
Q9NRC6	0	0	0	0	0	0	1	0	0	0	0.5	0
A6H8Y7	0	0	0	0	0	0	1	0	0	0	0.5	0
Q8NDH2	0	0	1	0	0	0	0	0	0	0	0.5	0
A2RRE5	0	0	0	0	0	0	1	0	0	0	0.5	0
A0A087WT	0	0	0	0	0	0	1	0	0	0	0.5	0
D6RGI5	0	0	1	0	0	0	0	0	0	0	0.5	0
A0A0A0MT	0	0	0	0	0	0	1	0	0	0	0.5	0
Q96PE2	0	0	1	0	0	0	0	0	0	0	0.5	0
Q9NP31	0	0	0	0	0	0	1	0	0	0	0.5	0
Q9Y2Z4	0	0	0	0	0	0	1	0	0	0	0.5	0
Q711Q0	0	0	0	0	0	0	1	0	0	0	0.5	0
D6R9Q9	0	0	0	0	0	0	1	0	0	0	0.5	0
Q8N3C0	0	0	0	0	0	0	1	0	0	0	0.5	0
P42575	0	0	0	0	0	0	1	0	0	0	0.5	0
F8WBW2	0	0	1	0	0	0	0	0	0	0	0.5	0
A0A075B7F	0	0	1	0	0	0	0	0	0	0	0.5	0
C9IYV2	0	0	1	0	0	0	0	0	0	0	0.5	0
A6NGJ6	0	0	0	0	0	0	1	0	0	0	0.5	0
A8MUF7	0	0	1	0	0	0	0	0	0	0	0.5	0
O14733	0	0	0	0	0	0	1	0	0	0	0.5	0
O43353	0	0	1	0	0	0	0	0	0	0	0.5	0
O60422	0	0	1	0	0	0	0	0	0	0	0.5	0
O60566	0	0	0	0	0	0	1	0	0	0	0.5	0
O75607	0	0	1	0	0	0	0	0	0	0	0.5	0
O75815	0	0	0	0	0	0	1	0	0	0	0.5	0
P05060	0	0	1	0	0	0	0	0	0	0	0.5	0
P12955	0	0	0	0	0	0	1	0	0	0	0.5	0
E9PIK5	0	0	1	0	0	0	0	0	0	0	0.5	0
E9PKL5	0	0	0	0	0	0	1	0	0	0	0.5	0
G3V4L3	0	0	1	0	0	0	0	0	0	0	0.5	0
C9J8M3	0	0	0	0	0	0	1	0	0	0	0.5	0
P35268	0	0	0	0	0	0	1	0	0	0	0.5	0
A0A0A0MS	0	0	0	0	0	0	1	0	0	0	0.5	0
C9JH72	0	0	0	0	0	0	1	0	0	0	0.5	0

P52952	0	0	0	0	0	0	1	0	0	0	0.5	0
A0A087X1E	0	0	1	0	0	0	0	0	0	0	0.5	0
F6RFD5	0	0	1	0	0	0	0	0	0	0	0.5	0
M0QZC5	0	0	0	0	0	0	1	0	0	0	0.5	0
J3KTJ3	0	0	0	0	0	0	1	0	0	0	0.5	0
P82094	0	0	1	0	0	0	0	0	0	0	0.5	0
E9PJF6	0	0	0	0	0	0	1	0	0	0	0.5	0
A0A0D9SFI	0	0	0	0	0	0	1	0	0	0	0.5	0
Q02809	0	0	0	0	0	0	1	0	0	0	0.5	0
Q04760	0	0	0	0	0	0	1	0	0	0	0.5	0
Q06124	0	0	0	0	0	0	1	0	0	0	0.5	0
Q08AD1	0	0	0	0	0	0	1	0	0	0	0.5	0
Q15437	0	0	0	0	0	0	1	0	0	0	0.5	0
Q2VY69	0	0	0	0	0	0	1	0	0	0	0.5	0
Q5T4S7	0	0	1	0	0	0	0	0	0	0	0.5	0
Q5VYS8	0	0	0	0	0	0	1	0	0	0	0.5	0
Q5VZK9	0	0	0	0	0	0	1	0	0	0	0.5	0
M0QX46	0	0	0	0	0	0	1	0	0	0	0.5	0
Q6UY01	0	0	0	0	0	0	1	0	0	0	0.5	0
H3BMJ2	0	0	0	0	0	0	1	0	0	0	0.5	0
A0A087WU	0	0	0	0	0	0	1	0	0	0	0.5	0
Q70CQ2	0	0	1	0	0	0	0	0	0	0	0.5	0
Q86W56	0	0	0	0	0	0	1	0	0	0	0.5	0
E5RHH7	0	0	0	0	0	0	1	0	0	0	0.5	0
A0A087X21	0	0	0	0	0	0	1	0	0	0	0.5	0
H0YMR4	0	0	1	0	0	0	0	0	0	0	0.5	0
Q8WYQ5	0	0	0	0	0	0	1	0	0	0	0.5	0
E7EN38	0	0	1	0	0	0	0	0	0	0	0.5	0
Q96A99	0	0	0	0	0	0	1	0	0	0	0.5	0
Q96E09	0	0	0	0	0	0	1	0	0	0	0.5	0
E9PPJ9	0	0	0	0	0	0	1	0	0	0	0.5	0
A8MVZ6	0	0	1	0	0	0	0	0	0	0	0.5	0
Q96MD7-1	0	0	1	0	0	0	0	0	0	0	0.5	0
Q9BUH6	0	0	1	0	0	0	0	0	0	0	0.5	0
Q9BXT5	0	0	0	0	0	0	1	0	0	0	0.5	0
Q9C0B0	0	0	0	0	0	0	1	0	0	0	0.5	0
E9PE10	0	0	0	0	0	0	1	0	0	0	0.5	0
H0YM60	0	0	0	0	0	0	1	0	0	0	0.5	0
F5H039	0	0	1	0	0	0	0	0	0	0	0.5	0
Q9NXB9	0	0	0	0	0	0	1	0	0	0	0.5	0
H0Y8C3	0	0	1	0	0	0	0	0	0	0	0.5	0
Q9UBB4	0	0	0	0	0	0	1	0	0	0	0.5	0
Q9UBN7	0	0	0	0	0	0	1	0	0	0	0.5	0
Q9UEG4	0	0	1	0	0	0	0	0	0	0	0.5	0
E9PIZ4	0	0	0	0	0	0	1	0	0	0	0.5	0
E9PBL0	0	0	1	0	0	0	0	0	0	0	0.5	0
Q5H909	0	0	1	0	0	0	0	0	0	0	0.5	0
A0A0A0MT	0	0	0	0	0	0	1	0	0	0	0.5	0
G3V4C6	0	0	0	0	0	0	1	0	0	0	0.5	0
C9JQG7	0	0	1	0	0	0	0	0	0	0	0.5	0
B1AMU3	0	0	0	0	0	0	1	0	0	0	0.5	0
H3BRS3	0	0	1	0	0	0	0	0	0	0	0.5	0
A0A087WV	0	0	1	0	0	0	0	0	0	0	0.5	0
C9JDM3	0	0	0	0	0	0	1	0	0	0	0.5	0
F8W8Y7	0	0	1	0	0	0	0	0	0	0	0.5	0
V9GYZ8	0	0	1	0	0	0	0	0	0	0	0.5	0
P62633	0	0	1	0	0	0	0	0	0	0	0.5	0
D6RAN6	0	0	0	0	0	0	1	0	0	0	0.5	0
O15111	0	0	1	0	0	0	0	0	0	0	0.5	0
O75663	0	0	1	0	0	0	0	0	0	0	0.5	0
B4DKY1	0	0	0	0	0	0	1	0	0	0	0.5	0

Q6IQ49	0	0	0	0	0	0	1	0	0	0	0.5	0
C9JYQ9	0	0	0	0	0	0	1	0	0	0	0.5	0
A0A087WV	0	0	0	0	0	0	1	0	0	0	0.5	0
B7Z493	0	0	0	0	0	0	1	0	0	0	0.5	0
Q9NW64	0	0	0	0	0	0	1	0	0	0	0.5	0
Q9Y5G6	0	0	0	0	0	0	1	0	0	0	0.5	0
E9PQP8	0	0	0	0	0	0	1	0	0	0	0.5	0
D6RIZ8	0	0	1	0	0	0	0	0	0	0	0.5	0
J3KRD8	0	0	0	0	0	0	1	0	0	0	0.5	0
A1A5B4	0	0	0	0	0	0	1	0	0	0	0.5	0
P09429	0	0	0	0	0	0	1	0	0	0	0.5	0
D6R9L5	0	0	1	0	0	0	0	0	0	0	0.5	0
A6NNN6	0	0	0	0	0	0	1	0	0	0	0.5	0
H3BND0	0	0	1	0	0	0	0	0	0	0	0.5	0
A0A087WZ	0	0	0	0	0	0	1	0	0	0	0.5	0
Q99543	0	0	0	0	0	0	1	0	0	0	0.5	0
Q9BV73	0	0	1	0	0	0	0	0	0	0	0.5	0
B8ZZZ9	0	0	0	0	0	0	1	0	0	0	0.5	0
A0A0D9SF2	0	0	0	0	0	0	1	0	0	0	0.5	0
P55073	0	0	1	0	0	0	0	0	0	0	0.5	0
Q07973	0	0	1	0	0	0	0	0	0	0	0.5	0
F5H478	0	0	0	0	0	0	1	0	0	0	0.5	0
K7EPZ9	0	0	1	0	0	0	0	0	0	0	0.5	0
Q12756	0	0	1	0	0	0	0	0	0	0	0.5	0
H0YDR7	0	0	0	0	0	0	1	0	0	0	0.5	0
A6NIV2	0	0	0	0	0	0	1	0	0	0	0.5	0
Q04656	0	0	1	0	0	0	0	0	0	0	0.5	0
Q9Y2X9	0	0	0	0	0	0	1	0	0	0	0.5	0
E5RHG6	0	0	0	0	0	0	1	0	0	0	0.5	0
F8VU51	0	0	0	0	0	0	1	0	0	0	0.5	0
Q86VD1	0	0	1	0	0	0	0	0	0	0	0.5	0
Q8N4E4	0	0	0	0	0	0	1	0	0	0	0.5	0
M0QXB0	0	0	0	0	0	0	1	0	0	0	0.5	0
C9J9J4	0	0	0	0	0	0	1	0	0	0	0.5	0
Q6ZW49	0	0	0	0	0	0	1	0	0	0	0.5	0
F8WEF8	0	0	1	0	0	0	0	0	0	0	0.5	0
J3KTQ5	0	0	1	0	0	0	0	0	0	0	0.5	0
Q8IWI9	0	0	1	0	0	0	0	0	0	0	0.5	0
H3BTH6	0	0	1	0	0	0	0	0	0	0	0.5	0
Q8N475	0	0	0	0	0	0	1	0	0	0	0.5	0
Q96PB1	0	0	0	0	0	0	1	0	0	0	0.5	0
D6R9W6	0	0	0	0	0	0	1	0	0	0	0.5	0
Q5JZB8	0	0	0	0	1	0	1	0	0.5	0	0.5	0
A0AVF1	0	0	1	0	0	0	0	0	0	0	0.5	0
I3L1Y9	0	0	0	0	0	0	1	0	0	0	0.5	0
A2A2Y4	0	0	1	0	0	0	0	0	0	0	0.5	0
A0A087WX	0	0	0	0	0	0	1	0	0	0	0.5	0
Q9NYZ3	0	0	0	0	0	0	1	0	0	0	0.5	0
Q9Y2H2	0	0	0	0	0	0	1	0	0	0	0.5	0
O60341	0	0	0	0	0	0	1	0	0	0	0.5	0
Q6PIU1	0	0	0	0	0	0	1	0	0	0	0.5	0
H0Y760	0	0	0	0	0	0	1	0	0	0	0.5	0
C9J798	0	0	1	0	0	0	0	0	0	0	0.5	0
P28482-2	0	0	0	0	0	2	0	2	0	1	0	1
E9PJF0	0	0	0	0	2	0	0	1	1	0	0	0.5
H0YD75	0	0	0	0	0	1	0	0	0	0.5	0	0
Q16659	0	0	0	0	1	0	0	0	0.5	0	0	0
P04259	0	1	0	0	0	0	0	0	0	0.5	0	0
P02538	12	0	0	0	2	0	0	0	7	0	0	0
K1M1_SHE	23	0	0	0	0	0	0	0	11.5	0	0	0
O94822	0	6	0	0	1	26	0	0	0.5	16	0	0

P08727	1	0	0	0	0	0	0	0	0.5	0	0	0
Q562R1	0	0	0	1	0	0	0	0	0	0	0	0.5
Q9Y573	0	4	0	7	0	7	0	7	0	5.5	0	7
O95678	1	0	0	0	0	0	0	0	0.5	0	0	0
P42025	0	0	0	1	0	0	0	1	0	0	0	1
K2M3_SHE	20	0	0	0	0	0	0	0	10	0	0	0
KRHB6_HU	8	0	0	0	0	0	0	0	4	0	0	0
K1H6_HUM	5	0	0	0	0	0	0	0	2.5	0	0	0
Q58FF8	1	0	0	0	0	0	0	0	0.5	0	0	0
C4AM86	1	0	0	0	0	0	0	0	0.5	0	0	0
E7ERL6	0	0	0	0	0	1	0	0	0	0.5	0	0
K2M2_SHE	3	0	0	0	0	0	0	0	1.5	0	0	0
Q99504	2	0	0	0	11	0	0	0	6.5	0	0	0
E7EQ64	1	1	0	0	0	2	0	2	0.5	1.5	0	1
E9PM09	1	0	0	0	0	0	0	0	0.5	0	0	0
K2M1_SHE	5	0	0	0	0	0	0	0	2.5	0	0	0
P31942	0	0	0	0	1	0	0	0	0.5	0	0	0
Q9Y5B6	1	3	0	1	0	1	0	2	0.5	2	0	1.5
O76041	0	0	0	0	0	0	0	3	0	0	0	1.5
P21281	1	0	0	0	4	1	0	0	2.5	0.5	0	0
G3V1S7	1	0	0	2	0	1	0	2	0.5	0.5	0	2
Q9P2R3	0	0	0	0	2	2	0	1	1	1	0	0.5
O75821	0	0	0	0	3	0	0	2	1.5	0	0	1
Q58FF6	0	0	0	0	1	1	0	0	0.5	0.5	0	0
B1AK85	1	1	0	1	0	0	0	0	0.5	0.5	0	0.5
A0A087WV	1	0	0	1	0	0	0	3	0.5	0	0	2
Q86YZ3	0	5	0	0	0	0	0	0	0	2.5	0	0
Q9UGR2	0	0	0	0	4	0	0	0	2	0	0	0
Q9Y3Y2	0	0	0	0	1	2	0	1	0.5	1	0	0.5
O14818	0	1	0	1	0	1	0	1	0	1	0	1
A8MQ02	0	0	0	0	4	0	0	0	2	0	0	0
Q5JX49	1	0	0	1	0	0	0	0	0.5	0	0	0.5
Q9BX84	0	0	0	0	1	0	0	1	0.5	0	0	0.5
Q06495	0	0	0	0	1	1	0	0	0.5	0.5	0	0
A0A087WV	0	0	0	0	1	0	0	1	0.5	0	0	0.5
H3BSW0	2	1	0	1	0	0	0	0	1	0.5	0	0.5
A0A087WX	0	0	0	0	0	2	0	0	0	1	0	0
F5H435	1	0	0	0	1	2	0	0	1	1	0	0
Q9UJX3	1	0	0	0	2	0	0	0	1.5	0	0	0
E9PF10	1	0	0	0	2	0	0	0	1.5	0	0	0
P15924	2	0	0	0	0	0	0	1	1	0	0	0.5
P20742	0	0	0	0	1	0	0	1	0.5	0	0	0.5
P30044	0	0	0	0	0	0	0	3	0	0	0	1.5
P31025	3	0	0	0	0	0	0	0	1.5	0	0	0
P31151	1	0	0	0	0	2	0	0	0.5	1	0	0
P15104	1	0	0	0	2	0	0	0	1.5	0	0	0
CASB_BOV	3	0	0	0	0	0	0	0	1.5	0	0	0
P35573	0	0	0	0	3	0	0	0	1.5	0	0	0
Q4KMP7	0	0	0	0	3	0	0	0	1.5	0	0	0
P51991	0	0	0	0	3	0	0	0	1.5	0	0	0
Q9Y678	0	0	0	0	2	0	0	1	1	0	0	0.5
Q5S007	0	0	0	1	0	2	0	0	0	1	0	0.5
E9PK41	0	0	0	0	1	1	0	1	0.5	0.5	0	0.5
C9J0J7	0	1	0	1	1	0	0	0	0.5	0.5	0	0.5
F6SS63	1	0	0	0	0	2	0	0	0.5	1	0	0
Q9P244	1	0	0	1	0	0	0	0	0.5	0	0	0.5
F8W079	0	1	0	1	0	0	0	0	0	0.5	0	0.5
Q9NWU2	0	0	0	1	0	0	0	1	0	0	0	1
Q9UKX3	0	1	0	0	1	0	0	0	0.5	0.5	0	0
F5H4R1	1	0	0	0	1	0	0	0	1	0	0	0
ALDOA_RA	1	0	0	0	0	0	0	1	0.5	0	0	0.5

A0A087X1(	0	1	0	0	1	0	0	0	0.5	0.5	0	0
F8VWS0	1	1	0	0	0	0	0	0	0.5	0.5	0	0
P07195	1	0	0	1	0	0	0	0	0.5	0	0	0.5
A0A087WL	2	0	0	0	0	0	0	0	1	0	0	0
A0A0C4DG	0	1	0	1	0	0	0	0	0	0.5	0	0.5
C9J2Y9	0	0	0	0	2	0	0	0	1	0	0	0
CASK_BOVI	2	0	0	0	0	0	0	0	1	0	0	0
P59665	2	0	0	0	0	0	0	0	1	0	0	0
M0R1L2	0	0	0	0	1	0	0	1	0.5	0	0	0.5
P20930	1	0	0	0	0	1	0	0	0.5	0.5	0	0
F5H459	0	0	0	0	1	0	0	1	0.5	0	0	0.5
Q96AG4	0	0	0	0	2	0	0	0	1	0	0	0
B7WPG3	0	0	0	0	2	0	0	0	1	0	0	0
A0A0A0MF	0	0	0	0	0	2	0	0	0	1	0	0
C9J3R0	1	0	0	0	1	0	0	0	1	0	0	0
B7ZKJ8	1	1	0	0	0	0	0	0	0.5	0.5	0	0
A0A0A0MF	0	0	0	0	0	0	0	2	0	0	0	1
Q5VU13-2	1	0	0	0	1	0	0	0	1	0	0	0
Q9NP98	0	0	0	0	1	1	0	0	0.5	0.5	0	0
K7EQQ8	0	0	0	0	2	0	0	0	1	0	0	0
Q9UPU7	1	0	0	0	0	1	0	0	0.5	0.5	0	0
Q96EF0	0	0	0	0	0	0	0	2	0	0	0	1
A0A087X2(	0	0	0	0	1	1	0	0	0.5	0.5	0	0
F5GX23	1	0	0	0	1	0	0	0	1	0	0	0
P53803	1	0	0	0	0	1	0	0	0.5	0.5	0	0
Q5T750	0	1	0	1	0	0	0	0	0	0.5	0	0.5
H0YL69	0	0	0	0	1	0	0	1	0.5	0	0	0.5
A0A0U1RQ	0	0	0	0	1	1	0	0	0.5	0.5	0	0
Q6P2C0	0	0	0	0	1	0	0	0	0.5	0	0	0
O75937	0	0	0	0	0	0	0	1	0	0	0	0.5
Q5QGS0	0	0	0	0	0	1	0	0	0	0.5	0	0
Q6IMI6	0	0	0	0	0	0	0	1	0	0	0	0.5
Q8N7X1	0	0	0	0	0	1	0	0	0	0.5	0	0
B1AH58	0	0	0	0	1	0	0	0	0.5	0	0	0
Q8NEZ3	0	0	0	0	0	0	0	1	0	0	0	0.5
Q9P2G4	0	0	0	0	0	1	0	0	0	0.5	0	0
Q4G0P3	0	0	0	0	1	0	0	0	0.5	0	0	0
A8MTJ6	0	0	0	0	0	1	0	0	0	0.5	0	0
A0A0J9YXJ(	0	0	0	0	0	0	0	1	0	0	0	0.5
F5H6B2	0	0	0	0	0	1	0	0	0	0.5	0	0
P31629	1	0	0	0	0	0	0	0	0.5	0	0	0
E7ESA6	1	0	0	0	0	0	0	0	0.5	0	0	0
Q13231-4	0	0	0	0	0	0	0	1	0	0	0	0.5
G3V3G9	0	0	0	0	1	0	0	0	0.5	0	0	0
Q9ULM3	0	0	0	0	0	1	0	0	0	0.5	0	0
C0MHM2	0	0	0	0	0	1	0	0	0	0.5	0	0
F8WBW9	1	0	0	0	0	0	0	0	0.5	0	0	0
K7EIR6	0	0	0	1	0	0	0	0	0	0	0	0.5
J3KNS5	1	0	0	0	0	0	0	0	0.5	0	0	0
H0YLZ8	0	0	0	1	0	0	0	0	0	0	0	0.5
Q6XUX3	0	0	0	0	1	0	0	0	0.5	0	0	0
A0A0C4DG	0	0	0	1	0	0	0	0	0	0	0	0.5
B4DGJ5	0	0	0	0	0	1	0	0	0	0.5	0	0
Q9Y6X0	1	0	0	0	0	0	0	0	0.5	0	0	0
Q68DA7-3	0	0	0	0	0	0	0	1	0	0	0	0.5
H3BR40	0	0	0	1	0	0	0	0	0	0	0	0.5
Q6ZVD7	0	1	0	0	0	0	0	0	0	0.5	0	0
A0A1B0GT(	0	0	0	0	1	0	0	0	0.5	0	0	0
Q9NQS3-3	0	1	0	0	0	0	0	0	0	0.5	0	0
J3QTJ6	0	1	0	0	0	0	0	0	0	0.5	0	0
Q7Z7H8	0	0	0	0	1	0	0	0	0.5	0	0	0

Q92539	0	0	0	1	0	0	0	0	0	0	0	0.5
J3KNK1	0	0	0	0	1	0	0	0	0.5	0	0	0
E5RGL8	0	0	0	0	1	0	0	0	0.5	0	0	0
O60271-9	0	0	0	0	1	0	0	0	0.5	0	0	0
P61244-5	0	0	0	0	0	1	0	0	0	0.5	0	0
Q6ZUT6	0	0	0	1	0	0	0	0	0	0	0	0.5
H7C2Y3	0	0	0	0	0	1	0	0	0	0.5	0	0
O43745	1	0	0	0	0	0	0	0	0.5	0	0	0
Q2M1P5	0	0	0	0	1	0	0	0	0.5	0	0	0
Q7Z7B7	0	0	0	0	1	0	0	0	0.5	0	0	0
E7ERS3	1	0	0	0	0	0	0	0	0.5	0	0	0
KRA61_SHE	1	0	0	0	0	0	0	0	0.5	0	0	0
A0A087WV	0	0	0	0	0	0	0	1	0	0	0	0.5
Q5VUA4	0	0	0	0	0	1	0	0	0	0.5	0	0
E7ER45	0	1	0	0	0	0	0	0	0	0.5	0	0
Q9NYQ8	0	1	0	0	0	0	0	0	0	0.5	0	0
O95711	0	0	0	0	0	1	0	0	0	0.5	0	0
Q9BRH9	0	0	0	0	0	1	0	0	0	0.5	0	0
Q9BRX2	0	0	0	0	1	0	0	0	0.5	0	0	0
B4E0T2	0	1	0	0	0	0	0	0	0	0.5	0	0
Q2L4Q9	0	1	0	0	0	0	0	0	0	0.5	0	0
Q99683	0	0	0	0	0	1	0	0	0	0.5	0	0
G3V3G3	0	0	0	0	0	1	0	0	0	0.5	0	0
H3BPR3	0	0	0	0	0	1	0	0	0	0.5	0	0
O96019	1	0	0	0	0	0	0	0	0.5	0	0	0
P12272-3	0	0	0	0	0	0	0	1	0	0	0	0.5
O00292	0	0	0	0	0	0	0	1	0	0	0	0.5
Q9H773	0	0	0	0	1	0	0	0	0.5	0	0	0
M0QYZ9	1	0	0	0	0	0	0	0	0.5	0	0	0
F8W061	0	1	0	0	0	0	0	0	0	0.5	0	0
Q86VW2	0	0	0	0	0	1	0	0	0	0.5	0	0
A0A075B6E	0	0	0	0	0	0	0	1	0	0	0	0.5
F8VVY9	0	0	0	0	0	1	0	0	0	0.5	0	0
C9IYI5	0	0	0	0	0	0	0	1	0	0	0	0.5
A6NFC9	0	0	0	0	0	1	0	0	0	0.5	0	0
P58005	0	0	0	0	0	1	0	0	0	0.5	0	0
Q6ZV70-2	1	0	0	0	0	0	0	0	0.5	0	0	0
P51878-3	0	0	0	1	0	0	0	0	0	0	0	0.5
Q96BN2	1	0	0	0	0	0	0	0	0.5	0	0	0
E9PC90	0	0	0	0	1	0	0	0	0.5	0	0	0
Q15910	0	1	0	0	0	0	0	0	0	0.5	0	0
P46199	0	0	0	0	0	1	0	0	0	0.5	0	0
P78524	1	0	0	0	0	0	0	0	0.5	0	0	0
Q14093	0	0	0	0	0	1	0	0	0	0.5	0	0
Q9NR48	0	0	0	0	1	0	0	0	0.5	0	0	0
F2Z388	0	0	0	0	0	1	0	0	0	0.5	0	0
A0A0D9SF6	1	0	0	0	0	0	0	0	0.5	0	0	0
A0A0A0MS	0	1	0	0	0	0	0	0	0	0.5	0	0
P09923	0	1	0	0	0	0	0	0	0	0.5	0	0
A0A087WU	1	0	0	0	0	0	0	0	0.5	0	0	0
B7ZBJ4	0	1	0	0	0	0	0	0	0	0.5	0	0
E9PF49	1	0	0	0	0	0	0	0	0.5	0	0	0
A0A087WU	0	0	0	0	0	1	0	0	0	0.5	0	0
A0A087WU	0	0	0	0	0	1	0	0	0	0.5	0	0
Q9BTV7	0	1	0	0	0	0	0	0	0	0.5	0	0
Q7Z2Y5	1	0	0	0	0	0	0	0	0.5	0	0	0
A4UGR9-4	0	0	0	0	1	0	0	0	0.5	0	0	0
A0A0A0MF	0	0	0	0	1	0	0	0	0.5	0	0	0
Q9Y4D7	0	1	0	0	0	0	0	0	0	0.5	0	0
F5GX86	0	0	0	1	0	0	0	0	0	0	0	0.5
A0A0A0MT	0	0	0	0	1	0	0	0	0.5	0	0	0

Q9UKL4	1	0	0	0	0	0	0	0	0.5	0	0	0
A0A0A0MT	0	0	0	0	1	0	0	0	0.5	0	0	0
P10412	1	0	0	0	0	0	0	0	0.5	0	0	0
F8WFC6	0	0	0	0	0	1	0	0	0	0.5	0	0
H7C4K7	0	0	0	0	1	0	0	0	0.5	0	0	0
A0A0A0MS	0	0	0	0	1	0	0	0	0.5	0	0	0
Q9BY10	1	0	0	0	0	0	0	0	0.5	0	0	0
Q9NQW5	0	0	0	0	0	1	0	0	0	0.5	0	0
G3V2R1	0	0	0	0	0	0	0	1	0	0	0	0.5
M0QZW4	0	0	0	0	0	1	0	0	0	0.5	0	0
Q16600	0	1	0	0	0	0	0	0	0	0.5	0	0
O14980	0	0	0	0	1	0	0	0	0.5	0	0	0
P78395	0	0	0	0	0	0	0	1	0	0	0	0.5
A0AUZ9	0	0	0	0	1	0	0	0	0.5	0	0	0
A0A096LNV	0	0	0	0	0	1	0	0	0	0.5	0	0
A6NLC5	0	0	0	1	0	0	0	0	0	0	0	0.5
A6NNN8	0	0	0	0	1	0	0	0	0.5	0	0	0
LYSC_HUM	1	0	0	0	0	0	0	0	0.5	0	0	0
O00203	1	0	0	0	0	0	0	0	0.5	0	0	0
A0A024R6X	0	0	0	0	1	0	0	0	0.5	0	0	0
O14529	1	0	0	0	0	0	0	0	0.5	0	0	0
O14640	0	0	0	0	1	0	0	0	0.5	0	0	0
G3V105	0	0	0	1	0	0	0	0	0	0	0	0.5
A4QPE4	0	0	0	1	0	0	0	0	0	0	0	0.5
H3BS03	0	0	0	0	1	0	0	0	0.5	0	0	0
O43347	0	0	0	0	1	0	0	0	0.5	0	0	0
O60503	0	0	0	0	1	0	0	0	0.5	0	0	0
O75159	0	0	0	0	1	0	0	0	0.5	0	0	0
O94776	0	0	0	1	0	0	0	0	0	0	0	0.5
C9JAT7	0	0	0	0	0	0	0	1	0	0	0	0.5
A8MUN2	0	0	0	0	1	0	0	0	0.5	0	0	0
P05109	1	0	0	0	0	0	0	0	0.5	0	0	0
P12273	1	0	0	0	0	0	0	0	0.5	0	0	0
P21817	0	0	0	1	0	0	0	0	0	0	0	0.5
P30048	0	0	0	0	1	0	0	0	0.5	0	0	0
H3BPE7	0	0	0	0	0	0	0	1	0	0	0	0.5
K7EKS1	0	0	0	0	1	0	0	0	0.5	0	0	0
P38606	1	0	0	0	0	0	0	0	0.5	0	0	0
C9JJ34	0	0	0	0	1	0	0	0	0.5	0	0	0
E9PI86	0	0	0	0	1	0	0	0	0.5	0	0	0
P49790	1	0	0	0	0	0	0	0	0.5	0	0	0
P49796-8	1	0	0	0	0	0	0	0	0.5	0	0	0
P51684	0	0	0	0	0	0	0	1	0	0	0	0.5
P52738	0	1	0	0	0	0	0	0	0	0.5	0	0
P53350	1	0	0	0	0	0	0	0	0.5	0	0	0
P58397	0	0	0	0	1	0	0	0	0.5	0	0	0
G5E9G7	0	0	0	0	1	0	0	0	0.5	0	0	0
B1AQK6	0	0	0	0	0	1	0	0	0	0.5	0	0
I6L8B7	1	0	0	0	0	0	0	0	0.5	0	0	0
F8VUA6	1	0	0	0	0	0	0	0	0.5	0	0	0
Q0ZLH3	1	0	0	0	0	0	0	0	0.5	0	0	0
Q13085	1	0	0	0	0	0	0	0	0.5	0	0	0
A0A0A0MT	0	0	0	0	0	0	0	1	0	0	0	0.5
Q14643	1	0	0	0	0	0	0	0	0.5	0	0	0
Q15024	0	0	0	0	1	0	0	0	0.5	0	0	0
H0YLX2	0	0	0	0	1	0	0	0	0.5	0	0	0
Q3SXZ3	0	0	0	0	0	0	0	1	0	0	0	0.5
Q5BKY6	0	0	0	1	0	0	0	0	0	0	0	0.5
Q5T5P0	1	0	0	0	0	0	0	0	0.5	0	0	0
F6XA08	0	0	0	1	0	0	0	0	0	0	0	0.5
Q63HQ2	0	1	0	0	0	0	0	0	0	0.5	0	0

Q6IA86	0	0	0	0	1	0	0	0	0.5	0	0	0
A0A0A0MS	0	0	0	0	1	0	0	0	0.5	0	0	0
Q6PL18	0	0	0	1	0	0	0	0	0	0	0	0.5
Q6UXQ4	0	1	0	0	0	0	0	0	0	0.5	0	0
Q6ZRI8	0	1	0	0	0	0	0	0	0	0.5	0	0
Q71F78	0	0	0	1	0	0	0	0	0	0	0	0.5
Q7Z4L9-2	0	0	0	1	0	0	0	0	0	0	0	0.5
Q8IXQ4-4	0	0	0	0	1	0	0	0	0.5	0	0	0
Q8IZD9	0	1	0	0	0	0	0	0	0	0.5	0	0
Q8IZU8	0	0	0	1	0	0	0	0	0	0	0	0.5
Q8N1D0	0	0	0	0	0	0	0	1	0	0	0	0.5
K7EL42	0	0	0	1	0	0	0	0	0	0	0	0.5
Q8NA70	0	0	0	0	1	0	0	0	0.5	0	0	0
Q8NEG0	0	0	0	1	0	0	0	0	0	0	0	0.5
H0Y6V6	0	0	0	0	1	0	0	0	0.5	0	0	0
Q8WXF1	0	0	0	0	1	0	0	0	0.5	0	0	0
C9JA69	0	0	0	1	0	0	0	0	0	0	0	0.5
A0A087X05	0	0	0	1	0	0	0	0	0	0	0	0.5
Q96B26	0	0	0	0	1	0	0	0	0.5	0	0	0
Q96FS4	0	0	0	1	0	0	0	0	0	0	0	0.5
Q96GW7	0	0	0	0	0	0	0	1	0	0	0	0.5
Q96J02	0	0	0	1	0	0	0	0	0	0	0	0.5
Q96M60	1	0	0	0	0	0	0	0	0.5	0	0	0
Q96Q91	0	0	0	1	0	0	0	0	0	0	0	0.5
Q96SQ9-2	0	0	0	1	0	0	0	0	0	0	0	0.5
E7ES68	0	0	0	0	1	0	0	0	0.5	0	0	0
Q9BTY7	0	0	0	0	1	0	0	0	0.5	0	0	0
Q9BVI0	0	0	0	0	1	0	0	0	0.5	0	0	0
Q9C0B6	0	0	0	1	0	0	0	0	0	0	0	0.5
Q9C0G6	0	0	0	1	0	0	0	0	0	0	0	0.5
Q9H330	0	0	0	1	0	0	0	0	0	0	0	0.5
Q9H3G5	1	0	0	0	0	0	0	0	0.5	0	0	0
Q9H501	0	1	0	0	0	0	0	0	0	0.5	0	0
Q9H6N6	0	0	0	0	0	0	0	1	0	0	0	0.5
H7C1U7	0	1	0	0	0	0	0	0	0	0.5	0	0
Q9H7R0	0	0	0	0	0	0	0	1	0	0	0	0.5
A0A075B6I	0	0	0	0	1	0	0	0	0.5	0	0	0
Q9H900	0	1	0	0	0	0	0	0	0	0.5	0	0
I3L139	0	0	0	0	1	0	0	0	0.5	0	0	0
Q9HCD5	0	0	0	0	1	0	0	0	0.5	0	0	0
Q9HCS5	1	0	0	0	0	0	0	0	0.5	0	0	0
Q9NQW8	0	1	0	0	0	0	0	0	0	0.5	0	0
Q9NRN7	1	0	0	0	0	0	0	0	0.5	0	0	0
Q9NTZ6	0	0	0	0	1	0	0	0	0.5	0	0	0
Q9NXG0	1	0	0	0	0	0	0	0	0.5	0	0	0
Q9NYU2	0	0	0	0	0	0	0	1	0	0	0	0.5
K7EKM6	0	0	0	0	1	0	0	0	0.5	0	0	0
Q9P2D3	0	0	0	0	1	0	0	0	0.5	0	0	0
Q9P2I0	0	0	0	0	0	0	0	1	0	0	0	0.5
E9PMX7	0	0	0	1	0	0	0	0	0	0	0	0.5
G3V2W1	0	1	0	0	0	0	0	0	0	0.5	0	0
Q9UKY3	0	0	0	0	0	1	0	0	0	0.5	0	0
H0YMN5	0	1	0	0	0	0	0	0	0	0.5	0	0
Q9UP83	0	0	0	0	1	0	0	0	0.5	0	0	0
A0A0U1RQ	0	0	0	0	1	0	0	0	0.5	0	0	0
G8JLP4	0	0	0	0	0	1	0	0	0	0.5	0	0
Q9Y6K8	0	0	0	1	0	0	0	0	0	0	0	0.5
A0A087WV	0	0	0	0	0	1	0	0	0	0.5	0	0
A0A1B0GU	0	0	0	1	0	0	0	0	0	0	0	0.5
F5H1Z8	0	0	0	1	0	0	0	0	0	0	0	0.5
F8VV97	1	0	0	0	0	0	0	0	0.5	0	0	0

F8WDC4	0	0	0	0	1	0	0	0	0.5	0	0	0
H0YC36	0	1	0	0	0	0	0	0	0	0.5	0	0
H3BPN6	0	0	0	1	0	0	0	0	0	0	0	0.5
Q5SXN9	0	0	0	1	0	0	0	0	0	0	0	0.5
B5MDF5	1	0	0	0	0	0	0	0	0.5	0	0	0
A2AB06	1	0	0	0	0	0	0	0	0.5	0	0	0
C9J730	0	1	0	0	0	0	0	0	0	0.5	0	0
H7C121	0	0	0	1	0	0	0	0	0	0	0	0.5
J3QLI3	0	0	0	0	0	0	0	1	0	0	0	0.5
O43182	0	1	0	0	0	0	0	0	0	0.5	0	0
P07205	0	0	0	0	0	0	0	1	0	0	0	0.5
P13985	0	1	0	0	0	0	0	0	0	0.5	0	0
P20264	0	1	0	0	0	0	0	0	0	0.5	0	0
P49915	1	0	0	0	0	0	0	0	0.5	0	0	0
B4DXD0	1	0	0	0	0	0	0	0	0.5	0	0	0
A0A0C4DG	0	0	0	0	0	1	0	0	0	0.5	0	0
Q6UXN9	0	0	0	0	1	0	0	0	0.5	0	0	0
I3L1V0	1	0	0	0	0	0	0	0	0.5	0	0	0
E9PMP7	0	0	0	1	0	0	0	0	0	0	0	0.5
Q96BJ8	0	1	0	0	0	0	0	0	0	0.5	0	0
H0Y7A5	0	0	0	0	0	0	0	1	0	0	0	0.5
Q9NX45	1	0	0	0	0	0	0	0	0.5	0	0	0
H0YC70	1	0	0	0	0	0	0	0	0.5	0	0	0
A0A1B0GTI	0	0	0	1	0	0	0	0	0	0	0	0.5
K7EKP8	1	0	0	0	0	0	0	0	0.5	0	0	0
A0A0A0MF	0	0	0	0	1	0	0	0	0.5	0	0	0
P14923	1	0	0	0	0	0	0	0	0.5	0	0	0
P46013	0	0	0	0	1	0	0	0	0.5	0	0	0
A0A087WV	1	0	0	0	0	0	0	0	0.5	0	0	0
J3QT83	1	0	0	0	0	0	0	0	0.5	0	0	0
C9J8F4	0	0	0	0	1	0	0	0	0.5	0	0	0
Q8NGJ4	1	0	0	0	0	0	0	0	0.5	0	0	0
C9JZB0	1	0	0	0	0	0	0	0	0.5	0	0	0
A0A1B0GU	1	0	0	0	0	0	0	0	0.5	0	0	0
K7EQD1	0	0	0	0	1	0	0	0	0.5	0	0	0
A0A0C4DG	0	0	0	0	1	0	0	0	0.5	0	0	0
A0A0C4DG	0	0	0	0	0	0	0	1	0	0	0	0.5
B1AJY5	0	0	0	1	0	0	0	0	0	0	0	0.5
Q13127	0	0	0	0	0	1	0	0	0	0.5	0	0
B8ZZ87	0	0	0	0	0	1	0	0	0	0.5	0	0
F5GXW1	0	0	0	0	1	0	0	0	0.5	0	0	0
Q96PQ5	0	0	0	1	0	0	0	0	0	0	0	0.5
Q9NY12	0	0	0	0	1	0	0	0	0.5	0	0	0
Q9Y421-2	0	0	0	0	1	0	0	0	0.5	0	0	0
A6NJV1	0	1	0	0	0	0	0	0	0	0.5	0	0
P51511	0	1	0	0	0	0	0	0	0	0.5	0	0
F8VVT9	0	0	0	0	1	0	0	0	0.5	0	0	0
A0A0A6YY	0	0	0	0	1	0	0	0	0.5	0	0	0
P08240	0	0	0	0	1	0	0	0	0.5	0	0	0
P34820-2	0	0	0	1	0	0	0	0	0	0	0	0.5
H0YLB9	0	0	0	0	1	0	0	0	0.5	0	0	0
K7ELC7	1	0	0	0	0	0	0	0	0.5	0	0	0
C9JKF1	0	0	0	0	1	0	0	0	0.5	0	0	0
A6PVH9	0	0	0	0	1	0	0	0	0.5	0	0	0
Q9BTM9	0	0	0	0	1	0	0	0	0.5	0	0	0
Q9H6T0	0	0	0	0	0	0	0	1	0	0	0	0.5
A6NCK2	1	0	0	0	0	0	0	0	0.5	0	0	0
B2RTY4	0	0	0	0	0	1	0	0	0	0.5	0	0
P0C853	1	0	0	0	0	0	0	0	0.5	0	0	0
A0A087WV	0	1	0	0	0	0	0	0	0	0.5	0	0
C9JPI6	1	0	0	0	0	0	0	0	0.5	0	0	0

A0A0A0MS	1	0	0	0	0	0	0	0	0.5	0	0	0
Q8N414	0	0	0	1	0	0	0	0	0	0	0	0.5
A0A0A0MC	0	0	0	0	0	0	0	1	0	0	0	0.5
H0YFK7	0	0	0	0	0	0	0	1	0	0	0	0.5
H3BNW8	0	0	0	0	1	0	0	0	0.5	0	0	0
K7EK23	0	0	0	0	1	0	0	0	0.5	0	0	0
E7EMV8	0	0	0	0	0	1	0	0	0	0.5	0	0
A6NGW2	0	0	0	1	0	0	0	0	0	0	0	0.5
E5RG74	0	0	0	0	1	0	0	0	0.5	0	0	0
Q68DN1	0	0	0	0	0	1	0	0	0	0.5	0	0
Q9NY15	0	0	0	0	1	0	0	0	0.5	0	0	0
A0A0A0MT	0	1	0	0	0	0	0	0	0	0.5	0	0
O75110	0	0	0	0	1	0	0	0	0.5	0	0	0
M0R1C8	0	0	0	1	0	0	0	0	0	0	0	0.5
P25391	1	0	0	0	0	0	0	0	0.5	0	0	0
J3KNB4	0	0	0	0	1	0	0	0	0.5	0	0	0
Q5M775	1	0	0	0	0	0	0	0	0.5	0	0	0
A0A087WT	0	0	0	0	1	0	0	0	0.5	0	0	0
Q9H871	1	0	0	0	0	0	0	0	0.5	0	0	0
F5H026	0	0	0	0	0	1	0	0	0	0.5	0	0
Q6IEY1	0	0	0	0	1	0	0	0	0.5	0	0	0
Q5T3J3	0	0	0	0	0	1	0	0	0	0.5	0	0
Q86X59	0	0	0	0	1	0	0	0	0.5	0	0	0
Q8N5G2	0	0	0	0	1	0	0	0	0.5	0	0	0
A0A0C4DF	0	0	0	0	0	1	0	0	0	0.5	0	0
A0A087X07	0	0	0	0	1	1	0	0	0.5	0.5	0	0
Q9Y3Q8	0	0	0	0	0	1	0	0	0	0.5	0	0
H0YIZ1	0	0	0	0	0	1	0	0	0	0.5	0	0
Q86WV7	0	1	0	0	0	0	0	0	0	0.5	0	0
Q8TD57	0	0	0	0	0	1	0	0	0	0.5	0	0
O94907	0	1	0	0	0	0	0	0	0	0.5	0	0
Q14393	0	0	0	1	0	0	0	0	0	0	0	0.5
A0A0G2JM	0	0	0	1	0	0	0	0	0	0	0	0.5
Q9H3C7	0	0	0	1	0	0	0	0	0	0	0	0.5
M0QYS1	0	0	0	1	0	0	0	0	0	0	0	0.5
Q9BZF3	0	0	0	0	1	0	0	0	0.5	0	0	0
Q9UMQ6	0	0	0	0	0	0	0	1	0	0	0	0.5
E5RIC9	1	0	0	0	0	0	0	0	0.5	0	0	0
C9JF14	0	1	0	0	0	0	0	0	0	0.5	0	0
J3KMY8	0	0	0	0	0	0	0	1	0	0	0	0.5
F8VWD7	0	0	0	0	1	0	0	0	0.5	0	0	0

Appendix C

All Protein IDs from PhAXA-MS with 4E-BP1 (T46C) as Bait

PROTID	Replicate 1 PSMs				Replicate 2 PSMs				Average PSMs			
	4E-BP1 (WT) + **1**	4E-BP1 (WT) ATP ctl	4E-BP1 (T46C) + **1**	4E-BP1 (T46C) ATP ctl	4E-BP1 (WT) + **1**	4E-BP1 (WT) ATP ctl	4E-BP1 (T46C) + **1**	4E-BP1 (T46C) ATP ctl	4E-BP1 (WT) + **1**	4E-BP1 (WT) ATP ctl	4E-BP1 (T46C) + **1**	4E-BP1 (T46C) ATP ctl
Q13541	1037	1085	607	643	2433	2252	1457	1357	1735	1668.5	1032	1000
TRYP_PIG	58	57	52	64	221	237	191	191	139.5	147	121.5	127.5
P11142	57	35	62	34	110	72	114	94	83.5	53.5	88	64
P42345	22	0	104	0	2	0	45	0	12	0	74.5	0
D6RBW1	68	70	61	72	76	64	79	68	72	67	70	70
P78347	37	25	36	27	74	78	102	92	55.5	51.5	69	59.5
P11021	44	43	44	22	85	64	72	79	64.5	53.5	58	50.5
P78527	40	0	66	6	11	0	31	3	25.5	0	48.5	4.5
P68363	31	24	43	49	24	14	50	53	27.5	19	46.5	51
P52272	1	1	26	20	1	0	58	39	1	0.5	42	29.5
A0A0G2JIW1	25	10	24	6	51	32	54	42	38	21	39	24
P07437	10	19	43	26	23	15	32	35	16.5	17	37.5	30.5
ALBU_BOVIN	53	50	51	84	14	17	20	11	33.5	33.5	35.5	47.5
Q13162	23	22	18	21	38	37	46	38	30.5	29.5	32	29.5
PRDX1_HUMAN	20	34	31	43	23	30	33	46	21.5	32	32	44.5
P04264	31	14	18	33	25	7	38	16	28	10.5	28	24.5
P13639	19	8	32	17	14	0	23	2	16.5	4	27.5	9.5
P17987	28	15	28	10	20	10	25	12	24	12.5	26.5	11
P49327	30	4	37	15	4	0	14	1	17	2	25.5	8
H0Y4R1	20	0	25	0	13	0	25	0	16.5	0	25	0
P68104	12	3	23	15	14	7	27	18	13	5	25	16.5
P30153	17	29	28	35	9	3	20	17	13	16	24	26
P50990	21	19	19	15	18	11	25	13	19.5	15	22	14
P13645	21	8	11	20	22	9	26	13	21.5	8.5	18.5	16.5
P35527	21	8	8	16	18	10	28	14	19.5	9	18	15
P60709	10	7	20	8	7	3	15	6	8.5	5	17.5	7
O14744	37	38	31	25	1	0	3	0	19	19	17	12.5
P63151	17	19	19	23	10	4	15	11	13.5	11.5	17	17
P08238	17	5	24	6	4	0	10	0	10.5	2.5	17	3
Q15393	14	15	22	14	6	1	12	5	10	8	17	9.5
Q8N122	21	21	25	18	6	1	8	3	13.5	11	16.5	10.5
P32119	10	17	18	22	11	13	15	13	10.5	15	16.5	17.5
E9PLK3	2	0	14	1	0	0	19	0	1	0	16.5	0.5
F5H5D3	0	0	19	22	0	0	14	0	0	0	16.5	11
Q9NUY8	0	0	18	0	0	0	15	0	0	0	16.5	0
P48643	17	6	14	7	14	3	17	8	15.5	4.5	15.5	7.5
P78371	13	3	12	6	15	7	19	14	14	5	15.5	10
Q99832	18	13	21	10	10	6	9	6	14	9.5	15	8
P10599	11	5	15	7	10	0	15	2	10.5	2.5	15	4.5
Q9BY77	1	3	1	1	12	12	28	22	6.5	7.5	14.5	11.5
P30041	15	10	14	10	12	3	14	3	13.5	6.5	14	6.5
P13797	13	0	12	1	5	0	16	0	9	0	14	0.5
Q16531	15	18	22	27	0	1	6	1	7.5	9.5	14	14
P68371	4	6	0	0	1	0	27	19	2.5	3	13.5	9.5
Q9BQA1	26	36	23	17	0	0	1	1	13	18	12	9
Q92598	16	3	18	0	3	0	6	0	9.5	1.5	12	0
P53396	12	2	16	2	6	0	8	0	9	1	12	1
P04350	4	0	23	24	0	0	0	0	2	0	11.5	12
Q9UJ70	3	0	15	0	1	0	8	0	2	0	11.5	0
Q15365	10	9	10	12	15	9	12	11	12.5	9	11	11.5
P11802	8	5	12	4	3	0	10	0	5.5	2.5	11	2
P22234	9	3	15	2	2	0	7	0	5.5	1.5	11	1
A0A0J9YVP6	13	9	9	12	7	8	11	10	10	8.5	10	11
F8W6I7	14	6	11	9	7	1	8	2	10.5	3.5	9.5	5.5
P40227	9	7	11	12	7	3	8	8	8	5	9.5	10
O60506	5	0	12	1	6	1	7	0	5.5	0.5	9.5	0.5
E9PB61	7	11	8	8	14	11	10	14	10.5	11	9	11

P49368	6	3	10	1	5	2	8	4	5.5	2.5	9	2.5
A0A0A0MQU4	9	12	9	10	4	2	8	2	6.5	7	8.5	6
Q9Y230	8	7	14	7	4	0	3	0	6	3.5	8.5	3.5
P62937	9	4	8	5	4	0	8	2	6.5	2	8	3.5
P46109	5	1	7	0	7	0	9	0	6	0.5	8	0
Q8TEX9	7	9	11	6	4	0	5	0	5.5	4.5	8	3
P07900	8	0	9	1	1	0	7	0	4.5	0	8	0.5
P07237	4	0	14	0	0	0	2	0	2	0	8	0
J3QRG6	3	2	5	4	5	0	10	1	4	1	7.5	2.5
Q71U36	0	0	0	0	0	0	15	5	0	0	7.5	2.5
O75190	0	0	6	7	0	0	9	8	0	0	7.5	7.5
P84090	5	5	8	9	9	5	6	8	7	5	7	8.5
Q15029	9	5	10	5	3	0	4	0	6	2.5	7	2.5
P62993	6	0	11	2	2	0	3	0	4	0	7	1
P13010	7	2	9	1	0	0	5	1	3.5	1	7	1
Q0VDG4	10	12	7	11	11	6	6	7	10.5	9	6.5	9
Q14011	7	6	5	4	7	4	8	7	7	5	6.5	5.5
P62714	6	0	13	25	5	4	0	0	5.5	2	6.5	12.5
P34932	10	2	11	1	0	0	2	0	5	1	6.5	0.5
P06748	7	1	7	1	0	1	6	1	3.5	1	6.5	1
P28482	5	7	10	10	1	0	3	2	3	3.5	6.5	6
P14618	3	1	12	10	3	0	1	0	3	0.5	6.5	5
Q5VWV2	1	0	5	1	1	0	8	1	1	0	6.5	1
A0A1C7CYX9	0	0	10	0	0	0	3	0	0	0	6.5	0
P52597	4	2	12	2	1	0	0	0	2.5	1	6	1
Q13085	1	0	11	0	0	0	1	0	0.5	0	6	0
Q14204	22	18	10	13	2	1	1	1	12	9.5	5.5	7
K22E_HUMAN	15	1	6	8	5	2	5	5	10	1.5	5.5	6.5
P19338	13	3	8	5	1	0	3	0	7	1.5	5.5	2.5
P67775	6	12	0	0	5	4	11	10	5.5	8	5.5	5
P00492	7	2	6	2	4	0	5	0	5.5	1	5.5	1
P98179	6	4	4	4	3	5	7	2	4.5	4.5	5.5	3
H0Y8C6	8	0	10	4	1	0	1	0	4.5	0	5.5	2
Q9HB71	5	0	5	0	3	0	6	0	4	0	5.5	0
P22314	6	1	9	4	1	0	2	0	3.5	0.5	5.5	2
A0A087WZT3	2	3	4	5	4	1	7	5	3	2	5.5	5
P30044	2	5	4	3	3	2	7	2	2.5	3.5	5.5	2.5
Q9P258	4	0	7	0	0	0	4	0	2	0	5.5	0
Q9BVC4	2	0	11	0	0	0	0	0	1	0	5.5	0
Q92616	2	0	10	0	0	0	1	0	1	0	5.5	0
A0A087WTP3	1	0	7	5	0	0	4	2	0.5	0	5.5	3.5
Q86X55	10	0	7	0	0	0	3	0	5	0	5	0
P50991	4	0	5	1	4	2	5	5	4	1	5	3
P22626	5	7	8	7	2	0	2	1	3.5	3.5	5	4
P27348	4	0	7	0	1	0	3	0	2.5	0	5	0
P63173	2	1	2	0	2	3	8	3	2	2	5	1.5
Q13395	4	0	8	1	0	0	2	0	2	0	5	0.5
E9PKG1	3	0	8	3	0	0	2	0	1.5	0	5	1.5
E9PCY7	8	7	4	6	1	0	5	1	4.5	3.5	4.5	3.5
A0A0A0MS07	2	2	5	4	6	6	4	6	4	4	4.5	5
G8JLD5	7	0	7	0	1	0	2	0	4	0	4.5	0
B0QY89	5	7	7	6	2	2	2	1	3.5	4.5	4.5	3.5
P55072	7	4	9	3	0	0	0	0	3.5	2	4.5	1.5
E7EUT5	2	2	3	0	2	0	6	2	2	1	4.5	1
A0A0U1RRM4	1	0	4	0	3	0	5	1	2	0	4.5	0.5
O60573	1	2	3	2	2	2	6	2	1.5	2	4.5	2
F8VPD4	3	0	9	6	0	0	0	0	1.5	0	4.5	3
P06733	1	2	4	2	2	1	5	1	1.5	1.5	4.5	1.5
Q9HA64	1	0	4	0	2	0	5	0	1.5	0	4.5	0
P17812	2	0	7	3	0	0	2	0	1	0	4.5	1.5
Q9HAV4	2	0	8	0	0	0	1	0	1	0	4.5	0
Q9BVA1	1	0	8	12	0	0	1	0	0.5	0	4.5	6
E9PL69	1	0	6	1	0	0	3	0	0.5	0	4.5	0.5
P09874	7	0	2	0	5	0	6	1	6	0	4	0.5
P60228	10	9	8	6	0	0	0	0	5	4.5	4	3

P27694	2	1	1	1	8	8	7	4	5	4.5	4	2.5
A0A075B6S2	4	5	4	4	5	5	4	5	4.5	5	4	4.5
Q6P2Q9	6	4	7	5	2	0	1	0	4	2	4	2.5
B4DV12	2	2	3	3	5	1	5	4	3.5	1.5	4	3.5
I3L397	1	3	4	2	5	1	4	2	3	2	4	2
P12277	3	0	5	1	1	0	3	0	2	0	4	0.5
P26641	3	0	5	0	0	0	3	0	1.5	0	4	0
Q8NBS9	2	7	5	4	0	1	3	0	1	4	4	2
P17858	0	0	8	8	0	0	0	0	0	0	4	4
P17655	12	3	5	0	3	0	2	0	7.5	1.5	3.5	0
E9PK25	5	2	4	2	4	0	3	2	4.5	1	3.5	2
P19474	8	5	7	10	0	0	0	0	4	2.5	3.5	5
A0A0A0MRJ6	6	1	6	1	2	0	1	0	4	0.5	3.5	0.5
P78406	7	3	5	6	0	0	2	0	3.5	1.5	3.5	3
P02538	3	0	0	0	3	0	7	0	3	0	3.5	0
Q12906	3	3	5	3	2	0	2	0	2.5	1.5	3.5	1.5
O14980	4	4	6	1	1	0	1	0	2.5	2	3.5	0.5
E5RJR5	4	1	3	1	1	0	4	1	2.5	0.5	3.5	1
P08243	2	0	4	1	2	0	3	0	2	0	3.5	0.5
P61978	2	0	3	0	2	0	4	0	2	0	3.5	0
P08779	1	0	1	0	2	2	6	2	1.5	1	3.5	1
Q13838	2	2	5	6	1	0	2	1	1.5	1	3.5	3.5
P51991	3	1	5	1	0	0	2	0	1.5	0.5	3.5	0.5
P23246	2	0	2	0	1	0	5	0	1.5	0	3.5	0
E9PC52	0	6	7	3	2	0	0	1	1	3	3.5	2
J3KTA4	0	0	2	2	2	0	5	0	1	0	3.5	1
P23526	2	0	4	3	0	0	3	0	1	0	3.5	1.5
Q9Y265	2	1	5	1	0	0	2	0	1	0.5	3.5	0.5
P31689	1	0	6	3	0	0	1	0	0.5	0	3.5	1.5
Q6DKJ4	1	0	2	0	0	0	5	0	0.5	0	3.5	0
Q14257	0	0	5	3	0	0	2	4	0	0	3.5	3.5
P54136	0	0	7	4	0	0	0	0	0	0	3.5	2
Q9Y3I0	0	0	3	0	0	0	4	0	0	0	3.5	0
A0A087WW66	7	3	4	2	0	0	2	0	3.5	1.5	3	1
P14866	5	0	4	1	2	0	2	0	3.5	0	3	0.5
D6RAF8	5	2	4	2	1	0	2	0	3	1	3	1
Q99615	5	0	5	0	1	0	1	0	3	0	3	0
B1AHC9	3	0	2	0	3	0	4	0	3	0	3	0
P37802	3	0	4	1	2	0	2	0	2.5	0	3	0.5
Q9BQ67	4	2	5	4	0	0	1	0	2	1	3	2
O15067	3	0	6	1	0	0	0	0	1.5	0	3	0.5
P22102	3	0	6	0	0	0	0	0	1.5	0	3	0
J3KQ32	1	0	2	0	2	0	4	0	1.5	0	3	0
G5E9A6	2	2	5	5	0	0	1	0	1	1	3	2.5
P31948	2	0	4	1	0	0	2	0	1	0	3	0.5
Q93009	2	0	2	0	0	0	4	0	1	0	3	0
Q96CX2	1	0	5	0	1	0	1	0	1	0	3	0
Q8NI35	1	1	6	6	0	0	0	0	0.5	0.5	3	3
P55060	1	0	5	0	0	0	1	0	0.5	0	3	0
Q9Y224	0	0	2	0	1	0	4	0	0.5	0	3	0
Q9NPA8	1	1	1	3	7	3	4	4	4	2	2.5	3.5
Q9UMS4	4	4	3	4	3	1	2	1	3.5	2.5	2.5	2.5
B4DY09	6	2	4	4	0	0	1	0	3	1	2.5	2
P49458	4	2	2	3	2	0	3	0	3	1	2.5	1.5
A0A087WYT3	5	0	2	0	1	0	3	0	3	0	2.5	0
Q09028	3	6	1	3	2	0	4	1	2.5	3	2.5	2
Q00839	3	0	4	1	2	0	1	1	2.5	0	2.5	1
TRY1_BOVIN	1	1	1	0	3	3	4	2	2	2	2.5	1
J3QLE5	2	1	3	2	2	1	2	2	2	1	2.5	2
P35606	4	2	5	1	0	0	0	0	2	1	2.5	0.5
F5H365	3	2	3	0	1	0	2	0	2	1	2.5	0
B0QZ18	4	0	4	0	0	0	1	0	2	0	2.5	0
Q9Y3Y2	1	1	1	0	2	1	4	3	1.5	1	2.5	1.5
Q15233	1	0	2	0	2	0	3	1	1.5	0	2.5	0.5
Q9NZL4	3	0	4	1	0	0	1	0	1.5	0	2.5	0.5

Q9Y3B4	1	0	3	0	2	0	2	1	1.5	0	2.5	0.5
J3KQ69	3	0	3	0	0	0	2	0	1.5	0	2.5	0
A0A087WTT1	2	4	2	3	0	0	3	0	1	2	2.5	1.5
C9J0J7	2	0	3	1	0	0	2	0	1	0	2.5	0.5
P62316	1	0	3	1	1	0	2	0	1	0	2.5	0.5
O75643	2	0	3	0	0	0	2	0	1	0	2.5	0
P38606	2	0	3	0	0	0	2	0	1	0	2.5	0
P45984	2	0	4	0	0	0	1	0	1	0	2.5	0
G5EA31	1	0	4	0	0	0	1	0	0.5	0	2.5	0
O95825	1	0	5	0	0	0	0	0	0.5	0	2.5	0
P12081	0	0	5	2	0	0	0	0	0	0	2.5	1
Q9H3U1	0	0	4	0	0	0	1	0	0	0	2.5	0
P02533	5	0	1	5	2	2	3	0	3.5	1	2	2.5
P62857	3	2	2	0	3	1	2	0	3	1.5	2	0
Q15208	6	1	4	1	0	0	0	0	3	0.5	2	0.5
O43390	5	4	3	1	0	0	1	0	2.5	2	2	0.5
P62913	2	0	2	0	3	1	2	2	2.5	0.5	2	1
Q16543	5	0	3	0	0	0	1	0	2.5	0	2	0
H3BLZ8	2	0	2	2	2	0	2	0	2	0	2	1
Q9BYB4	4	0	3	0	0	0	1	0	2	0	2	0
A0A087WVQ6	3	5	4	5	0	0	0	0	1.5	2.5	2	2.5
O43242	3	4	3	2	0	1	1	0	1.5	2.5	2	1
F8W079	3	1	4	5	0	0	0	0	1.5	0.5	2	2.5
P07195	3	0	4	0	0	0	0	1	1.5	0	2	0.5
P53602	3	0	4	0	0	0	0	0	1.5	0	2	0
Q08499-12	1	1	0	2	1	7	4	4	1	4	2	3
E9PDE8	2	0	4	0	0	0	0	0	1	0	2	0
J3QRS3	1	2	2	2	1	0	2	2	1	1	2	2
Q13200	2	2	3	2	0	0	1	0	1	1	2	1
Q13347	2	2	4	1	0	0	0	0	1	1	2	0.5
A0A087WWU8	2	0	4	0	0	0	0	0	1	0	2	0
P04080	1	0	1	0	1	0	3	0	1	0	2	0
P39019	0	0	0	0	2	0	4	0	1	0	2	0
Q13435	0	0	0	0	2	0	4	0	1	0	2	0
A0A0U1RR32	0	2	2	1	1	0	2	3	0.5	1	2	2
G3V1N2	1	0	4	2	0	0	0	0	0.5	0	2	1
H9KV75	1	0	3	1	0	0	1	0	0.5	0	2	0.5
P05387	1	0	2	0	0	0	2	0	0.5	0	2	0
P41250	1	0	2	0	0	0	2	0	0.5	0	2	0
Q93008	1	0	4	0	0	0	0	0	0.5	0	2	0
P55795	0	0	4	0	0	0	0	1	0	0	2	0.5
P51116	0	0	3	1	0	0	1	1	0	0	2	1
P61221	0	0	3	2	0	0	1	0	0	0	2	1
Q15773	0	0	2	2	0	0	2	0	0	0	2	1
Q6IA86	0	0	4	1	0	0	0	0	0	0	2	0.5
E9PJH4	0	0	1	0	0	0	3	0	0	0	2	0
P48147	0	0	3	0	0	0	1	0	0	0	2	0
Q14012	0	0	4	0	0	0	0	0	0	0	2	0
Q6PJG6	0	0	4	0	0	0	0	0	0	0	2	0
P23284	6	5	2	2	2	2	1	1	4	3.5	1.5	1.5
E9PMI6	5	6	3	2	0	0	0	0	2.5	3	1.5	1
P35244	3	2	0	2	2	1	3	1	2.5	1.5	1.5	1.5
Q9H4A4	4	1	3	4	0	0	0	0	2	0.5	1.5	2
P47813	2	0	1	1	2	1	2	3	2	0.5	1.5	2
Q7RTV0	1	1	2	3	3	1	1	0	2	1	1.5	1.5
E7EMB3	2	0	2	1	2	0	1	0	2	0	1.5	0.5
P62269	0	0	0	0	4	1	3	2	2	0.5	1.5	1
Q9UNE7	3	1	2	0	1	0	1	0	2	0.5	1.5	0
P35998	3	2	3	3	0	0	0	1	1.5	1	1.5	2
Q9UJ68	1	3	3	3	1	0	0	0	1	1.5	1.5	1.5
O00303	2	2	2	2	0	0	1	0	1	1	1.5	1
P61163	2	2	1	1	0	0	2	0	1	1	1.5	0.5
P62310	2	2	2	1	0	0	1	0	1	1	1.5	0.5
Q13561	1	1	2	1	1	0	1	1	1	0.5	1.5	1
Q13409-2	1	2	0	0	1	0	3	0	1	1	1.5	0

P60842	2	0	1	1	0	0	2	0	1	0	1.5	0.5
CAS1_BOVIN	1	0	2	0	1	0	1	1	1	0	1.5	0.5
J3QT28	2	0	3	0	0	0	0	0	1	0	1.5	0
Q7KZF4	2	0	3	0	0	0	0	0	1	0	1.5	0
E7EX29	1	1	3	2	0	0	0	0	0.5	0.5	1.5	1
E5RHG8	1	2	3	2	0	0	0	0	0.5	1	1.5	1
K7ERF1	1	4	2	1	0	0	1	0	0.5	2	1.5	0.5
P62318	1	1	2	1	0	0	1	0	0.5	0.5	1.5	0.5
Q96J01	1	0	3	2	0	0	0	0	0.5	0	1.5	1
P61758	1	0	3	3	0	0	0	0	0.5	0	1.5	1.5
P62195	1	1	2	1	0	0	1	0	0.5	0.5	1.5	0.5
P04818	1	1	2	1	0	0	1	0	0.5	0.5	1.5	0.5
Q9BWJ5	1	1	3	1	0	0	0	0	0.5	0.5	1.5	0.5
O43175	0	0	3	2	1	0	0	0	0.5	0	1.5	1
A0A087X2I1	1	1	2	0	0	0	1	0	0.5	0.5	1.5	0
P13489	1	0	3	1	0	0	0	0	0.5	0	1.5	0.5
GSTP1_HUMAN	0	1	2	0	1	0	1	0	0.5	0.5	1.5	0
P52564	1	0	2	0	0	0	1	0	0.5	0	1.5	0
Q9BUF5	0	0	3	4	0	0	0	0	0	0	1.5	2
D6R9P3	0	0	3	0	0	0	0	0	0	0	1.5	0
H3BR35	0	0	3	3	0	0	0	0	0	0	1.5	1.5
O00170	0	0	3	3	0	0	0	0	0	0	1.5	1.5
Q9GZP4	0	0	3	3	0	0	0	0	0	0	1.5	1.5
E9PJM3	0	0	3	2	0	0	0	0	0	0	1.5	1
A0A0A6YY92	0	0	3	1	0	0	0	0	0	0	1.5	0.5
Q8N5X7	0	0	3	1	0	0	0	0	0	0	1.5	0.5
A0A0C4DGH5	0	0	2	0	0	0	1	0	0	0	1.5	0
A6NIH7	0	0	3	0	0	0	0	0	0	0	1.5	0
E9PLT0	0	0	3	0	0	0	0	0	0	0	1.5	0
H0Y650	0	0	3	0	0	0	0	0	0	0	1.5	0
K7EK33	0	0	3	0	0	0	0	0	0	0	1.5	0
P19623	0	0	2	0	0	0	1	0	0	0	1.5	0
P63167	0	0	2	0	0	0	1	0	0	0	1.5	0
Q8N3R9	0	0	3	0	0	0	0	0	0	0	1.5	0
Q9NRN7	0	0	3	0	0	0	0	0	0	0	1.5	0
P31151	3	4	2	1	2	0	0	0	2.5	2	1	0.5
P37108	2	0	1	0	2	0	1	0	2	0	1	0
Q8NC51	4	1	2	0	0	0	0	0	2	0.5	1	0
P43487	3	0	2	0	1	0	0	0	2	0	1	0
E7EQU1	1	0	0	0	2	1	2	0	1.5	0.5	1	0
P48556	2	3	1	3	1	0	1	0	1.5	1.5	1	1.5
P26639	3	0	2	1	0	0	0	0	1.5	0	1	0.5
E9PHA6	2	0	2	0	1	0	0	0	1.5	0	1	0
K7EN45	2	0	2	0	1	0	0	0	1.5	0	1	0
EFC4EBP1	1	1	0	2	1	3	2	1	1	2	1	1.5
A0A087WXI3	2	1	1	1	0	0	1	0	1	0.5	1	0.5
P01859	1	2	2	2	1	0	0	1	1	1	1	1.5
Q9Y383	2	1	2	1	0	0	0	0	1	0.5	1	0.5
D3YTI2	1	1	1	0	1	1	1	0	1	1	1	0
Q9UHV9	1	0	1	2	1	0	1	0	1	0	1	1
H3BQN4	2	1	2	0	0	0	0	0	1	0.5	1	0
O00232	2	1	1	0	0	0	1	0	1	0.5	1	0
O75131	2	0	0	0	0	0	2	0	1	0	1	0
P12955	2	0	1	0	0	0	1	0	1	0	1	0
Q14236	2	0	2	0	0	0	0	0	1	0	1	0
P68032	1	0	2	1	0	0	0	0	0.5	0	1	0.5
F8VZX2	0	0	0	1	1	0	2	0	0.5	0	1	0.5
F5H2F4	0	0	1	0	1	0	1	0	0.5	0	1	0
P62258	1	0	2	1	0	0	0	0	0.5	0	1	0.5
Q8N0Z9-2	1	0	1	2	0	0	1	0	0.5	0	1	1
Q9BW04	1	1	2	0	0	0	0	0	0.5	0.5	1	0
C9J381	1	0	2	0	0	0	0	0	0.5	0	1	0
Q9BTE3	1	0	2	2	0	0	0	0	0.5	0	1	1
J3QLI9	0	1	1	0	1	1	1	1	0.5	1	1	0.5
F5GX77	1	0	2	2	0	0	0	0	0.5	0	1	1

P52907	1	0	2	0	0	0	0	0	0.5	0	1	0
Q8TF72	1	1	1	1	0	0	1	0	0.5	0.5	1	0.5
C9JIZ0	1	0	1	1	0	0	1	0	0.5	0	1	0.5
P11413	1	1	2	0	0	0	0	0	0.5	0.5	1	0
P08708	0	0	0	0	1	1	2	0	0.5	0.5	1	0
M0R0K9	1	0	2	0	0	0	0	0	0.5	0	1	0
P11172	1	0	2	0	0	0	0	0	0.5	0	1	0
Q5MNZ6	1	0	2	0	0	0	0	0	0.5	0	1	0
Q96QK1	1	0	2	0	0	0	0	0	0.5	0	1	0
Q9Y4C2	1	0	2	0	0	0	0	0	0.5	0	1	0
B1AHB1	0	0	2	0	1	0	0	0	0.5	0	1	0
B7Z6Z4	0	5	2	2	0	0	0	0	0	2.5	1	1
Q8NBF2	0	0	2	5	0	0	0	0	0	0	1	2.5
K7ERV3	0	2	1	1	0	0	1	0	0	1	1	0.5
P59025	0	0	1	1	0	0	1	0	0	0	1	0.5
B4DXZ6	0	0	0	0	0	0	2	1	0	0	1	0.5
P25398	0	2	2	0	0	0	0	0	0	1	1	0
Q13547	0	1	2	1	0	0	0	0	0	0.5	1	0.5
Q4G163	0	0	2	0	0	0	0	0	0	0	1	0
Q9Y5L4	0	0	2	2	0	0	0	0	0	0	1	1
B1AMS2	0	0	2	1	0	0	0	0	0	0	1	0.5
C9JZW3	0	0	2	1	0	0	0	0	0	0	1	0.5
G5E9W3	0	0	1	1	0	0	1	0	0	0	1	0.5
Q15024	0	0	2	1	0	0	0	0	0	0	1	0.5
A0A087WUW6	0	0	2	0	0	0	0	0	0	0	1	0
A0A087X2G1	0	0	0	0	0	0	2	0	0	0	1	0
A0A0C4DGX4	0	0	2	0	0	0	0	0	0	0	1	0
A0A1B0GTC3	0	0	2	0	0	0	0	0	0	0	1	0
C9JSQ1	0	0	1	0	0	0	1	0	0	0	1	0
E5RGS4	0	0	1	0	0	0	1	0	0	0	1	0
E7EPP6	0	0	1	0	0	0	1	0	0	0	1	0
F5H2T0	0	0	2	0	0	0	0	0	0	0	1	0
H0Y8B3	0	0	2	0	0	0	0	0	0	0	1	0
I3L2B0	0	0	1	0	0	0	1	0	0	0	1	0
J3KTM9	0	0	1	0	0	0	1	0	0	0	1	0
K7EIN2	0	0	2	0	0	0	0	0	0	0	1	0
M0R1M5	0	0	0	0	0	0	2	0	0	0	1	0
P11678	0	0	1	0	0	0	1	0	0	0	1	0
P14735	0	0	2	0	0	0	0	0	0	0	1	0
P26196	0	0	1	0	0	0	1	0	0	0	1	0
P56537	0	0	2	0	0	0	0	0	0	0	1	0
Q06330	0	0	2	0	0	0	0	0	0	0	1	0
Q8IXB1	0	0	2	0	0	0	0	0	0	0	1	0
Q8WUM4	0	0	2	0	0	0	0	0	0	0	1	0
Q9BPU6	0	0	0	0	0	0	2	0	0	0	1	0
B7Z9C2	2	1	1	0	2	0	0	0	2	0.5	0.5	0
H3BPE7	3	1	1	1	1	0	0	0	2	0.5	0.5	0.5
P29508	2	2	1	1	1	0	0	0	1.5	1	0.5	0.5
O60826	3	0	1	0	0	0	0	0	1.5	0	0.5	0
P31153	2	0	1	0	1	0	0	0	1.5	0	0.5	0
Q66LE6	2	1	1	3	0	0	0	1	1	0.5	0.5	2
P13647	2	0	0	2	0	0	1	0	1	0	0.5	1
CASB_BOVIN	2	0	1	2	0	0	0	0	1	0	0.5	1
P05204	2	1	1	0	0	1	0	2	1	1	0.5	1
E9PM69	2	2	0	1	0	0	1	0	1	1	0.5	0.5
H0YIE9	2	0	1	1	0	0	0	0	1	0	0.5	0.5
Q86YZ3	2	0	1	3	0	0	0	0	1	0	0.5	1.5
O00231	2	1	0	1	0	0	1	0	1	0.5	0.5	0.5
P62851	2	1	1	1	0	0	0	0	1	0.5	0.5	0.5
A0A087X2D0	1	1	0	1	1	0	1	0	1	0.5	0.5	0.5
A0A0B4J1R6	1	1	1	1	1	0	0	0	1	0.5	0.5	0.5
K7EKP8	2	0	1	1	0	0	0	0	1	0	0.5	0.5
P00338	2	0	1	1	0	0	0	0	1	0	0.5	0.5
D6RG13	1	0	0	0	1	0	1	1	1	0	0.5	0.5
B5MCX3	2	0	1	0	0	0	0	0	1	0	0.5	0

E9PRH9	2	0	1	0	0	0	0	0	1	0	0.5	0
F8WCF6	2	0	1	0	0	0	0	0	1	0	0.5	0
Q9BTY7	2	0	1	0	0	0	0	0	1	0	0.5	0
Q9H773	2	0	1	0	0	0	0	0	1	0	0.5	0
H0YC04	1	0	1	0	1	0	0	0	1	0	0.5	0
P34931	1	2	1	1	0	0	0	0	0.5	1	0.5	0.5
A0A0C4DGB6	1	3	1	0	0	0	0	0	0.5	1.5	0.5	0
P27361	0	0	1	1	1	0	0	0	0.5	0	0.5	0.5
P62191	1	5	0	1	0	0	1	1	0.5	2.5	0.5	1
O76041	1	0	0	1	0	1	1	0	0.5	0.5	0.5	0.5
Q96JK2	1	4	1	2	0	0	0	0	0.5	2	0.5	1
C9JKF1	0	1	1	1	1	0	0	0	0.5	0.5	0.5	0.5
Q96DG6	1	4	1	1	0	0	0	0	0.5	2	0.5	0.5
D6RAX2	1	1	1	2	0	0	0	0	0.5	0.5	0.5	1
F6RFD5	1	0	1	0	0	0	0	0	0.5	0	0.5	0
O00487	1	1	0	2	0	0	1	0	0.5	0.5	0.5	1
Q96R54	1	0	0	0	0	1	1	0	0.5	0.5	0.5	0
Q9NZR2	0	0	0	1	1	0	1	0	0.5	0	0.5	0.5
A0A087WV05	1	2	1	0	0	0	0	0	0.5	1	0.5	0
A0A087WYS6	1	1	1	1	0	0	0	0	0.5	0.5	0.5	0.5
E9PMD7	1	1	1	1	0	0	0	0	0.5	0.5	0.5	0.5
H3BM60	1	1	1	1	0	0	0	0	0.5	0.5	0.5	0.5
O75037	1	1	1	1	0	0	0	0	0.5	0.5	0.5	0.5
O75348	1	0	1	0	0	0	0	0	0.5	0	0.5	0
P04004	1	2	1	0	0	0	0	0	0.5	1	0.5	0
Q9Y294	1	1	1	0	0	0	0	0	0.5	0.5	0.5	0
P14174	0	1	0	1	1	0	1	0	0.5	0.5	0.5	0.5
A0A087WX29	1	0	1	1	0	0	0	0	0.5	0	0.5	0.5
A0A0A0MSX9	1	0	1	1	0	0	0	0	0.5	0	0.5	0.5
A0A0C4DGL3	1	1	1	0	0	0	0	0	0.5	0.5	0.5	0
K7EPK0	1	0	1	1	0	0	0	0	0.5	0	0.5	0.5
O00483	1	0	0	0	0	1	1	0	0.5	0.5	0.5	0
O15085	1	0	1	0	0	0	0	1	0.5	0	0.5	0.5
O43592	1	0	1	1	0	0	0	0	0.5	0	0.5	0.5
B5MCP9	0	0	0	0	1	1	1	0	0.5	0.5	0.5	0
G3V1S7	0	0	0	0	1	0	1	1	0.5	0	0.5	0.5
H7C3G1	0	0	0	0	1	0	1	1	0.5	0	0.5	0.5
Q9UM47	0	0	1	0	1	1	0	0	0.5	0.5	0.5	0
Q9Y4R8	0	0	1	1	1	0	0	0	0.5	0	0.5	0.5
A0A087X027	1	0	1	0	0	0	0	0	0.5	0	0.5	0
A0A087X1R4	1	0	1	0	0	0	0	0	0.5	0	0.5	0
A0A0D9SFL3	1	0	1	0	0	0	0	0	0.5	0	0.5	0
A0A0G2JIC2	1	0	1	0	0	0	0	0	0.5	0	0.5	0
A8MWD9	1	0	1	0	0	0	0	0	0.5	0	0.5	0
B4E0K5	1	0	1	0	0	0	0	0	0.5	0	0.5	0
B8ZZU8	1	0	1	0	0	0	0	0	0.5	0	0.5	0
C9IZ80	1	0	1	0	0	0	0	0	0.5	0	0.5	0
C9JZD1	1	0	1	0	0	0	0	0	0.5	0	0.5	0
E9PF46	1	0	1	0	0	0	0	0	0.5	0	0.5	0
H0Y580	1	0	1	0	0	0	0	0	0.5	0	0.5	0
J3KPM9	1	0	1	0	0	0	0	0	0.5	0	0.5	0
K7ENA8	1	0	1	0	0	0	0	0	0.5	0	0.5	0
M0R261	1	0	1	0	0	0	0	0	0.5	0	0.5	0
P25705	1	0	1	0	0	0	0	0	0.5	0	0.5	0
P58546	1	0	0	0	0	0	1	0	0.5	0	0.5	0
P62306	1	0	1	0	0	0	0	0	0.5	0	0.5	0
Q05519	1	0	1	0	0	0	0	0	0.5	0	0.5	0
Q96DI7	1	0	1	0	0	0	0	0	0.5	0	0.5	0
Q9BYN0	1	0	0	0	0	0	1	0	0.5	0	0.5	0
Q9H1R2	1	0	1	0	0	0	0	0	0.5	0	0.5	0
Q9H3P7	1	0	1	0	0	0	0	0	0.5	0	0.5	0
Q9NSY0-2	1	0	1	0	0	0	0	0	0.5	0	0.5	0
Q9UPV7	1	0	1	0	0	0	0	0	0.5	0	0.5	0
O15397	0	0	1	0	1	0	0	0	0.5	0	0.5	0
Q5T3E1	0	0	1	0	1	0	0	0	0.5	0	0.5	0

Q562R1	0	0	0	0	0	0	1	0	0	0	0.5	0
A0A024QZP7	0	0	1	0	0	0	0	0	0	0	0.5	0
E7ESI2	0	0	1	0	0	0	0	0	0	0	0.5	0
O76003	0	1	1	4	0	0	0	0	0	0.5	0.5	2
P07996	0	0	0	0	0	1	1	0	0	0.5	0.5	0
P14625	0	0	1	0	0	0	0	0	0	0	0.5	0
P43686	0	2	0	0	0	1	1	0	0	1.5	0.5	0
P45983	0	0	0	0	0	1	1	0	0	0.5	0.5	0
P62829	0	0	1	3	0	0	0	0	0	0	0.5	1.5
Q01813	0	0	1	0	0	0	0	0	0	0	0.5	0
Q9NVP2	0	0	0	3	0	0	1	0	0	0	0.5	1.5
A0A087WT12	0	1	0	1	0	0	1	0	0	0.5	0.5	0.5
B1AKJ5	0	0	1	2	0	0	0	0	0	0	0.5	1
O60814	0	1	0	1	0	0	1	0	0	0.5	0.5	0.5
O75506	0	0	1	2	0	0	0	0	0	0	0.5	1
P08237	0	0	1	1	0	0	0	0	0	0	0.5	0.5
P33993	0	0	1	2	0	0	0	0	0	0	0.5	1
Q13643	0	1	1	0	0	1	0	0	0	1	0.5	0
Q15181	0	0	1	2	0	0	0	0	0	0	0.5	1
Q6TFL3	0	1	0	0	0	0	1	1	0	0.5	0.5	0.5
Q6TFL3-3	0	0	0	1	0	0	1	1	0	0	0.5	1
Q8NBK3	0	0	1	2	0	0	0	0	0	0	0.5	1
Q9NUP9	0	1	1	1	0	0	0	0	0	0.5	0.5	0.5
A0A024RA52	0	1	1	0	0	0	0	0	0	0.5	0.5	0
A0A0B4J207	0	1	0	0	0	0	1	0	0	0.5	0.5	0
A2RRP1	0	0	1	0	0	0	0	1	0	0	0.5	0.5
B1AHE4	0	0	1	1	0	0	0	0	0	0	0.5	0.5
D6RCP9	0	1	1	0	0	0	0	0	0	0.5	0.5	0
F6TLX2	0	0	1	1	0	0	0	0	0	0	0.5	0.5
H3BN98	0	0	0	0	0	0	1	1	0	0	0.5	0.5
J3KNF4	0	0	1	1	0	0	0	0	0	0	0.5	0.5
P07814	0	1	1	0	0	0	0	0	0	0.5	0.5	0
P12004	0	1	1	0	0	0	0	0	0	0.5	0.5	0
P14854	0	0	1	1	0	0	0	0	0	0	0.5	0.5
P31025	0	1	1	0	0	0	0	0	0	0.5	0.5	0
Q01581	0	0	1	1	0	0	0	0	0	0	0.5	0.5
Q04760	0	0	1	1	0	0	0	0	0	0	0.5	0.5
Q8N1N4	0	0	0	0	0	0	1	0	0	0	0.5	0
Q9BUA3	0	0	1	1	0	0	0	0	0	0	0.5	0.5
A0A087WXX9	0	0	1	0	0	0	0	0	0	0	0.5	0
A0A087X0B7	0	0	0	0	0	0	1	0	0	0	0.5	0
A0A0A0MTI9	0	0	1	0	0	0	0	0	0	0	0.5	0
A0A0U1RQC5	0	0	1	0	0	0	0	0	0	0	0.5	0
A3KFL1	0	0	0	0	0	0	1	0	0	0	0.5	0
B0QYA4	0	0	0	0	0	0	1	0	0	0	0.5	0
B1AK87	0	0	1	0	0	0	0	0	0	0	0.5	0
B3KQ25	0	0	1	0	0	0	0	0	0	0	0.5	0
B4DWH1	0	0	0	0	0	0	1	0	0	0	0.5	0
B4E3M2	0	0	1	0	0	0	0	0	0	0	0.5	0
B5MD17	0	0	1	0	0	0	0	0	0	0	0.5	0
C9J2Y4	0	0	1	0	0	0	0	0	0	0	0.5	0
C9J2Y9	0	0	1	0	0	0	0	0	0	0	0.5	0
C9J3R0	0	0	1	0	0	0	0	0	0	0	0.5	0
C9JUY3	0	0	1	0	0	0	0	0	0	0	0.5	0
C9JV77	0	0	1	0	0	0	0	0	0	0	0.5	0
D6RBM8	0	0	0	0	0	0	1	0	0	0	0.5	0
E3W980	0	0	0	0	0	0	1	0	0	0	0.5	0
E7EMG7	0	0	1	0	0	0	0	0	0	0	0.5	0
E7EMZ0	0	0	0	0	0	0	1	0	0	0	0.5	0
E7EWC5	0	0	1	0	0	0	0	0	0	0	0.5	0
E7EWD3	0	0	0	0	0	0	1	0	0	0	0.5	0
E9PFW2	0	0	1	0	0	0	0	0	0	0	0.5	0
E9PMM9	0	0	0	0	0	0	1	0	0	0	0.5	0
F5H6T1	0	0	1	0	0	0	0	0	0	0	0.5	0
F8W1B7	0	0	0	0	0	0	1	0	0	0	0.5	0

G3V4T5	0	0	1	0	0	0	0	0	0	0	0.5	0
H0YCK3	0	0	1	0	0	0	0	0	0	0	0.5	0
H0YHR9	0	0	1	0	0	0	0	0	0	0	0.5	0
I3L106	0	0	1	0	0	0	0	0	0	0	0.5	0
M0R1Q8	0	0	1	0	0	0	0	0	0	0	0.5	0
M0R338	0	0	0	0	0	0	1	0	0	0	0.5	0
O00165	0	0	0	0	0	0	1	0	0	0	0.5	0
O14787-2	0	0	1	0	0	0	0	0	0	0	0.5	0
O14965	0	0	0	0	0	0	1	0	0	0	0.5	0
O43252	0	0	1	0	0	0	0	0	0	0	0.5	0
O43543	0	0	1	0	0	0	0	0	0	0	0.5	0
O75419	0	0	1	0	0	0	0	0	0	0	0.5	0
P15259	0	0	1	0	0	0	0	0	0	0	0.5	0
P23280	0	0	1	0	0	0	0	0	0	0	0.5	0
P28562	0	0	1	0	0	0	0	0	0	0	0.5	0
P32241-2	0	0	0	0	0	0	1	0	0	0	0.5	0
P49770	0	0	1	0	0	0	0	0	0	0	0.5	0
P59510-2	0	0	1	0	0	0	0	0	0	0	0.5	0
P60174	0	0	0	0	0	0	1	0	0	0	0.5	0
Q07973	0	0	1	0	0	0	0	0	0	0	0.5	0
Q08945	0	0	1	0	0	0	0	0	0	0	0.5	0
Q0VDF9	0	0	1	0	0	0	0	0	0	0	0.5	0
Q12852	0	0	1	0	0	0	0	0	0	0	0.5	0
Q13451	0	0	1	0	0	0	0	0	0	0	0.5	0
Q15084	0	0	0	0	0	0	1	0	0	0	0.5	0
Q52LJ0	0	0	0	0	0	0	1	0	0	0	0.5	0
Q5T1S4	0	0	1	0	0	0	0	0	0	0	0.5	0
Q5T6H7	0	0	1	0	0	0	0	0	0	0	0.5	0
Q5W0B1	0	0	1	0	0	0	0	0	0	0	0.5	0
Q6ZVT6-2	0	0	1	0	0	0	0	0	0	0	0.5	0
Q7Z2T5	0	0	1	0	0	0	0	0	0	0	0.5	0
Q7Z6Z7	0	0	1	0	0	0	0	0	0	0	0.5	0
Q86Y25	0	0	1	0	0	0	0	0	0	0	0.5	0
Q8NFU7	0	0	0	0	0	0	1	0	0	0	0.5	0
Q8WXH2	0	0	1	0	0	0	0	0	0	0	0.5	0
Q96P70	0	0	1	0	0	0	0	0	0	0	0.5	0
Q96PK6-5	0	0	1	0	0	0	0	0	0	0	0.5	0
Q9BRX2	0	0	1	0	0	0	0	0	0	0	0.5	0
Q9BWD1	0	0	1	0	0	0	0	0	0	0	0.5	0
Q9H069	0	0	0	0	0	0	1	0	0	0	0.5	0
Q9NWU2	0	0	1	0	0	0	0	0	0	0	0.5	0
Q9NX55	0	0	1	0	0	0	0	0	0	0	0.5	0
Q9UBB9	0	0	0	0	0	0	1	0	0	0	0.5	0
Q9UBF6	0	0	1	0	0	0	0	0	0	0	0.5	0
Q9UBQ7	0	0	0	0	0	0	1	0	0	0	0.5	0
Q9Y3Z3	0	0	1	0	0	0	0	0	0	0	0.5	0
S4R3T0	0	0	0	0	0	0	1	0	0	0	0.5	0
A0A0C4DGQ5	6	1	0	0	2	0	0	0	4	0.5	0	0
Q14344	1	1	0	1	3	1	0	0	2	1	0	0.5
E7EQ64	1	0	0	1	2	0	0	0	1.5	0	0	0.5
P05109	0	0	0	1	3	0	0	0	1.5	0	0	0.5
Q15008	2	1	0	1	1	0	0	0	1.5	0.5	0	0.5
F8W1S1	1	0	0	0	1	0	0	0	1	0	0	0
Q9H361	2	0	0	0	0	0	0	2	1	0	0	1
A0A0A0MRG9	0	0	0	1	2	0	0	3	1	0	0	2
A6PVX3	1	1	0	1	1	0	0	0	1	0.5	0	0.5
Q9NQ29	2	0	0	0	0	0	0	0	1	0	0	0
O14929	2	0	0	0	0	0	0	0	1	0	0	0
P62304	2	0	0	0	0	0	0	0	1	0	0	0
Q92572	2	0	0	0	0	0	0	0	1	0	0	0
Q9Y3F4	2	0	0	0	0	0	0	0	1	0	0	0
P81605	1	2	0	1	0	0	0	4	0.5	1	0	2.5
Q9Y657	1	2	0	1	0	0	0	0	0.5	1	0	0.5
Q15751	0	0	0	1	1	0	0	0	0.5	0	0	0.5
A0A087X0G5	1	0	0	0	0	2	0	0	0.5	1	0	0

H0Y614	1	1	0	1	0	0	0	0	0.5	0.5	0	0.5
Q5D862	1	0	0	0	0	1	0	1	0.5	0.5	0	0.5
Q9UP83	1	1	0	1	0	0	0	0	0.5	0.5	0	0.5
A0A1B0GU80	0	0	0	1	1	1	0	0	0.5	0.5	0	0.5
M0R132	0	0	0	0	1	1	0	1	0.5	0.5	0	0.5
Q562F6	0	1	0	0	1	1	0	0	0.5	1	0	0
Q9Y5H6	0	0	0	0	1	0	0	2	0.5	0	0	1
E7EX17	1	1	0	0	0	0	0	0	0.5	0.5	0	0
E9PL10	1	1	0	0	0	0	0	0	0.5	0.5	0	0
H3BQH3	1	1	0	0	0	0	0	0	0.5	0.5	0	0
O95398-2	1	0	0	1	0	0	0	0	0.5	0	0	0.5
P49643	1	0	0	1	0	0	0	0	0.5	0	0	0.5
P49915	1	1	0	0	0	0	0	0	0.5	0.5	0	0
Q8NFC6	1	1	0	0	0	0	0	0	0.5	0.5	0	0
H3BSW0	0	0	0	0	1	0	0	1	0.5	0	0	0.5
Q99459	0	0	0	0	1	1	0	0	0.5	0.5	0	0
Q9P2P6	0	0	0	1	1	0	0	0	0.5	0	0	0.5
Q9UPU7	0	0	0	0	1	0	0	1	0.5	0	0	0.5
A0A0X1KG71	1	0	0	0	0	0	0	0	0.5	0	0	0
A8MT37	1	0	0	0	0	0	0	0	0.5	0	0	0
A8MTY9	1	0	0	0	0	0	0	0	0.5	0	0	0
B4DKY1	1	0	0	0	0	0	0	0	0.5	0	0	0
C9J5P6	1	0	0	0	0	0	0	0	0.5	0	0	0
E5RI99	1	0	0	0	0	0	0	0	0.5	0	0	0
E9PAV3	1	0	0	0	0	0	0	0	0.5	0	0	0
E9PHS0	1	0	0	0	0	0	0	0	0.5	0	0	0
F8W810	1	0	0	0	0	0	0	0	0.5	0	0	0
G3V3M6	1	0	0	0	0	0	0	0	0.5	0	0	0
G3V4W4	1	0	0	0	0	0	0	0	0.5	0	0	0
H0Y4E5	1	0	0	0	0	0	0	0	0.5	0	0	0
J3KNE3	1	0	0	0	0	0	0	0	0.5	0	0	0
O43172	1	0	0	0	0	0	0	0	0.5	0	0	0
P03891	1	0	0	0	0	0	0	0	0.5	0	0	0
P14923	1	0	0	0	0	0	0	0	0.5	0	0	0
Q09161	1	0	0	0	0	0	0	0	0.5	0	0	0
Q12874	1	0	0	0	0	0	0	0	0.5	0	0	0
Q15645	1	0	0	0	0	0	0	0	0.5	0	0	0
Q5SYB0-2	1	0	0	0	0	0	0	0	0.5	0	0	0
Q86U90	1	0	0	0	0	0	0	0	0.5	0	0	0
Q8N8D9	1	0	0	0	0	0	0	0	0.5	0	0	0
Q8N8L2	1	0	0	0	0	0	0	0	0.5	0	0	0
Q96GM8	1	0	0	0	0	0	0	0	0.5	0	0	0
Q9HB03	1	0	0	0	0	0	0	0	0.5	0	0	0
B2RPK0	0	0	0	0	1	0	0	0	0.5	0	0	0
B5ME19	0	0	0	0	1	0	0	0	0.5	0	0	0
E7ERC4	0	0	0	0	1	0	0	0	0.5	0	0	0
F8VQQ8	0	0	0	0	1	0	0	0	0.5	0	0	0
K7EKB9	0	0	0	0	1	0	0	0	0.5	0	0	0
O43379-2	0	0	0	0	1	0	0	0	0.5	0	0	0
O75934	0	0	0	0	1	0	0	0	0.5	0	0	0
P05412	0	0	0	0	1	0	0	0	0.5	0	0	0
P26678	0	0	0	0	1	0	0	0	0.5	0	0	0
P48751	0	0	0	0	1	0	0	0	0.5	0	0	0
P54296	0	0	0	0	1	0	0	0	0.5	0	0	0
Q7Z7K2	0	0	0	0	1	0	0	0	0.5	0	0	0
Q96HQ2	0	0	0	0	1	0	0	0	0.5	0	0	0
Q96NY8	0	0	0	0	1	0	0	0	0.5	0	0	0
Q9NS62	0	0	0	0	1	0	0	0	0.5	0	0	0
Q9UJX2	0	0	0	0	1	0	0	0	0.5	0	0	0
Q05639	0	0	0	1	0	0	0	0	0	0	0	0.5
C9JUM1	0	0	0	1	0	0	0	0	0	0	0	0.5
Q8TEB1	0	9	0	4	0	0	0	0	0	4.5	0	2
A0A087WX41	0	0	0	0	0	1	0	0	0	0.5	0	0
A0A087WUW9	0	0	0	3	0	0	0	0	0	0	0	1.5
P30048	0	1	0	2	0	0	0	0	0	0.5	0	1

P54687	0	0	0	3	0	0	0	0	0	0	0	1.5
A0A087WWM6	0	2	0	0	0	0	0	0	0	1	0	0
C9J8P9	0	1	0	1	0	0	0	0	0	0.5	0	0.5
G3V3W4	0	1	0	1	0	0	0	0	0	0.5	0	0.5
H3BUZ6	0	1	0	1	0	0	0	0	0	0.5	0	0.5
K7ELC7	0	1	0	1	0	0	0	0	0	0.5	0	0.5
N0DVX5	0	1	0	1	0	0	0	0	0	0.5	0	0.5
O60884	0	0	0	2	0	0	0	0	0	0	0	1
Q5SY68	0	1	0	1	0	0	0	0	0	0.5	0	0.5
Q9Y3E2	0	0	0	2	0	0	0	0	0	0	0	1
Q9Y678	0	1	0	1	0	0	0	0	0	0.5	0	0.5
A0A087WTN8	0	1	0	0	0	0	0	0	0	0.5	0	0
A0A087WUB1	0	0	0	0	0	1	0	0	0	0.5	0	0
A0A087WYC6	0	0	0	0	0	0	0	1	0	0	0	0.5
A0A087WYD6	0	0	0	1	0	0	0	0	0	0	0	0.5
A0A0A0MRV0	0	0	0	1	0	0	0	0	0	0	0	0.5
A0A0A0MSS2	0	0	0	1	0	0	0	0	0	0	0	0.5
A0A0A0MTS7	0	0	0	1	0	0	0	0	0	0	0	0.5
A0A0B4J1R5	0	0	0	1	0	0	0	0	0	0	0	0.5
A0A0B4J1X7	0	1	0	0	0	0	0	0	0	0.5	0	0
A0A0C4DFX2	0	0	0	1	0	0	0	0	0	0	0	0.5
A0A0C4DG21	0	0	0	0	0	0	0	1	0	0	0	0.5
A0A0C4DGF8	0	0	0	0	0	0	0	1	0	0	0	0.5
A0A0D9SFZ1	0	0	0	0	0	1	0	0	0	0.5	0	0
A0A0G2JMX7	0	0	0	1	0	0	0	0	0	0	0	0.5
A0A0U1RRB6	0	0	0	0	0	1	0	0	0	0.5	0	0
A0A1B0GWD6	0	1	0	0	0	0	0	0	0	0.5	0	0
A1XBS5	0	0	0	0	0	0	0	1	0	0	0	0.5
A6NER6	0	0	0	1	0	0	0	0	0	0	0	0.5
B1AH59	0	0	0	0	0	0	0	1	0	0	0	0.5
B1AKR6	0	0	0	1	0	0	0	0	0	0	0	0.5
B1AQK6	0	1	0	0	0	0	0	0	0	0.5	0	0
B7Z4B8	0	0	0	0	0	0	0	1	0	0	0	0.5
B7Z4C8	0	0	0	0	0	0	0	1	0	0	0	0.5
C9J4I9	0	1	0	0	0	0	0	0	0	0.5	0	0
C9JK86	0	0	0	0	0	0	0	1	0	0	0	0.5
E9PC47	0	0	0	0	0	1	0	0	0	0.5	0	0
E9PM04	0	0	0	1	0	0	0	0	0	0	0	0.5
E9PMG9	0	1	0	0	0	0	0	0	0	0.5	0	0
E9PRF2	0	0	0	0	0	1	0	0	0	0.5	0	0
F8VVT9	0	0	0	1	0	0	0	0	0	0	0	0.5
F8W9P2	0	0	0	0	0	0	0	1	0	0	0	0.5
G5E9M4	0	0	0	1	0	0	0	0	0	0	0	0.5
H3BNW8	0	0	0	0	0	0	0	1	0	0	0	0.5
H7BZ54	0	0	0	1	0	0	0	0	0	0	0	0.5
H7C346	0	0	0	1	0	0	0	0	0	0	0	0.5
H7C5S0	0	0	0	1	0	0	0	0	0	0	0	0.5
H9KV93	0	0	0	0	0	1	0	0	0	0.5	0	0
I3L1D5	0	0	0	1	0	0	0	0	0	0	0	0.5
J3KNW5	0	0	0	0	0	0	0	1	0	0	0	0.5
K7EIK4	0	0	0	0	0	0	0	1	0	0	0	0.5
O14514	0	0	0	1	0	0	0	0	0	0	0	0.5
O15212	0	0	0	1	0	0	0	0	0	0	0	0.5
O60522	0	1	0	0	0	0	0	0	0	0.5	0	0
O60551	0	0	0	0	0	1	0	0	0	0.5	0	0
O75592	0	0	0	0	0	1	0	0	0	0.5	0	0
O95278	0	1	0	0	0	0	0	0	0	0.5	0	0
P01037	0	1	0	0	0	0	0	0	0	0.5	0	0
P01570	0	0	0	1	0	0	0	0	0	0	0	0.5
P05386	0	0	0	1	0	0	0	0	0	0	0	0.5
P15927	0	1	0	0	0	0	0	0	0	0.5	0	0
P20618	0	1	0	0	0	0	0	0	0	0.5	0	0
P21399	0	0	0	1	0	0	0	0	0	0	0	0.5
P41212	0	0	0	1	0	0	0	0	0	0	0	0.5
P55884	0	1	0	0	0	0	0	0	0	0.5	0	0

Q15056	0	1	0	0	0	0	0	0	0	0.5	0	0
Q3KQV3	0	0	0	0	0	1	0	0	0	0.5	0	0
Q4J6C6	0	1	0	0	0	0	0	0	0	0.5	0	0
Q502W7	0	1	0	0	0	0	0	0	0	0.5	0	0
Q5TB80	0	0	0	0	0	1	0	0	0	0.5	0	0
Q5VU13-2	0	1	0	0	0	0	0	0	0	0.5	0	0
Q5VUC0	0	0	0	0	0	0	0	1	0	0	0	0.5
Q5VYS8	0	0	0	0	0	0	0	1	0	0	0	0.5
Q6NSW5	0	0	0	0	0	0	0	1	0	0	0	0.5
Q6P0N0	0	1	0	0	0	0	0	0	0	0.5	0	0
Q6WRI0	0	0	0	0	0	0	0	1	0	0	0	0.5
Q7L0X2	0	0	0	0	0	1	0	0	0	0.5	0	0
Q8IWV7	0	1	0	0	0	0	0	0	0	0.5	0	0
Q8TB03	0	0	0	1	0	0	0	0	0	0	0	0.5
Q92674	0	1	0	0	0	0	0	0	0	0.5	0	0
Q96BQ3	0	1	0	0	0	0	0	0	0	0.5	0	0
Q96N38-2	0	1	0	0	0	0	0	0	0	0.5	0	0
Q9BPW9	0	0	0	1	0	0	0	0	0	0	0	0.5
Q9BRF8	0	0	0	1	0	0	0	0	0	0	0	0.5
Q9BU76	0	0	0	0	0	1	0	0	0	0.5	0	0
Q9NP61	0	1	0	0	0	0	0	0	0	0.5	0	0
Q9NP77	0	1	0	0	0	0	0	0	0	0.5	0	0
Q9NTX9	0	0	0	0	0	0	0	1	0	0	0	0.5
Q9Y219	0	0	0	0	0	1	0	0	0	0.5	0	0
Q9Y238-3	0	0	0	1	0	0	0	0	0	0	0	0.5

Appendix D

All Protein IDs from PhAXA-MS with 4E-BP1 (S101C) as Bait

| | | PSMs | | |
DEFLINE	4E-BP1 (WT) + **1**	4E-BP1 (WT) ATP ctl	4E-BP1 (S101C) + **1**	4E-BP1 (S101C) ATP ctl
Eukaryotic translation initiation factor 4E-bindii	2264	2405	2220	2584
sp TRYP_PIG	204	214	224	299
Keratin, type II cytoskeletal 1 OS=Homo sapiens	44	30	169	40
Keratin, type I cytoskeletal 10 OS=Homo sapien	30	30	136	27
Isoform of P06730, Eukaryotic translation initia	126	147	113	134
Heat shock cognate 71 kDa protein OS=Homo s	136	119	108	88
Keratin, type II cytoskeletal 2 epidermal OS=Ho	18	14	85	11
78 kDa glucose-regulated protein OS=Homo sap	102	97	80	97
General transcription factor II-I OS=Homo sapie	43	50	71	36
Isoform of P0DMV9, Heat shock 70 kDa protein	36	38	48	22
Peroxiredoxin-4 OS=Homo sapiens GN=PRDX4 I	53	43	46	37
Tubulin alpha-1B chain OS=Homo sapiens GN=T	29	25	41	32
Tubulin beta chain OS=Homo sapiens GN=TUBE	36	22	39	30
sp PRDX1_HUMAN	39	33	26	42
T-complex protein 1 subunit theta OS=Homo sa	27	24	26	23
T-complex protein 1 subunit alpha OS=Homo sa	23	16	25	14
Thioredoxin OS=Homo sapiens GN=TXN PE=1 S\	12	1	22	3
Elongation factor 2 OS=Homo sapiens GN=EEF2	11	1	17	1
Poly(rC)-binding protein 1 OS=Homo sapiens GI	11	17	16	13
T-complex protein 1 subunit beta OS=Homo sap	14	11	16	5
Keratin, type II cytoskeletal 1b OS=Homo sapier	0	0	16	0
Elongation factor 1-alpha 1 OS=Homo sapiens C	14	8	15	10
sp ALBU_BOVIN	28	71	14	34
Isoform of Q9BY77, Polymerase delta-interactii	8	10	14	10
T-complex protein 1 subunit eta OS=Homo sapi	12	8	14	5
Keratin, type II cytoskeletal 5 OS=Homo sapiens	0	0	14	0
Keratin, type I cytoskeletal 9 OS=Homo sapiens	22	17	13	15
Isoform of Q86V81, THO complex subunit 4 OS=	10	10	13	6
Cytoplasmic dynein 1 heavy chain 1 OS=Homo s	4	6	13	7
DNA-dependent protein kinase catalytic subuni	6	1	13	1
Poly [ADP-ribose] polymerase 1 OS=Homo sapic	6	0	13	0
Keratinocyte proline-rich protein OS=Homo sap	0	0	13	0
Tubulin beta-4B chain OS=Homo sapiens GN=TI	2	0	11	0
Peroxiredoxin-2 OS=Homo sapiens GN=PRDX2 I	12	10	11	11
Isoform of P48643, T-complex protein 1 subuni	13	11	11	5
Actin, cytoplasmic 1 OS=Homo sapiens GN=ACT	12	6	11	7
Peroxiredoxin-6 OS=Homo sapiens GN=PRDX6 I	11	6	11	8
T-complex protein 1 subunit zeta OS=Homo sap	12	7	10	4

Protein				
Serine/threonine-protein phosphatase 2A 65 kD	11	7	10	5
Enhancer of rudimentary homolog OS=Homo sa	10	9	9	10
Isoform of Q9UHX1, Poly(U)-binding-splicing fac	11	12	9	7
Isoform of P13797, Plastin-3 OS=Homo sapiens	8	0	9	0
Filaggrin-2 OS=Homo sapiens GN=FLG2 PE=1 SV	3	4	9	0
Keratin, type I cytoskeletal 14 OS=Homo sapien	3	0	8	3
Isoform of P01857, Ig gamma-1 chain C region (	8	6	8	10
Cold-inducible RNA-binding protein OS=Homo s	5	6	8	10
Splicing factor 3B subunit 3 OS=Homo sapiens C	5	4	8	7
Peptidyl-prolyl cis-trans isomerase A OS=Homo	11	3	8	2
Isoform of P12268, Inosine-5_-monophosphate	16	0	8	0
Regulatory-associated protein of mTOR OS=Hor	6	1	8	2
T-complex protein 1 subunit gamma OS=Homo	3	2	8	2
Isoform of P49327, Fatty acid synthase OS=Hon	7	0	8	0
Isoform of P22234, Multifunctional protein ADE	5	1	8	1
Serine/threonine-protein phosphatase 2A catal	6	4	7	6
T-complex protein 1 subunit delta OS=Homo sa	1	2	7	2
Heat shock protein HSP 90-beta OS=Homo sapi	4	1	7	1
Isoform of P63241, Eukaryotic translation initia	3	1	7	2
Serine/threonine-protein phosphatase 2A 55 kD	8	4	6	5
RNA-binding protein 3 OS=Homo sapiens GN=R	6	5	6	6
Isoform of P09651, Heterogeneous nuclear ribo	6	5	6	6
Heterogeneous nuclear ribonucleoprotein R OS	3	0	6	1
Calpain-2 catalytic subunit OS=Homo sapiens G	4	0	6	0
Nucleolin OS=Homo sapiens GN=NCL PE=1 SV=:	1	0	6	3
ATP-citrate synthase OS=Homo sapiens GN=AC	3	0	6	0
Isoform of P05783, Keratin, type I cytoskeletal :	8	5	5	7
Isoform of Q08499, Isoform 12 of cAMP-specifi	5	7	5	5
Peroxiredoxin-5, mitochondrial OS=Homo sapie	5	3	5	3
Cyclin-dependent kinase 4 OS=Homo sapiens G	4	0	5	2
Isoform of Q14103, Heterogeneous nuclear ribo	3	1	5	2
Crk-like protein OS=Homo sapiens GN=CRKL PE	4	0	5	0
Isoform of Q92598, Heat shock protein 105 kDa	3	0	5	1
Heterogeneous nuclear ribonucleoprotein L OS	3	1	5	0
Non-POU domain-containing octamer-binding	3	0	5	0
Keratin, type II cytoskeletal 78 OS=Homo sapiei	0	0	5	0
Isoform of P05090, Apolipoprotein D (Fragmen	0	0	5	0
DNA damage-binding protein 1 OS=Homo sapie	3	3	4	6
Secernin-3 OS=Homo sapiens GN=SCRN3 PE=1 :	5	3	4	3
Eukaryotic translation initiation factor 3 subuni	3	2	4	4
Isoform of P23528, Cofilin-1 OS=Homo sapiens	3	4	4	2
Signal recognition particle 9 kDa protein OS=Ho	4	2	4	2
Heterogeneous nuclear ribonucleoproteins A2/	1	1	4	6
Nucleophosmin OS=Homo sapiens GN=NPM1 P	3	0	4	0
RuvB-like 2 OS=Homo sapiens GN=RUVBL2 PE=	2	2	4	1
Heterogeneous nuclear ribonucleoprotein F OS	1	0	4	0
Synaptic functional regulator FMR1 OS=Homo s	1	1	4	1

Histone-arginine methyltransferase CARM1 OS=	1	0	4	0
Isoform of P14618, Pyruvate kinase OS=Homo s	1	0	4	0
Actin, alpha cardiac muscle 1 OS=Homo sapiens	1	0	3	0
Isoform of Q9H3K6, BolA-like protein 2 OS=Hor	7	3	3	3
Histone-binding protein RBBP4 OS=Homo sapie	6	3	3	2
Isoform of Q16576, Histone-binding protein RB	0	0	3	2
sp TRY1_BOVIN	3	3	3	3
Isoform of Q96I15, Selenocysteine lyase OS=Ho	3	2	3	4
Transcription and mRNA export factor ENY2 OS	4	3	3	2
Peptidyl-prolyl cis-trans isomerase B OS=Homo	4	1	3	3
Cystatin-B OS=Homo sapiens GN=CSTB PE=1 SV	4	0	3	3
Low molecular weight phosphotyrosine protein	3	1	3	2
Heterogeneous nuclear ribonucleoprotein K OS	4	0	3	0
Isoform of P22061, Protein-L-isoaspartate O-m	4	0	3	0
Hypoxanthine-guanine phosphoribosyltransfera	3	0	3	1
Elongation factor 1-gamma OS=Homo sapiens (	1	0	3	1
Isoform of P19484, Transcription factor EB (Fra	1	0	3	1
Isoform of P04406, Glyceraldehyde-3-phosphat	2	0	3	0
Mitogen-activated protein kinase 1 OS=Homo s	0	0	3	2
X-ray repair cross-complementing protein 5 OS=	1	0	3	0
Serpin B12 OS=Homo sapiens GN=SERPINB12 P	0	0	3	0
Specifically androgen-regulated gene protein O	0	0	3	0
Isoform of P25311, Zinc-alpha-2-glycoprotein C	0	0	3	0
Isoform of Q15366, Poly(rC)-binding protein 2 (	0	0	2	0
Pre-mRNA-processing factor 19 OS=Homo sapie	3	3	2	2
PHD finger-like domain-containing protein 5A C	3	2	2	3
Band 3 anion transport protein OS=Homo sapie	4	4	2	0
116 kDa U5 small nuclear ribonucleoprotein co	3	1	2	1
Isoform of P0CG47, Polyubiquitin-B OS=Homo s	1	3	2	3
Isoform of P63162, Small nuclear ribonucleopro	2	1	2	2
14-3-3 protein epsilon OS=Homo sapiens GN=Y	2	1	2	1
Serine/threonine-protein kinase mTOR OS=Hon	3	0	2	0
Eukaryotic translation initiation factor 1A, X-chr	2	1	2	0
Protein S100-A7 OS=Homo sapiens GN=S100A7	1	0	2	2
40S ribosomal protein S28 OS=Homo sapiens G	3	0	2	0
Dermcidin OS=Homo sapiens GN=DCD PE=1 SV=	1	1	2	1
Protein RCC2 OS=Homo sapiens GN=RCC2 PE=1	3	0	2	0
Isoform of O15372, Eukaryotic translation initia	2	0	2	1
26S protease regulatory subunit 7 OS=Homo sa	1	0	2	1
Isoform of P27348, 14-3-3 protein theta (Fragn	2	0	2	0
Growth factor receptor-bound protein 2 OS=Hc	2	0	2	0
Isoform of Q99829, Copine-1 OS=Homo sapiens	2	0	2	0
Chromatin target of PRMT1 protein OS=Homo s	0	1	2	1
Isoform of Q99615, DnaJ homolog subfamily C	2	0	2	0
26S protease regulatory subunit 6B OS=Homo s	1	0	2	1
Caspase recruitment domain-containing protein	1	0	2	1
Eukaryotic translation initiation factor 3 subuni	1	1	2	0

Protein				
Isoform of Q9UJ70, N-acetyl-D-glucosamine kin	0	0	2	0
Transgelin-2 OS=Homo sapiens GN=TAGLN2 PE	1	0	2	0
Isoform of P52272, Heterogeneous nuclear ribo	1	0	2	0
Macrophage migration inhibitory factor OS=Ho	1	0	2	0
Ribonuclease P protein subunit p38 OS=Homo s	0	1	2	0
Plasminogen activator inhibitor 1 RNA-binding	1	0	2	0
Isoform of P26599, Polypyrimidine tract-bindin	1	0	2	0
Isoform of Q92841, Probable ATP-dependent R	0	0	2	0
Isoform of P17844, Probable ATP-dependent RI	0	0	2	0
Filaggrin OS=Homo sapiens GN=FLG PE=1 SV=3	0	0	2	0
Asparagine synthetase [glutamine-hydrolyzing]	0	0	2	0
Splicing factor, proline- and glutamine-rich OS=	0	0	2	0
Heterogeneous nuclear ribonucleoprotein A3 O	0	0	2	0
Isoform of P25205, DNA replication licensing fa	0	0	2	0
Caspase-14 OS=Homo sapiens GN=CASP14 PE=	0	0	2	0
Isoform of Q96DR8, Mucin-like protein 1 OS=H	0	0	2	0
Isoform of Q13867, Bleomycin hydrolase (Fragr	0	0	2	0
U5 small nuclear ribonucleoprotein 200 kDa he	0	0	2	0
Isoform of P15170, Eukaryotic peptide chain re	0	0	2	0
Tubulin beta-2A chain OS=Homo sapiens GN=TI	0	0	1	0
Keratin, type I cytoskeletal 27 OS=Homo sapien	0	0	1	0
sp EFC4EBP1	2	2	1	4
sp GSTP1_HUMAN	2	3	1	3
Isoform of Q7RTS7, Keratin, type II cytoskeletal	0	0	1	0
Heterogeneous nuclear ribonucleoprotein Q OS	3	1	1	1
Isoform of Q03431, Parathyroid hormone/para	4	3	1	1
Isoform of P31943, Heterogeneous nuclear ribo	5	0	1	0
Isoform of P63173, 60S ribosomal protein L38 (	3	3	1	1
Isoform of P60660, Myosin light polypeptide 6	3	1	1	2
Isoform of P63208, S-phase kinase-associated p	4	1	1	0
Isoform of Q15185, Prostaglandin E synthase 3	6	0	1	0
Isoform of P19105, Myosin regulatory light cha	2	2	1	2
Non-histone chromosomal protein HMG-17 OS	3	1	1	1
Isoform of Q15370, Elongin-B OS=Homo sapien	3	0	1	0
Thioredoxin domain-containing protein 5 OS=H	0	1	1	4
Isoform of Q8TAT6, Nuclear protein localizatior	1	1	1	0
Eukaryotic translation initiation factor 3 subuni	2	1	1	2
Isoform of P42771, Cyclin-dependent kinase inl	3	0	1	1
26S proteasome non-ATPase regulatory subuni	1	1	1	2
Isoform of P84103, Serine/arginine-rich-splicing	1	1	1	2
Isoform of O94952, F-box only protein 21 (Frag	2	0	1	2
Isoform of Q9UKF6, Cleavage and polyadenylat	2	1	1	1
Isoform of P17980, 26S protease regulatory sul	2	0	1	2
Isoform of Q9H0R5, Guanylate binding protein	2	0	1	1
Isoform of Q9H2I8, Leucine-rich repeat-contain	1	1	1	1
Isoform of P20929, Nebulin OS=Homo sapiens (	1	1	1	0
Isoform of Q92945, Far upstream element-bind	2	0	1	0

BTB/POZ domain-containing protein KCTD12 OS	2	0	1	0
Isoform of Q9UBQ5, Eukaryotic translation initi	1	0	1	1
Isoform of P02724, Glycophorin OS=Homo sapi	0	1	1	1
FRAS1-related extracellular matrix protein 3 OS	0	1	1	1
Replication protein A 70 kDa DNA-binding subu	1	1	1	0
Isoform of P55884, Eukaryotic translation initia	1	0	1	1
Isoform of Q15008, 26S proteasome non-ATPas	1	0	1	1
Histone H2B type 1-K OS=Homo sapiens GN=HI	1	1	1	0
Isoform of P06576, ATP synthase subunit beta,	1	0	1	1
Calcyclin-binding protein OS=Homo sapiens GN	2	0	1	0
Isoform of O00429, Dynamin-1-like protein (Fra	2	0	1	0
Isoform of P04632, Calpain small subunit 1 (Fra	2	0	1	0
Isoform of P06753, Tropomyosin alpha-3 chain	2	0	1	0
Isoform of O95757, Heat shock 70 kDa protein	2	0	1	0
Dynein light chain 1, cytoplasmic OS=Homo sap	1	0	1	0
Trifunctional purine biosynthetic protein adeno	0	0	1	1
Stress-induced-phosphoprotein 1 OS=Homo sap	1	0	1	0
Isoform of Q9NTJ3, Structural maintenance of c	1	0	1	0
Isoform of Q13148, TAR DNA-binding protein 4	0	0	1	1
Immunoglobulin heavy constant gamma 2 OS=H	1	0	1	0
Coatomer subunit beta_ OS=Homo sapiens GN=	1	0	1	0
Isoform of Q6L8Q7, 2_,5_-phosphodiesterase 1	0	0	1	1
Isoform of Q9BYB4, Guanine nucleotide-binding	1	0	1	0
Prefoldin subunit 2 OS=Homo sapiens GN=PFDN	1	0	1	0
Isoform of P05114, Non-histone chromosomal	1	0	1	0
Esterase OVCA2 OS=Homo sapiens GN=OVCA2	0	1	1	0
StAR-related lipid transfer protein 9 OS=Homo :	1	0	1	0
Isoform of Q9Y678, Coatomer subunit gamma-:	0	1	1	0
Small nuclear ribonucleoprotein Sm D3 OS=Hor	0	1	1	0
Isoform of P35080, Profilin OS=Homo sapiens G	1	0	1	0
Isoform of P15880, 40S ribosomal protein S2 O:	1	0	1	0
Isoform of Q9HA64, Ketosamine-3-kinase (Frag	1	0	1	0
Putative annexin A2-like protein OS=Homo sapi	0	0	1	0
sp ANXA5_HUMAN	0	0	1	0
Eukaryotic translation initiation factor 3 subuni	0	0	1	0
Isoform of O00410, Importin-5 (Fragment) OS=	0	0	1	0
Isoform of O95336, 6-phosphogluconolactonas	0	0	1	0
Isoform of O95447, Lebercilin-like protein (Frag	0	0	1	0
Alpha-2-HS-glycoprotein OS=Homo sapiens GN=	0	0	1	0
Cystathionine beta-synthase-like protein OS=Ho	0	0	1	0
Isoform of P11940, Polyadenylate-binding prote	0	0	1	0
Prolactin-inducible protein OS=Homo sapiens G	0	0	1	0
Fibrillin-1 OS=Homo sapiens GN=FBN1 PE=1 SV:	0	0	1	0
Histidine ammonia-lyase OS=Homo sapiens GN	0	0	1	0
Isoform of P53992, Protein transport protein Se	0	0	1	0
Isoform of Q14240, Eukaryotic initiation factor	0	0	1	0
Desmoglein-1 OS=Homo sapiens GN=DSG1 PE=	0	0	1	0

Synaptic vesicular amine transporter OS=Homo	0	0	1	0
Isoform of Q13526, Peptidyl-prolyl cis-trans iso	0	0	1	0
Isoform of Q15436, Protein transport protein S	0	0	1	0
KN motif and ankyrin repeat domain-containing	0	0	1	0
Isoform of Q6DKJ4, Nucleoredoxin OS=Homo sa	0	0	1	0
Isoform of Q6H8Q1, Actin-binding LIM protein	0	0	1	0
Suprabasin OS=Homo sapiens GN=SBSN PE=1 S	0	0	1	0
BRCA1-associated protein OS=Homo sapiens GI	0	0	1	0
DnaJ homolog subfamily C member 10 OS=Hom	0	0	1	0
Isoform of Q8N9I9, Probable E3 ubiquitin-prote	0	0	1	0
Arrestin domain-containing protein 2 OS=Homc	0	0	1	0
Mucin-16 OS=Homo sapiens GN=MUC16 PE=1	0	0	1	0
Isoform of Q9Y383, Putative RNA-binding prote	0	0	1	0
Conserved oligomeric Golgi complex subunit 5	0	0	1	0
1-phosphatidylinositol 3-phosphate 5-kinase OS	0	0	1	0
Isoform of Q96FF7, Uncharacterized protein MI	0	0	1	0
Isoform of P08493, Isoform 2 of Matrix Gla pro	0	0	1	0
Pre-B-cell leukemia transcription factor 2 OS=H	0	0	1	0
Isoform of P58546, Myotrophin OS=Homo sapie	0	0	1	0
Isoform of P62316, Small nuclear ribonucleopro	0	0	1	0
Eukaryotic translation initiation factor 3 subuni	0	0	1	0
Isoform of Q8TAC2, Josephin-2 (Fragment) OS=	0	0	1	0
Isoform of Q96SN8, CDK5 regulatory subunit-as	0	0	1	0
Splicing factor 3B subunit 5 OS=Homo sapiens C	0	0	1	0
dCTP pyrophosphatase 1 OS=Homo sapiens GN	0	0	1	0
CMP-N-acetylneuraminate-beta-galactosamide	0	0	1	0
Uncharacterized protein OS=Homo sapiens GN=	0	0	1	0
Isoform of Q9H9A5, CCR4-NOT transcription co	0	0	1	0
Isoform of P26368, Splicing factor U2AF 65 kDa	0	0	1	0
Isoform of Q86YA3, HCG21296, isoform CRA_a	0	0	1	0
Isoform of O15197, Ephrin type-B receptor 6 OS	0	0	1	0
Isoform of Q6MZP7, Isoform 2 of Protein lin-54	0	0	1	0
Isoform of Q8NA56, Tetratricopeptide repeat p	0	0	1	0
Ubiquitin carboxyl-terminal hydrolase 40 OS=H	0	0	1	0
ADM2 OS=Homo sapiens GN=ADM2 PE=2 SV=1	0	0	1	0
Isoform of Q8TB05, UBA-like domain-containing	0	0	1	0
Isoform of P55209, Nucleosome assembly prote	0	0	1	0
60S ribosomal protein L11 OS=Homo sapiens G	0	0	1	0
Claudin-8 OS=Homo sapiens GN=CLDN8 PE=1 S	0	0	1	0
E3 ubiquitin-protein ligase UBR3 OS=Homo sap	0	0	1	0
Isoform of Q9NZI2, Kv channel-interacting prote	0	0	1	0
Retinoblastoma-like protein 2 OS=Homo sapien	0	0	1	0
Paraneoplastic antigen-like protein 5 OS=Homo	0	0	1	0
Isoform of Q9UFE4, Coiled-coil domain-contain	0	0	1	0
Zinc finger protein 648 OS=Homo sapiens GN=Z	0	0	1	0
Isoform of Q9GZM8, Nuclear distribution prote	0	0	1	0
Isoform of Q9BXK5, Bcl-2-like protein 13 OS=Hc	0	0	1	0

Titin OS=Homo sapiens GN=TTN PE=1 SV=1	0	0	1	0
Protein pelota homolog OS=Homo sapiens GN=	0	0	1	0
Isoform of Q9NPH5, NADPH oxidase 4 OS=Hom	0	0	1	0
Isoform of Q6P4R8, Nuclear factor-related to ka	0	0	1	0
Isoform of P53602, Diphosphomevalonate deca	0	0	1	0
Isoform of O75821, Eukaryotic translation initia	0	0	1	0
Isoform of Q13509, HCG1983504, isoform CRA_	0	0	0	1
Immunoglobulin kappa variable 2D-29 OS=Hom	6	4	0	3
Isoform of Q7Z4L5, Tetratricopeptide repeat pr	0	4	0	1
Heat shock protein HSP 90-alpha OS=Homo sap	4	0	0	1
Isoform of Q8N1B3, Cyclin-related protein FAM	0	2	0	2
Isoform of M0R082, Uncharacterized protein O	3	4	0	0
Isoform of Q9BUL8, Programmed cell death 10,	1	1	0	1
Isoform of Q96N23, Cilia- and flagella-associate	0	0	0	3
Isoform of P24941, Cyclin-dependent kinase 2 (	1	0	0	0
Serine/threonine-protein kinase MAK OS=Home	0	2	0	0
Isoform of P33316, Deoxyuridine 5_-triphospha	1	3	0	1
Isoform of Q99460, 26S proteasome non-ATPas	2	1	0	2
Isoform of P08670, Vimentin (Fragment) OS=Ho	1	2	0	1
Dynactin subunit 2 OS=Homo sapiens GN=DCTN	3	1	0	0
Isoform of P36941, Tumor necrosis factor recep	1	1	0	0
Peptidyl-prolyl cis-trans isomerase OS=Homo sa	1	0	0	0
Solute carrier family 2, facilitated glucose trans	1	2	0	0
Pre-mRNA-processing-splicing factor 8 OS=Hom	1	1	0	1
Protein arginine N-methyltransferase 5 OS=Hor	2	0	0	1
26S proteasome non-ATPase regulatory subunit	2	1	0	0
Probable maltase-glucoamylase 2 OS=Homo sa	0	0	0	3
Isoform of Q92839, Hyaluronan synthase 1 OS=	2	1	0	0
Creatine kinase B-type OS=Homo sapiens GN=C	3	0	0	0
26S protease regulatory subunit 8 OS=Homo sa	1	0	0	1
Cytoplasmic dynein 1 intermediate chain 2 OS=	1	1	0	0
Bifunctional glutamate/proline--tRNA ligase OS	0	1	0	1
Isoform of P27708, CAD protein (Fragment) OS=	1	0	0	1
Isoform of Q8N3X6, Ligand-dependent nuclear	0	1	0	1
26S proteasome non-ATPase regulatory subunit	1	0	0	1
Isoform of P00441, Superoxide dismutase [Cu-Z	2	0	0	0
Isoform of A0A0U1RRH7, Histone H2A OS=Hom	0	1	0	1
Isoform of P62333, 26S protease regulatory sul	0	0	0	2
Interleukin enhancer-binding factor 3 OS=Homo	1	0	0	1
Isoform of Q3ZCQ8, Isoform 2 of Mitochondrial	0	0	0	2
Isoform of Q9HCF6, TRPM3 protein OS=Homo s	0	0	0	2
DNA-directed RNA polymerases I, II, and III subu	1	1	0	0
Fer-1-like protein 6 OS=Homo sapiens GN=FER1	1	0	0	1
Heat shock 70 kDa protein 4 OS=Homo sapiens	2	0	0	0
U11/U12 small nuclear ribonucleoprotein 35 kD	1	1	0	0
Isoform of Q5JVF3, Isoform 4 of PCI domain-cor	2	0	0	0
Isoform of O60232, Sjoegren syndrome/scleroc	1	1	0	0

Isoform of Q96MR6, Cilia- and flagella-associate	0	2	0	0
Isoform of P61247, 40S ribosomal protein S3a (	1	1	0	0
Transmembrane protein 239 OS=Homo sapiens	1	1	0	0
Isoform of Q8WZA1, Protein O-linked-mannose	0	2	0	0
Isoform of P51991, Heterogeneous nuclear ribo	1	0	0	0
Phosphoribosylformylglycinamidine synthase O	2	0	0	0
Sphingosine-1-phosphate lyase 1 OS=Homo sap	1	0	0	1
26S proteasome non-ATPase regulatory subuni	2	0	0	0
sp CAS1_BOVIN	0	0	0	1
sp K2M2_SHEEP	0	0	0	1
Laminin subunit alpha-5 OS=Homo sapiens GN=	0	1	0	0
Isoform of O15294, UDP-N-acetylglucosamine--	0	0	0	1
Endonuclease domain-containing 1 protein OS=	0	1	0	0
Isoform of O95819, Mitogen-activated protein	0	0	0	1
Aspartate aminotransferase, mitochondrial OS=	0	0	0	1
Protein S100-A8 OS=Homo sapiens GN=S100A8	0	0	0	1
Phosphoglycerate mutase 2 OS=Homo sapiens	1	0	0	0
Isoform of P18754, Regulator of chromosome c	1	0	0	0
Isoform of P24394, Interleukin-4 receptor subu	0	1	0	0
Isoform of P31995, Low affinity immunoglobuli	0	1	0	0
Glycerol kinase OS=Homo sapiens GN=GK PE=1	0	1	0	0
Isoform of P35244, Replication protein A 14 kD	0	1	0	0
Isoform of P35637, RNA-binding protein FUS OS	0	1	0	0
Isoform of P45984, Mitogen-activated protein I	0	1	0	0
Isoform of P47756, Capping protein (Actin filam	1	0	0	0
Vacuolar protein sorting-associated protein 41	0	0	0	1
Coatomer subunit beta OS=Homo sapiens GN=(	0	1	0	0
LIM domain kinase 2 OS=Homo sapiens GN=LIM	0	0	0	1
Uncharacterized protein (Fragment) OS=Homo	1	0	0	0
Isoform of P60981, Destrin OS=Homo sapiens G	1	0	0	0
Isoform of P62888, 60S ribosomal protein L30 (	1	0	0	0
Isoform of Q00978, Interferon regulatory facto	0	1	0	0
ATP-dependent 6-phosphofructokinase, platele	0	0	0	1
Isoform of Q12768, WASH complex subunit 5 O	0	0	0	1
Isoform of Q12769, Nuclear pore complex prote	0	0	0	1
26S proteasome non-ATPase regulatory subuni	0	0	0	1
Isoform of Q13459, Unconventional myosin-IXk	0	1	0	0
Protein Tob2 OS=Homo sapiens GN=TOB2 PE=1	0	1	0	0
Unhealthy ribosome biogenesis protein 2 homo	0	0	0	1
Calponin-3 OS=Homo sapiens GN=CNN3 PE=1 S	1	0	0	0
ELAV-like protein 1 OS=Homo sapiens GN=ELAV	1	0	0	0
Zinc finger protein 425 OS=Homo sapiens GN=Z	0	0	0	1
PDZ domain-containing RING finger protein 4 O	1	0	0	0
Zinc finger protein 467 OS=Homo sapiens GN=Z	0	1	0	0
Isoform of Q86XX4, Extracellular matrix protein	1	0	0	0
Hornerin OS=Homo sapiens GN=HRNR PE=1 SV=	0	0	0	1
Isoform of Q8IXL7, Methionine-R-sulfoxide redu	0	1	0	0

pre-rRNA processing protein FTSJ3 OS=Homo sa	1	0	0	0
Uncharacterized protein C17orf53 OS=Homo sa	1	0	0	0
Isoform of Q8N5X7, Eukaryotic translation initia	1	0	0	0
Olfactory receptor 52E4 OS=Homo sapiens GN=	0	0	0	1
AP-3 complex subunit sigma-1 OS=Homo sapien	1	0	0	0
Isoform of Q92608, Dedicator of cytokinesis pro	0	0	0	1
Isoform of Q92736, Ryanodine receptor 2 OS=H	0	1	0	0
Glomulin OS=Homo sapiens GN=GLMN PE=1 SV	1	0	0	0
Isoform of Q93009, Ubiquitin carboxyl-termina	1	0	0	0
Isoform of Q96G01, BICD1 protein OS=Homo sa	1	0	0	0
Isoform of Q96K80, Zinc finger CCCH domain-co	0	1	0	0
Probable G-protein coupled receptor 101 OS=H	0	0	0	1
Isoform of Q99497, Protein deglycase DJ-1 OS=	1	0	0	0
Membrane-associated phosphatidylinositol trar	0	0	0	1
Isoform of Q9UBW7, Zinc finger MYM-type pro	0	1	0	0
Isoform of Q9UI30, Multifunctional methyltrans	1	0	0	0
Isoform of Q9UKV5, E3 ubiquitin-protein ligase	0	0	0	1
Isoform of Q9UL40, Zinc finger protein 346 OS=	1	0	0	0
Isoform of Q9UPR5, Sodium/calcium exchanger	1	0	0	0
Carbohydrate sulfotransferase 2 OS=Homo sap	1	0	0	0
FACT complex subunit SPT16 OS=Homo sapiens	1	0	0	0
CD2-associated protein OS=Homo sapiens GN=(	0	0	0	1
Uncharacterized protein OS=Homo sapiens PE=	1	0	0	0
Sjoegren syndrome nuclear autoantigen 1 OS=H	1	0	0	0
Isoform of Q9ULX6, A-kinase anchor protein 8-l	1	0	0	0
Isoform of O15519, CASP8 and FADD-like apopt	0	1	0	0
Putative small nuclear ribonucleoprotein G-like	1	0	0	0
Isoform of O60610, Protein diaphanous homolc	0	1	0	0
Low-density lipoprotein receptor-related prote	1	0	0	0
Solute carrier family 22 member 3 OS=Homo sa	0	0	0	1
Isoform of P07203, Glutathione peroxidase OS=	0	0	0	1
TFIIH basal transcription factor complex helicas	0	1	0	0
Isoform of P41252, Isoleucine--tRNA ligase, cyt	1	0	0	0
Arfaptin-1 OS=Homo sapiens GN=ARFIP1 PE=1 :	0	1	0	0
Isoform of Q02297, Isoform 10 of Pro-neuregul	1	0	0	0
Isoform of Q58DX5, Isoform 2 of Inactive N-ace	0	0	0	1
Osteoclast stimulatory transmembrane protein	1	0	0	0
Zinc finger protein 407 OS=Homo sapiens GN=Z	1	0	0	0
Protocadherin-18 OS=Homo sapiens GN=PCDH:	1	0	0	0
Isoform of Q8NBL1, Protein O-glucosyltransfera	1	0	0	0
Isoform of Q8N2M8, CLK4-associating serine/ar	0	0	0	1
Isoform of P23381, Tryptophan--tRNA ligase, cy	0	0	0	1
Isoform of P12110, Collagen alpha-2(VI) chain (	1	0	0	0
KN motif and ankyrin repeat domain-containing	0	0	0	1
Isoform of Q5U5Z8, Cytosolic carboxypeptidase	0	0	0	1
Immunoglobulin superfamily member 2 OS=Ho	1	0	0	0
Isoform of Q9P267, Methyl-CpG-binding domai	1	0	0	0

Protein				
Isoform of Q6ZRI0, Isoform 2 of Otogelin OS=H	1	0	0	0
Peroxidasin-like protein OS=Homo sapiens GN=	1	0	0	0
Isoform of P38159, RNA-binding motif protein,	0	1	0	0
Isoform of Q00532, Cyclin-dependent kinase-lik	0	0	0	1
Isoform of Q92599, Septin-8 OS=Homo sapiens	1	0	0	0
Isoform of Q86YC2, Partner and localizer of BR(	0	0	0	1
Protein bicaudal D homolog 2 OS=Homo sapien	0	0	0	1
Isoform of Q6ZPD9, Probable C-mannosyltransf	1	0	0	0
Isoform of Q9NQ69, LIM/homeobox protein Lh	0	0	0	1
Receptor-transporting protein 1 OS=Homo sapi	0	0	0	1
Zinc finger protein 468 OS=Homo sapiens GN=Z	1	0	0	0
Isoform of Q8WVK7, Spindle and kinetochore-a	1	0	0	0
Sorting nexin-9 OS=Homo sapiens GN=SNX9 PE	1	0	0	0
Zinc finger protein 491 OS=Homo sapiens GN=Z	0	0	0	1
Isoform of P13725, Oncostatin-M OS=Homo saj	0	1	0	0
Transcription factor SOX-11 OS=Homo sapiens (	0	1	0	0
Isoform of P47755, F-actin-capping protein sub	1	0	0	0
40S ribosomal protein S25 OS=Homo sapiens G	1	0	0	0
Isoform of Q99426, Tubulin-folding cofactor B (	1	0	0	0
Isoform of P20290, Transcription factor BTF3 (F	0	0	0	1
Isoform of P32929, Isoform 2 of Cystathionine ;	1	0	0	0
Nuclear pore complex protein Nup107 OS=Hom	0	0	0	1
Solute carrier family 22 member 12 OS=Homo ;	0	0	0	1
DNA replication factor Cdt1 OS=Homo sapiens (	1	0	0	0
Thyroid transcription factor 1-associated protei	0	1	0	0
Protein sel-1 homolog 1 OS=Homo sapiens GN=	0	0	0	1
Dual oxidase 1 OS=Homo sapiens GN=DUOX1 P	0	1	0	0
B-cell lymphoma/leukemia 11A OS=Homo sapie	1	0	0	0
E3 ubiquitin-protein ligase TRIM71 OS=Homo si	1	0	0	0
Exportin-2 OS=Homo sapiens GN=CSE1L PE=1 S	1	0	0	0
Acetylcholine receptor subunit delta OS=Homo	0	1	0	0
2_-5_-oligoadenylate synthase-like protein OS=	1	0	0	0
Zinc finger and BTB domain-containing protein	0	1	0	0
Isoform of Q9Y4E5, Isoform 3 of E3 SUMO-prot	0	1	0	0
Transmembrane 6 superfamily member 2 OS=H	0	0	0	1
Structural maintenance of chromosomes flexib	0	0	0	1
ATP-binding cassette sub-family C member 9 O!	1	0	0	0
Isoform of P35443, Thrombospondin-4 OS=Hor	1	0	0	0
Isoform of Q96HE7, ERO1-like protein alpha OS	0	0	0	1
Actin-like protein 8 OS=Homo sapiens GN=ACTI	1	0	0	0
Follistatin-related protein 3 OS=Homo sapiens (	1	0	0	0
Nucleolar pre-ribosomal-associated protein 1 C	1	0	0	0
Guanine nucleotide-binding protein subunit alp	0	0	0	1
Isoform of P62158, Calmodulin OS=Homo sapie	0	1	0	0
Ubiquitin-like-conjugating enzyme ATG3 OS=Hc	0	0	0	1
Protein Shroom4 OS=Homo sapiens GN=SHRO(	0	0	0	1
Isoform of P60891, Ribose-phosphate pyrophos	1	0	0	0

Nestin OS=Homo sapiens GN=NES PE=1 SV=2	1	0	0	0
Immunoglobulin superfamily member 10 OS=H	0	0	0	1
Isoform of Q9BYT3, Serine/threonine-protein k	0	0	0	1
Isoform of Q9NVF9, Ethanolamine kinase 2 (Fra	0	1	0	0
Tripeptidyl-peptidase 1 OS=Homo sapiens GN=ˈ	0	1	0	0
Isoform of Q5K651, Sterile alpha motif domain-	1	0	0	0
Isoform of Q8WV37, Zinc finger protein 480 (Fr	0	0	0	1
Isoform of O94916, Isoform A of Nuclear factor	1	0	0	0
Inorganic pyrophosphatase OS=Homo sapiens (	1	0	0	0
Isoform of Q92887, Canalicular multispecific or	1	0	0	0
Isoform of Q14938, Isoform 2 of Nuclear factor	1	0	0	0
Isoform of O75334, Liprin-alpha-2 (Fragment) (	1	0	0	0
Ankyrin repeat domain-containing protein 61 O	1	0	0	0
Isoform of P16112, Aggrecan core protein OS=ŀ	1	0	0	0
Transcription elongation factor A protein 1 OS=	1	0	0	0
Isoform of P35241, Radixin OS=Homo sapiens (	0	1	0	0
Cysteine/serine-rich nuclear protein 1 OS=Hom	0	1	0	0
Isoform of O95180, Voltage-dependent T-type (	0	0	0	1
Myomesin-2 OS=Homo sapiens GN=MYOM2 PE	0	1	0	0
Putative zinc finger protein 840 OS=Homo sapie	0	1	0	0
Isoform of Q674X7, Kazrin OS=Homo sapiens G	1	0	0	0
Elongation factor 1-beta OS=Homo sapiens GN=	1	0	0	0
Heart- and neural crest derivatives-expressed p	0	0	0	1
Calsyntenin-2 OS=Homo sapiens GN=CLSTN2 PE	0	1	0	0
Alpha-mannosidase 2 OS=Homo sapiens GN=M	1	0	0	0
Isoform of O75095, Multiple epidermal growth	0	0	0	1
Isoform of Q8IZF3, Adhesion G protein-coupled	0	1	0	0
Protein bassoon OS=Homo sapiens GN=BSN PE:	0	0	0	1
Isoform of Q8TES7, Fas-binding factor 1 (Fragm	1	0	0	0
Mucin-13 OS=Homo sapiens GN=MUC13 PE=1 !	1	0	0	0

Appendix E

All Protein IDs from PhAXA-MS with 4E-BP1 (T46C) as Bait in Mitotic Cells

PROTID	DEFLINE	PSMs			
		4E-BP1 (WT) + **1**	4E-BP1 (WT) ATP ctl	4E-BP1 (T46C) + **1**	4E-BP1 (T46C) ATP ctl
Q13541	Eukaryotic translation initiation factor 4E-bind	2396	2556	1803	1764
TRYP_PIG	sp TRYP_PIG	228	255	255	246
P06730-3	Isoform of P06730, Isoform 3 of Eukaryotic tr	64	73	92	75
P78347	General transcription factor II-I OS=Homo sap	61	55	75	56
P11142	Heat shock cognate 71 kDa protein OS=Homc	36	13	75	23
ALBU_BOV	sp ALBU_BOVIN	33	34	53	47
P68363	Tubulin alpha-1B chain OS=Homo sapiens GN:	23	25	46	53
P42345	Serine/threonine-protein kinase mTOR OS=Hc	7	0	45	0
PRDX1_HU	sp PRDX1_HUMAN	33	22	44	32
A0A0G2JIW	Isoform of P0DMV9, Heat shock 70 kDa prote	26	5	39	14
P52272	Heterogeneous nuclear ribonucleoprotein M	0	0	38	33
K1C10_HUI	sp K1C10_HUMAN	16	23	35	22
P04264	Keratin, type II cytoskeletal 1 OS=Homo sapie	12	40	34	34
Q13162	Peroxiredoxin-4 OS=Homo sapiens GN=PRDX4	25	29	31	31
P50990	T-complex protein 1 subunit theta OS=Homo	14	13	29	15
P68371	Tubulin beta-4B chain OS=Homo sapiens GN=	2	1	28	27
P68104	Elongation factor 1-alpha 1 OS=Homo sapiens	6	3	27	10
P78527	DNA-dependent protein kinase catalytic subu	6	0	27	2
P07437	Tubulin beta chain OS=Homo sapiens GN=TUI	21	9	26	21
P35527	Keratin, type I cytoskeletal 9 OS=Homo sapier	21	26	24	23
H0Y4R1	Isoform of P12268, Inosine-5_-monophospha	7	0	24	0
P30153	Serine/threonine-protein phosphatase 2A 65	10	2	23	10
Q71U36	Tubulin alpha-1A chain OS=Homo sapiens GN	0	0	22	0
Q14204	Cytoplasmic dynein 1 heavy chain 1 OS=Homc	15	12	22	13
P17987	T-complex protein 1 subunit alpha OS=Homo	11	9	20	11
K22E_HUM	sp K22E_HUMAN	3	13	19	13
P10599	Thioredoxin OS=Homo sapiens GN=TXN PE=1	12	1	17	3
P11021	78 kDa glucose-regulated protein OS=Homo s	10	18	16	12
P60709	Actin, cytoplasmic 1 OS=Homo sapiens GN=A(	11	6	15	9
Q15393	Splicing factor 3B subunit 3 OS=Homo sapiens	7	8	15	9
Q0VDG4	Secernin-3 OS=Homo sapiens GN=SCRN3 PE=	7	9	14	10
P48643	T-complex protein 1 subunit epsilon OS=Hom	0	5	14	3
F6VRR5	Isoform of Q9BY77, Polymerase delta-interac	19	10	13	15
Q15365	Poly(rC)-binding protein 1 OS=Homo sapiens (	8	7	13	14
P63151	Serine/threonine-protein phosphatase 2A 55	9	3	13	6
P67775	Serine/threonine-protein phosphatase 2A cat	3	4	13	8
P08238	Heat shock protein HSP 90-beta OS=Homo sa	9	1	13	3
Q9Y230	RuvB-like 2 OS=Homo sapiens GN=RUVBL2 PE	5	4	13	3
A0A0U1RQ	Isoform of P49327, Fatty acid synthase OS=Hc	1	0	13	0

A0A0J9YVP	Isoform of Q9UHX1, Poly(U)-binding-splicing 1	8	10	12	8
P30041	Peroxiredoxin-6 OS=Homo sapiens GN=PRDX(	7	7	12	4
A0A087WT	Isoform of Q92945, Far upstream element-bir	3	0	12	3
Q9NUY8	TBC1 domain family member 23 OS=Homo sa	0	0	12	1
E9PB61	Isoform of Q86V81, THO complex subunit 4 C	13	12	11	11
P40227	T-complex protein 1 subunit zeta OS=Homo s	4	4	11	5
O75190	DnaJ homolog subfamily B member 6 OS=Hor	0	0	11	7
P14866	Heterogeneous nuclear ribonucleoprotein L C	4	0	11	0
P46109	Crk-like protein OS=Homo sapiens GN=CRKL F	3	0	11	0
E9PLK3	Isoform of P55786, Puromycin-sensitive amin	0	0	11	0
F8W6I7	Isoform of P09651, Heterogeneous nuclear ri	10	8	10	5
P62937	Peptidyl-prolyl cis-trans isomerase A OS=Hor	9	5	10	7
Q99832	T-complex protein 1 subunit eta OS=Homo sa	5	1	10	5
P13639	Elongation factor 2 OS=Homo sapiens GN=EEI	6	1	10	1
P32119	Peroxiredoxin-2 OS=Homo sapiens GN=PRDX.	2	12	9	7
Q09028	Histone-binding protein RBBP4 OS=Homo sap	6	7	9	8
P84090	Enhancer of rudimentary homolog OS=Homo	6	7	9	6
A0A087WZ	Isoform of Q9H3K6, BolA-like protein 2 OS=H(	3	2	9	5
F5GWF6	Isoform of P78371, T-complex protein 1 subu	6	4	9	5
Q9Y265	RuvB-like 1 OS=Homo sapiens GN=RUVBL1 PE	2	0	9	1
B4DUR8	Isoform of P49368, T-complex protein 1 subu	0	0	9	0
P07900	Heat shock protein HSP 90-alpha OS=Homo s;	1	1	7	0
P63173	60S ribosomal protein L38 OS=Homo sapiens	5	4	7	2
Q8N122	Regulatory-associated protein of mTOR OS=H	7	2	7	1
O60506	Heterogeneous nuclear ribonucleoprotein Q (	3	1	7	2
P12956	X-ray repair cross-complementing protein 6 C	1	0	7	1
E9PCY7	Isoform of P31943, Heterogeneous nuclear ri	1	0	7	0
Q9UMS4	Pre-mRNA-processing factor 19 OS=Homo sap	8	9	6	8
P22626	Heterogeneous nuclear ribonucleoproteins A.	10	6	6	0
B4DV12	Isoform of P0CG47, Polyubiquitin-B OS=Homc	6	6	6	4
Q9Y3Y2	Chromatin target of PRMT1 protein OS=Homc	4	6	6	3
A0A0A0MC	Isoform of Q96I15, Selenocysteine lyase OS=F	3	2	6	5
H3BLZ8	Isoform of Q92841, Probable ATP-dependent	6	1	6	0
Q13838	Spliceosome RNA helicase DDX39B OS=Homo	0	0	6	6
J3KTA4	Isoform of P17844, Probable ATP-dependent	2	1	6	0
E9PBS1	Isoform of P22234, Multifunctional protein Al	2	0	6	0
P11802	Cyclin-dependent kinase 4 OS=Homo sapiens	1	0	6	0
P62993	Growth factor receptor-bound protein 2 OS=I	1	0	6	0
Q9HA64	Ketosamine-3-kinase OS=Homo sapiens GN=F	1	0	6	0
J3KQ32	Isoform of Q9NTK5, Obg-like ATPase 1 OS=Hc	1	0	6	0
A0A1C7CY	Isoform of Q16555, Dihydropyrimidinase-rela	0	0	6	0
Q9Y3I0	tRNA-splicing ligase RtcB homolog OS=Homo	0	0	6	0
P02533	Keratin, type I cytoskeletal 14 OS=Homo sapi	8	4	5	4
Q14011	Cold-inducible RNA-binding protein OS=Homc	4	5	5	7
TRY1_BOVI	sp TRY1_BOVIN	5	4	5	3
D6W5Y5	Isoform of Q14011, Cold inducible RNA bindir	0	0	5	0
Q9NPA8	Transcription and mRNA export factor ENY2 C	5	3	5	6

Accession	Description				
A0A0A0MS	Isoform of P01857, Ig gamma-1 chain C region	5	3	5	0
Q7RTV0	PHD finger-like domain-containing protein 5A	2	3	5	2
H3BPE7	Isoform of P35637, RNA-binding protein FUS	1	2	5	3
Q13435	Splicing factor 3B subunit 2 OS=Homo sapiens	2	1	5	3
E9PM69	Isoform of P17980, 26S protease regulatory s	1	2	5	1
P00492	Hypoxanthine-guanine phosphoribosyltransfe	1	1	5	1
P13010	X-ray repair cross-complementing protein 5 C	1	1	5	0
P26641	Elongation factor 1-gamma OS=Homo sapiens	1	0	5	1
A0A0A0MS	Isoform of P13797, Plastin-3 OS=Homo sapier	2	0	5	0
P42771	Cyclin-dependent kinase inhibitor 2A OS=Hon	1	0	5	0
Q92598	Heat shock protein 105 kDa OS=Homo sapien	1	0	5	0
P31689	DnaJ homolog subfamily A member 1 OS=Hor	0	0	5	0
O43175	D-3-phosphoglycerate dehydrogenase OS=Ho	0	0	5	0
Q13885	Tubulin beta-2A chain OS=Homo sapiens GN=	0	0	4	0
A0A075B6S	Immunoglobulin kappa variable 2D-29 OS=Ho	3	6	4	4
H0Y6E7	Isoform of P38159, RNA-binding motif protein	4	4	4	3
P62857	40S ribosomal protein S28 OS=Homo sapiens	7	1	4	2
P62913	60S ribosomal protein L11 OS=Homo sapiens	4	1	4	3
Q13409-2	Isoform of Q13409, Isoform 2B of Cytoplasmi	3	4	4	0
P50991	T-complex protein 1 subunit delta OS=Homo s	3	1	4	1
GSTP1_HUI	sp GSTP1_HUMAN	1	2	4	2
P09874	Poly [ADP-ribose] polymerase 1 OS=Homo sap	5	0	4	0
P06733	Alpha-enolase OS=Homo sapiens GN=ENO1 P	1	1	4	2
E7EMB3	Isoform of P62158, Calmodulin OS=Homo sap	2	1	4	1
P52597	Heterogeneous nuclear ribonucleoprotein F C	1	0	4	0
Q9UJ70	N-acetyl-D-glucosamine kinase OS=Homo sap	1	0	4	0
Q9HB71	Calcyclin-binding protein OS=Homo sapiens G	2	0	4	0
P53396	ATP-citrate synthase OS=Homo sapiens GN=A	1	0	4	0
Q9BVC4	Target of rapamycin complex subunit LST8 OS	1	0	4	0
H3BND8	Isoform of Q93009, Ubiquitin carboxyl-termir	0	0	4	0
O14744	Protein arginine N-methyltransferase 5 OS=H	0	0	4	0
Q9BUF5	Tubulin beta-6 chain OS=Homo sapiens GN=T	0	0	3	2
E7EQ64	Isoform of P07477, Trypsin-1 OS=Homo sapie	3	5	3	3
E9PC52	Isoform of Q16576, Histone-binding protein F	0	0	3	1
P98179	RNA-binding protein 3 OS=Homo sapiens GN=	6	4	3	4
P23284	Peptidyl-prolyl cis-trans isomerase B OS=Hom	4	6	3	3
O43390	Heterogeneous nuclear ribonucleoprotein R C	3	1	3	2
Q08499-12	Isoform of Q08499, Isoform 12 of cAMP-spec	4	3	3	3
E9PK25	Isoform of P23528, Cofilin-1 OS=Homo sapier	3	2	3	4
Q99459	Cell division cycle 5-like protein OS=Homo sap	3	4	3	1
P62269	40S ribosomal protein S18 OS=Homo sapiens	3	3	3	1
P09661	U2 small nuclear ribonucleoprotein A_ OS=Ho	0	4	3	2
Q16531	DNA damage-binding protein 1 OS=Homo sap	1	2	3	3
A0A087X2I	Isoform of P84103, Serine/arginine-rich-splici	1	3	3	2
Q9Y383	Putative RNA-binding protein Luc7-like 2 OS=I	2	2	3	2
P51991	Heterogeneous nuclear ribonucleoprotein A3	3	1	3	2
C9J4W5	Isoform of Q9GZV4, Eukaryotic translation ini	3	1	3	2

J3QLE5	Isoform of P63162, Small nuclear ribonucleop	2	1	3	2
P19338	Nucleolin OS=Homo sapiens GN=NCL PE=1 SV	2	1	3	2
P05204	Non-histone chromosomal protein HMG-17 C	3	1	3	1
Q15029	116 kDa U5 small nuclear ribonucleoprotein c	1	0	3	2
P35998	26S protease regulatory subunit 7 OS=Homo :	1	1	3	2
A0A0A0MF	Isoform of Q12905, Interleukin enhancer-binc	1	1	3	2
D6RAF8	Isoform of Q14103, Heterogeneous nuclear ri	2	1	3	1
Q12874	Splicing factor 3A subunit 3 OS=Homo sapiens	2	1	3	1
A0A087WY	Isoform of Q15185, Prostaglandin E synthase	3	1	3	0
P62316	Small nuclear ribonucleoprotein Sm D2 OS=H	0	1	3	2
O00483	Cytochrome c oxidase subunit NDUFA4 OS=H	0	2	3	1
G3V4N7	Isoform of P12277, Creatine kinase B-type (Fr	0	1	3	1
P28482	Mitogen-activated protein kinase 1 OS=Homc	0	1	3	1
P37802	Transgelin-2 OS=Homo sapiens GN=TAGLN2 F	2	0	3	0
A0A0A0MF	Isoform of P22061, Protein-L-isoaspartate O-r	2	0	3	0
O75934	Pre-mRNA-splicing factor SPF27 OS=Homo sap	2	0	3	0
P30044	Peroxiredoxin-5, mitochondrial OS=Homo sap	0	0	3	1
P02765	Alpha-2-HS-glycoprotein OS=Homo sapiens G	0	0	3	1
P31948	Stress-induced-phosphoprotein 1 OS=Homo s	1	0	3	0
E7EUT5	Isoform of P04406, Glyceraldehyde-3-phosph	1	0	3	0
K7EPP7	Isoform of Q99615, DnaJ homolog subfamily (	1	0	3	0
P23280	Carbonic anhydrase 6 OS=Homo sapiens GN=	1	0	3	0
Q16543	Hsp90 co-chaperone Cdc37 OS=Homo sapiens	0	0	3	0
Q13395	Probable methyltransferase TARBP1 OS=Hom	0	0	3	0
ALBU_HUM	sp ALBU_HUMAN	0	0	2	0
A0A087WL	Isoform of Q8N1B3, Cyclin-related protein FA	2	5	2	4
H7C3G1	Isoform of Q9H8V3, Protein ECT2 (Fragment)	2	2	2	1
O14602	Eukaryotic translation initiation factor 1A, Y-c	3	3	2	2
CAS1_BOVI	sp CAS1_BOVIN	2	3	2	2
A0A087WT	Isoform of P11940, Polyadenylate-binding pro	4	2	2	1
P01859	Immunoglobulin heavy constant gamma 2 OS	2	2	2	2
Q9Y6G9	Cytoplasmic dynein 1 light intermediate chair	3	2	2	1
A0A087WV	Isoform of Q00610, Clathrin heavy chain OS=I	1	4	2	0
P62318	Small nuclear ribonucleoprotein Sm D3 OS=H	3	1	2	1
A0A087WZ	Isoform of O15372, Eukaryotic translation init	0	1	2	3
B7Z6Z4	Isoform of P60660, Myosin light polypeptide (	2	1	2	1
Q15233	Non-POU domain-containing octamer-binding	3	1	2	0
M0QXL5	Isoform of P22087, rRNA 2_-O-methyltransfe	0	2	2	1
P43686	26S protease regulatory subunit 6B OS=Homc	1	1	2	1
P14174	Macrophage migration inhibitory factor OS=H	2	1	2	0
P11678	Eosinophil peroxidase OS=Homo sapiens GN=	0	0	2	0
P61163	Alpha-centractin OS=Homo sapiens GN=ACTR	1	0	2	1
B5ME19	Eukaryotic translation initiation factor 3 subu	1	1	2	0
A0A087WV	Isoform of P21333, Filamin-A OS=Homo sapie	1	0	2	1
J3QRS3	Isoform of P19105, Myosin regulatory light ch	1	1	2	0
Q8NBS9	Thioredoxin domain-containing protein 5 OS=	1	0	2	1
F8W883	Isoform of Q9Y6X6, Unconventional myosin-X	1	1	2	0

Q12906	Interleukin enhancer-binding factor 3 OS=Hor	1	1	2	0
E9PQ57	Isoform of P78406, mRNA export factor OS=H	2	0	2	0
P31153	S-adenosylmethionine synthase isoform type-	2	0	2	0
P06748	Nucleophosmin OS=Homo sapiens GN=NPM1	2	0	2	0
B0QY89	Isoform of Q9Y262, Eukaryotic translation init	0	0	2	1
B5MCA4	Isoform of P16422, Epithelial cell adhesion m	0	0	2	1
Q8NBF2	NHL repeat-containing protein 2 OS=Homo sa	0	0	2	1
Q9UHV9	Prefoldin subunit 2 OS=Homo sapiens GN=PFI	0	0	2	1
Q5JZ02	Isoform of Q96S44, TP53-regulating kinase OS	0	0	2	1
P17812	CTP synthase 1 OS=Homo sapiens GN=CTPS1	1	0	2	0
A0A087WV	Isoform of P06753, Tropomyosin alpha-3 chai	1	0	2	0
F5H365	Isoform of Q15436, Protein transport protein	1	0	2	0
I3L0J9	Isoform of Q6P2Q9, Pre-mRNA-processing-sp	1	0	2	0
O75643	U5 small nuclear ribonucleoprotein 200 kDa h	1	0	2	0
P13489	Ribonuclease inhibitor OS=Homo sapiens GN=	0	0	2	0
A0A0U1RR	Isoform of P26599, Polypyrimidine tract-bind	0	0	2	0
P04080	Cystatin-B OS=Homo sapiens GN=CSTB PE=1 S	0	0	2	0
E5RJR5	Isoform of P63208, S-phase kinase-associated	0	0	2	0
Q13263	Transcription intermediary factor 1-beta OS=I	0	0	2	0
E9PEB5	Isoform of Q96AE4, Far upstream element-bii	0	0	2	0
B1ALA9	Isoform of P60891, Ribose-phosphate pyroph	0	0	2	0
E7EWB4	Isoform of Q9BPU6, Dihydropyrimidinase-rela	0	0	2	0
P23526	Adenosylhomocysteinase OS=Homo sapiens (	0	0	2	0
Q13129	Zinc finger protein Rlf OS=Homo sapiens GN=	0	0	2	0
Q9H773	dCTP pyrophosphatase 1 OS=Homo sapiens G	0	0	2	0
Q92896	Golgi apparatus protein 1 OS=Homo sapiens (	0	0	2	0
Q00839	Heterogeneous nuclear ribonucleoprotein U (	0	0	2	0
Q9NP60	X-linked interleukin-1 receptor accessory prot	0	0	2	0
H0Y8C6	Isoform of O00410, Importin-5 (Fragment) OS	0	0	2	0
G8JLD5	Isoform of O00429, Dynamin-1-like protein O	0	0	2	0
E7EQB9	Isoform of O15160, DNA-directed RNA polym	0	0	2	0
O95373	Importin-7 OS=Homo sapiens GN=IPO7 PE=1	0	0	2	0
P00338	L-lactate dehydrogenase A chain OS=Homo sa	0	0	2	0
P05386	60S acidic ribosomal protein P1 OS=Homo sap	0	0	2	0
H7BZ94	Isoform of P07237, Protein disulfide-isomeras	0	0	2	0
P62714	Serine/threonine-protein phosphatase 2A cat	3	0	1	0
P30154	Serine/threonine-protein phosphatase 2A 65	0	0	1	0
O75190-2	Isoform of O75190, Isoform B of DnaJ homolo	0	0	1	4
EFC4EBP1	sp EFC4EBP1	1	1	1	0
O75909	Cyclin-K OS=Homo sapiens GN=CCNK PE=1 SV	1	4	1	2
P62195	26S protease regulatory subunit 8 OS=Homo :	2	3	1	1
P81605	Dermcidin OS=Homo sapiens GN=DCD PE=1 S	2	2	1	2
P60228	Eukaryotic translation initiation factor 3 subu	3	1	1	2
P55036	26S proteasome non-ATPase regulatory subu	2	2	1	1
P57081	tRNA (guanine-N(7)-)-methyltransferase non-	2	0	1	1
P62851	40S ribosomal protein S25 OS=Homo sapiens	2	2	1	1
D6RG13	Isoform of P61247, 40S ribosomal protein S3a	1	2	1	1

Q2TAM9	Tumor suppressor candidate gene 1 protein C	2	1	1	1
A6NFY0	Isoform of Q00013, 55 kDa erythrocyte meml	0	0	1	1
Q13347	Eukaryotic translation initiation factor 3 subu	0	2	1	1
O43660	Pleiotropic regulator 1 OS=Homo sapiens GN=	0	1	1	0
A0A024QZI	Isoform of P06493, Cell division cycle 2, G1 to	1	0	1	0
P27694	Replication protein A 70 kDa DNA-binding sul	1	1	1	1
P07814	Bifunctional glutamate/proline--tRNA ligase C	1	0	1	1
A0A0A0MS	Isoform of P41252, Isoleucine--tRNA ligase, cy	1	1	1	1
Q16650	T-box brain protein 1 OS=Homo sapiens GN=T	1	1	1	1
A0A1B0GT	Isoform of P08670, Vimentin (Fragment) OS=l	2	1	1	0
P08579	U2 small nuclear ribonucleoprotein B__ OS=H	0	2	1	0
P00519	Tyrosine-protein kinase ABL1 OS=Homo sapie	0	1	1	1
P62258	14-3-3 protein epsilon OS=Homo sapiens GN=	0	0	1	2
A0A087X2I	Isoform of P62333, 26S protease regulatory s	0	1	1	1
E5RFI6	Isoform of Q92769, Histone deacetylase 2 (Fr	0	1	1	1
A0A0A0MS	Isoform of P51531, Probable global transcript	0	0	1	2
K7ERY7	Isoform of P61353, 60S ribosomal protein L27	1	1	1	0
J3KP15	Isoform of Q01130, Serine/arginine-rich-splici	1	1	1	0
G3V1D4	Isoform of Q9NUP9, Lin-7 homolog C (C. elega	1	0	1	1
J3KRI4	Isoform of O43237, Cytoplasmic dynein 1 ligh	1	1	1	0
H3BSW0	Isoform of Q8N9N7, Leucine-rich repeat-cont	1	1	1	0
Q9NRC6	Spectrin beta chain, non-erythrocytic 5 OS=H	1	0	1	1
A0A087WV	Isoform of Q9UBQ5, Eukaryotic translation in	1	1	1	0
Q9UKZ4	Teneurin-1 OS=Homo sapiens GN=TENM1 PE=	1	1	1	0
E7EQG2	Isoform of Q14240, Eukaryotic initiation facto	2	0	1	0
A0A087WV	Isoform of Q99460, 26S proteasome non-ATP	2	0	1	0
Q9P258	Protein RCC2 OS=Homo sapiens GN=RCC2 PE=	2	0	1	0
C9J381	Isoform of P20839, Inosine-5_-monophospha	0	0	1	0
Q8TBZ5	Zinc finger protein 502 OS=Homo sapiens GN=	0	1	1	0
A8MUF7	Isoform of P02100, Hemoglobin subunit epsil	0	0	1	1
J3QRY4	Isoform of O00231, 26S proteasome non-ATP	0	0	1	1
O00232	26S proteasome non-ATPase regulatory subu	0	1	1	0
A0A087WZ	Isoform of Q03938, Zinc finger protein 90 OS=	0	0	1	1
Q00577	Transcriptional activator protein Pur-alpha OS	0	1	1	0
A0A087WV	Isoform of Q06033, Inter-alpha-trypsin inhibi	0	0	1	1
Q13200	26S proteasome non-ATPase regulatory subu	0	0	1	1
H0YCQ8	Isoform of Q7L2H7, Eukaryotic translation init	0	0	1	1
Q96M95	Coiled-coil domain-containing protein 42 OS=	0	0	1	1
K7EJT5	Isoform of P35268, 60S ribosomal protein L22	0	1	1	0
H0Y7R1	Isoform of Q8TBZ2, MYCBP-associated protei	0	1	1	0
Q8WTU2	Scavenger receptor cysteine-rich domain-con	0	0	1	1
F8WA32	Isoform of Q9BZW7, Testis-specific gene 10 p	0	1	1	0
Q12767-2	Isoform of Q12767, Isoform 2 of Transmembr	0	0	1	1
H0YKH9	Isoform of P49641, Alpha-mannosidase 2x (Fr	0	0	1	1
F5GWN5	Isoform of O00750, Phosphatidylinositol 4-ph	0	0	1	1
Q86VD1	MORC family CW-type zinc finger protein 1 OS	0	1	1	0
Q9BYB4	Guanine nucleotide-binding protein subunit b	1	0	1	0

C9JZD1	Isoform of O15145, Actin-related protein 2/3	1	0	1	0
O43143	Pre-mRNA-splicing factor ATP-dependent RN/	1	0	1	0
B8ZZL3	Isoform of O60573, Eukaryotic translation init	1	0	1	0
A0A0U1RR	Isoform of A0A0U1RRH7, Histone H2A OS=Hc	1	0	1	0
P08243	Asparagine synthetase [glutamine-hydrolyzin;	1	0	1	0
A0A0B4J1R	Isoform of P29401, Transketolase OS=Homo s	1	0	1	0
A0A0D9SE1	Isoform of P47755, F-actin-capping protein su	1	0	1	0
P61978	Heterogeneous nuclear ribonucleoprotein K (	1	0	1	0
H0YA86	Isoform of A6NEF3, Golgin subfamily A memb	1	0	1	0
Q9Y2V2	Calcium-regulated heat-stable protein 1 OS=H	0	0	1	0
O00165	HCLS1-associated protein X-1 OS=Homo sapie	0	0	1	0
O00170	AH receptor-interacting protein OS=Homo sap	0	0	1	0
O14980	Exportin-1 OS=Homo sapiens GN=XPO1 PE=1	0	0	1	0
O15371	Eukaryotic translation initiation factor 3 subu	0	0	1	0
O75306-2	Isoform of O75306, Isoform 2 of NADH dehyd	0	0	1	0
C9JIZ0	Isoform of O95777, LSM8 homolog, U6 small	0	0	1	0
O95881	Thioredoxin domain-containing protein 12 OS	0	0	1	0
A0A075B71	Isoform of P08708, 40S ribosomal protein S17	0	0	1	0
P0DN76	Splicing factor U2AF 35 kDa subunit-like prote	0	0	1	0
P12955	Xaa-Pro dipeptidase OS=Homo sapiens GN=PI	0	0	1	0
B4DNK4	Isoform of P14618, Pyruvate kinase OS=Homc	0	0	1	0
P19474	E3 ubiquitin-protein ligase TRIM21 OS=Homo	0	0	1	0
P22102	Trifunctional purine biosynthetic protein ader	0	0	1	0
E9PJH4	Isoform of P23396, 40S ribosomal protein S3	0	0	1	0
J3KQ69	Isoform of P25205, DNA replication licensing	0	0	1	0
P25398	40S ribosomal protein S12 OS=Homo sapiens	0	0	1	0
A0A0C4DG	Isoform of P33316, DUTP pyrophosphatase, is	0	0	1	0
C9J0J7	Isoform of P35080, Profilin OS=Homo sapiens	0	0	1	0
B5MC59	Isoform of P35244, Replication protein A 14 k	0	0	1	0
P41227	N-alpha-acetyltransferase 10 OS=Homo sapie	0	0	1	0
H3BUM9	Isoform of P41240, Tyrosine-protein kinase C!	0	0	1	0
J3KPM9	Isoform of P42224, Signal transducer and acti	0	0	1	0
P42285	Superkiller viralicidic activity 2-like 2 OS=Hom	0	0	1	0
B1AK85	Isoform of P47756, F-actin-capping protein su	0	0	1	0
B4DXZ6	Isoform of P51114, Fragile X mental retardati	0	0	1	0
A8MU27	Isoform of P55854, Small ubiquitin-related m	0	0	1	0
P55884	Eukaryotic translation initiation factor 3 subu	0	0	1	0
A0A0U1RQ	Uncharacterized protein (Fragment) OS=Hom	0	0	1	0
C9JL85	Isoform of P58546, Myotrophin OS=Homo sap	0	0	1	0
A0A0A6YY(	Protein ARPC4-TTLL3 OS=Homo sapiens GN=/	0	0	1	0
D6R9I9	Isoform of P61221, ATP-binding cassette sub-	0	0	1	0
B4DWR3	Isoform of P61758, Prefoldin subunit 3 OS=Hc	0	0	1	0
P62310	U6 snRNA-associated Sm-like protein LSm3 O	0	0	1	0
P62701	40S ribosomal protein S4, X isoform OS=Hom	0	0	1	0
E9PR30	Isoform of P35544, 40S ribosomal protein S3(	0	0	1	0
A0A0A0MS	Isoform of Q14192, Four and a half LIM doma	0	0	1	0
Q14566	DNA replication licensing factor MCM6 OS=Hc	0	0	1	0

Q15056	Eukaryotic translation initiation factor 4H OS=	0	0	1	0
Q15717	ELAV-like protein 1 OS=Homo sapiens GN=EL/	0	0	1	0
B5MCZ9	Isoform of Q16769, Glutaminyl-peptide cyclo	0	0	1	0
Q3KQU3	MAP7 domain-containing protein 1 OS=Homo	0	0	1	0
Q52LJ0	Protein FAM98B OS=Homo sapiens GN=FAM9	0	0	1	0
J3QTJ6	Isoform of Q5CZC0, Fibrous sheath-interactin	0	0	1	0
C9JKF1	Isoform of Q5K651, Sterile alpha motif domai	0	0	1	0
B4DEH8	Isoform of Q86U42, Polyadenylate-binding pr	0	0	1	0
K7EQA8	Isoform of Q86X55, Histone-arginine methyltr	0	0	1	0
B1AP52	Isoform of Q8TEW0, Partitioning defective 3 h	0	0	1	0
Q8WXX5	DnaJ homolog subfamily C member 9 OS=Hor	0	0	1	0
A0A087X2(	Isoform of Q92499, ATP-dependent RNA helic	0	0	1	0
K7EIN2	Isoform of Q9BRJ7, Protein syndesmos (Fragn	0	0	1	0
Q96M86	Dynein heavy chain domain-containing protei	0	0	1	0
A0A1B0GU	Isoform of Q96N23, Cilia- and flagella-associa	0	0	1	0
M0QX71	Isoform of Q9BQ67, Glutamate-rich WD repea	0	0	1	0
Q9BQA1	Methylosome protein 50 OS=Homo sapiens G	0	0	1	0
Q9BYX2	TBC1 domain family member 2A OS=Homo sa	0	0	1	0
E9PJP1	Isoform of Q9H7C9, Mth938 domain-containi	0	0	1	0
F6TLX2	Isoform of Q9HC38, Glyoxalase domain-conta	0	0	1	0
Q9P2Q2	FERM domain-containing protein 4A OS=Hom	0	0	1	0
C9JHK9	Isoform of Q9UG63, ATP-binding cassette sut	0	0	1	0
Q9Y3Z3	Deoxynucleoside triphosphate triphosphohyd	0	0	1	0
H0Y4N6	Isoform of O14786, Neuropilin-1 (Fragment) (	0	0	1	0
K9M1A9	Isoform of K9M1U5, Interferon lambda-4 OS=	0	0	1	0
E7EQB2	Isoform of P02788, Lactotransferrin (Fragmer	0	0	1	0
C9J712	Isoform of P35080, Profilin OS=Homo sapiens	0	0	1	0
O15294	UDP-N-acetylglucosamine--peptide N-acetylg	0	0	1	0
O75348	V-type proton ATPase subunit G 1 OS=Homo s	0	0	1	0
P41250	Glycine--tRNA ligase OS=Homo sapiens GN=G	0	0	1	0
P53350	Serine/threonine-protein kinase PLK1 OS=Hoi	0	0	1	0
Q86VV8	Rotatin OS=Homo sapiens GN=RTTN PE=1 SV=	0	0	1	0
Q8NC51	Plasminogen activator inhibitor 1 RNA-binding	0	0	1	0
H0Y339	Isoform of Q8NHY2, E3 ubiquitin-protein ligas	0	0	1	0
P20618	Proteasome subunit beta type-1 OS=Homo sa	0	0	1	0
M0QXK4	Isoform of P39019, 40S ribosomal protein S19	0	0	1	0
A0A0A0MF	Isoform of Q8IW50, Protein FAM219A OS=Ho	0	0	1	0
Q9UBB9	Tuftelin-interacting protein 11 OS=Homo sapi	0	0	1	0
F2Z388	Isoform of P42766, 60S ribosomal protein L35	0	0	1	0
Q9BWJ5	Splicing factor 3B subunit 5 OS=Homo sapiens	0	0	1	0
K7EL89	Isoform of P19623, Spermidine synthase (Frag	0	0	1	0
H7BZU1	Isoform of P41091, Eukaryotic translation init	0	0	1	0
Q53F19	Nuclear cap-binding protein subunit 3 OS=Ho	0	0	1	0
Q9GZP4	PITH domain-containing protein 1 OS=Homo s	0	0	1	0
Q9UQE7	Structural maintenance of chromosomes prot	0	0	1	0
E9PKN4	Isoform of O75534, Cold shock domain-conta	0	0	1	0
C9JM43	Isoform of Q6ZSS3, Zinc finger protein 621 (Fr	0	0	1	0

A0A096LP1	Isoform of Q8ND56, Protein LSM14 homolog	0	0	1	0
A8MW50	Isoform of P07195, L-lactate dehydrogenase (	0	0	1	0
Q9P2P6	StAR-related lipid transfer protein 9 OS=Home	0	0	1	0
A6NMZ7	Collagen alpha-6(VI) chain OS=Homo sapiens	0	0	1	0
B1ALD9	Isoform of Q15063, Periostin OS=Homo sapie	0	0	1	0
H0YCK3	Isoform of P55265, Double-stranded RNA-spe	0	0	1	0
F8WDP8	Isoform of Q8N841, Tubulin polyglutamylase	0	0	1	0
Q8TB03	Uncharacterized protein CXorf38 OS=Homo sa	0	0	1	0
F8VPD4	Isoform of P27708, CAD protein OS=Homo sa	0	0	1	0
O00479	High mobility group nucleosome-binding dom	0	0	1	0
P0DN79	Cystathionine beta-synthase-like protein OS=	0	0	1	0
A0A0C4DG	Isoform of Q86VP6, Cullin-associated NEDD8-	0	0	1	0
Q8TE59	A disintegrin and metalloproteinase with thro	0	0	1	0
Q9HAV4	Exportin-5 OS=Homo sapiens GN=XPO5 PE=1	0	0	1	0
Q14674	Separin OS=Homo sapiens GN=ESPL1 PE=1 SV	0	0	1	0
J3KTM9	Isoform of Q14974, Importin subunit beta-1 (	0	0	1	0
A0A087X1|	Isoform of P20929, Nebulin OS=Homo sapien	0	0	1	0
D6R9P3	Isoform of Q99729, Heterogeneous nuclear ri	0	0	1	0
C9K0F9	Isoform of Q92794, Histone acetyltransferase	0	0	1	0
O94826	Mitochondrial import receptor subunit TOM7	0	0	1	0
P20023	Complement receptor type 2 OS=Homo sapie	0	0	1	0
E7ENZ3	Isoform of P48643, T-complex protein 1 subu	11	5	0	3
P68032	Actin, alpha cardiac muscle 1 OS=Homo sapie	0	3	0	0
Q04695	Keratin, type I cytoskeletal 17 OS=Homo sapie	0	4	0	4
P02538	Keratin, type II cytoskeletal 6A OS=Homo sapi	0	0	0	4
P13647	Keratin, type II cytoskeletal 5 OS=Homo sapie	0	1	0	1
Q6NUN7	Uncharacterized protein C11orf63 OS=Homo	1	1	0	5
A6NIJ5	Putative protein FAM90A20P OS=Homo sapie	3	7	0	0
F8VXH9	Isoform of Q15366, Poly(rC)-binding protein 2	0	0	0	0
Q9NZL6	Ral guanine nucleotide dissociation stimulato	0	0	0	3
Q8NFD2	Ankyrin repeat and protein kinase domain-co	3	0	0	0
F8W1S1	Isoform of Q7RTS7, Keratin, type II cytoskelet	0	1	0	0
O95470	Sphingosine-1-phosphate lyase 1 OS=Homo sa	1	2	0	0
F8W079	Isoform of P06576, ATP synthase subunit beta	1	2	0	2
P23246-2	Isoform of P23246, Isoform Short of Splicing f	3	1	0	0
P54296	Myomesin-2 OS=Homo sapiens GN=MYOM2	1	2	0	1
A0A0A0MT	Isoform of Q6ZN11, Zinc finger protein 793 O	1	0	0	1
E9PGM7	Isoform of O94988, Protein FAM13A OS=Hom	0	0	0	3
D6R9A6	Isoform of P26583, High mobility group prote	2	0	0	0
S4R3T0	Isoform of M0R082, Uncharacterized protein	2	0	0	1
Q4ZG55	Protein GREB1 OS=Homo sapiens GN=GREB1	1	2	0	0
A0A0D9SFI	Isoform of Q8TAT6, Nuclear protein localizatic	1	2	0	0
Q9UPU7	TBC1 domain family member 2B OS=Homo sa	1	2	0	0
P62191	26S protease regulatory subunit 4 OS=Homo	0	1	0	0
A0A0D9SF!	Isoform of O00571, ATP-dependent RNA helic	0	0	0	1
E5RHG6	Isoform of O75347, Tubulin-specific chaperor	0	1	0	1
H0YBW5	Isoform of Q8WVK2, U4/U6.U5 small nuclear	0	2	0	0

J3QL71	Isoform of Q96FV2, Secernin-2 OS=Homo sap	0	1	0	1
E9PDH4	Isoform of Q9Y2I7, 1-phosphatidylinositol 3-p	0	1	0	1
O43506	Disintegrin and metalloproteinase domain-co	0	1	0	1
G3V1N2	Isoform of P69905, HCG1745306, isoform CR	0	0	0	2
G3V198	Isoform of Q12769, Nuclear pore complex pro	0	2	0	0
K7EJS6	Isoform of Q92918, Mitogen-activated protei	0	1	0	1
P63167	Dynein light chain 1, cytoplasmic OS=Homo sa	2	0	0	0
Q9ULD9	Zinc finger protein 608 OS=Homo sapiens GN=	1	1	0	0
D6RFZ2	Isoform of Q0IIM8, TBC1 domain family mem	2	0	0	0
B2RPK0	Putative high mobility group protein B1-like 1	2	0	0	0
A0A087X0(	Isoform of Q9BVV2, Fibronectin type III doma	1	0	0	1
C9J808	Isoform of Q9BYG3, MKI67 FHA domain-inter	1	0	0	1
P53803	DNA-directed RNA polymerases I, II, and III su	1	1	0	0
F8WBW2	Isoform of Q9UFE4, Coiled-coil domain-conta	1	1	0	0
Q96HU1	Small G protein signaling modulator 3 OS=Hor	1	0	0	1
K7EN45	Isoform of Q13526, Peptidyl-prolyl cis-trans is	2	0	0	0
A0A0A0MF	Isoform of Q96SN8, CDK5 regulatory subunit-	2	0	0	0
E9PFE2	Isoform of Q9UHL9, General transcription fac	1	0	0	1
O60519	cAMP-responsive element-binding protein-lik	0	0	0	1
P11441	Ubiquitin-like protein 4A OS=Homo sapiens G	0	1	0	0
B4DQ67	Isoform of P49590, Probable histidine--tRNA l	0	0	0	1
Q15427	Splicing factor 3B subunit 4 OS=Homo sapiens	0	0	0	1
Q5T280	Putative methyltransferase C9orf114 OS=Hon	0	0	0	1
A0A0D9SG	Isoform of Q6P1N9, Putative deoxyribonuclea	0	1	0	0
Q7L1I2	Synaptic vesicle glycoprotein 2B OS=Homo sa	0	1	0	0
Q86U38	Nucleolar protein 9 OS=Homo sapiens GN=N(	0	0	0	1
Q8IVB5	LIX1-like protein OS=Homo sapiens GN=LIX1L	0	1	0	0
H0YD40	Isoform of Q8IZC6, Collagen alpha-1(XXVII) ch	0	0	0	1
C9J5X9	Isoform of Q8NB91, Fanconi anemia group B	0	0	0	1
A0A1B0GX(	Isoform of Q969T4, Ubiquitin-conjugating enz	0	0	0	1
F5GWH4	Isoform of Q96EP1, E3 ubiquitin-protein ligase	0	1	0	0
Q9NVP2	Histone chaperone ASF1B OS=Homo sapiens (	0	0	0	1
Q9P109	Beta-1,3-galactosyl-O-glycosyl-glycoprotein b	0	1	0	0
Q9P227	Rho GTPase-activating protein 23 OS=Homo s	0	1	0	0
J3QQJ0	Isoform of Q9UHR5, SAP30-binding protein (F	0	1	0	0
B3KPX4	Isoform of Q9UJ83, 2-hydroxyacyl-CoA lyase 1	0	1	0	0
Q9UKN8	General transcription factor 3C polypeptide 4	0	1	0	0
Q9Y3B4	Splicing factor 3B subunit 6 OS=Homo sapiens	0	1	0	0
F8WDC4	Isoform of Q8NBL1, Protein O-glucosyltransfe	0	0	0	1
Q8N3T6	Transmembrane protein 132C OS=Homo sapi	0	1	0	0
Q96PQ1	Sialic acid-binding Ig-like lectin 12 OS=Homo s	0	0	0	1
Q99543	DnaJ homolog subfamily C member 2 OS=Hor	0	0	0	1
Q9HC44	Vasculin-like protein 1 OS=Homo sapiens GN=	0	0	0	1
Q14344	Guanine nucleotide-binding protein subunit a	0	1	0	0
Q99962	Endophilin-A1 OS=Homo sapiens GN=SH3GL2	0	1	0	0
Q9UKS7-5	Isoform of Q9UKS7, Isoform 5 of Zinc finger p	0	1	0	0
Q9Y5B6	PAX3- and PAX7-binding protein 1 OS=Homo	0	0	0	1

A0A0B4J25	Isoform of P61626, Lysozyme C OS=Homo sap	0	1	0	0
D6RGK3	Isoform of Q16594, Transcription initiation fa	0	0	0	1
A0A0A0MS	Isoform of Q9Y6M7, Anion exchange protein	0	1	0	0
A4D2P6	Delphilin OS=Homo sapiens GN=GRID2IP PE=3	0	1	0	0
K7EPW3	Isoform of P10072, Krueppel-related zinc fing	0	0	0	1
Q9NXL6	SID1 transmembrane family member 1 OS=H	0	1	0	0
H7C319	Isoform of Q9UHB7, AF4/FMR2 family membe	0	0	0	1
H3BUU9	Isoform of P55287, Cadherin-11 OS=Homo sa	0	0	0	1
H3BPG7	Isoform of Q6FI81, Anamorsin OS=Homo sapi	0	0	0	1
K7EKB9	Isoform of P15923, Transcription factor E2-al	0	1	0	0
Q13136	Liprin-alpha-1 OS=Homo sapiens GN=PPFIA1	0	0	0	1
O00443	Phosphatidylinositol 4-phosphate 3-kinase C2	0	0	0	1
Q9P2F8	Signal-induced proliferation-associated 1-like	0	1	0	0
G3V295	Isoform of P60900, Proteasome subunit alpha	0	0	0	1
Q5TA15	Isoform of O15056, Synaptojanin-2 (Fragment	0	1	0	0
Q9Y2W2	WW domain-binding protein 11 OS=Homo sap	0	0	0	1
U3KQH8	Isoform of P24310, Cytochrome c oxidase sut	0	1	0	0
O96004	Heart- and neural crest derivatives-expressed	0	1	0	0
Q7RTY3	Serine protease 45 OS=Homo sapiens GN=PR!	0	0	0	1
P11498	Pyruvate carboxylase, mitochondrial OS=Hom	0	1	0	0
H0Y607	Isoform of Q96BN6, Protein FAM149B1 (Frag	0	1	0	0
A6NNM8	Tubulin polyglutamylase TTLL13P OS=Homo s	0	1	0	0
P25445-7	Isoform of P25445, Isoform 7 of Tumor necro	0	0	0	1
A2VEC9-2	Isoform of A2VEC9, Isoform 2 of SCO-spondin	1	0	0	0
O95400	CD2 antigen cytoplasmic tail-binding protein 2	1	0	0	0
D3YTI2	Isoform of P24666, Low molecular weight pho	1	0	0	0
E9PS50	Isoform of P62277, 40S ribosomal protein S13	1	0	0	0
E9PKU4	Isoform of P62917, 60S ribosomal protein L8	1	0	0	0
D6RER2	Isoform of Q13634, Cadherin-18 OS=Homo sa	1	0	0	0
Q15034	Probable E3 ubiquitin-protein ligase HERC3 O	1	0	0	0
C9IZX4	Isoform of Q6P9H4, Connector enhancer of ki	1	0	0	0
E7ENR6	Isoform of Q8TBG4, Ethanolamine-phosphate	1	0	0	0
A2A304	Isoform of Q96NH3, Protein broad-minded (F	1	0	0	0
Q96QD8	Sodium-coupled neutral amino acid transport	1	0	0	0
Q9BU76	Multiple myeloma tumor-associated protein 2	1	0	0	0
Q9H5V9	UPF0428 protein CXorf56 OS=Homo sapiens (	1	0	0	0
Q9NR30	Nucleolar RNA helicase 2 OS=Homo sapiens G	1	0	0	0
F5GX77	Isoform of Q9UI30, Multifunctional methyltra	1	0	0	0
Q9UKP5	A disintegrin and metalloproteinase with thro	1	0	0	0
Q9Y2S6	Translation machinery-associated protein 7 O	1	0	0	0
A0A182DW	Zinc finger protein 812, pseudogene OS=Hom	1	0	0	0
E9PJP2	Isoform of Q5TF21, Protein SOGA3 OS=Homo	1	0	0	0
P17655	Calpain-2 catalytic subunit OS=Homo sapiens	1	0	0	0
B5MD17	Isoform of P83916, Chromobox protein homc	1	0	0	0
H0YAE2	Isoform of Q0JRZ9, F-BAR domain only protei	1	0	0	0
Q14938-2	Isoform of Q14938, Isoform 2 of Nuclear facto	1	0	0	0
Q6P3R8	Serine/threonine-protein kinase Nek5 OS=Ho	1	0	0	0

Q6UXC1	Apical endosomal glycoprotein OS=Homo sap	1	0	0	0
Q70JA7	Chondroitin sulfate synthase 3 OS=Homo sapi	1	0	0	0
P55060	Exportin-2 OS=Homo sapiens GN=CSE1L PE=1	1	0	0	0
A0A087WZ	Isoform of Q8N162, Olfactory receptor 8H2 C	1	0	0	0
P51571	Translocon-associated protein subunit delta C	1	0	0	0
A0A087WX	Isoform of Q06787, Synaptic functional regula	1	0	0	0
Q8WZ82	Esterase OVCA2 OS=Homo sapiens GN=OVCA	1	0	0	0
Q08211	ATP-dependent RNA helicase A OS=Homo sap	1	0	0	0
Q16739	Ceramide glucosyltransferase OS=Homo sapie	1	0	0	0
E7ER45	Isoform of O43451, Maltase-glucoamylase, in	1	0	0	0
A8MXE2	Putative UDP-GlcNAc:betaGal beta-1,3-N-ace	1	0	0	0
P14410	Sucrase-isomaltase, intestinal OS=Homo sapie	1	0	0	0
A0A087WV	Isoform of Q8IVF4, Dynein heavy chain 10, ax	1	0	0	0
Q96JW4	Solute carrier family 41 member 2 OS=Homo	1	0	0	0
P09619	Platelet-derived growth factor receptor beta	1	0	0	0
B1AHC5	Isoform of Q96EK2, PHD finger protein 21B O	1	0	0	0
E7ETF4	Isoform of O60701, UDP-glucose 6-dehydroge	1	0	0	0
Q9H568	Actin-like protein 8 OS=Homo sapiens GN=AC	1	0	0	0